



## City Research Online

### City, University of London Institutional Repository

---

**Citation:** Ekaireb, S.E. (1990). Dispersion of chemicals and reactions of dispersed chemicals. (Unpublished Doctoral thesis, City, University of London)

This is the accepted version of the paper.

This version of the publication may differ from the final published version.

---

**Permanent repository link:** <https://openaccess.city.ac.uk/id/eprint/29135/>

**Link to published version:**

**Copyright:** City Research Online aims to make research outputs of City, University of London available to a wider audience. Copyright and Moral Rights remain with the author(s) and/or copyright holders. URLs from City Research Online may be freely distributed and linked to.

**Reuse:** Copies of full items can be used for personal research or study, educational, or not-for-profit purposes without prior permission or charge. Provided that the authors, title and full bibliographic details are credited, a hyperlink and/or URL is given for the original metadata page and the content is not changed in any way.

TO MY FAMILY WITH MUCH LOVE

DISPERSION OF CHEMICALS  
AND  
REACTIONS OF DISPERSED CHEMICALS

A THESIS SUBMITTED FOR THE  
DEGREE OF DOCTOR OF PHILOSOPHY  
IN THE FACULTY OF SCIENCE AT  
THE CITY UNIVERSITY, LONDON

BY  
SALLY ELIZABETH EKAIREB

Department of Chemistry,  
The City University,  
London.

April, 1990

DISPERSION OF CHEMICALS  
AND  
REACTIONS OF DISPERSED CHEMICALS

CONTENTS

	<b>Page</b>
ABSTRACT	5
CHAPTER ONE           DISPERSION	6
CHAPTER TWO           THE MAGNETIC TREATMENT OF FLUIDS	
- CRYSTAL NUCLEATION	64
CHAPTER THREE        CEMENT	161
CHAPTER FOUR         DISPERSION STUDIES	215

ACKNOWLEDGEMENTS

I would like to express my sincere gratitude to Prof. J.D. Donaldson for his help and guidance throughout the course of this work. I am similarly indebted to Dr. S.M. Grimes and Dr. S.J. Clark for their advice and assistance.

Thanks are due to the staff of the Department of Physics, for use of the optical instruments, particularly Mr. M. Phillips for his kind assistance. I also wish to thank the staff of the Department of Civil Engineering for the use of their facilities and the provision of valuable material.

Much appreciation is offered to the technical staff at The City University for microanalytical work and to Mr. C.J. Whitehead for his help with the Particle Size Analyzer.

My grateful thanks are extended to the SERC for the award of a CASE studentship. Moreover, I should like to acknowledge Dr. M. Christoforou and Dr. I. Abrahams.

Finally, a special thanks must go to my family and friends for their whole-hearted support and encouragement during the course of this study.

DECLARATION

I grant powers of discretion to the University Librarian to allow this thesis to be copied, in whole or in part, without further reference to me. This permission covers single copies made for study purposes, subject to the normal conditions of acknowledgement.

*Sally Ekaireb.*

Sally Ekaireb.

ABSTRACT

Two aspects of the chemistry of dispersion of materials in fluids are studied, (1) the dispersion of fine powders in fluids to enhance reactivity and (2) the interaction between magnetic fields and charged species in fluids.

The problems arising from a conflict between (i) the use of fine powders to optimize reactivity and (ii) the health hazards of fine powders and the decreased reactivity resulting from reaction of these powders with the atmosphere are considered for tin(II) carboxylate catalysts, calcium hydroxide-processing aids for fluoroelastomers and cobalt oxide ruminant feedstocks.

Fine particle suspensions and crystal nuclei dispersed in fluids have high surface charges that can react with an applied magnetic field. The effects of magnetic fields on charged species are studied for precipitation reactions of calcium sulphate and calcium phosphate and for suspensions of cementaceous materials in water. The effects of magnetic fields on the solubility of barium sulphate and calcium phosphate in water are also reported.

It is shown that the magnetic treatment of fluids can have a profound effect on the behaviour of charged species in fluids. Changes in particle size, morphology and solubility arising from the interaction between the field and the changes at the solid-fluid interface are discussed in terms of possible field-charge mechanisms.

The major factors affecting the behaviour of species in magnetic fields are considered to be (i) the separation of positive and negative charges by opposite helical motion in the field and (ii) the direct interaction of the field with the highly charged surfaces of crystal nuclei and dispersed fine particles.

CHAPTER ONE

DISPERSION

	Page
1.1 Introduction	7
1.2 Definition of a Colloid	8
1.3 Classification of Colloidal Systems	10
1.4 Formation of Colloids	13
1.5 The Electric Double Layer	20
1.6 Stability of Colloidal Systems	30
1.7 Solid-Liquid and Liquid-Liquid Interfaces	40
1.8 Sols	41
1.9 Gels	42
1.10 Emulsions	47
1.11 Microemulsions	51
1.12 Association Colloids	52
1.13 Objectives	60
References	61

CHAPTER ONE

DISPERSION

1.1 Introduction

The physical and chemical behaviour of very small particles of materials can vastly differ from that of the bulk. Differences in physical properties will be associated with high surface charge to volume and flocculation effects, while differences in chemical properties will arise from the availability of large surface areas for reaction. Both the physical and chemical aspects of fine particles are considered in this thesis.

Physical property effects are considered in studies of the influence of magnetic fields on dispersed fine particles and on crystal nuclei which provide a specific example of small particle science.

The chemical property effects are considered in studies of the reactivity of dispersed fine particles of catalysts and processing aids.

This introductory chapter contains a description of the general characteristics of colloids, as they are among the

best understood fine particles, and is extended to account for crystal nucleation processes.

## 1.2 Definition of a Colloid

The significance of particle size was inherent in Graham's definition of a 'colloid' in 1861 [1] [2]. The term is derived from the Greek word 'κολλᾶ' meaning 'glue', although the etymology of the term is now largely irrelevant. However, the word in its original context was used to describe systems which exhibited slow rates of diffusion through a porous membrane of which glue was a typical example.

Colloid science, being an interdisciplinary subject depends, for its progress on developments in other fields, notably physics and physical chemistry.

The microscopic observations of botanist, Robert Brown (hence Brownian motion), experiments on the scattering of light by small particles by Tyndall and the ultramicroscopic observations of Zsigmondy all showed that colloidal particles exist in a size range where the energy of random bombardment by solvent molecules is adequate to maintain their distribution throughout the medium against the

sedimentary action of gravity. These observations led Ostwald (1907) to a more precise definition of a colloidal system: *one in which one or more of the components of the dispersed phase has at least one dimension within the range of  $10^3$  to  $1\mu$  (3)*. The dispersed phase (or discontinuous phase) is that which is uniformly distributed (in a finely divided state) in a dispersion medium (or continuous phase) or solvent, i.e. it generally applies to systems containing large molecules and/or small particles. The adjective 'microheterogeneous' provides an apt description of most colloidal systems.

Systems in which only one dimension falls within this size range include lamellar systems such as clay platelets and soap films; in asbestos and substances containing fibres there are two such dimensions, whilst in particulate dispersions all three dimensions are within the colloidal size range. The units of a colloidal system need not be discrete; continuous network systems such as porous solids, gels (discussed in detail in Section 1.9) and foams are also classified as colloids. The limits specified are not rigid, e.g. in emulsions and slurries, particles of larger dimensions may be present. Moreover, like other class distinctions, the extremities are unmistakable, but the line of demarcation between colloidal and non-colloidal systems is indefinite.

The major factors contributing to the overall nature of a colloidal system are as follows:

Particle size

Particle shape and flexibility

Surface (including electrical) properties

Particle-particle interactions

Particle-solvent interactions

### 1.3 Classification of Colloidal Systems

Colloidal systems may be categorized into three major groups [4]:

- (i) Colloidal dispersions, e.g. sols and emulsions, are thermodynamically unstable due to their high surface free energy and are irreversible systems, that is, they are not readily reconstituted after phase separation.
- (ii) True solutions of macromolecular material (natural or synthetic), e.g. gels, resins, rubber, plastics, are thermodynamically stable and reversible, i.e. they are readily reconstituted after phase separation of solute from solvent.

(iii) Association colloids, e.g. soap, detergents and other surfactants form aggregates, 'micelles', in water.

Dispersions in which particles are of uniform size are referred to as 'monodispersed', whereas a variation in particle size is found in colloids of a 'polydispersed' nature. Under certain conditions, particles may adhere to one another to form aggregates of successively increasing size, which may, despite the tendency of thermal motion to keep them in suspension, separate out under gravity and change with time. 'Flocculation' is the process used to describe the formation of an initially formed, rather open aggregate, or 'floc', which may or may not separate out. If the aggregate changes to, or is produced in, a much denser form, it is said to undergo 'coagulation' with the formation of a 'coagulum'. An aggregate usually separates out either by 'creaming' (if it is less dense than the medium) or by 'sedimentation' (if it is more dense than the medium). Flocculation can be reversed in the process of 'deflocculation', whereas coagulation is generally irreversible (some coagulated systems can be redispersed under favourable conditions).

Aggregation results in the formation of a variety of shapes which do not necessarily correspond to those of the primary particles.

TABLE 1.1 Some typical colloidal systems

Dispersed phase	Dispersion medium	Class	Examples
<b>DISPERSED SYSTEMS</b>			
Liquid	Gas	Liquid aerosol	Fog, mist, liquid sprays
Solid	Gas	Solid aerosol	Industrial smokes, dust
Gas	Liquid	Foam	Foam on soap solns., fire-extinguisher foam
Liquid	Liquid	Emulsion	Milk, butter, mayonnaise, pharmaceutical creams, cosmetics
Solid	Liquid	Sol, colloidal suspension, paste (high solid conc.)	Inorganic sols (Au, AgI, S, metallic hydroxides), toothpaste
Gas	Solid	Solid foam	Expanded plastics
Liquid	Solid	Solid emulsion	Opal, pearl
Solid	Solid	Solid suspension	Pigmented plastics
		Xerogels	Microporous oxides, "silica gel", porous glass, microporous carbons, zeolites
<b>MACROMOLECULAR COLLOIDS</b>			
Macro-molecules	Solvent	Gels	Jellies, glue
<b>ASSOCIATION COLLOIDS</b>			
Micelles	Solvent	-	Soap/water, detergent/water, dye solns.

TABLE 1.1 Some typical colloidal systems (contd.)

Dispersed phase	Dispersion medium	Class	Examples
<b>BIOCOLLOIDS</b>			
Corpuscles	Serum		Blood
Hydroxy-apatite	Collagen		Bone
Proteins	Lipids		Cell membranes, muscle
<b>THREE-PHASE COLLOIDAL SYSTEMS (MULTIPLE COLLOIDS)</b>			
Coexisting phases			
Porous rock	Oil	Water	Oil-bearing rock
Porous solid	Liquid	Vapour	Capillary condensed vapours
Mineral	Water	Air bubbles or oil droplets	Mineral flotation
Oil	Aqueous phase	Water	Double emulsions

1.4 Formation of Colloids

Colloidal suspensions can either be prepared by the degradation of bulk matter (comminution and dispersion methods) or by aggregation of atomic or molecular species (nucleation and growth). Examples of the former route include the formation of pigment dispersions, and herbicide and pesticide formulations, whilst examples of the latter include the production of silver bromide sols used in

photography, aqueous oxide dispersions (e.g. alumina or silica), and polymer lattices (both aqueous and non-aqueous). However, these dispersions will only remain metastable or colloidally stable if the repulsive forces are sufficiently large to inhibit coagulation or flocculation.

Dispersion of bulk material by grinding in a colloid mill or by ultrasonics does not generally lead to extensive subdivision, owing to the tendency of smaller particles to reunite under the influence of the mechanical and attractive forces involved - the caking of dry powders is a common problem in practice. After prolonged grinding the distribution of particles reaches an equilibrium. Fine dispersions can be achieved by the incorporation of an inert diluent to reduce the chances of particles encountering one another during grinding, or by wet-milling [5] in the presence of a surface-active material (see Section 1.12). The former technique is exemplified by the preparation of a sulphur sol containing particles in the upper colloidal range: a mixture of sulphur and glucose are ground, the powder dispersed in water and the dissolved glucose removed from the sol by dialysis.

Colloids prepared by the aggregation of atomic or molecular species involves the formation of clusters, or *embryos*, of a new phase in an existing bulk phase and is accompanied by

an increase in free energy. As the magnitude of the embryo increases, it passes through an intermediate size range of 1-10nm, at which stage it is termed the *critical nucleus* and the free energy passes through a maximum. Further growth results in a decrease in free energy and acts as a stimulus for spontaneous growth of the nucleus.

Scale formation is an example of crystal growth and should thus be considered in this context. Since much of the research carried out in the present work was either directly or indirectly concerned with the effects of magnetic fields on crystal growth, it is appropriate to explain the mechanism via which it proceeds.

Crystal growth involves the following stages [6], [7]:

1. Nucleation - the formation of centres of crystallization.
2. Transport of reactants to the crystal-solution interface.
3. Adsorption of ions/molecules from the interface onto the crystal surface.
4. Surface diffusion to energetically favourable growth positions on the crystal surface and thereby incorporation into the crystal lattice.
5. Growth - advance of liquid-solid (or vapour-solid) interface.

The initial rate of nucleation depends on the degree of

supersaturation of the liquid phase (or the gas) with respect to the component whose growth is required, i.e. the solution should contain a greater concentration of solute than that corresponding to the equilibrium solubility at the temperature under consideration. Too little supersaturation will result in an unacceptably slow growth rate. (At the other extreme of the supersaturation range, the rate of condensation exceeds the rate at which the atoms or molecules can be incorporated into the crystal lattice, leading to the breakdown of the single-crystal interface and the onset of non-uniform cellular or dendritic growth.) The relative rates of nucleation and crystal growth determine the particle size of the precipitate formed. A high degree of dispersion is obtained when the rate of nucleation is high and the rate of crystal growth is low. For soluble materials, as used in this work, there is a tendency for the smaller particles to redissolve and recrystallize on the larger ones as the precipitate is allowed to age (Ostwald ripening). In any dispersion, a dynamic equilibrium exists whereby the rates of dissolution and deposition of the dispersed phase balance in order that the saturation solubility of the dispersed material in the dispersion medium is maintained.

The influence of the degree of supersaturation is well-illustrated by von Weimarn's results (1908) [8] for the

precipitation of barium sulphate from barium thiocyanate and manganese sulphate, respectively:



At very low concentrations, ca.  $10^{-4}$  to  $10^{-3}$  mol dm<sup>-3</sup>, the supersaturation is sufficient for extensive nucleation to occur, but crystal growth is limited by the availability of material, with the result that a sol (see Section 1.8) is formed. At moderate concentrations, ca.  $10^{-2}$  to  $10^{-1}$  mol dm<sup>-3</sup>, the extent of nucleation is not much greater, but more material is available for crystal growth and a coarse filterable precipitate is formed.

At higher concentrations, ca. 2 to 3 mol dm<sup>-3</sup>, the high viscosity of the medium retards the rate of crystal growth sufficiently to allow time for more extensive nucleation and the formation of numerous small particles. Due to their close proximity, the barium sulphate crystals will tend to link and the dispersion will take the form of a translucent, semi-solid gel (see Section 1.9).

Clearly, this shows that the particle size of a precipitate decreases with increasing concentration of the reactants.

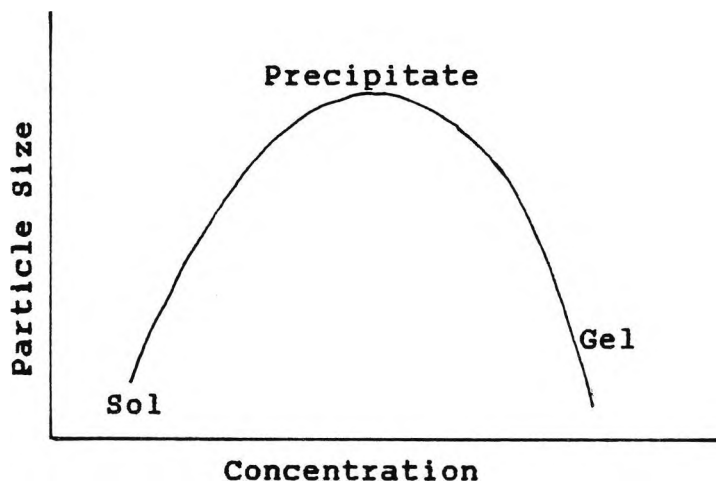


FIGURE 1.1 The dependence of particle size on reagent concentration for the precipitation of a sparingly soluble material.

It is possible to distinguish between two types of nucleation. 'Homogeneous nucleation' occurs spontaneously when all parts of the parent phase are identical and is a consequence of thermal fluctuations in atomic positions. Usually, however, it is much easier for 'heterogeneous nucleation' to occur in which nucleation takes place preferentially on impurities, seed crystals, metal surfaces and at defect centres due to the lower activation energy required. A metastable region [9] [10], i.e. a considerable barrier, associated with the necessity of large compositional fluctuations and hence long range diffusion of ions, has to be surmounted in order for phase separation to occur. Kinetically, nucleation and growth processes often take place only slowly.

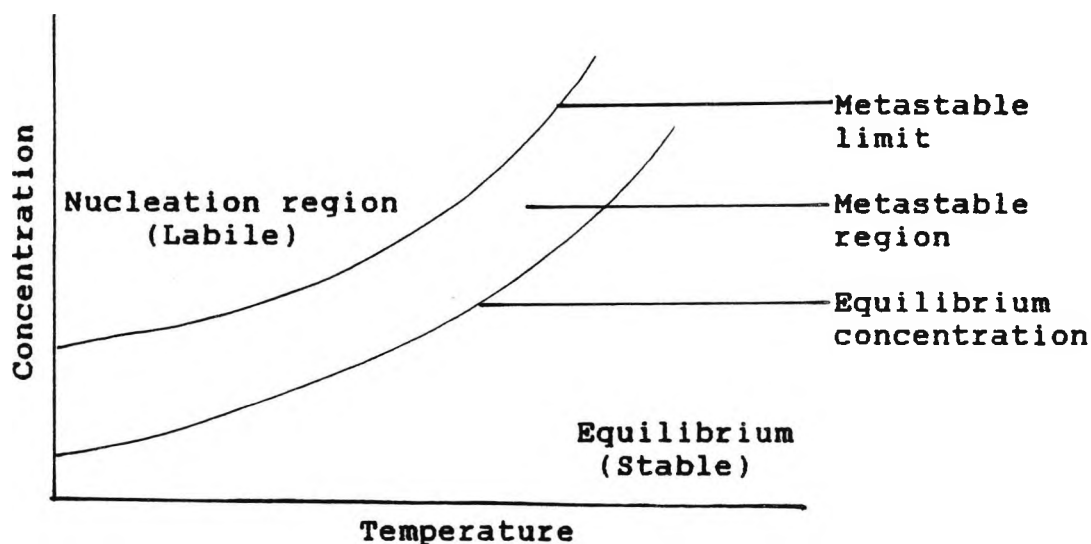


FIGURE 1.2 Representation of the stable, metastable and labile (nucleating) region of a system undergoing crystallization.

In a pure system the width of the metastable region is thermodynamically given by the free energy of formation of the nucleus (activation energy). Therefore, in most cases, the presence of dissolved impurities determine the width of the metastable region, i.e. heterogeneous nucleation is the dominant mechanism during scale formation. In these systems, nucleation occurs either on the impurities suspended in the water, or directly on the metal surfaces. When formed, the nuclei develop into visible crystals (scale). Apart from temperature and pressure changes, pH, particle volume, particle density and the density of the dispersion medium all affect crystal growth and thus, scale formation.

Moreover, it is not only the gravitational field and applied centrifugal fields [11] which affect the behaviour of particulate suspensions, but the application of electric fields or magnetic fields to charged particles. The main effect of an external field to which particles can respond, is to perturb the homogeneous distribution of particles present (singlets and any flocs).

Rates of nucleation are profoundly affected by the presence of adsorbed materials, surface-active agents and macromolecules.

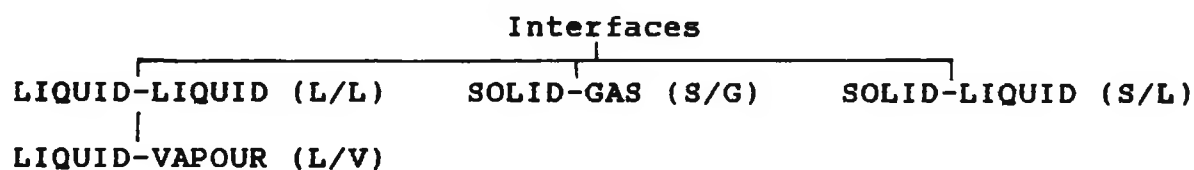
### 1.5 The Electric Double Layer

The physical properties of colloidal systems are largely governed by the fact that a significant proportion of molecules lie in or are associated with interfacial regions (the term 'surface' is commonly used when one of the phases is a gas or a vapour) as a consequence of the high surface area to volume ratio of particles in the dispersed phase.

An interface may be considered, from a thermodynamic standpoint, either as a mathematical plane or as a distinct phase having a finite thickness and may be one or several

molecules thick. Matter at the interface generally exhibits different physical and energy characteristics from that of the bulk. The study of interfaces has grown into a distinct branch of chemistry - surface chemistry.

The physical properties of an interface are determined by the states of matter concerned. The usual classification is as follows:



Since the dispersions chosen for study in this work involve solid-liquid and liquid-liquid systems, only the nature of these interfaces shall be considered.

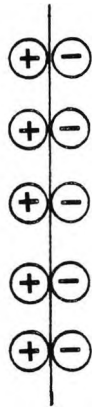
The behaviour of colloidal particles is substantially affected by the fact that they are small, highly charged species (Reuss, 1808). Most substances acquire a surface charge when brought into contact with a polar (aqueous) medium, the possible charging mechanisms being ionization, ion adsorption and ion dissolution. Ions of opposite charge, *counter-ions*, are attracted towards the surface and ions of like charge, *co-ions* are repelled from the surface. This, together with the mixing tendency of thermal motion,

engenders the formation of an electric double layer composed of a charged surface and a neutralizing excess of counter-ions over co-ions distributed in a diffuse manner in the polar medium. The theory of the electric double layer concerns this distribution of ions and hence, the magnitude of the electric potentials which develop in the locality of the charged surface.

The concept of an electric double layer was introduced by Helmholtz, in 1879, who envisaged an arrangement of charges in two parallel planes forming, in effect, a 'molecular condenser' as shown in Fig. 1.3.

However, thermal motion causes the counter-ions to be spread out in space, forming a diffuse double layer. Therefore, the model is only valid for a rather concentrated electrolyte solution. The more dilute the electrolyte the larger the distances will be where the ions forming the solution part of the double layer can escape by thermal motion.

The Helmholtz model of the electric double layer is inadequate in explaining several features of electrokinetic phenomena. The model proposes a minute double layer that approximates to molecular dimensions. Yet, hydrodynamic investigations have shown that the area of discontinuity



Layer of ions at solid surface and rigidly held layer of oppositely charged ions in solution.

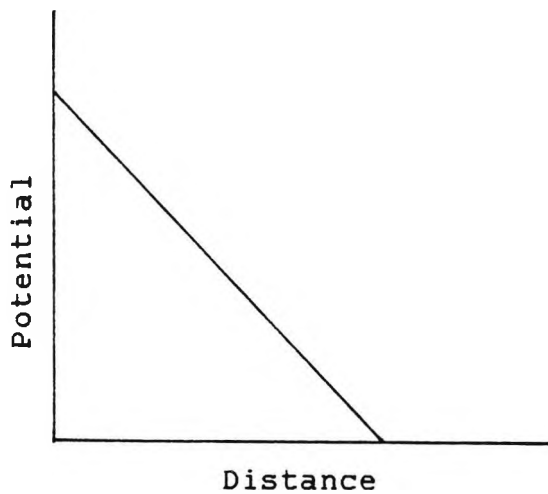


**FIGURE 1.3** The Helmholtz model of the structure of the electric double layer.

(slipping plane) is always in the liquid phase at a comparatively great distance from the interface when the solid and liquid phases move relative to each other. The thickness of the liquid layer that has 'adhered' to the solid surface under these conditions is, in any case greater than the thickness of the Helmholtz electric double layer.

Futhermore, if the Helmholtz theory were correct, the streaming potential should not be observed. The streaming potential is set up when a liquid flows through a capillary or porous plug under the influence of a pressure gradient and carries counter-ions with it, i.e. it arises from the displacement of the double layer by the flowing liquid. Electrophoresis and electroosmosis would also be impossible under these circumstances.

The Gouy-Chapman theory (1910-1913) serves as a refinement of the Helmholtz model. The theory regards the electric double layer as consisting of two regions (illustrated in Fig. 1.5): an inner region which may include adsorbed ions, and a diffuse region in which ions are distributed in a manner influenced by electric forces and random thermal motion.

The action of the electric field prevails in the immediate vicinity of the interface. As the distance from the

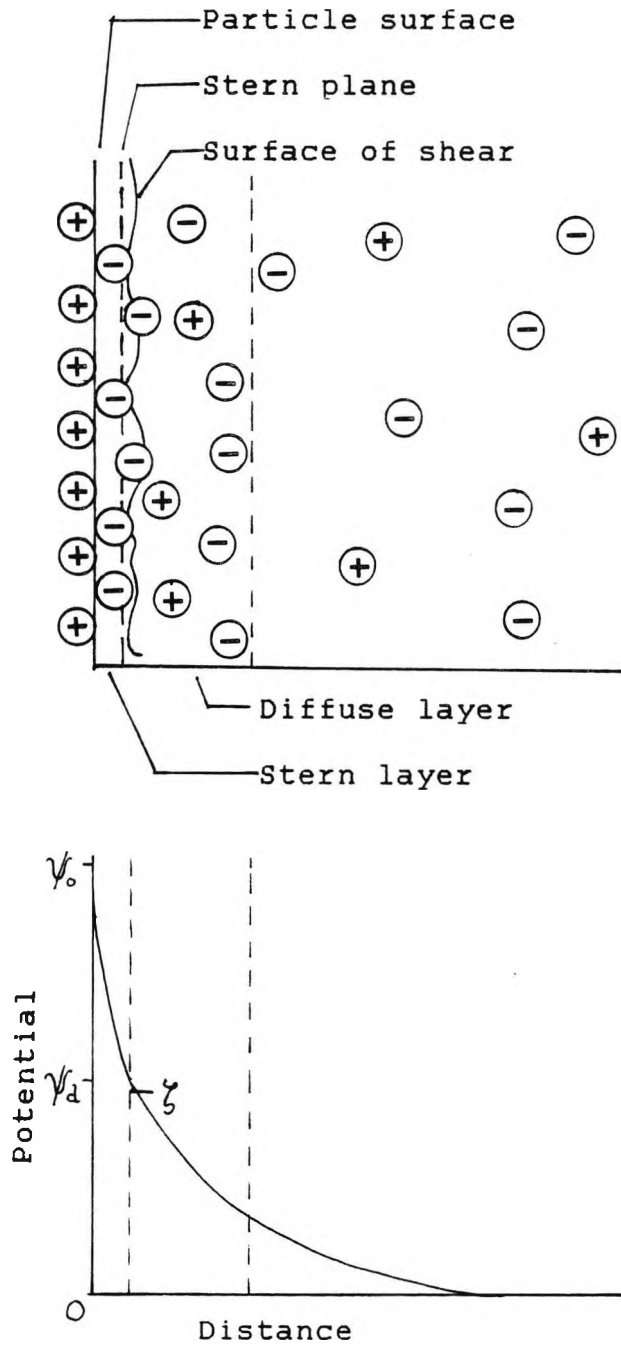


**FIGURE 1.4** Schematic representation of the structure of the electric double layer according to Stern's theory.

interface increases, the intensity of the field gradually decreases and counter-ions of the double layer become more dispersed owing to thermal motion. Hence, the concentration of counter-ions diminishes and becomes equal to that of the ions in the bulk of the liquid. This explains how the equilibrium diffuse layer of counter-ions, connected with the solid, originates. A dynamic equilibrium exists in the layer. Conversely, co-ions are repelled from the solid phase (by electrostatic forces) and penetrate deeply into solution.

The potential drop is not linear, but an exponential function of distance [12], i.e. the number of counter-ions at the charged surface of a solid phase decreases with distance according to the Boltzmann distribution law; the number of co-ions increases according to the same law. The potential has a range of the order of thickness of the electric double layer.

Thus, the Gouy-Chapman model accounts for the variation in electric potential with distance from the interface. Numerical treatment of this model yields information for surfaces of spherical and cylindrical shape.

The shortcomings of the Gouy-Chapman diffuse double layer theory are as follows:-

- (i) The dielectric constant is assumed to be independent of distance from the surface, yet it is known to vary with the electric field strength for a dipolar liquid such as water. The errors entailed by this assumption, though, are thought to negligible.
  
- (ii) The ions in the diffuse part of the double layer are assumed to be point charges. This assumption is unsatisfactory in two respects. Firstly, the number of point ions that can be concentrated into unit volume is infinite, while for actual ions this number is strictly limited by their volume. Therefore, the theory predicts absurdly high local ion concentrations. Secondly, point ions may approach infinitely close to the surface, but for real ions, the distance of closest approach to the surface is determined by the hydrated ionic radii. (This correction is incorporated in the Stern theory described below.)
  
- (iii) The surface is assumed to be uniformly charged rather than, as it actually does, contain discrete ions or electrons. The diffuse layer, in reality, consists of overlapping ionic atmospheres of individual surface charges, and the potential in the plane parallel to the surface fluctuates from place to place depending on the degree of overlap of these atmospheres. Thus,

the Gouy-Chapman potentials are average potentials, but the errors incurred are likely to be minor.

These difficulties are overcome to a considerable extent by the Stern model (1924) in which the double layer is divided into two parts separated by a plane - the Stern plane - located at about a hydrated ion's radius from the surface (see Fig. 1.4). The model also considers the possibility of specific ion adsorption.

Specifically adsorbed ions are those which are attached (albeit temporarily) to the surface by electrostatic and/or van der Waals forces strongly enough to overcome thermal agitation. They may be dehydrated, at least in the direction of the surface. The centres of any specifically adsorbed ions are located in the Stern layer, i.e. between the surface and the Stern plane. Ions with centres located beyond the Stern plane form the diffuse part of the double layer, outlined by the Gouy-Chapman treatment.

The potential changes from  $\psi_0$  (the surface or wall potential) to  $\psi_s$  (the Stern potential) in the Stern layer, and decays from  $\psi_s$  to zero in the diffuse double layer.

In the absence of specific ion adsorption, the charge densities at the surface and at the Stern plane are equal.

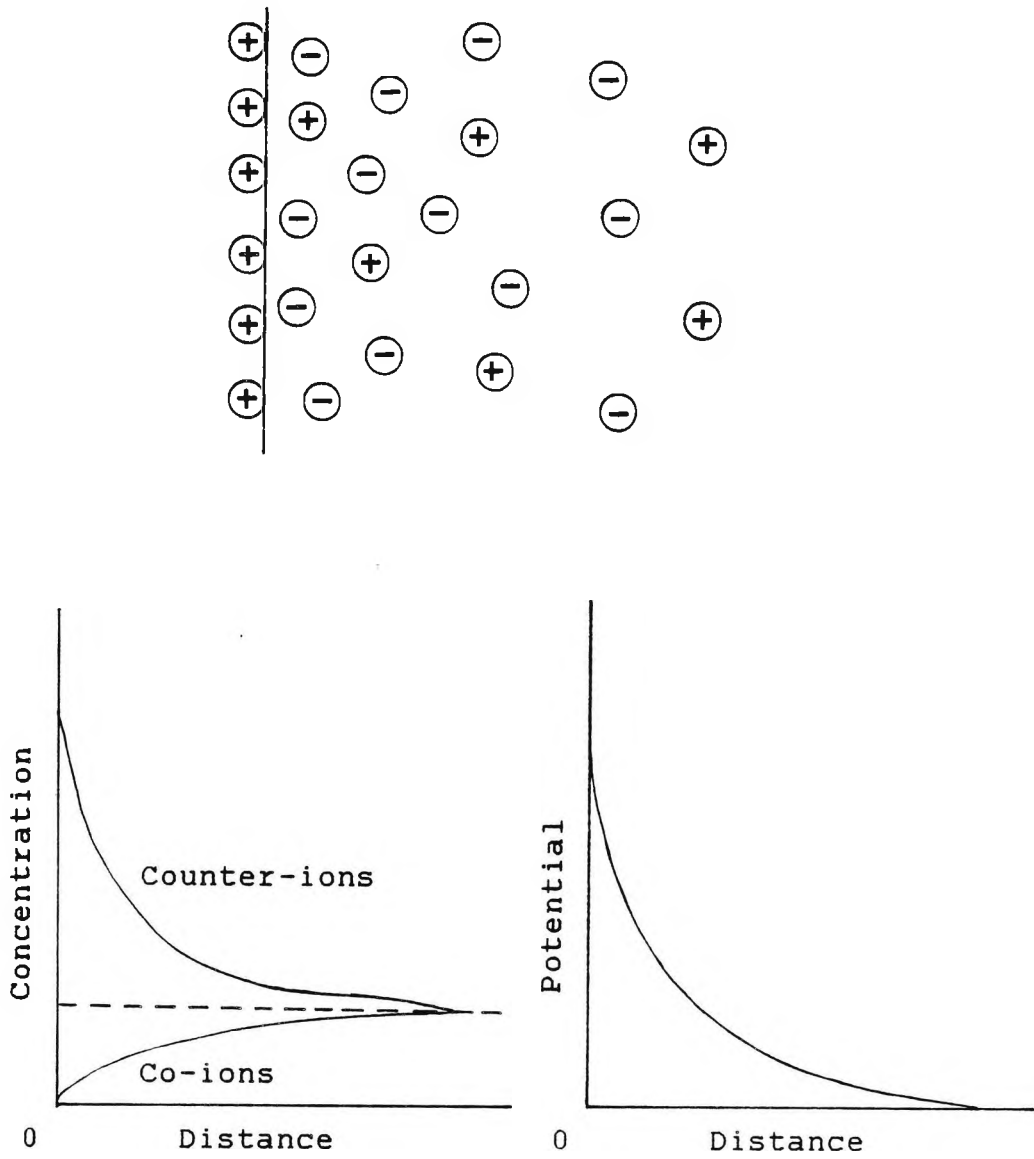


**FIGURE 1.5** Schematic representation of a diffuse electric double layer.

When specific adsorption occurs, counter-ion adsorption usually predominates over co-ion adsorption and a typical double layer situation prevails.

More recent developments [13] have taken into account the discrete nature of charges. When two charged surfaces and their associated double layers are brought together, the double layers overlap and an excess of ions of one type is built up in the liquid phase between the particles. The surfaces repel each other with a force dependent on the electrolyte concentration and the electrical charge or potential of the particle surface.

#### 1.6 Stability of Colloidal Systems

Generally in dispersions of fine particles in a liquid, e.g. suspensions and emulsions, frequent encounters between particles occur due to Brownian motion, gravity (creaming, sedimentation) and convection. Whether such collisions result in permanent contact or whether the particles rebound and remain free is determined by the forces between them. A dispersion is stable in the colloid-chemical sense when its particles remain permanently free.

In a stable dispersion, where the particles are similarly

charged, electrostatic repulsive forces predominate, preventing particles from adhering since these forces are of longer range than the van der Waals. The magnitude of repulsion is gauged roughly by the zeta potential, i.e. the potential at the dividing line between the fixed and mobile portions of the double layer. If the zeta potential is sufficiently high, the charges constitute a potential barrier to coagulation and the colloidal system is stable. The zeta potential is expressed as

$$\zeta = \frac{4\pi ed}{D}$$

where  $\zeta$  is the potential drop across the double layer;  $e$ , the electric charge of the double layer;  $d$ , the thickness and,  $D$ , the dielectric constant.

The zeta potential is obtained from electrokinetic measurements, of which electrophoresis, electro-osmosis, streaming potentials and streaming currents are the most familiar [14].

Particle-solvent affinity also promotes stability mainly by mechanical means, which can be considered in terms of the positive desolvation free energy change accompanying aggregation.

Potential  
Energy

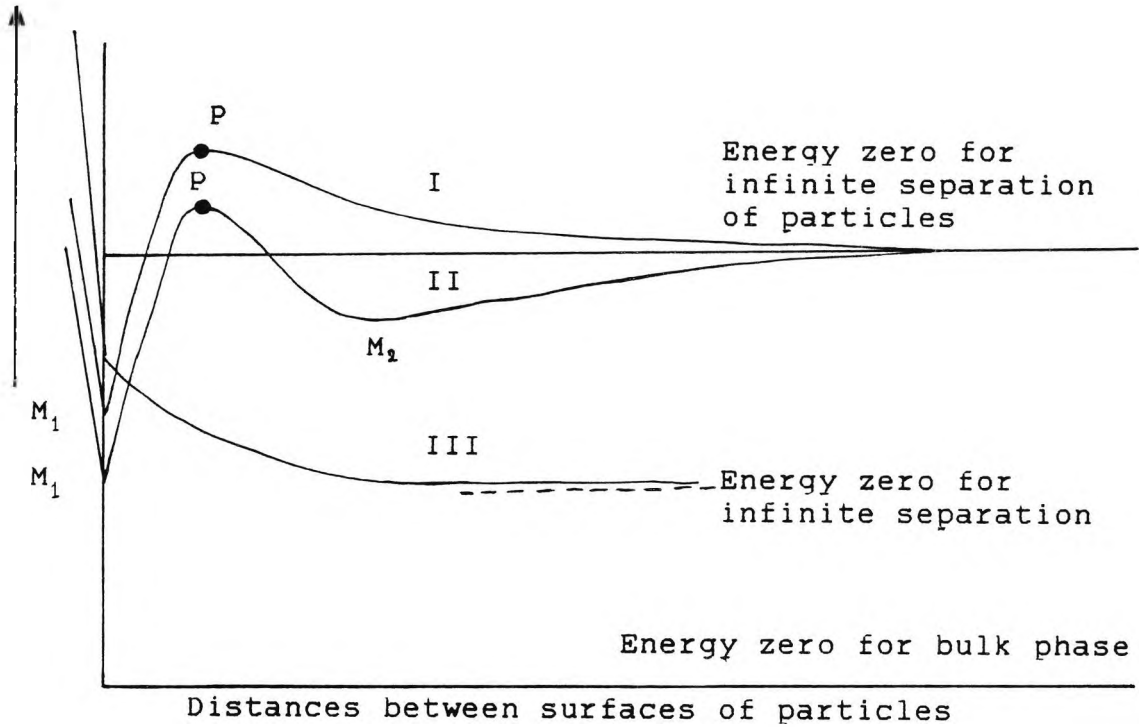


**FIGURE 1.6** Mutual potential energy of two colloidal particles as a function of distance of separation between their surfaces:

- I curve with primary maximum, P, and primary minimum, M<sub>1</sub>
- II curve with primary maximum, P, primary minimum, M<sub>1</sub>, and secondary minimum, M<sub>2</sub>
- III curve for spontaneous (unactivated) dispersion.

The charge on colloidal particles can be neutralized by the addition of an electrolyte to the suspension. Ions having the opposite charge to that on a particle are attracted towards the particle; on close approach, these ions lower the charge on the particle (lower than the zeta potential), and reduce the repulsion between particles, that is, the added electrolyte causes a compression of the diffuse parts of the double layer around the particle and may, in addition, exert a specific effect through ion adsorption into the Stern layer. The local ionic concentration is proportional to the distance from the surface. Coagulation ensues when the range of double layer repulsive interaction is sufficiently reduced, particles have enough kinetic energy to surmount the barrier, and are permitted to approach closely for van der Waals forces to predominate. The *critical coagulation concentration* is reached when the forces between particles are attractive at all distances. Under certain conditions, the potential energy curve may exhibit a secondary minimum, as shown in Fig. 1.6, giving rise to a loose, easily reversible flocculation.

The classical DLVO theory, proposed independently by Derjaguin and Landau (USSR) [15], and Verwey and Overbeek (Netherlands) [16], in the 1940s, concerns the stability of lyophobic sols, particularly in relation to added electrolyte, in terms of the energy changes which occur when

particles approach one another. The repulsive electrostatic forces are superimposed on the attractive van der Waals forces to give a series of potential energy curves as a function of interparticle distance.

Three types of intermolecular attraction are recognized: that arising from molecules containing permanent dipoles; dipolar molecules inducing dipoles in other molecules; and that between non-polar molecules or particles resulting from the interaction between the fluctuating polarization of regions of one body induced by fluctuations in the electron density distribution of another. The latter, the London-van der Waals dispersion force, varies inversely with the seventh power of intermolecular distance, although for larger colloidal particles the distance approximates to the inverse square. These forces, incidently, enable the liquefaction of monoatomic gases such as hydrogen and helium.

When two similarly charged colloidal particles, with their associated double layers approach each other, interaction gradually develops. The range of this repulsion, approximately  $2\psi$  (the 'thickness' of the double layer is characterized by  $\psi$ ) is inversely proportional to the square root of the concentration of the electrolyte solution, the double layer contracting with increasing concentration;

conversely, it is augmented as the bulk electrolyte concentration decreases.

The repulsion can be interpreted in different ways:

(i) The two overlapping electron clouds, of the same sign, repel one another (Born repulsion) in a manner analogous to the electron clouds enveloping atoms and molecules.

(ii) The double layers may be envisaged as screening the charges on the colloidal particles from one another. From a distance, charged particles with their neutralizing double layers may appear to be uncharged entities, but when in close proximity, the screening is incomplete and the particles recognize each other as partially charged co-ions, consequently repelling each other.

Thus, at the point of aggregation,

$$\psi = Be^{-\kappa D} - AD^{-2}$$

repulsive	attractive
force	force
(+ve)	(-ve)

where  $\psi$  is the net force; A, the Hamaker constant; B, a

constant;  $K$ , a constant; and,  $D$ , the distance.

As  $D \longrightarrow 0$ , repulsive force  $\longrightarrow \infty$

and attractive force  $\longrightarrow -\infty$ , i.e. aggregation.

As  $D \longrightarrow \infty$ , repulsive and attractive forces  $\longrightarrow 0$

Colloid stability is then interpreted in terms of the nature of the interaction energy-distance curve, as illustrated in Fig. 1.7.

Coagulation rates are generally measured under *perikinetic* (non-agitated) conditions, where particle-particle encounters are solely the result of Brownian motion. Particle aggregation can sometimes be brought about by *orthokinetic* (agitated) conditions. In the case of large particles such as in emulsions, orthokinetic aggregation can occur at  $10^4$  times the perikinetic rate, but with smaller particles, agitation has relatively little effect on their rate of aggregation.

Therefore, the mechanism by which particles repel one another depends upon the charge on the particle (and hence on the potential at the surface) and on the electrolyte concentration, both of which affect the range of the repulsive force. The Schultz-Hardy rule [17] maintains

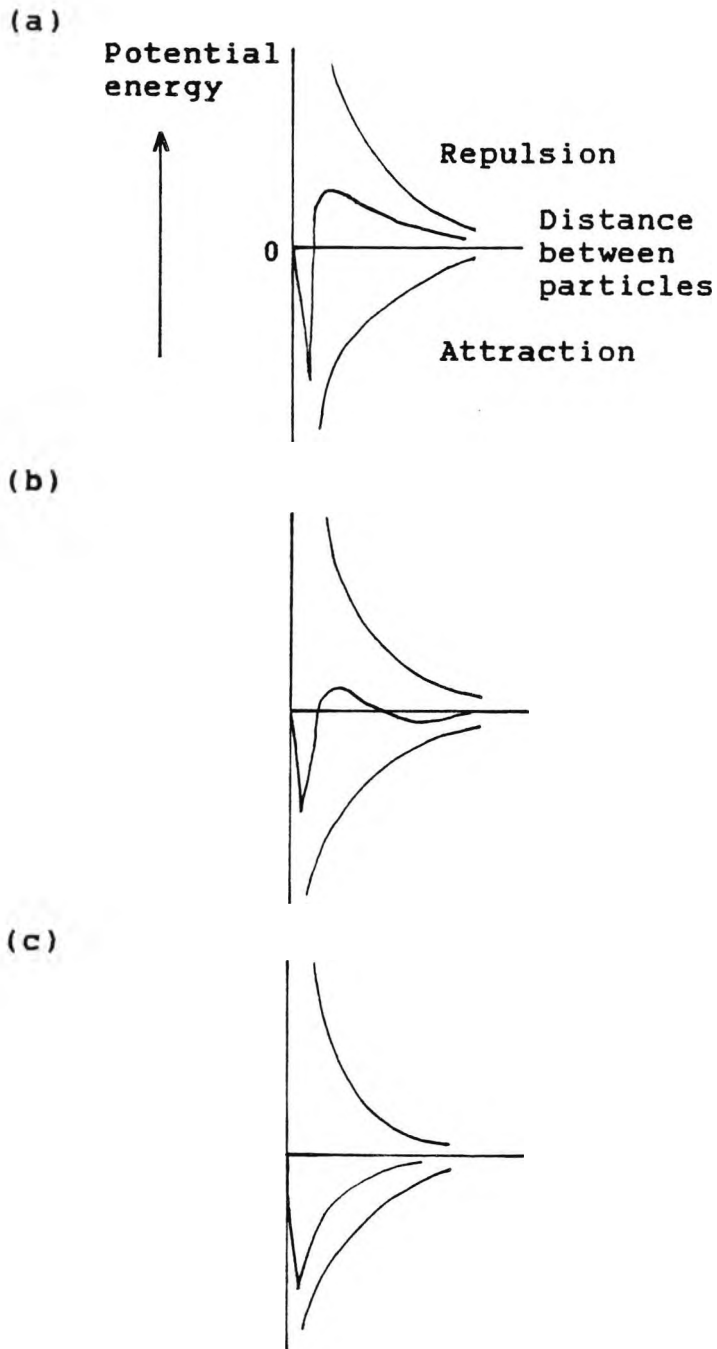


FIGURE 1.7 Resultant potential energy curves obtained by summation of attraction and repulsion contributions for (a) low (stable: large barrier to coagulation, (b) medium and (c) high electrolyte concentrations (unstable: as concentration of counter-ions increases, curve collapses back), i.e. forces of repulsion too weak, coagulation ensues).

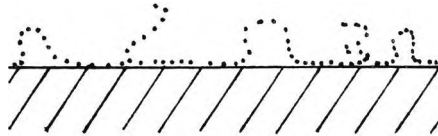
that highly charged ions are much more effective in coagulating colloids than those of lower charge.

### Steric Stabilization

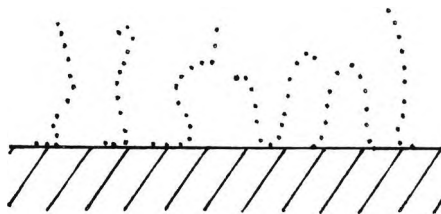
Steric stabilization concerns the 'protection' of colloidal dispersions by adsorbed macromolecules, usually block copolymers [e.g. poly (ethylene oxide) surfactants]. The lyophobic (see Section 1.8) part (the 'anchor' group) adheres strongly to the particle surface, whilst the lyophilic chain trails freely in the dispersion medium. This mechanism of stabilization follows from Faraday's observation that gelatin protects a gold sol against flocculation. Today, the phenomenon is exploited in many paint formulations.

The mechanism is dependent on the nature of the polymers, their adsorption characteristics, and the solutions. Polymers can adopt various configurations, many of which are eliminated in the presence of an adsorbing surface. At low temperatures, if the adsorption forces are large, and the solvent is poor for the lyophilic moieties of the adsorbed polymer, a high proportion of polymer segments lie on the surface (Fig. 1.8a), interpenetration of polymer chains is favoured and attraction results; interpenetration progresses to the point where it is impeded by elastic

(a)



(b)



(c)

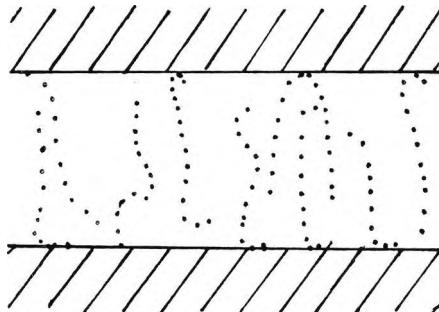


**FIGURE 1.8** Typical conformation of polymer molecules:

- (a) adsorbed with high adsorption energy per segment, low temperature, poor solvent,
- (b) adsorbed with low adsorption energy per segment, high temperature, good solvent,
- (c) adsorption on two surfaces approaching one another, showing how mutual interference of chains reduces the number of possible configurations.

repulsion. Conversely, at higher temperatures, with weaker adsorption from a better solvent, a greater proportion of polymer chains extend out from the surface (Fig. 1.8b), interpenetration is not favoured and repulsion ensues.

The mutual interference of chains further reduces the number of accessible configurations, (Fig. 1.8c). Since the number of arrangements available to a system without changing its energy is directly related to its entropy, this implies a reduction in entropy, and hence an increase in free energy.

If charged colloidal dispersions are stabilized by a polymer (especially a polyelectrolyte) then both electrostatic and steric effects are involved. In other circumstances, as in the case of dilute polymer solutions, remote segments of polymer chains may be adsorbed on separate particles, causing them to be drawn together, leading to *bridging flocculation*, important in water treatment.

### 1.7 Solid-liquid and Liquid-liquid Interfaces

The following theoretical treatment attempts to provide a more detailed description of the characteristics of solid-liquid and liquid-liquid interfaces as exemplified by sols, gels, emulsions and association colloids.

### 1.8 Sols

Sols generally include colloidal dispersions of solids in liquids and are classified according to the affinity of the particles for the medium, as *lyophobic* (liquid-hating) or *lyophilic* (liquid-loving). If the medium is aqueous, the terms *hydrophobic* and *hydrophilic* are used.

Solutions of macromolecules and association colloids are of the lyophilic type and form spontaneously when brought into contact. They are true solutions and are thermodynamically stable, whereas lyophobic sols, e.g. dispersions of powdered silica or alumina in water, do not form spontaneously and hence, in principle, are thermodynamically unstable.

Lyophilic surfaces can be made lyophobic and *vice versa*, e.g. clean glass surfaces which are hydrophilic can be made hydrophobic by a coating of wax; conversely the droplets in a hydrocarbon oil-in-water emulsion, which are hydrophobic can be made hydrophilic by the addition of protein to the emulsion, the protein molecules being adsorbed onto the droplet surfaces.

More recently, non-aqueous dispersions of magnetic and non-magnetic powders have attracted considerable attention as a result of their applications in the electronic industry.

Such powders can be used for recording tapes and discs, magnets, electrodes, and so on.

The usage of the terms 'lyophilic' and 'lyophobic' are somewhat illogical. 'Lyophobic' traditionally describes dispersions produced by mechanical or chemical action; however, in such cases (e.g. dispersions of powdered alumina or silica in water), a high affinity between the particles and the dispersion medium often exist, i.e. the particles are really lyophilic. Similarly, if the term 'lyophobic' is taken to imply no affinity between the dispersed phase and dispersion medium (an unreal situation), then the particles would not be wetted, or solvated, and no dispersion could, in fact, be formed. 'Lyophilic' describes soluble macromolecular material, yet, lyophobic regions are often present, e.g. proteins contain both hydrophobic (hydrocarbon groups) and hydrophilic (peptide linkages, and amino and carboxyl substituents) segments.

### 1.9 Gels

Gels are essentially dispersions in which the attractive interactions between elements of the dispersed phase are so strong that the system develops a rigid network structure, and, under small stresses behaves elastically. The

dispersed phase may envelop the entire dispersion medium forming, effectively, a pseudo-solid. Gels often exhibit thixotropy: intermolecular attractions and entanglements are overcome and the extent of solvent immobilization is reduced on shearing, while Brownian motion restores the system to its original condition when left to stand.

The dispersed phase may consist of solid particles (e.g. clay platelets), macromolecules (e.g. gelatine), or surfactant molecules (e.g. soaps). Thus, concentrated suspensions of clay or latex particles form gels. Other examples include densely filled lubricating greases (inorganic gel greases) and gelled paints. Domestic examples encompass those formed by hydrophilic polymers (mostly of biological origin), which swell spontaneously in contact with water, but because of the strong bonds between individual molecules, retain a degree of rigidity. Rubber swollen by aromatic hydrocarbons is yet another example.

#### Forces Leading to Gel Formation

Electrostatic forces, van der Waals forces, or chemical bonding may result in gel formation. Interestingly, in some charge-stabilized dispersions above a critical concentration, addition of electrolyte engenders gelation rather than distinct flocs. In this sense, gelation may be

regarded as the formation of an extended, continuous floc occupying the whole system.

Various types of gel abound: lamellar gels, e.g. those formed by soaps which are essentially micellar systems, and at particular concentrations extend and interlock to form a continuous network; macromolecular aqueous gels in which the structure is controlled primarily by hydrogen bonding, although if polyelectrolytes (macromolecular compounds containing many ionizable groups within the same molecule) are concerned, ionic forces also contribute, e.g. often block copolymers containing polysaccharide and/or protein chains.

Gel formation is markedly dependent on the pH and electrolyte concentration, both of which affect the attractive forces leading to rigidity, and on temperature which affects the thermal motion of the polymer chains. This explains why a gelatine solution is liquid-like at high temperatures and forms a jelly when cooled. Similarly, gelling may be induced by the addition of an electrolyte to a polyelectrolyte solution.

Gels are sometimes classified as either elastic or rigid. Gelatin is an example of the former type, silica gel of the latter, but this division is not strict, as even silica has

a certain amount of elasticity. Gelatin gel may revert to the sol on heating and is thus a reversible gel.

Sol-gel processes are important in the preparation of nuclear fuel in the form of spherical particles of uniform size.

Rigid gels, e.g. vulcanized rubber, are formed by covalent bonding of polymeric systems, in the presence of the appropriate crosslinking agent. Their elasticity is usually maintained up to high stresses.

Xerogels, of which silica gel is a typical example, are porous solids, consisting of a network structure, that have been dried. Silica will not liquify to the sol on any simple treatment and is therefore considered to be an irreversible gel.

#### Swelling Properties of Gels

Gel formation is a spontaneous reaction. Since the macromolecules contain hydrophilic substituents, water can diffuse into the gel, but soluble units cannot diffuse out. Thus, swelling may be regarded as an osmotic phenomenon, the network behaving like a semi-permeable membrane. Imbibition occurs spontaneously causing a stretching of the network,

which in turn, imposes a pressure on the imbibed water. If the cohesion of the network is strong enough, swelling will cease when the internal pressure is equal to the osmotic pressure of the 'internal solution'. Significant water penetration of a weak network will lead to disintegration under the internal pressure and the polymer will go into solution. However, aggregates of the polymer may persist and influence the rheological properties of the solution.

A similar situation is observed in the swelling of rubber. The isoprene units, when not a constituent of the rubber molecule, are soluble in aromatic hydrocarbons, but when incorporated in the polymer network, they are constrained to remain as part of the gel.

Swelling pressures can reach high values, enabling the breakage of rocks: a dry wooden wedge can be driven into a fissure and then the wood wet. Yet severe problems may arise in civil engineering, since the swelling pressures in clays developed under certain conditions are sufficient to lift a moderate-sized building.

The network structure initially formed is not always the most stable (or compact), a situation offset by the relatively slow diffusion of portions of the polymer chains. This exerts an increased osmotic pressure on the imbibed

liquid which then exudes from the gel. The slow expulsion of imbibed liquid is called *syneresis*.

### 1.10 Emulsions

An emulsion is a dispersed system in which both phases are liquids, usually one being water or an aqueous solution, and the other an oil or another water-immiscible liquid. The globules of a dispersed fluid are generally between  $0.1\mu\text{m}$  and  $10\mu\text{m}$  in diameter, although they can be well above the accepted colloidal size range, thus tending to be larger than the particles in sols. If the oil is the dispersed phase, the emulsion is termed an *oil-in-water* (O/W) emulsion; if the aqueous medium is the dispersed phase, the emulsion is termed a *water-in-oil* (W/O) emulsion. In some special cases, a *bicontinuous* emulsion may be formed, in which one phase forms a continuous network in the other.

Emulsions are of considerable industrial importance, for example, in the manufacture of foodstuffs (especially dairy produce), pharmaceutical preparations, cosmetics, horticultural and insecticide sprays, paints and bituminous products, etc.

The formation of an O/W or a W/O emulsion is dependent on

several factors. Generally, the phase present in the lower quantity is the dispersed phase; if the phase volumes are approximately equal, other factors will determine the type of emulsion formed.

The formation of an emulsion involves an increase in the interfacial area between the two phases and is accompanied by an increase in free energy, i.e. its formation is facilitated by a lower interfacial tension (less work required).

The visual appearance of an emulsion reflects the influence of droplet size on light scattering, and varies from milky-white-opaque, with large droplets, through blue-white, then grey-translucent, to transparent for microemulsion (see Section 1.11) droplets.

There are a number of methods by which an emulsion type may be identified:

- (i) An O/W emulsion generally has a creamy consistency, whereas a W/O emulsion feels greasy.
- (ii) The emulsion mixes readily with a liquid which is miscible with its dispersion medium. For example, on the addition of water to an O/W emulsion, the emulsion is diluted; the addition of oil manifests

itself as a separate layer. That milk can be diluted with water indicates that it is an O/W emulsion, whilst mayonnaise can be blended with more oil.

- (iii) The emulsion is readily coloured by dyes which are soluble in the dispersion medium.
- (iv) O/W emulsions usually have a much higher electrical conductivity than W/O emulsions.

Emulsification is facilitated and emulsion stability often promoted by the addition of *emulsifying agents* or *emulsifiers* which adsorb at the interface preventing coagulation and coalescence. Thus, emulsifying agents for W/O or O/W dispersions are surface-active materials (or surfactants) consisting of molecules with both polar and non-polar groups (amphiphilic) with an appropriate HLB (hydrophile-lipophile balance), so that adsorption at the interface involves the orientation of adsorbed molecules with the hydrophilic moiety lying in the aqueous phase and the lyophilic portion in the oil phase.

Emulsions, like foams, can also be stabilized by finely divided solids, provided the properties of the solid/liquid/liquid interface are appropriately adjusted.

The following factors favour emulsion stability:

- (i) Low interfacial tension;
- (ii) A mechanically strong and elastic interfacial film - the stability of emulsions due to proteins arises from the mechanical protection afforded by the adsorbed films enveloping the droplets rather from a reduction of interfacial tension;
- (iii) Electric double layer repulsions - particularly important for O/W emulsions;
- (iv) Relatively small volume of dispersed phase;
- (v) Narrow droplet size distribution - larger droplets are less unstable than smaller droplets owing to their smaller area-to-volume ratio, thus tending to grow at the expense of smaller droplets. If this process continues, the emulsion will break. Emulsions with a fairly uniform droplet size will be less prone to this affect;
- (vi) High viscosity - retards rates of creaming, coalescence, etc.

### De-emulsification

The breaking of an emulsion, or de-emulsification, is of practical importance, for example, in creaming, breaking and inversion of milk to obtain butter, and the breaking of W/O oilfield emulsions. Agents for this purpose have to be capable of displacing the stabilizing surfactant, leaving a non-stabilized interface. The precise nature of those in use has not been revealed, but many of them are polymeric materials. Several other techniques are used commercially to accelerate de-emulsification including centrifugal separation, freezing, distillation and filtration. Emulsions can also be broken by the application of intense electric fields, the principal factors involved being electrophoresis in the case of O/W emulsions and droplet deformation in the case of W/O emulsions. It is interesting to speculate on the effect a magnetic field might have in this context.

#### 1.11 Microemulsions

Microemulsions occupy a place between coarse emulsions and micelles, their droplet diameters ranging from 0.01-0.1 $\mu$ m. They are effectively monodispersed and unlike coarse emulsions are thermodynamically stable.

Microemulsions were first discovered empirically by Schulman, who found that the addition of a fourth component, a *co-surfactant* (often an alcohol), to an emulsion consisting of oil, water and a surfactant led to the formation of a clear, apparently homogeneous phase. Microemulsions have been subject to intense study in recent years, particularly with regard to enhanced oil recovery from porous rock.

#### 1.12 Association Colloids

In contrast to the colloidal dispersions described hitherto, *association colloids* constitute a class in which nucleation is absent and growth spontaneous. The finite size of such structures often tends towards the lower end of the colloidal size range, constrained by geometric and energy factors. Association colloids are composed of highly surface-active substances (or surfactants), a common feature amongst which is that they are all amphiphilic, i.e. the molecules contain both polar and non-polar regions. These materials encompass ionic (including anionic, cationic and ampholytic) and non-ionic compounds.

### Physico-Chemical Properties of Surfactant Solutions

The physical properties, such as turbidity, electrical conductance, surface tension, osmotic pressure, solubilization and n.m.r. spectral features, of dilute solutions of certain surfactants, when plotted as a function of concentration, exhibit abrupt changes at a distinct point.

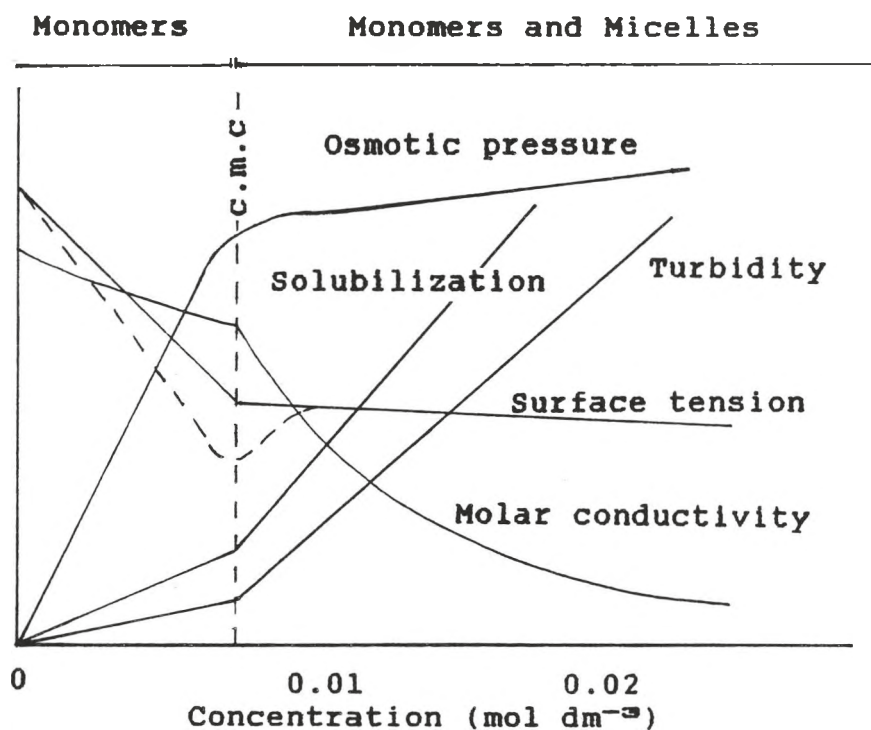


FIGURE 1.9 Variation of the properties of a solution of a surfactant with concentration.

McBain [18] suggested that such seemingly anomalous behaviour is consistent with the formation of organized

aggregates of molecules, or *micelles*, in which the hydrophobic hydrocarbon chains are orientated towards the interior of the micelle, leaving the hydrophilic groups in contact with the aqueous medium. The concentration above which micellization becomes appreciable is termed the *critical micelle concentration* (c.m.c.). Micellization is therefore an alternative mechanism to adsorption by which the interfacial energy might decrease. Van der Waals forces are involved in aggregation whilst counter-ion binding stabilizes structures. For ionic surfactants, monomer activity decreases with increasing surfactant concentration above the c.m.c.

However, association colloids embrace not only micelles, but more complex forms, such as cell membranes.

#### Variation of C.M.C. with Chemical Structure

- (i) Increasing the hydrocarbon chain length lowers the c.m.c. In aqueous media, the c.m.c. of ionic surfactants may be approximately halved by the addition of each  $-CH_2$  group; for non-ionic surfactants, the c.m.c. may be reduced by a factor of as much as ten for each additional  $-CH_2$  group. Above the  $C_{12}$  member of an homologous series, the c.m.c. tends to remain approximately constant,

probably as a result of coiling of the long hydrocarbon chains in the water phase [19].

- (ii) Hydrocarbon chain structure - branching and double bonds increase the c.m.c. For sodium alkyl sulphates, the c.m.c. increases as the sulphate group is moved the terminal position.
  
- (iii) Polar head group - the c.m.c. for a given alkyl chain length is much lower for non-ionic than ionic surfactants; zwitterions fall in between. For non-ionic surfactants, the c.m.c. is affected by the size and nature of the hydrophilic group; for ionic surfactants, the type of head group affects the c.m.c., and on addition of more ionic groups, the c.m.c. is reduced by the screening action of the added ions, i.e. less repulsion between charged groups at the periphery of micelles.
  
- (iv) Valency of counter-ions, e.g. for dodecylsulphates an inverse relationship exists between the oxidation state of the counter-ions and the c.m.c.

#### Other Factors Affecting C.M.C

- (i) In general, micellization is an exothermic process,

therefore at elevated temperatures the c.m.c. increases, but SDS is exceptional: the curve exhibits a minimum between 20-25°C, indicating that micellization is entirely entropy related here.

- (ii) Krafft phenomenon - above a certain temperature, the *Krafft point*, solubilities rapidly increase.
- (iii) Charge buried in micelle - the smaller the charge, the higher the c.m.c. (i.e. not buried very deeply resulting in greater electrostatic repulsion between charged head groups).

#### Micelle Size and Shape

The following factors favour an increase in micelle size: an increase in alkyl chain length, an increase in surfactant concentration and the addition of electrolyte. An increase in temperature engenders a decrease in size.

Evidence (from X-ray diffraction data, viscosity measurements, n.m.r., etc.) indicates that micelles, when initially formed, usually contain between 50-100 molecules and are roughly spherical in shape, although at higher concentrations and under the appropriate conditions, they may adopt disc-like [20], cylindrical, ellipsoid, laminar or

vesicular shapes.

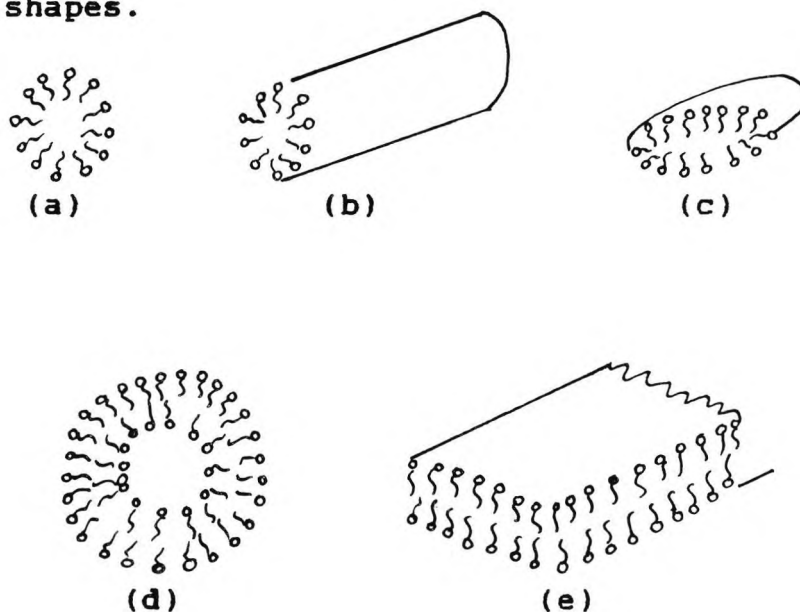


FIGURE 1.10 Some types of micellar structure.  
(a) spherical, (b) cylindrical, (c) disc-like,  
(d) spherical vesicle, (e) lamella.  
The head groups are shown as circles.

### Structure of Micelles

Micelles behave as colloidal units, with the distinction that there is a dynamic interchange between the monomer units of the micelles and those in solution. This also confers upon micelles the important property of solubilizing many otherwise insoluble materials. For amphipathic materials, there is rapid counter-ion exchange between the micellar surface and bulk solution.

### Solubilization

The ability of micelles to solubilize large amounts of non-polar substances by incorporating them into their interior can only be explained if the core is fluid-like; for example, the dye xylenol orange dissolves only sparingly in pure water, but gives a deep red solution with sodium dodecyl sulphate (SDS) present above its c.m.c. Even for high alkyl chain lengths, the melting points of alkanes lie below ambient temperature, thus providing further evidence of a liquid-like interior.

Harkins *et al* point out [21] [22] that the balance of electrostatic and hydrophobic interactions can be such as to cause the locus of solubilization to be anywhere in the micelle from close to the surface to the inner core. Moreover, there appears to be some degree of mobility within the micelle ('translational diffusion'). Solubilization generally increases with increasing hydrocarbon chain length and micelle size. For aromatic compounds, it is more difficult to predict the solubilization site. In the case of benzene, its alkyl derivatives and naphthalene the location is predominantly in the interfacial region at low solubilize concentrations.

The laminar phase occurs as the solubilize saturation

limit is exceeded and is probably a consequence of induced visco-elasticity.

Solubilization is of practical importance in the formulation of pharmaceutical products containing water-insoluble ingredients [23], detergency, emulsion polymerization and micellar catalysts of organic reactions [24].

### Hydration

Aniansson recently examined the dynamic protrusion of methylene groups from the hydrocarbon core of micelles (both spherical and rod) and found that every third methylene group protrudes beyond the general boundary of the micelle. This explains the partial exit of monomers from micelles and also bears significance to water penetration into micelles. Additional evidence suggests that water does not penetrate further than the beta-carbon.

Micellization permits strong interaction between water molecules (hydrogen bonding) which would be prevented if the surfactant was in solution in the monomeric form. This is often referred to as the *hydrophobic effect*.

### 1.13 Objectives

Two different aspects of dispersed materials are studied, viz. (i) the effects of magnetic fields on dispersed particles and charged species in fluids (Chapters Two and Three) and (ii) the use of dispersion to increase the reactivity and stability of reactants (Chapter Four).

REFERENCES

1. Graham, T., *Philos. Trans. R. Soc. London*, 1861, 151, 183.
2. Everett, D.H., 'Colloids in the World Around Us', *Chem. Br.*, 1981, 17, 377.
3. Science Research Council, 'Colloid Science', SRC, U.K., 1972.
4. Shaw, D.J., 'Introduction to Colloid and Surface Chemistry', 3rd Edn., Butterworths, London, 1980.
5. Parfitt, G.D., 'Dispersion of Powders in Liquids', Elsevier, London, 1969.
6. Goodman, G.H.L., 'Crystal Growth - Theory and Techniques', Vol.I, Plenum, London, 1974.
7. Vere, A.W., 'Crystal Growth - Principles and Progress', Plenum, New York, 1987.
8. Laitinen, H.A. and Harris, W.E., 'Chemical Analysis', 2nd Edn., McGraw-Hill, New York, 1975.
9. West, A.R., 'Solid State Chemistry and its Applications', Wiley and Sons Ltd., U.K., 1984.
10. Ellingsen, F. and Fjeldsend, O., 'A Review of Scale Formation and Scale Prevention, with Emphasis on Magnetic Water Treatment', Citation Unknown.
11. Vincent, B., 'The Stability of Particulate Suspensions', *Chem. Ind.*, London, 1980, 218.
12. Overbeek, J.Th.G., 'Recent Developments in the

- Understanding of Colloid Stability', *J. Colloid Interface Sci.*, 1977, 58, 408.
13. Aveyard, R. and Haydon, D.A., 'An Introduction to the Principles of Surface Chemistry', Cambridge University Press, 1973.
  14. Tadros, Th.F., (editor), 'Solid-Liquid Dispersions', Academic Press, London, 1987.
  15. Deryagin, B.V. and Landau, L., *Acta Phys. Chim. URSS*, 1941, 14, 633.
  16. Verwey, E.J.W. and Overbeek, J.Th.G., 'Theory of the Stability of Lyophobic Colloids', Elsevier, 1948.
  17. Overbeek, J.Th.G., 'The Rule of Schultz and Hardy', *Pure Appl. Chem.*, 1980, 52, 1151.
  18. McBain, J.W. and Bakr, A.M., *J. Am. Chem. Soc.*, 1926, 48, 690.
  19. Mukerjee, P., 'The Nature of the Association Equilibria and Hydrophobic Bonding in Aqueous Solutions of Association Colloids', *Advan. Colloid Interface Sci.*, 1967, 1, 241-275.
  20. Everett, D.H., "Basic Principles of Colloid Science", Royal Society of Chemistry, London, 1988.
  21. Harkins, W.D., Mattoon, R.W. and Mittelmann, R., *J. Chem. Phys.*, 1947, 15, 763.
  22. Fischer, E.K., 'Colloidal Dispersions', Wiley and Sons, Inc., 1959.
  23. Elworthy, P.H., Florence, A.T. and MacFarlane, C.B., 'Solubilisation by Surface Active Agents', Chapman and

Hall, 1968.

24. Cordes, E. (editor), 'Reaction Kinetics in Micelles',  
Plenum, 1973.

CHAPTER TWO

THE MAGNETIC TREATMENT OF FLUIDS - CRYSTAL NUCLEATION

	Page	
2.1	Introduction	65
2.2	Manufacture of HDL Magnetic Units	71
2.3	Experimental Techniques	73
2.3.1	Particle Size Analysis	74
2.3.2	Microscopy	78
2.3.3	X-ray Powder Diffraction	85
2.3.4	Chromatography	90
2.4	Solubility Experiments	97
2.4.1	Determination of Calcium Phosphate Solubility following Magnetic Treatment of Solution	97
2.4.2	Determination of Barium Sulphate Solubility following Magnetic Treatment of Solution	101
2.5	Precipitation Experiments	101
2.5.1	Precipitation of Calcium Sulphate under Conditions of Varying Magnetic Field Strength	101
2.5.2	Precipitation of Calcium Phosphate under Conditions of Varying Magnetic Field Strength	103
2.5.3	Precipitation of Barium Sulphate: A Comparison of Effects Observed after passing a Solution through a Magnetic Field and through a Dummy	117
2.6	Results	117
2.7	Discussion	138
	References	158

CHAPTER TWO

THE MAGNETIC TREATMENT OF FLUIDS - CRYSTAL NUCLEATION

2.1 Introduction

The magnetic treatment of fluids is not a new area of research, but one that has inspired interest for over fifty years in various parts of the world. Although a plethora of literature is presently available on the subject, there have been no recent detailed studies and much controversy still surrounds it. Many writers expound the virtues of the application of a magnetic field with particular emphasis on the erosion of scale, citing their own observations with no real scientific back-up, whilst others dismiss this, again, with no reasoned scientific argument.

The formation of solid deposits of scale in heat exchanger systems where liquids at different temperatures are in contact with pipes and walls of containment systems is a global problem, the costs of alleviating which are considerable. The most common scale-forming precipitate is calcium carbonate from hard water, but other precipitates, such as calcium sulphate dihydrate and calcium phosphate, also cause problems in industry. The effect of magnetic treatment on scale control was first detected in

the 1930s and magnetic devices designed specifically for this purpose can significantly minimize time, energy and costs.

Scale formation is an example of crystal growth which has been discussed in the introductory chapter. The point of inception for most of the experiments described in this work, is the nucleation stage which may be considered in terms of crystallization nuclei dispersed in a fluid. The possibility that magnetic fields affect dispersed nuclei is explored.

Several theories have been postulated in an attempt to provide a scientific explanation for the mode by which a magnetic field affects fluids.

These hypotheses may broadly be divided into two groups: the first assume that the magnetic field affects the structure of water itself, the second that it can only act on the suspension or the solution.

Joshi and Kamat [1] report changes in the physical properties of water after being subjected to a magnetic field. The properties investigated were surface tension, pH and the dielectric constant. They claim that the changes

brought about by a magnetic field are permanent. They further advocate that the pH of neutral water increases after flowing through a magnetic field which they attribute to a change in the ionization constant of water under the influence of a magnetic field resulting in a decrease in the concentration of hydronium ions.

V.I. Klassen *et al* [2] studied the changes in the I.R. spectra of magnetically treated water. The authors maintain that the magnetic field is responsible for structural changes in the water. However, there is reason to believe these measurements are incorrect due to the inclusion of impurities in the dissolved water.

W. Drost-Hansen *et al* [3] also support the view that water is structurally modified as a result of magnetic treatment, although their work does not directly address the issue, but rather is concerned with other properties of structurally modified interfacial water referred to as "Vicinal water". The theory, Elissen [4] concludes, is implausible and would contravene the Second Law of Thermodynamics which maintains that as energy is taken up by one body it must be given up in like amount by another body, whether the energy is electrical, mechanical, or chemical, i.e. energy must come from some source which must be expended, and not from a permanent nonexpendable source.

However, some observers dispute whether a magnetic field affects water and aqueous solutions at all. Physicists have calculated that even a magnetic field of 100,000 gauss is insufficient to influence particles within atoms. Yet this view has been discredited on the grounds that in order to produce even substantial effects, the initial force does not need to be large. Raisen [5] argues that this is demonstrated by the Zeeman effect, in which electron energy levels in an atom are split by only 5,000 to 15,000 gauss. The controlling action of weak forces, and of magnetic forces in particular, and the exploitation of weak forces as a controlling factor in science and engineering has been documented by Vonsovsky [6]. It should be noted that the aforementioned calculations generally assume that it is necessary for hydrogen bonds to be ruptured; but many investigators claim that the structural changes often depend on geometric distortions of the ice-like framework which require only the bending of the hydrogen bonds, and therefore less energy.

Minenko and Petrov [7] have published a theory for the magnetic treatment, presuming the efficiency of the treatment to be proportional to the Lorentz force acting on the particle moving in a magnetic field. They claim that the most important factor affecting precipitation in this period is nucleation and that the change in the growth part of

precipitation is evident after about five minutes.

Ellingsen and Fjeldsend [8] suggested that some changes in the surface or double layer surrounding colloidal particles occur following magnetic treatment, thus controlling the rate of precipitation. Their studies further showed that magnetic water treatment influences the formation of calcite.

Speranski [9] is also convinced that 'magnetic coagulation' occurs in water passing through a magnetic field. According to this mechanism, the raw water contains coarsely dispersed and colloidally dispersed iron oxides which are magnetized in the field and then adhere to each other by magnetic coagulation.

Duffy [10] [11] conducted experiments to determine the effect of magnetic fields on water, aqueous solutions, the corrosion of steel, and the effect of iron compounds on the precipitation of calcium carbonate. According to his results, magnetization was found not to alter the structure of water, but increased the corrosion rate of 1018 steel by 18.6%. His results further suggest that magnetic treatment increases the Fe(III) concentration in solution thus inhibiting the nucleation and/or growth of crystalline scale.

The influence of a magnetic field on aqueous solutions is reported to last for several hours after having passed through the field. Ellingsen and Kristiansen [12] report changes in the rate of precipitation of calcium carbonate after subjecting a solution to magnetic treatment which they attribute to what they unscientifically term a 'memory effect'.

Recent work at The City University [13] has shown that the effects of magnetic fields on fluids can involve changes in particle size, crystallinity, crystal morphology, crystal phase, solubility and rate of precipitation of the scale forming precipitates.

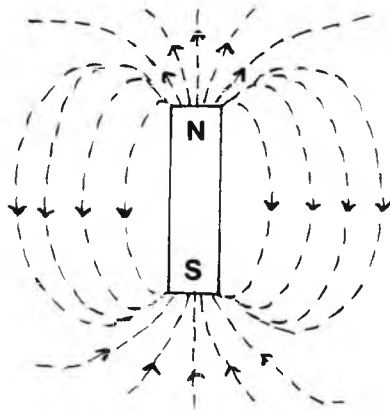
In controlled experiments [14], it was found that the major effect of a magnetic field on calcium carbonate precipitation was a change in particle size. This increase in size resulted in a reduction in the surface area and surface charges and therefore in the ability of the calcite crystals to adhere together to form scale. The main effect of the field is thus, to act as a crystal growth modifier and hence is a scale preventor. Descaling is a secondary downstream effect because the water is no longer supersaturated in calcite due to the crystallization of larger particles. In most heat-exchanger experiments, the calcite phase is the normal phase precipitated in the

presence or absence of a magnetic field, but in some special cases, for example, in evaporation experiments with boiling water, calcite and aragonite were found to precipitate in the ratio of 4:1, respectively, in the absence of a field and 1:4 in the presence of a field.

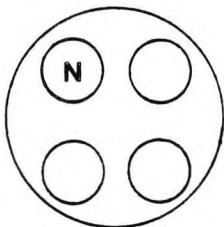
In this work, solubility and precipitation experiments were performed with a view to gaining a greater insight into the effects of the magnetic treatment of fluids and to ascribe a possible scientific basis to the observed effects. The products were characterized by particle size analysis, microscopy, X-ray powder diffraction and chromatography.

## 2.2 Manufacture of HDL Magnetic Units.

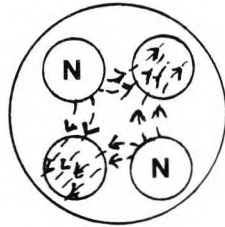
The magnetic units used in this work were supplied by HDL Fluid Dynamics Limited and take the form of cylindrical stainless steel tubes 3.8cm in diameter and 25.5cm long. The tubes are interiorly mounted with four solid cylindrical bars. The tubes contain either 0, 1, 2, 3 or 4 permanent magnetic bars depending on the field strength of the magnet (see Fig. 2.1), the complement being made up of non-magnetic bars. HDL magnets consist of 24 per cent cobalt, 14 per cent nickel, 8 per cent aluminium and 3 per cent copper [15]. The balance is iron. Magnetic Developments Limited



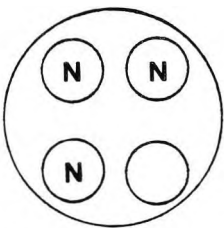
Longitudinal section showing magnetic field created by bar magnet.



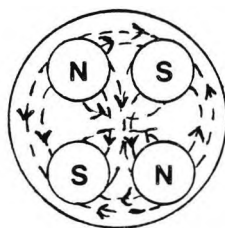
1M (0.3-1.2 kilogauss)



2M (1.1-1.3 kilogauss)



3M (1.0-2.0 kilogauss)



4M (2.75 kilogauss)

Transverse sections through HDL units showing configuration of magnetic bars.

FIGURE 2.1.

manufacture the magnets by melting the raw materials [16] in a high frequency furnace at 1100°C, then pouring them into sand castings. The bars are "fast cooled" to prevent the formation of the  $\alpha$ -phase of iron, since the irregular crystals of this polymorph inhibit the performance of the magnets. Heating the rough castings to 930°C cleans and tempers them, whilst subsequent cooling at a controlled rate in a magnetic field produces permanent magnets. The magnets are coated with polytetrafluoroethylene (PTFE) which is highly resistant to oxidation and chemical attack. It also serves to strengthen the magnets. PTFE prevents corrosion in, for example, abrasive phosphate systems. The direction of fluid flow is through the horizontal poles of the magnets, and constrictions in the tubes - venturis - vary the rate at which fluid flows through the units. Since the magnets are permanent, they need no external power connection. The ends are threaded to fit the pipework of a scaled up, or clean system. In this study, polyvinyl chloride piping and other plastic materials were employed wherever possible to minimize contamination.

### 2.3 Experimental Techniques

The experimental techniques, as mentioned in Section 2.1,

used to study crystallization were as follows: particle size analysis, optical and electron microscopy, X-ray powder diffraction and ion chromatography. A description of each will now be presented.

### 2.3.1 Particle Size Analysis

All particle size measurements were out carried on a MALVERN 2600/3600 Particle Sizer, a complete measurement tool for the analysis of particle size distributions in the range of 1 to 1800 microns. The instrument can measure the size distribution by weight of

- Solids in gas or liquid suspension
- Liquid droplets in gas or other immiscible liquids
- Gas bubbles in liquid

All samples for which the particle size was measured in this work were solid in liquid suspensions.

The instrument uses the principle of Fraunhofer Diffraction from the particles as the measurement means, as illustrated in Fig. 2.2. A low power visible laser transmitter produces a parallel, monochromatic beam of light to illuminate the particles. The incident light is diffracted by the particles to give a stationary diffraction pattern regardless of

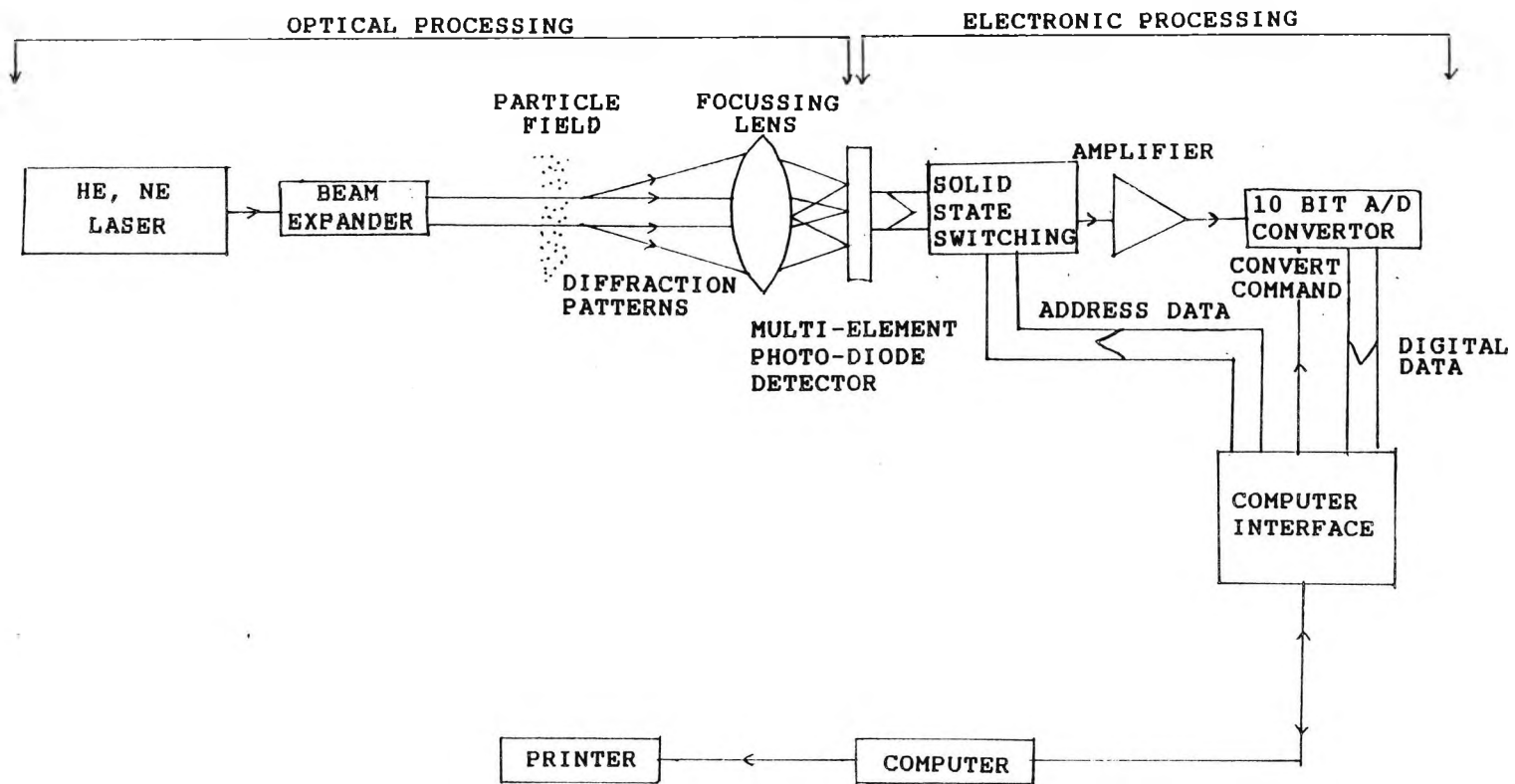


FIGURE 2.2 Basic opto-electric system for obtaining particle size and distribution.

MALVERN 2500/3500 PARTICLE SIZER VA. 1

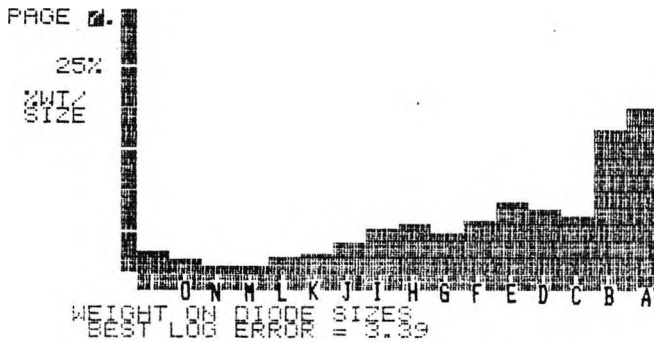
MALVERN INSTRUMENTS LTD, SPRING LAKE, MALVERN, ENGLAND.

PRINTING RESULTS FROM DATA BLOCK 1

TIME 06-03-20 RUN NO. 34 LOG ERROR = 3.39

SAMPLE CONCENTRATION = 0.0512 % BY VOLUME  
OBSCURATION = 0.26

	SIZE BAND		CUMULATIVE	WEIGHT	CUMULATIVE	LIGHT ENERGY	
	UPPER	LOWER	WT BELOW	IN BAND	WT ABOVE	COMPUTED	MEASURED
A	1128.0	523.2	79.6	20.5	0.0	613	598
B	523.2	320.7	62.2	17.3	20.5	634	643
C	320.7	225.6	55.1	7.1	37.8	688	675
D	225.6	168.6	47.4	7.7	44.9	770	769
E	168.6	129.3	38.6	0.8	52.6	942	942
F	129.3	100.3	32.0	6.6	61.4	1166	1163
G	100.3	78.0	26.9	5.1	68.0	1403	1381
H	78.0	60.7	20.8	6.0	73.2	1609	1618
I	60.7	47.3	15.5	5.4	79.2	1821	1820
J	47.3	36.9	11.7	3.7	84.5	2005	1993
K	36.9	29.0	9.0	2.7	88.3	2047	2032
L	29.0	22.8	7.0	2.0	91.0	2027	2047
M	22.8	18.1	5.0	1.2	93.0	2028	2018
N	18.1	14.5	4.6	1.2	94.2	2041	1993
O	14.5	11.6	2.9	1.0	95.4	2034	2014



S.E.E.

FIGURE 2.3 Computer printout representing particle size distribution.

particle motion. As particles enter and leave the illuminated area, the diffraction pattern 'evolves' always reflecting the instantaneous size distribution in this area. Thus, by integration over a suitable period and a continuous flux of particles through the illuminated area, a representative bulk sample of the particles may contribute to the final measured diffraction pattern.

A Fourier transform lens [17] focusses the diffraction pattern onto a multi-element photo-electric detector which produces an analogue signal proportional to received light intensity. This detector is interfaced directly to a computer allowing it to read the diffraction pattern and perform the necessary integration digitally.

The computer then finds the size distribution that gives the closest fitting diffraction pattern. The size distribution of the sample by weight may be displayed graphically on the VDU screen or printed as a hard copy result. The size distribution can be presented as the weight in size bands, the cumulative weight below a size and the cumulative weight above a size, depending on whichever is required.

The MALVERN 2600/3600 Particle Sizer comprises the following component sub-systems:

1. Optical measurement unit
2. Sample cell and measurement technique
3. Computer system
4. Application software package
5. High speed line printer

### 2.3.2 Microscopy

Observation of materials such as minerals, ceramics and biological material is difficult owing to their small size and lack of contrast. These complications are overcome with the aid of specially designed microscopes. Various types of microscope are available and can be divided into two groups: optical and electron. With both techniques, the sample can be viewed in transmission (the beam of light or electrons passes through the sample) or in reflection (the beam of light or electrons is reflected off the sample surface).

#### Optical Microscopy

The *polarizing* or *petrographic microscope* is a transmission instrument. Samples usually take the form of fine powders or thin slices severed from a solid piece. It is widely used in geology and mineralogy and can be used profitably in solid



optical properties of the solid.

The principal components of a polarizing microscope are indicated in Fig. 2.5. The source may emit either white or monochromatic light. Only light rays whose vibrational direction is parallel to the polarizer is permitted to pass through. The resulting plane polarized light passes through lenses, apertures and accessories (not shown) and on to the sample which is mounted on the microscope stage.

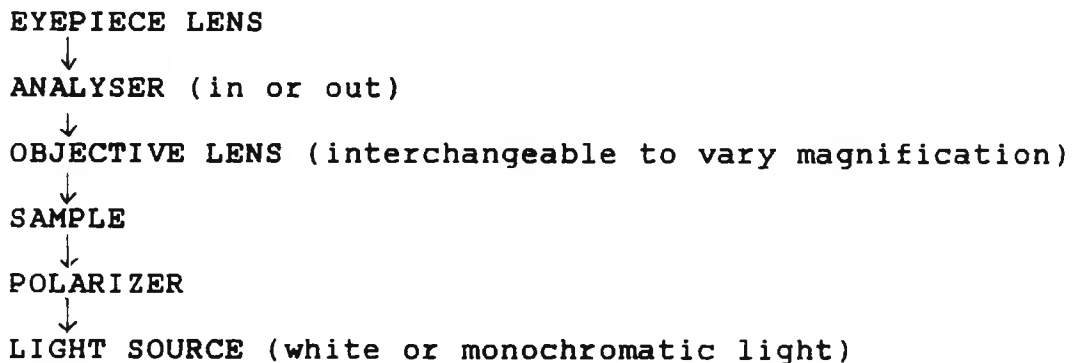


FIGURE 2.5 Basic components of a polarizing microscope.

Light transmitted by the sample and immersion liquid is detected by the objective lens. The instrument usually has several of these, of different magnification, which are readily interchangeable. The analyser may be placed in or out of the path of light. It is similar to the polarizer but

is orientated so that its vibrational direction is at  $90^\circ$  to that of the polarizer. When the analyser is 'in', only light vibrating in the correct direction is permitted to pass through and on to the eyepiece. When the analyser is 'out', the microscope behaves as a simple magnifying microscope.

The reflected light microscope is similar to the transmission one with the exception that the source and objective lens are on the same side of the sample. It is used to examine solid aggregates of opaque material such as metals, minerals and ceramics. The information derived from this technique primarily concerns the texture of the solid, i.e. the phases present; their identification; the number, size and distribution of particles.

Optical microscopy is applied in the determination of crystal morphology and symmetry; phase identification, purity and homogeneity; and crystal defects.

### Electron Microscopy

The optical microscope, although of tremendous importance, is limited by its resolving power. The 'limit of resolution' is defined as the minimum distance between two points that allows for their discrimination as two separate entities.

The electron microscope, initially constructed by Knoll and Hruska [19], in Berlin, in 1931, is an extremely versatile instrument, capable of providing structural information over a wide range of magnification. Its development in recent years has, revolutionized various aspects of science, in particular, the entire concept of the cell. The technique permits a direct study of biological ultrastructure.

In overall design, the electron microscope is similar to the optical microscope with fundamental deviations in the mode of illumination and type of lenses used. This microscope uses a beam of electrons analogous to a light source. The beam is focused by magnetic or electrostatic fields, which function as lenses, to produce a clear image.

In the *transmission electron microscope*, (TEM) so called because the electrons used to form the image pass through the specimen, a tungsten filament or cathode emits a stream of electrons which are accelerated by an electric potential in a vacuum tube. If the electrons, which have a relatively poor penetrating power were not kept under high vacuum [20] they would be scattered and absorbed by gas molecules in the microscope. This places special requirements on the specimen, which must be dry and non-volatile. The electron beam is then deflected by electromagnetic lenses. The condenser lenses are placed in

tandem to allow focusing of a very small, intense spot of electrons on the specimen. Transmitted electrons then pass through a sequence of lenses including an objective, intermediate and projector lens. The lenses are arranged so that successively magnified images are formed by each individual lens in the sequence.

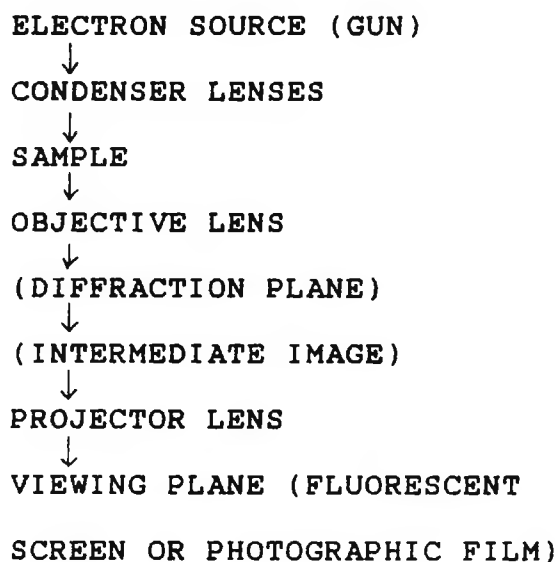


FIGURE 2.6 Basic components of a transmission electron microscope.

The final lens in the sequence focuses the magnified image onto a fluorescent screen, coated with a layer of crystals that respond to electron bombardment by emitting visible light. In this way, the electron image is converted to a visual image, permanent records of which are produced by exposing a photographic plate to the electron beam at the

level of the screen. The image formed on the fluorescent screen depends on the dispersion of electrons (electron scattering) by the atomic nuclei present in the object. This dispersion is determined by the thickness of the object, the molecular packing, and, in particular, by the atomic number. The greater the atomic number, the greater is the resultant dispersion. The resolving power depends on the wavelength ( $\lambda = 0.005\text{nm}$ ) as in the light microscope. The resolution reached is 0.3 to 0.5nm, and the final magnification can be  $10^6$  or more [21].

The *scanning electron microscope* (SEM) is an invaluable instrument for surveying materials under high magnification and providing information on particle sizes and shapes. Electrons from the electron gun are focused onto a small spot, 50 to 100Å in diameter, on the surface of the sample. The electron beam is scanned systematically over the sample. Both X-rays and secondary electrons (high-energy electrons released by excited molecules) are emitted by the sample; the former are used for chemical analysis and the latter are used to build up an image of the sample surface which is displayed on a screen. The limitation with SEM instruments is that the lower limit of resolution is approximately 100Å. A recent advance has been the development of the *scanning transmission electron microscope* (STEM) which combines the scanning feature of the SEM with the

intrinsically higher resolution obtainable with the TEM. This technique was taken advantage of in the examination of the barium sulphate crystals.

Finally, with high resolution electron microscopy (HREM) it is possible, under favourable conditions, to obtain information on an atomic scale, by direct lattice imaging. Resolutions of ca. 2Å have been achieved. However, it must be emphasized that this does not mean the demise of conventional crystallography.

### 2.3.3 X-ray Powder Diffraction

X-ray powder diffraction is a physical technique used in the characterization of solids. It has been in use since the early part of this century for the 'fingerprint' identification of crystalline materials and for the determination of crystal structures.

The principles of X-ray powder diffraction are illustrated in Fig. 2.7.1. A monochromatic beam of X-rays strikes a finely powdered sample, which, ideally, consists of randomly orientated crystals. In such a sample, the various lattice planes are also randomly orientated. Thus, for each set of planes, at least some crystals must be orientated at the

Bragg angle,  $\theta$ , to the incident beam and so diffraction occurs for these crystals and planes. The diffracted beam may be detected either by surrounding the sample with a strip of photographic film (Debye-Scherrer and Guinier focusing methods) or by using a movable detector, such as a Geiger counter, connected to a chart recorder (diffractometer).

The original powder method, Debye-Scherrer method, is used little nowadays, although its mode of operation is instructive. For a given set of lattice points, the diffracted radiation forms the surface of a cone, as shown in Fig. 2.7.2. The only requirement for diffraction is that the planes be at the angle,  $\theta$ , to the incident beam. In finely powdered samples, crystals are positioned randomly about the incident beam and the resulting diffracted beams appear to be emitted from the sample as cones of radiation. Since the Bragg angle is  $\theta$ , the angle between diffracted and undiffracted beams is  $2\theta$ , and the angle of the cone is  $4\theta$ . Each cone of radiation is produced by a different set of planes. A thin strip of film wrapped around the sample detects the cones which appear as arcs, symmetrical about the two orifices in the film (these allow entry and exit of the incident and undiffracted beams). Finely ground samples produce a continuous line; in coarser samples, relatively few particles are present and so, do not satisfy the

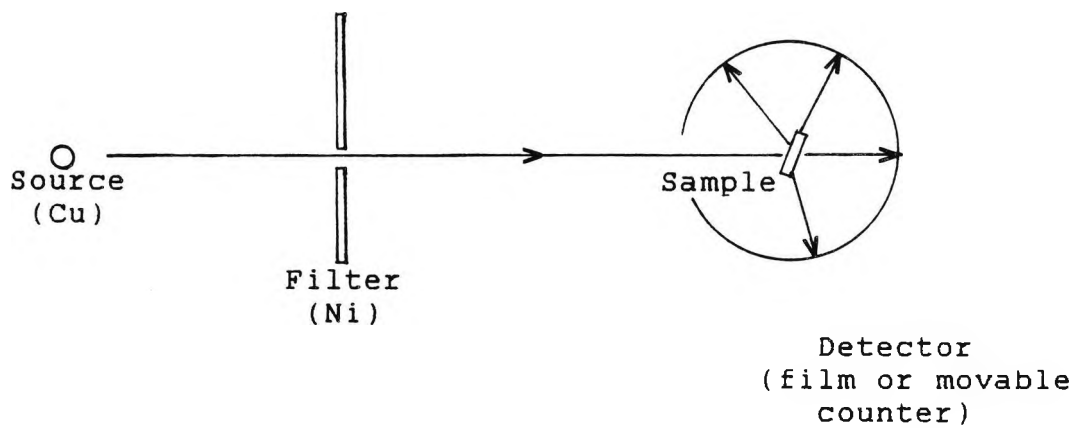


FIGURE 2.7.1 X-ray powder diffraction.

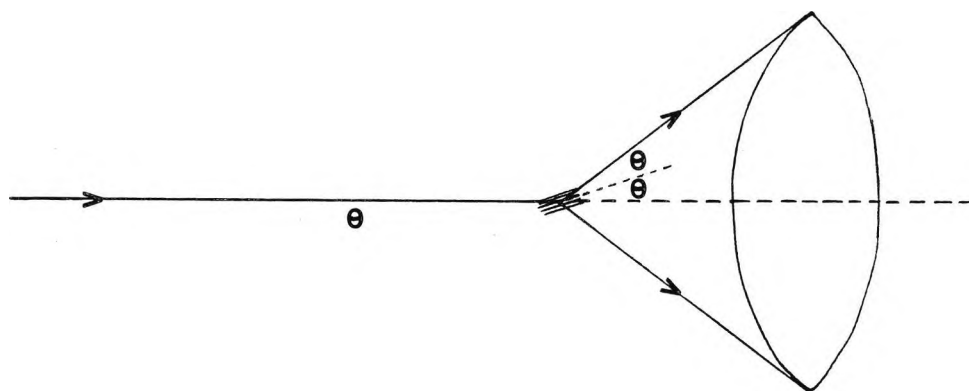


FIGURE 2.7.2 The formation of a cone of diffracted radiation in the powder method.

assumption that they lie in all possible orientations which may result in the arcs being 'spotty'.

To obtain the d-spacing, the separation, S, between pairs of corresponding arcs is measured and by knowing the radius, R, the following expression is applied:

$$S/2\pi R = 4\theta /360$$

From this,  $2\theta$  and therefore d may be obtained for each pair of arcs.

Modern film methods, such as Guinier focusing methods, make use of a convergent, intense incident beam. A bent single crystal of quartz or graphite is placed between the X-ray source and the sample to obtain a convergent beam. The orientation of the bent crystal is adjusted so that it diffracts the incident beam and converts it from a divergent to a convergent one. The beam then strikes the sample and the diffracted beams are arranged to focus at the surface of the film.

Another modern powder technique, as implemented in this work, is diffractometry. Again, a convergent beam is used and the resolution fairly good. Another advantage of this method is the reduction in exposure time (typically 10

minutes to 1 hour). The instrument has a proportional scintillation or Geiger counter as the detector which is connected to a chart recorder. The counter is usually set to scan over a range of  $2\theta$  values at a constant velocity. Generally, the range  $10$  to  $80^\circ 2\theta$  is sufficient to cover the most useful part of the powder pattern. The output to chart paper consists of a plot of peaks against values of  $2\theta$ . A Philips PW1051 diffractometer with  $\text{CuK}\alpha$  ( $\lambda = 1.5418\text{\AA}$ ) was used in this work.

#### Interpretation

The principle features of a powder pattern are the d-spacings and intensities. The d-spacings (positions) of the lines in a powder pattern are governed by the values of the unit cell parameters ( $a, b, c, \alpha, \beta, \gamma$ ). The intensities provide information on the types of atoms present in the sample. Intensities are recorded relative to the intensity of the strongest line of the pattern which is arbitrarily assigned 100. For a particular substance, the line positions are essentially fixed and are characteristic of that substance. Intensities may vary somewhat from sample to sample, depending on the method of sample preparation and instrumental conditions.

An important use of the powder method is the qualitative analysis of crystalline phases. For the identification of

unknown crystalline materials, an invaluable reference source is "The Powder Diffraction File" (Joint Committee on Powder Diffraction Standards, U.S.A.); (supplementary data are issued annually).

#### 2.3.4 Chromatography

Chromatographic techniques depend principally on the variation in the rate at which different components of a mixture migrate through a stationary phase under the influence of a mobile phase. During a chromatographic separation, solute molecules are continually moving back and forth between the stationary and mobile phases. While they are in the mobile phase, they are carried forward with it but remain virtually stationary during the time spent in the stationary phase. The rate of migration of each solute is therefore determined by the proportion of time it spends in the mobile phase, or in other words, by its distribution ratio. The process whereby a solute is transferred from a mobile to a stationary phase is known as 'sorption'.

#### Ion-Exchange Chromatography

##### (High Performance Ion Chromatography - HPIC)

In the solubility experiments involving barium sulphate, HPIC was implemented in determining the concentration of

sulphate ions, the barium ions being directly proportional to the latter.

Ion-exchange separations are limited to samples containing ionized or partially ionized solutes; it is used in the separation of anionic and cationic species. The process concerns an interchange of ions of like sign between the solution and an essentially insoluble solid in contact with the solution. The stationary phase consists of a polystyrene based resin crosslinked with divinylbenzene (DVB) and contains fixed charged groups and mobile counter-ions which can be reversibly exchanged for those of a solute carrying a like charge, as the mobile phase travels through the system. The proportion of DVB is 2 to 20% [22] and results in a three-dimensional cross-linked structure that is rigid, porous and highly insoluble. The extent of cross-linking, expressed as the weight percent of DVB, affects the rigidity of the structure and the pore size. A low degree of cross-linking produces beads which swell appreciably when in contact with a polar solvent and have large pores enabling ions to diffuse into the structure and exchange rapidly. This phenomenon of 'swelling' results from the osmotic pressure set up when a resin bead, which can be considered to be a concentrated electrolytic solution, is surrounded by a more dilute polar solution. Solvent flows into the bead and distends the structure in an attempt to reduce the

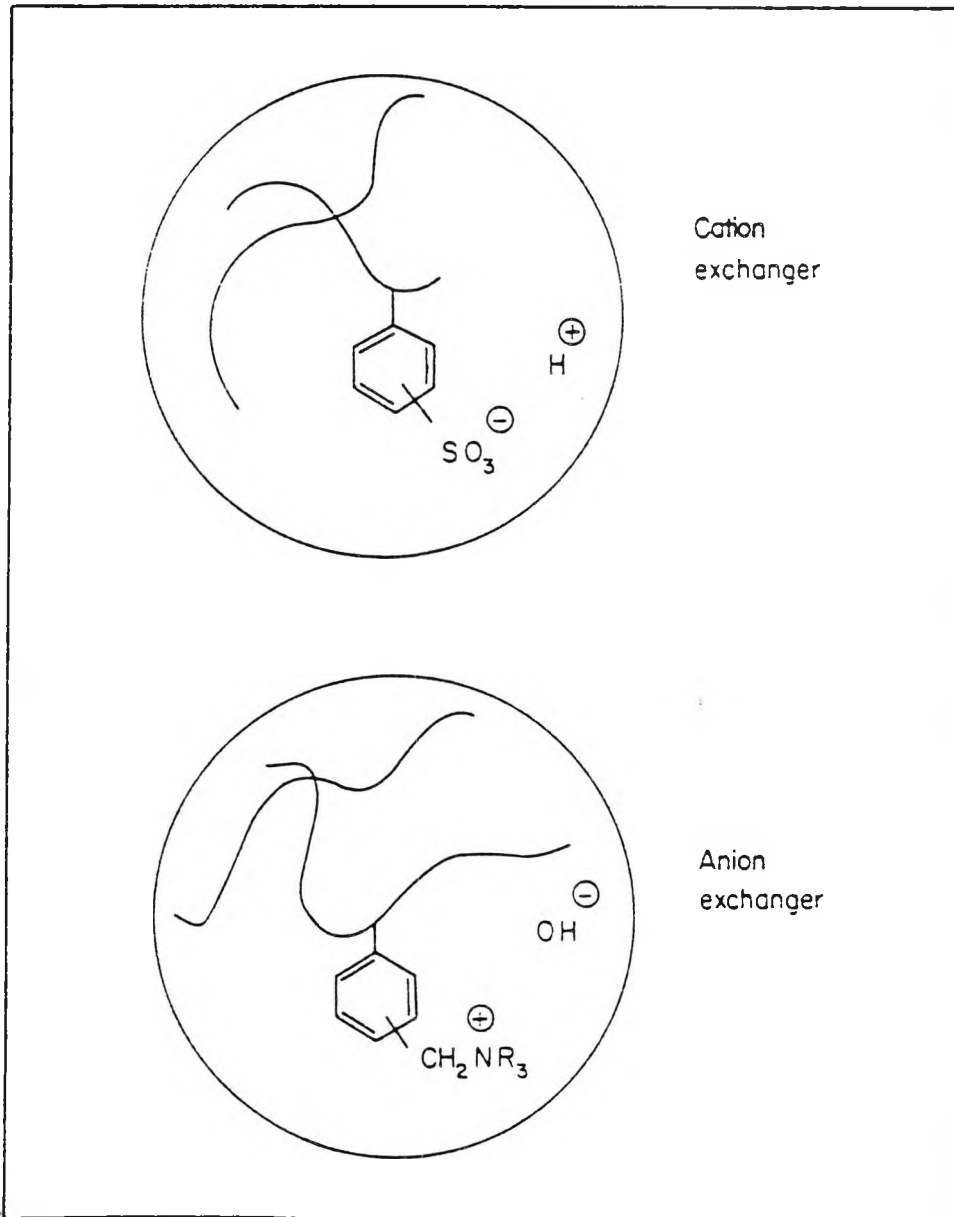


FIGURE 2.8 Representation of common forms of ion-exchanger.

osmotic pressure by dilution. Resins with a high degree of cross-linking have smaller pores and are more rigid. The degree of cross-linking and thus pore size is controlled by the polymerization process.

For the exchange of cations, the exchange function is usually a sulphonate group; whereas for the analysis of anions, a quaternary ammonium group is commonly employed. The different rates of migration result from variations in the affinity of the stationary phase for different ionic species. The mobile phase contains an ion of low resin affinity, and the separated components collected at the bottom of the column are thus accompanied by a relatively high concentration of this ion. Procedures often adopted in ion-exchange chromatography are 'gradient elution', involving continuous variation in the composition of the eluting agent, 'stepwise elution', in which the composition is altered at specific points during the separation, and 'complexing elution', where a reagent which forms complexes of varying stability with the sample components is included in the solution. Acids, bases and buffers are most widely used as eluting agents.

#### The Ion Chromatographic System

The major components of a modern chromatographic system, as used in this work and developed by Dionex are illustrated in

Fig. 2.9.

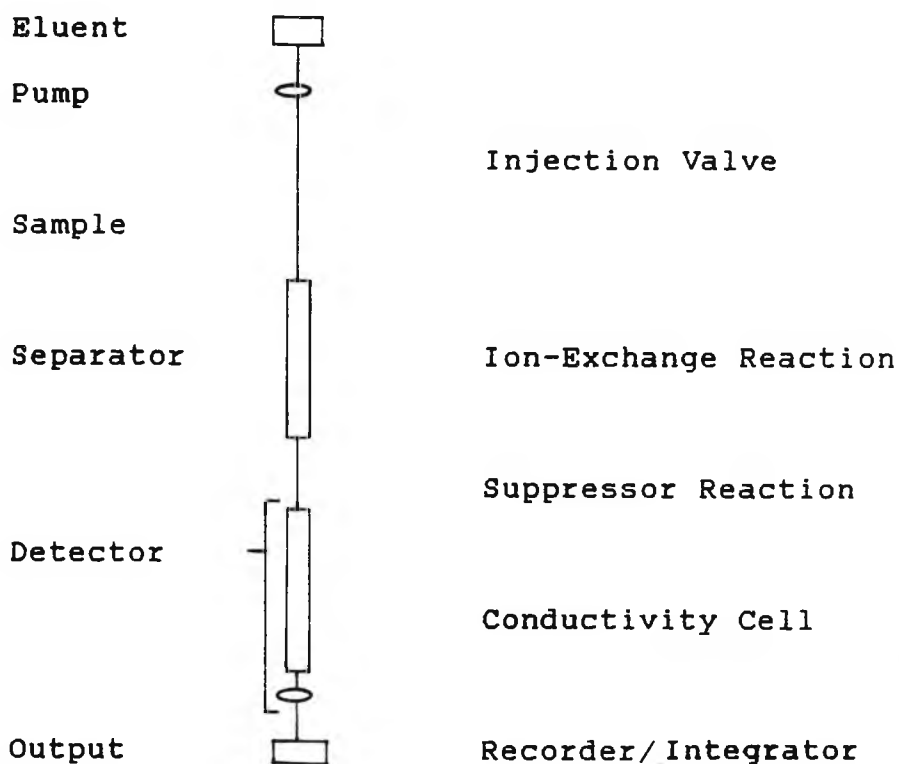


FIGURE 2.9 Basic components of an ion chromatograph.

The mobile phase is pumped through the chromatographic system by a double reciprocating pump [23]. A pulse-free flow, necessary for both UV/Vis and amperometric detectors, is ensured by a complex electronic control of the pump.

The samples are introduced into the system via a loop injector shown schematically in Fig. 2.10. The two outlets of the sample loop which is loaded at atmospheric pressure, are joined by a three-way valve. After the valve is

switched the sample is transported onto the column by the mobile phase.

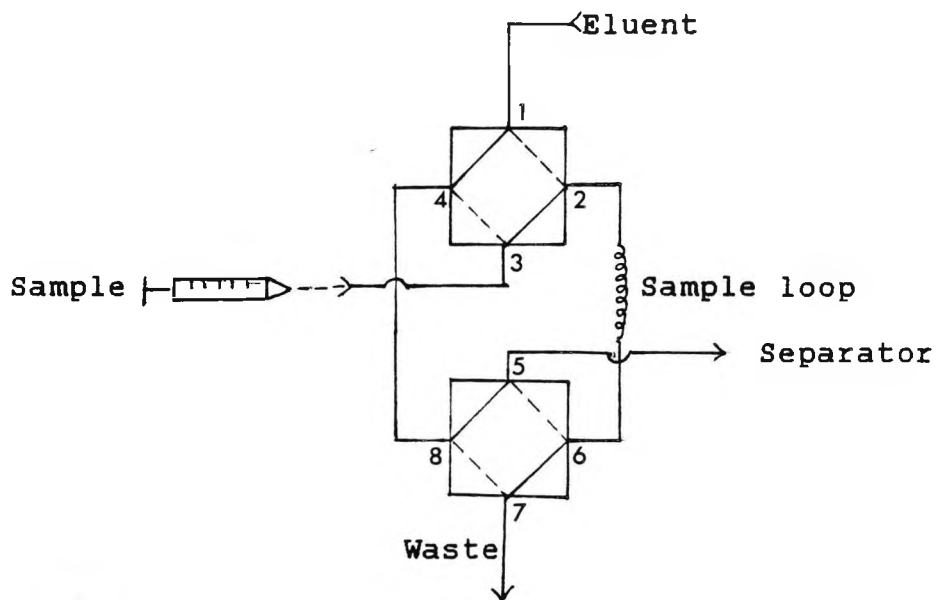


FIGURE 2.10 The loop injector.

The two ion-exchange columns are coupled in series and form the most important part of the chromatograph. The selection of a suitable stationary phase as well as of the appropriate chromatographic parameters, determines the quality of the analysis. The column bodies are fabricated with inert materials and are generally operated at room temperature. In some instances, such as in the analysis of carbohydrates and amino acids, it is necessary to thermostat the columns at elevated temperatures.

The performance of a detector (which serves to identify and

quantify the species being analyzed) is assessed on the following criteria:

Linearity

Resolution

Noise

The most widely used detector in ion-exchange chromatography is the conductivity detector. This detection system usually incorporates a suppressor device that serves to chemically reduce the background conductivity of the eluent which, simultaneously, converts the species of interest into a more conductive form. UV/Vis, amperometric, and fluorescence detectors are sometimes used in addition to the conductivity detector.

The chromatogram is obtained via a recorder or computer. Quantitative results are derived from a calculation of peak areas, or peak heights, that are proportional to the concentration of the species being determined. Simplification of the data reduction task is frequently accomplished via digital **integrators** or personal computers.

## 2.4. Solubility Experiments

### 2.4.1 Determination of Calcium Phosphate Solubility following Magnetic Treatment of Solution.

A saturated solution of calcium phosphate was pumped through a magnetic unit, M, (the dimensions of which are quoted in Section 2.2) of known field strength for five days using the apparatus shown in Fig. 2.11. The saturated solution also passed through a sintered column, A, containing 20g  $\text{Ca}_3(\text{PO}_4)_2$  before re-emerging into the reservoir. At various intervals, 25ml aliquots were pipetted from the tank into a conical flask. 2ml caustic soda (2M NaOH) followed by a small quantity of murexide indicator (mixed and ground thoroughly with NaCl until homogeneous, c.a. 0.1g indicator to 25g NaCl) were added to each sample which was then titrated against 0.01M EDTA solution to determine the  $\text{Ca}^{2+}$  concentration. The colour change at the end point was from pink to purple. Each titration was performed in duplicate. The procedure was then repeated using another magnetic unit, followed by a non-magnetic unit as a control. A graph of concentration against time was plotted as illustrated in Fig. 2.12.

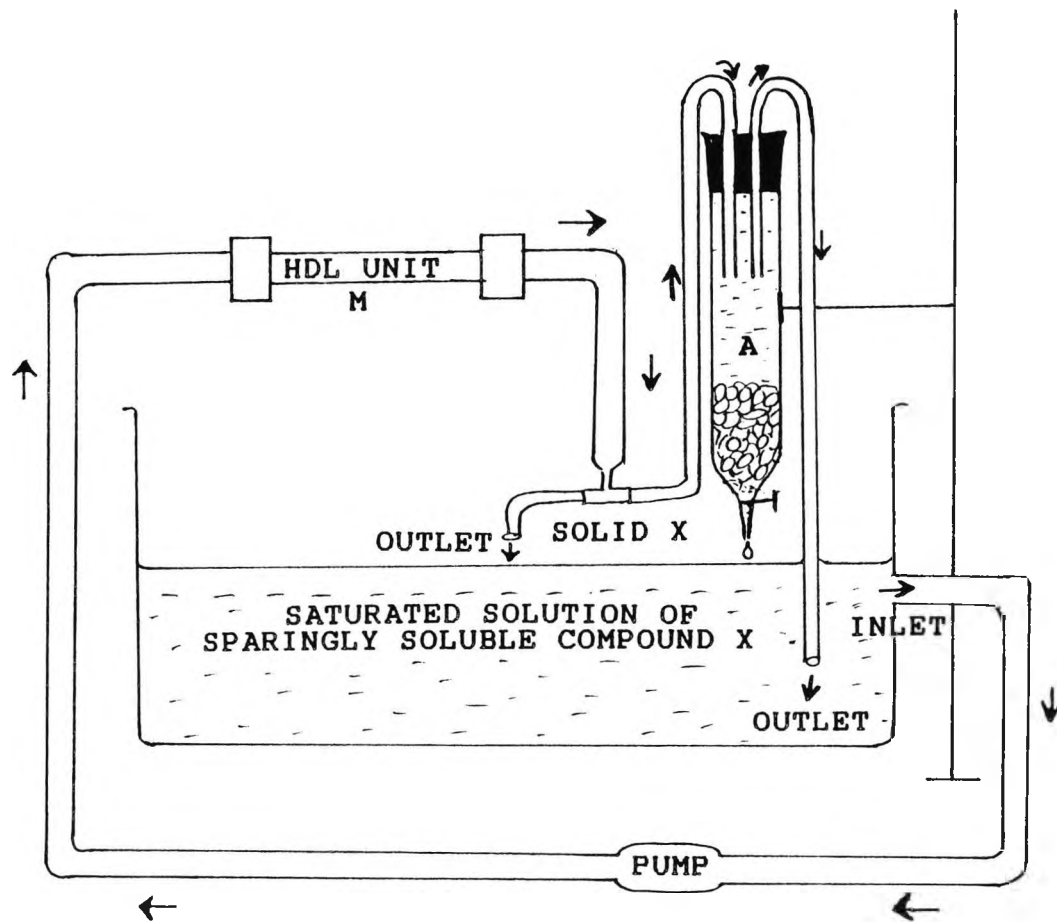


FIGURE 2.11 General set-up of apparatus used in solubility experiments.

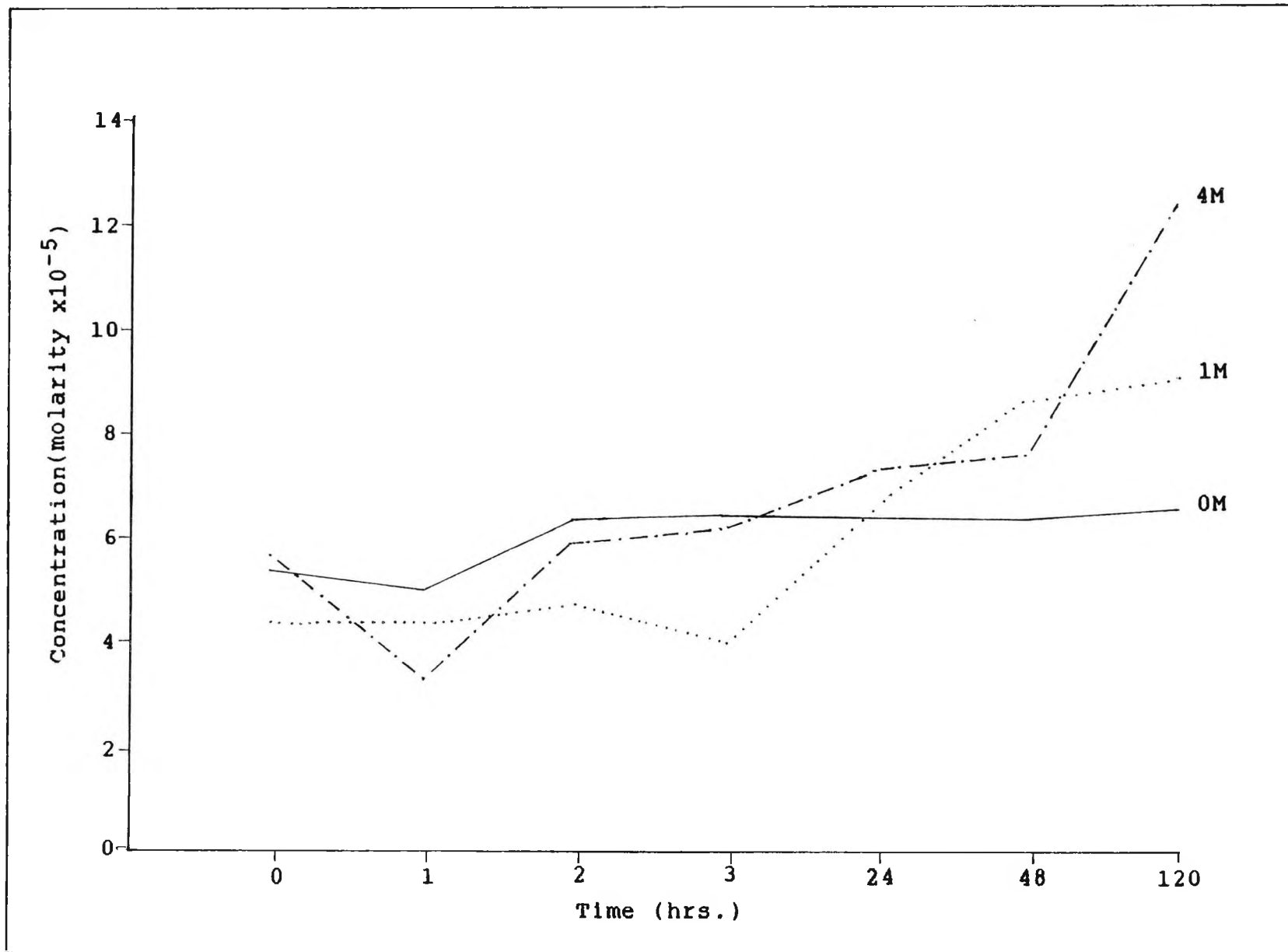


FIGURE 2.12

Variation in the concentration of a calcium phosphate solution with time after subjection to H.D.L. units containing 4,1 and 0 magnetic bars (4M, 1M and 0M).

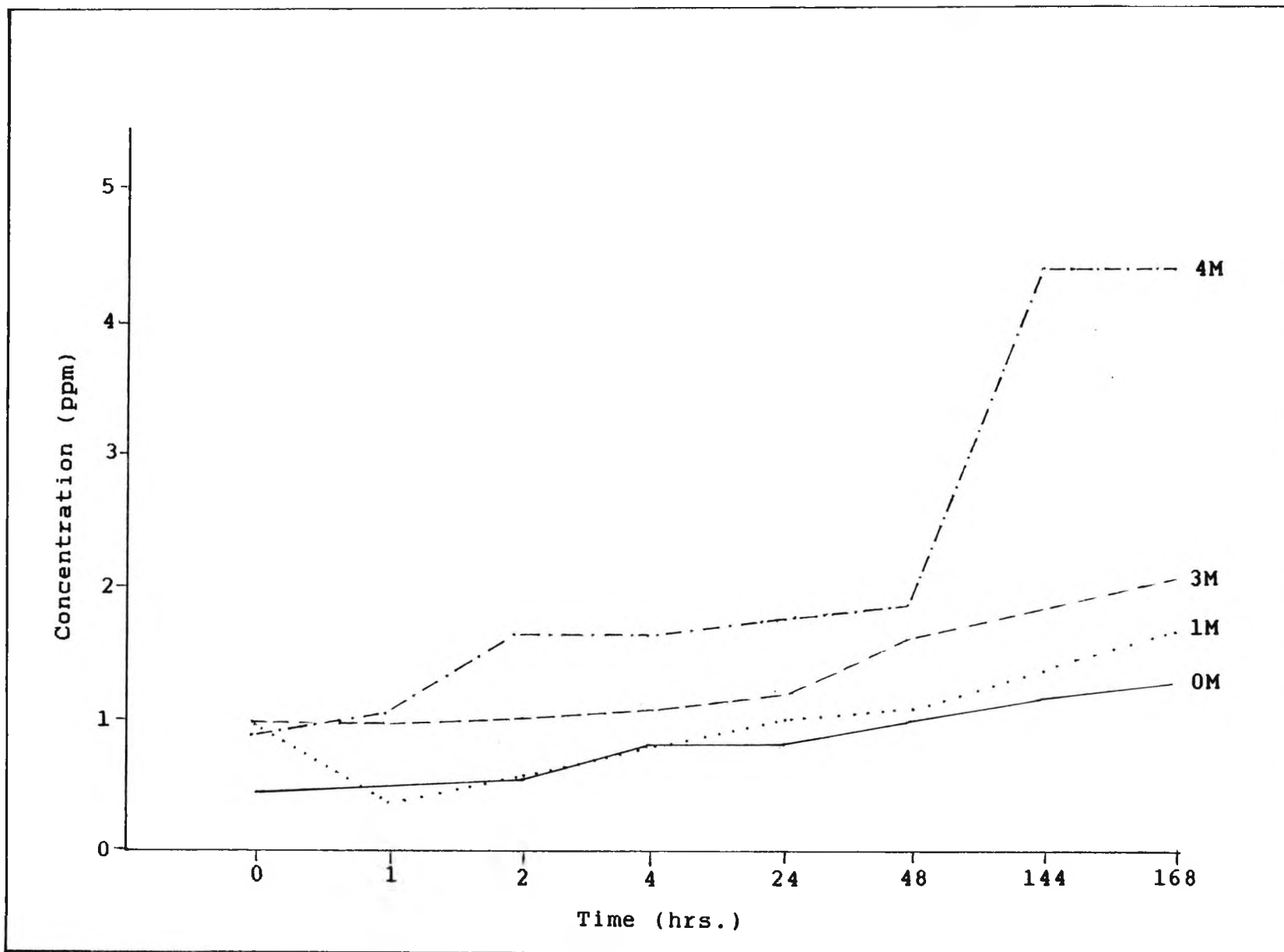


FIGURE 2.13 Variation in the concentration of a barium sulphate solution with time after subjection to H.D.L. units containing 4,3,1 and 0 magnetic bars (4M, 3M, 1M and 0M).

2.4.2 Determination of Barium Sulphate Solubility  
following Magnetic Treatment of Solution.

A saturated solution of  $\text{BaSO}_4$  was passed through a known magnetic field for seven days, applying the same experimental set-up as shown Fig. 2.11. Samples were collected from the tank at timed intervals and the  $\text{SO}_4^{2-}$  concentration was determined by ion chromatography, the principles of which have been discussed in Section 2.3.4. This experiment was repeated with one other magnet and a control. The graph of concentration against time is set out in Fig. 2.13.

2.5 Precipitation Experiments

2.5.1 Precipitation of Calcium Sulphate under Conditions  
of Varying Magnetic Field Strength.

A saturated solution of  $\text{CaSO}_4 \cdot 2\text{H}_2\text{O}$  was passed through a magnetic field using the apparatus illustrated in Fig. 2.14, a modification of that shown in Fig. 2.11. At various intervals, 20ml aliquots were collected from the tank and 2ml of calcium chloride (50g per 100ml) added to each sample fairly rapidly followed by the dropwise addition of 2ml of sodium sulphate (50g per 100ml) to precipitate calcium sulphate dihydrate. Units of differing field strengths were then used in repeat runs followed by a run using a control.

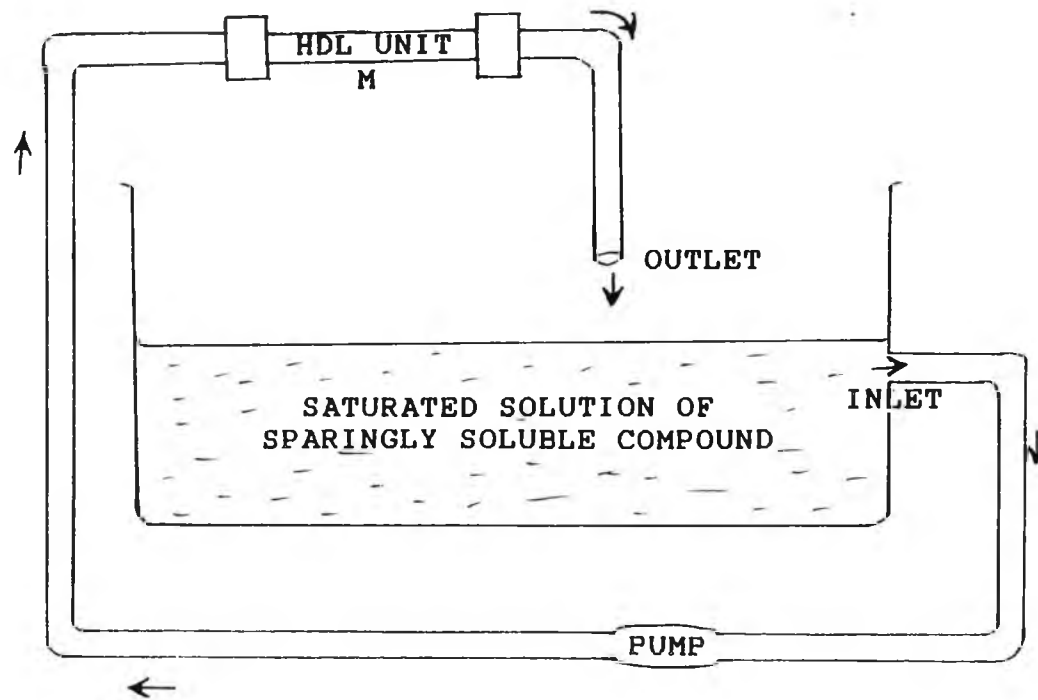


FIGURE 2.14 General set-up of apparatus used in precipitation experiments.

Particle size measurements were carried out on the precipitates and the data are shown in Figs. 2.15 - 2.21. The optical micrographs obtained are shown in Figs. 2.22 and 2.23. X-ray powder patterns for the precipitates are shown in Fig. 2.24.

Another experiment was performed in which a saturated solution of  $\text{CaSO}_4 \cdot 2\text{H}_2\text{O}$  was pumped through a magnetic field for a duration of 5 hours, after which 20ml aliquots were collected and evaporated to dryness under an I.R. lamp. The distance between the sample and lamp was kept constant throughout the experiment. The time taken for complete evaporation to occur was found to be approximately 21 hours. Samples were then examined by optical microscopy (see Fig. 2.25).

#### 2.5.2 Precipitation of Calcium Phosphate under Conditions of Varying Magnetic Field Strength.

A saturated solution of calcium phosphate was circulated through the magnetic system, described earlier (see Fig. 2.14) for 2 days. At timed intervals, 50ml aliquots were taken from the tank. 2ml  $\text{CaCl}_2$  solution (50g per 100ml) followed by 2ml  $(\text{NH}_4)_3\text{PO}_4$  solution (15g per 250ml) were added to the latter to form a precipitate. This was repeated using two other magnets and a control unit. The

FIGURE 2.15 Percentage weight above against particle size of calcium sulphate precipitated after two minutes following treatment with HDL units containing four, three, one and zero magnetic bars (hence 4M, 3M, 1M and 0M).

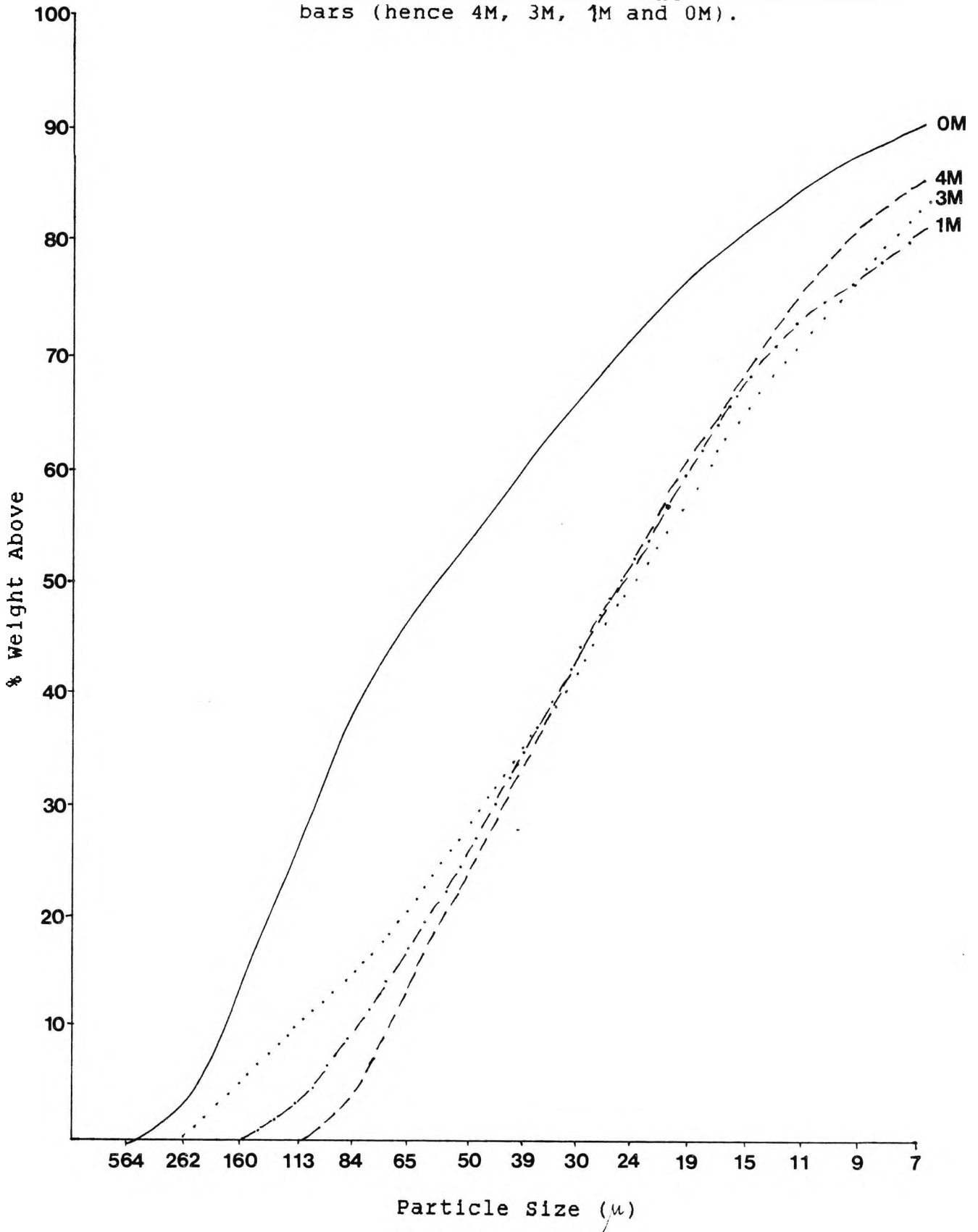


FIGURE 2.16 Percentage weight above against particle size of calcium sulphate precipitated after one and a half hours following treatment with HDL units containing four, three, one and zero magnetic bars (hence 4M, 3M, 1M and 0M).

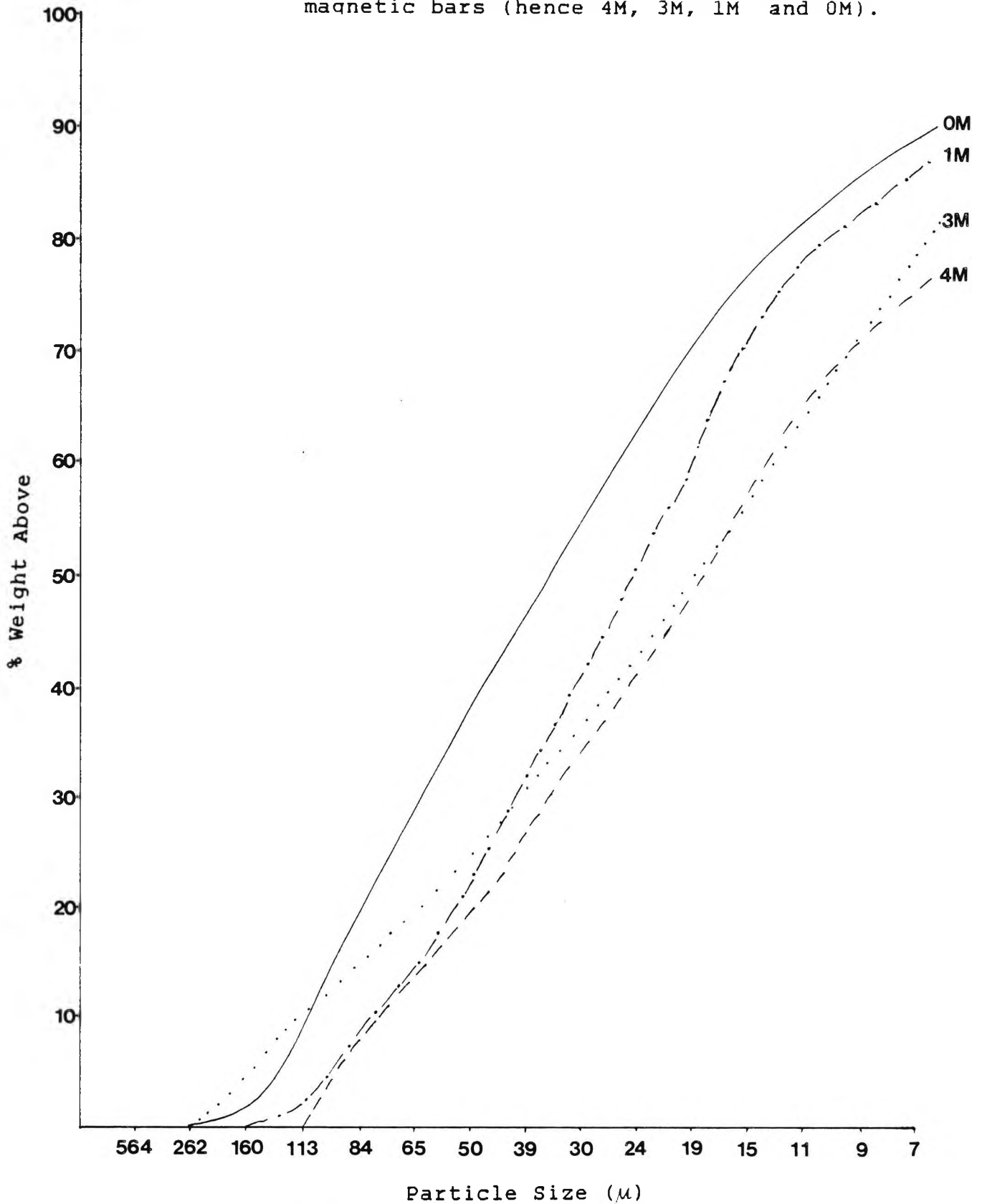


FIGURE 2.17 Percentage weight above against particle size of calcium sulphate precipitated after two and a half hours following treatment with HDL units containing four, three, one and zero magnetic bars (hence 4M, 3M, 1M and 0M).

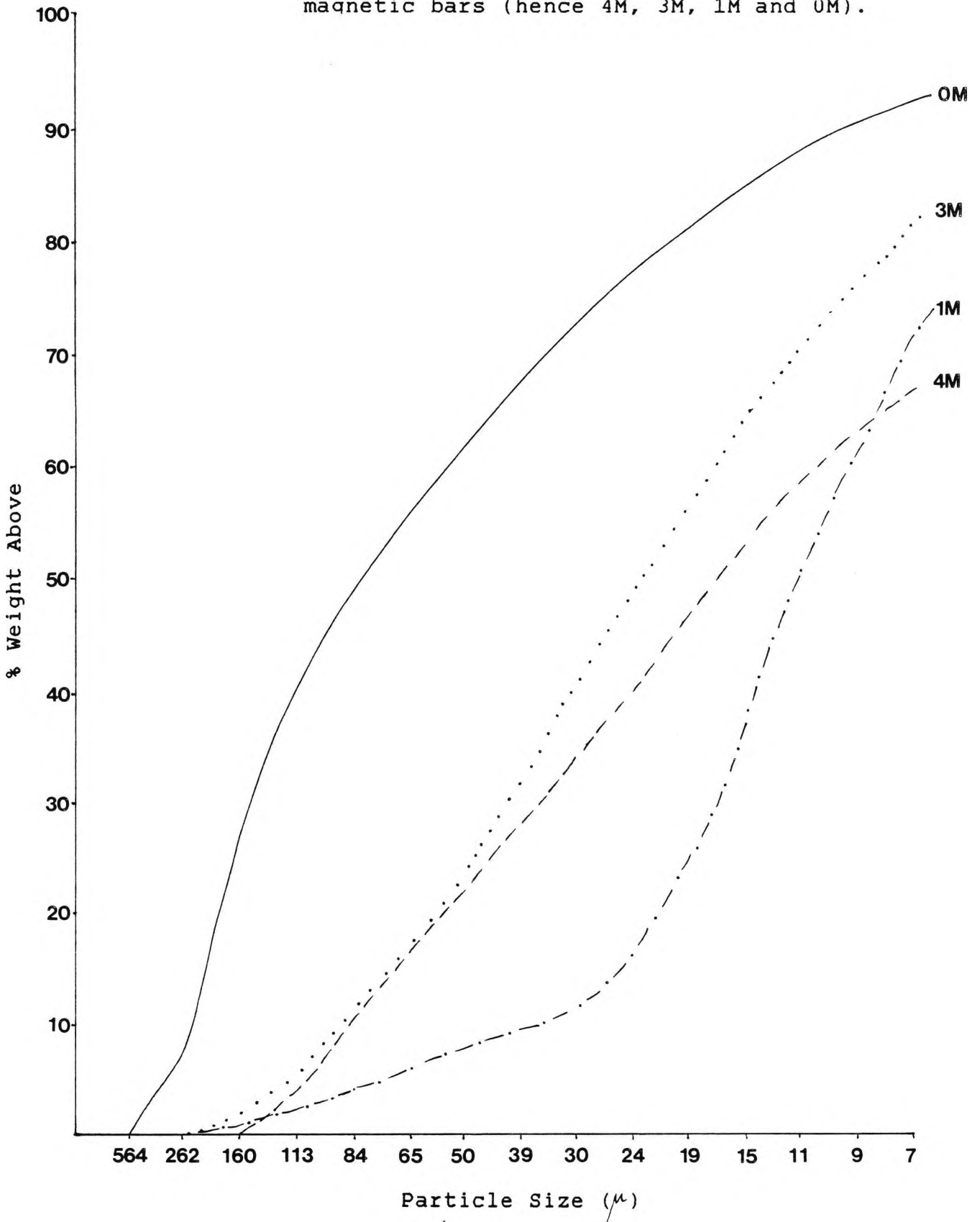


FIGURE 2.18 Percentage weight above against particle size of calcium sulphate precipitated after four and a half hours following treatment with HDL units containing four, three, one and zero magnetic bars (hence 4M, 3M, 1M and 0M).

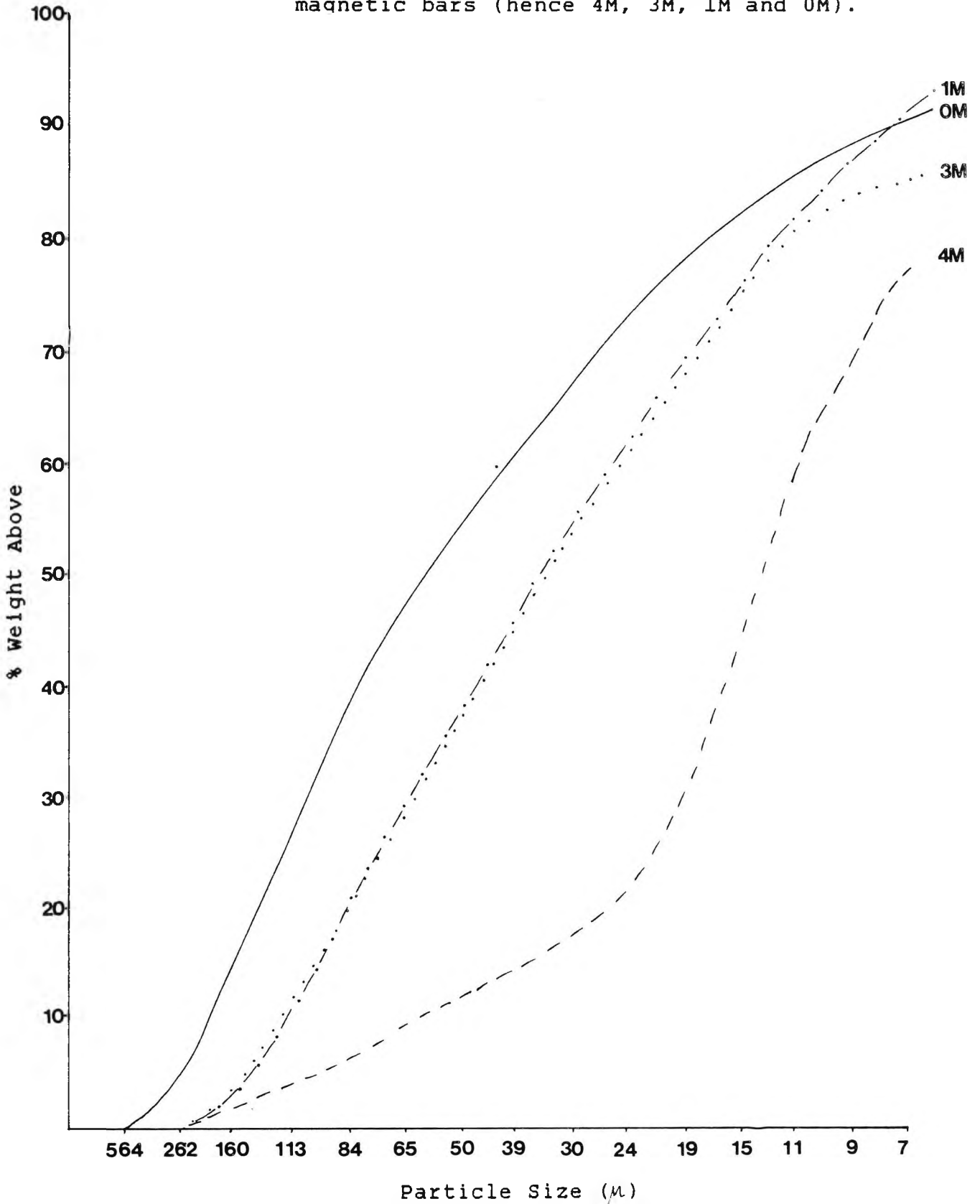


FIGURE 2.19 Percentage weight above against particle size of calcium sulphate precipitated after one day following treatment with HDL units containing four, three, one and zero magnetic bars (hence 4M, 3M, 1M and 0M).

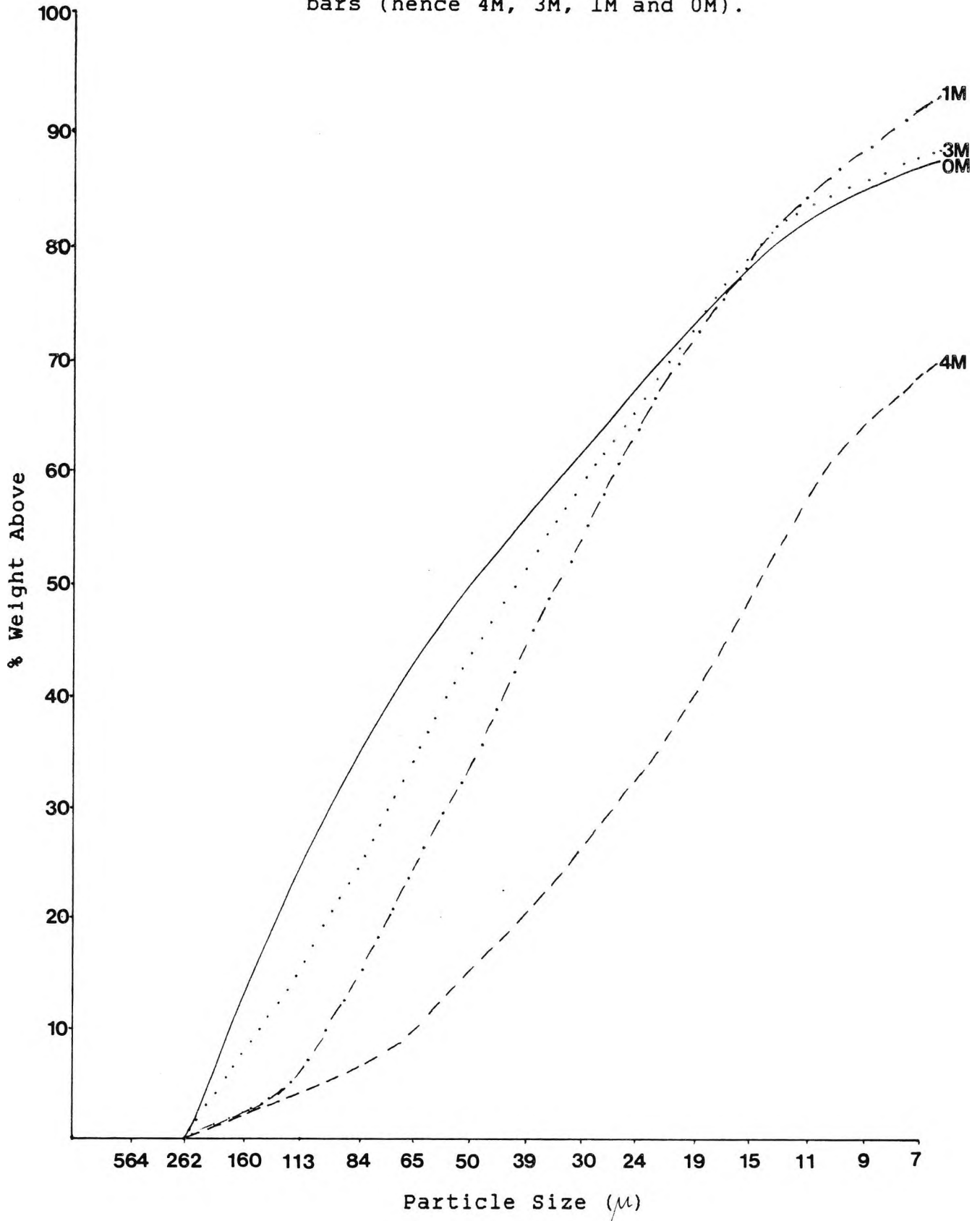


FIGURE 2.20 Percentage weight above against particle size of calcium sulphate precipitated after two days following treatment with HDL units containing four, three, one and zero magnetic bars (hence 4M, 3M, 1M and 0M).

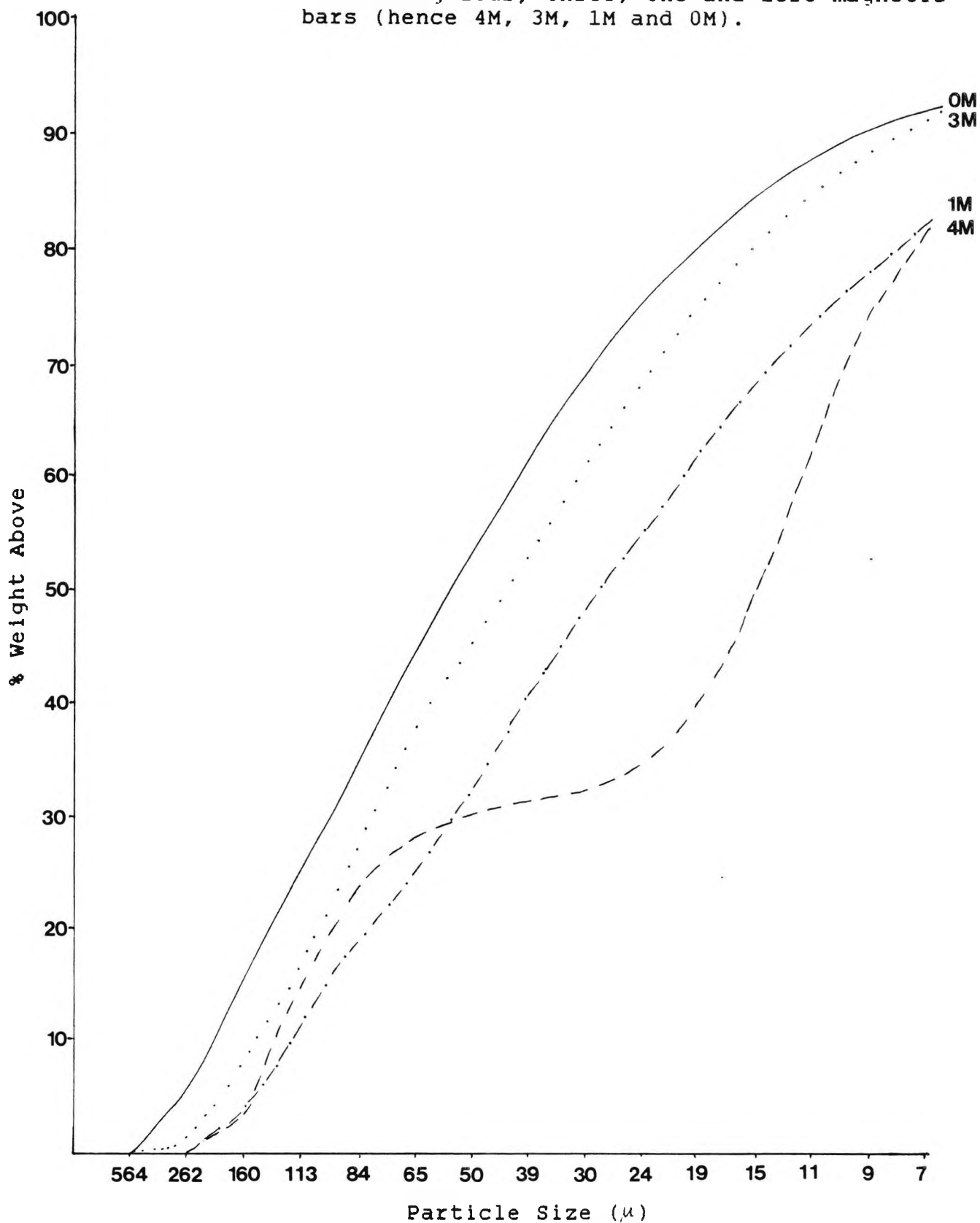
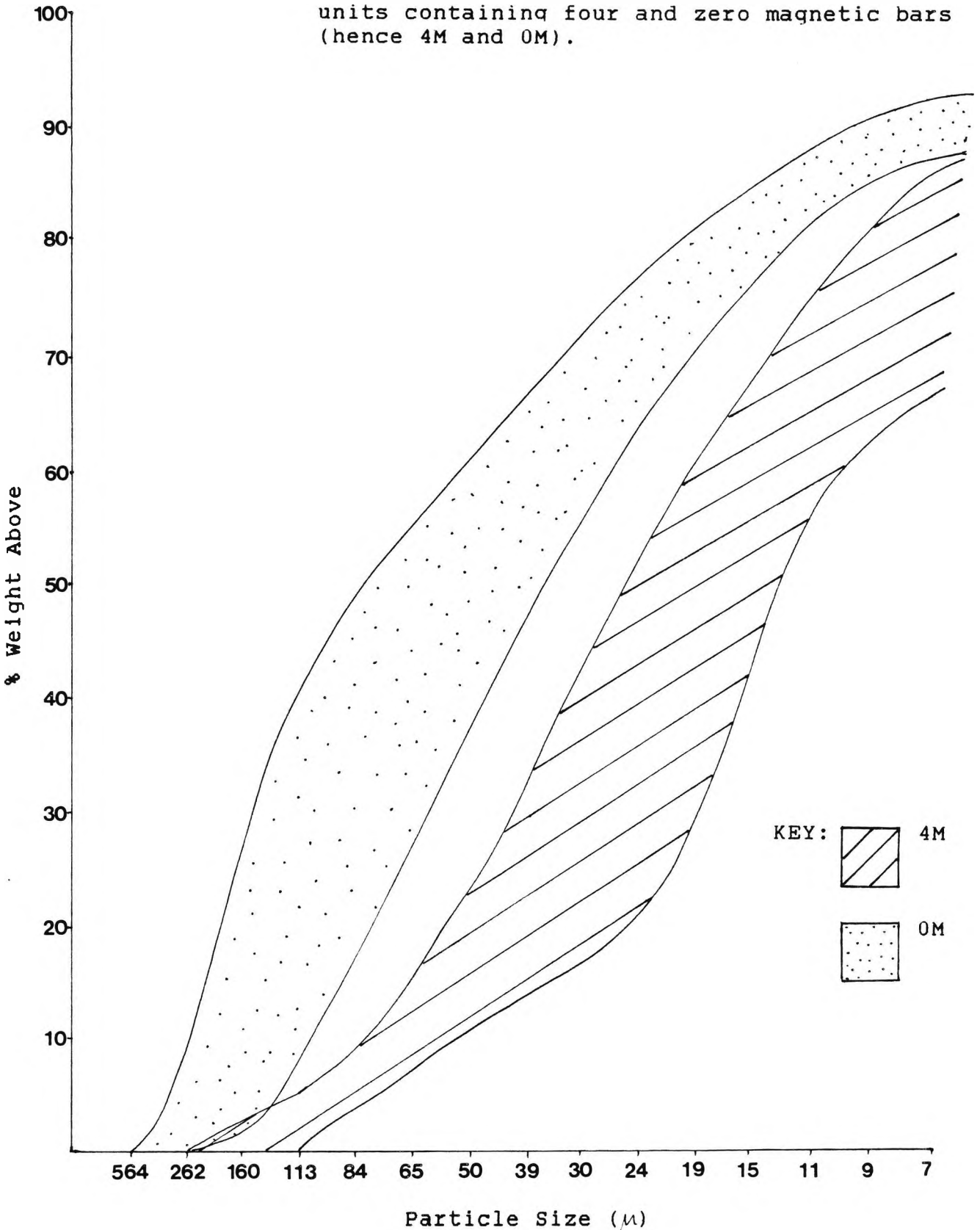
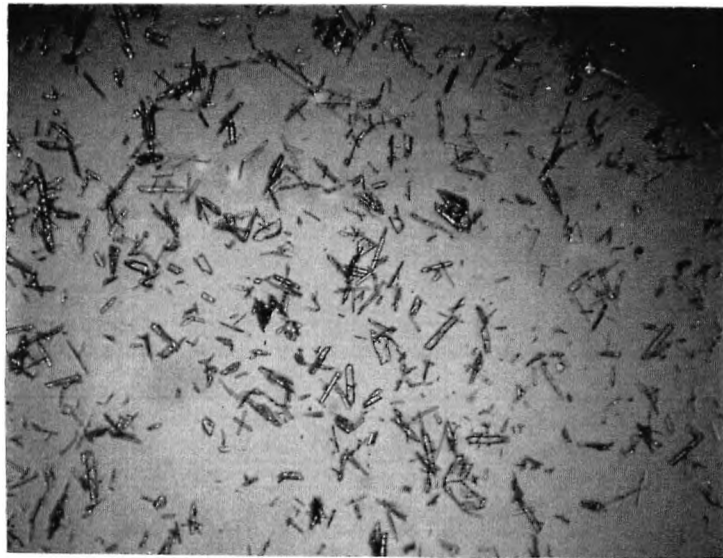
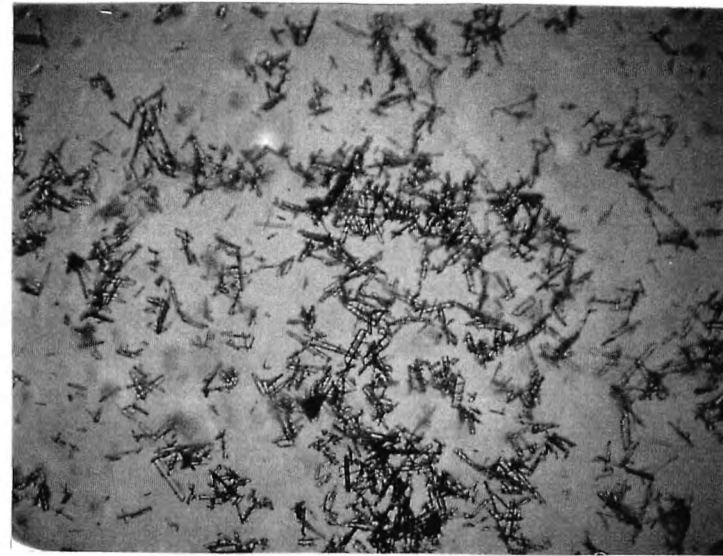


FIGURE 2.21 Compilation of data depicted in Figures 2.15 - 2.20 showing percentage weight above against particle size of calcium sulphate precipitated following treatment with HDL units containing four and zero magnetic bars (hence 4M and 0M).





(a) 4M



(b) 3M



(c) 1M

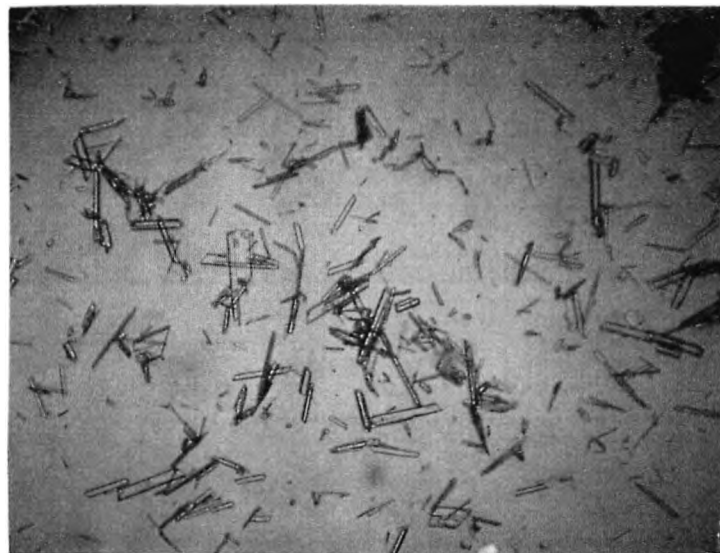


(d) 0M

**FIGURE 2.22** Optical Micrographs showing calcium sulphate dihydrate crystals precipitated, following treatment for one and a half hours with (a) four, (b) three, (c) one and (d) zero magnetic bars (hence 4M, 3M, 1M and 0M) [x50].



(a) 4M



(b) 3M

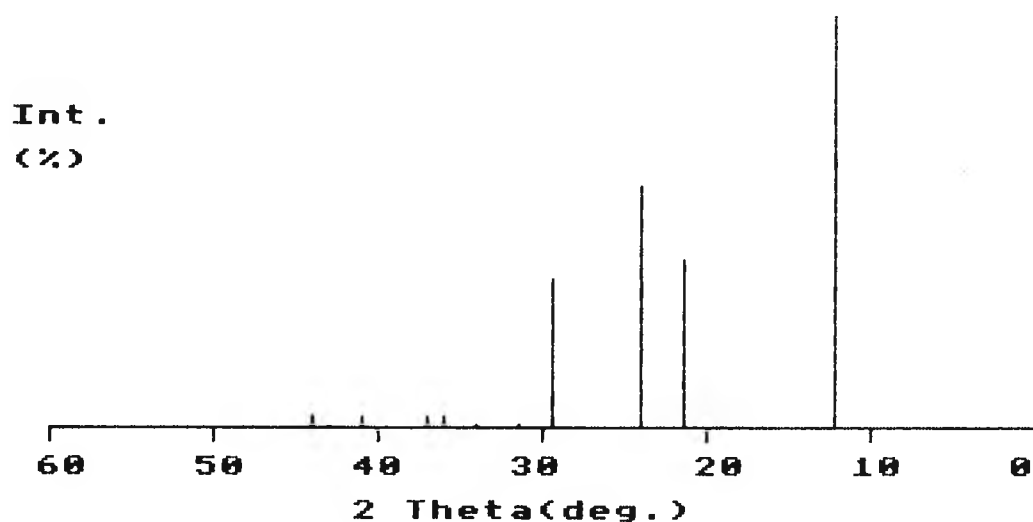


(c) 1M



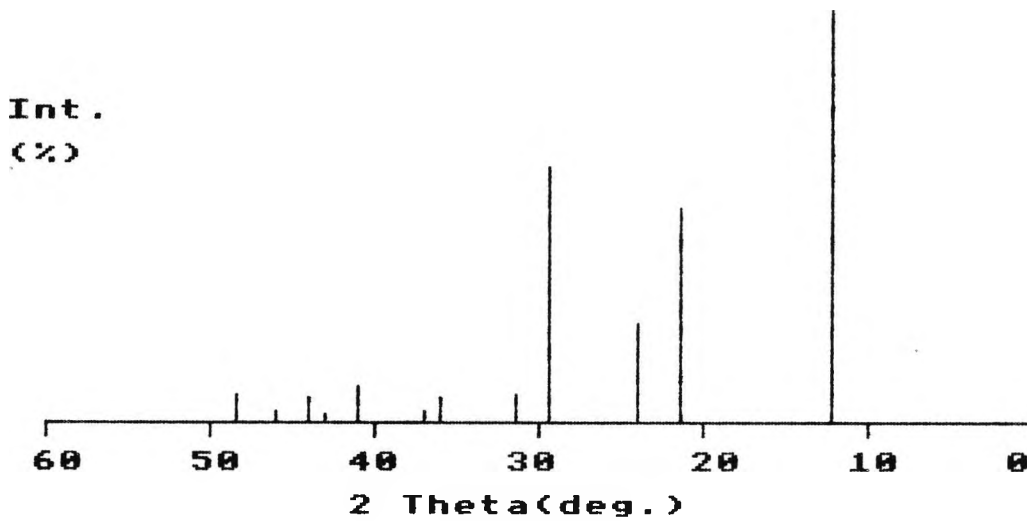
(d) 0M

**FIGURE 2.23** Optical Micrographs showing calcium sulphate dihydrate crystals precipitated, following treatment for four and a half hours with (a) four, (b) three, (c) one and (d) zero magnetic bars (hence 4M, 3M, 1M and 0M) [x50].



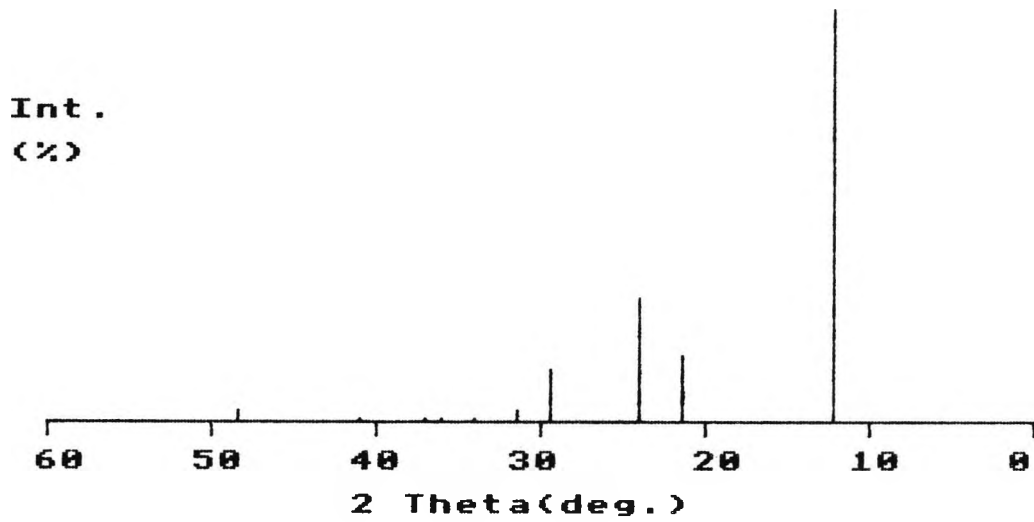
Rel. Int.	2theta	d
100	12.2	7.249
41	21.5	4.130
60	24.0	3.705
37	29.5	3.026
1	31.5	2.838
1	34.0	2.635
3	36.0	2.493
3	37.0	2.428
3	41.0	2.200
1	43.0	2.102
3	44.0	2.056

FIGURE 2.24(a) X-ray powder diffraction pattern for calcium sulphate dihydrate crystals precipitated following treatment for two days with a control unit.



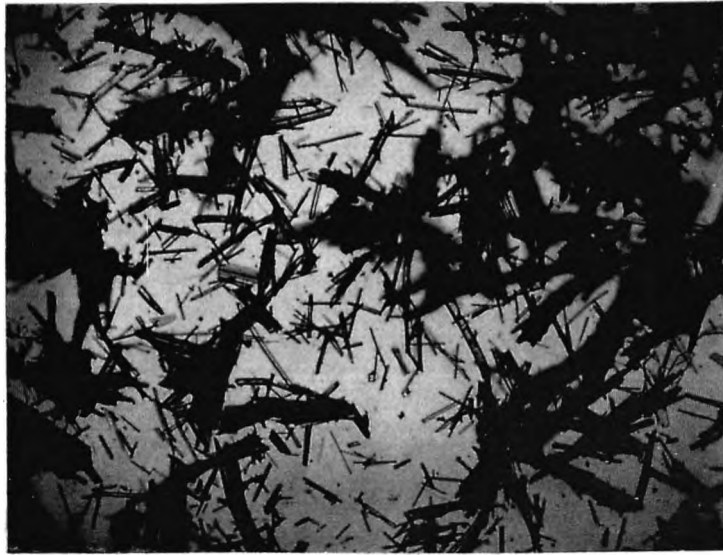
Rel. Int.	2theta	d
100	12.2	7.249
52	21.5	4.130
24	24.0	3.705
62	29.5	3.026
8	31.5	2.838
7	36.0	2.493
3	37.0	2.428
10	41.0	2.200
2	43.0	2.102
7	44.0	2.056
3	46.0	1.971
8	48.5	1.875

FIGURE 2.24(b) X-ray powder diffraction pattern for calcium sulphate dihydrate crystals precipitated following treatment for two days with a unit containing one magnetic bar.



Rel. Int.	2theta	d
100	12.2	7.249
17	21.5	4.130
30	24.0	3.705
13	29.5	3.026
3	31.5	2.838
1	34.0	2.635
1	36.0	2.493
1	37.0	2.428
1	41.0	2.200
3	48.5	1.875

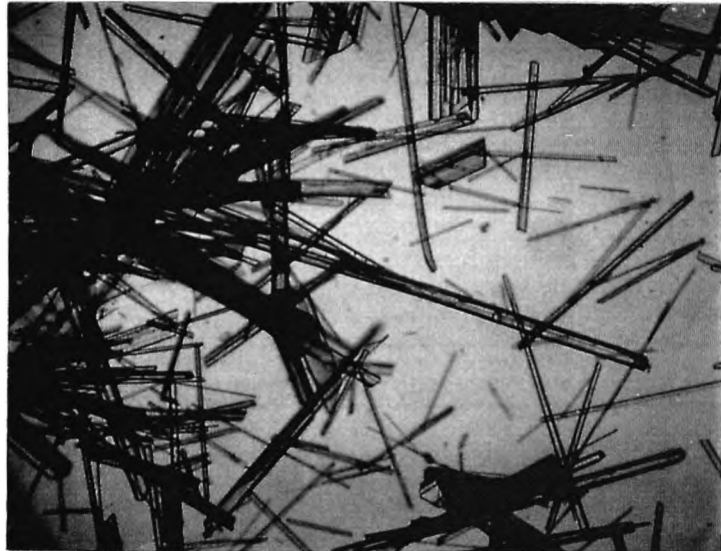
FIGURE 2.24(c) X-ray powder diffraction pattern for calcium sulphate dihydrate crystals precipitated following treatment for two days with a unit containing four magnetic bars.



(a) 4M



(b) 3M



(c) 2M



(d) 0M

**FIGURE 2.25** Optical micrographs showing calcium sulphate dihydrate crystals precipitated and evaporated, following treatment for five hours with (a) four, (b) three, (c) two and (d) zero magnetic bars (hence 4M, 3M, 2M and 0M) [x100].

particle size data are in Figs. 2.26 - 2.37. The optical micrographs obtained are shown in Figs. 2.38 and 2.39. Fig. 2.40 contains the X-ray powder diffraction results.

### 2.5.3 Precipitation of Barium Sulphate: A Comparison of the Effects Observed after passing a Solution through a Magnetic Field and through a Dummy.

5.0 litres of a 0.1M solution of  $\text{BaCl}_2 \cdot 2\text{H}_2\text{O}$  were passed through a known magnetic field for a duration of two hours. At timed intervals, 100ml aliquots were collected and 50ml of a saturated solution of  $\text{Na}_2\text{SO}_4 \cdot 10\text{H}_2\text{O}$  slowly added. This procedure was repeated using a control unit. The optical micrographs obtained are shown in Fig. 2.41.

## 2.6 Results

### Solubility Experiments

The solubility of both calcium phosphate and barium sulphate was found to increase, following magnetic treatment, in the case of the former, by 10%. Interestingly, these results are consistent with those obtained by Wheeler [24], at The City University, who found that the solubility of aluminium hydroxide increased after magnetic treatment, and with observations made on zinc phosphate solubilities in

FIGURE 2.26 Percentage weight above against particle size of calcium phosphate crystals precipitated after two and a half hours following treatment with HDL units containing four and zero magnetic bars (hence 4M and 0M).

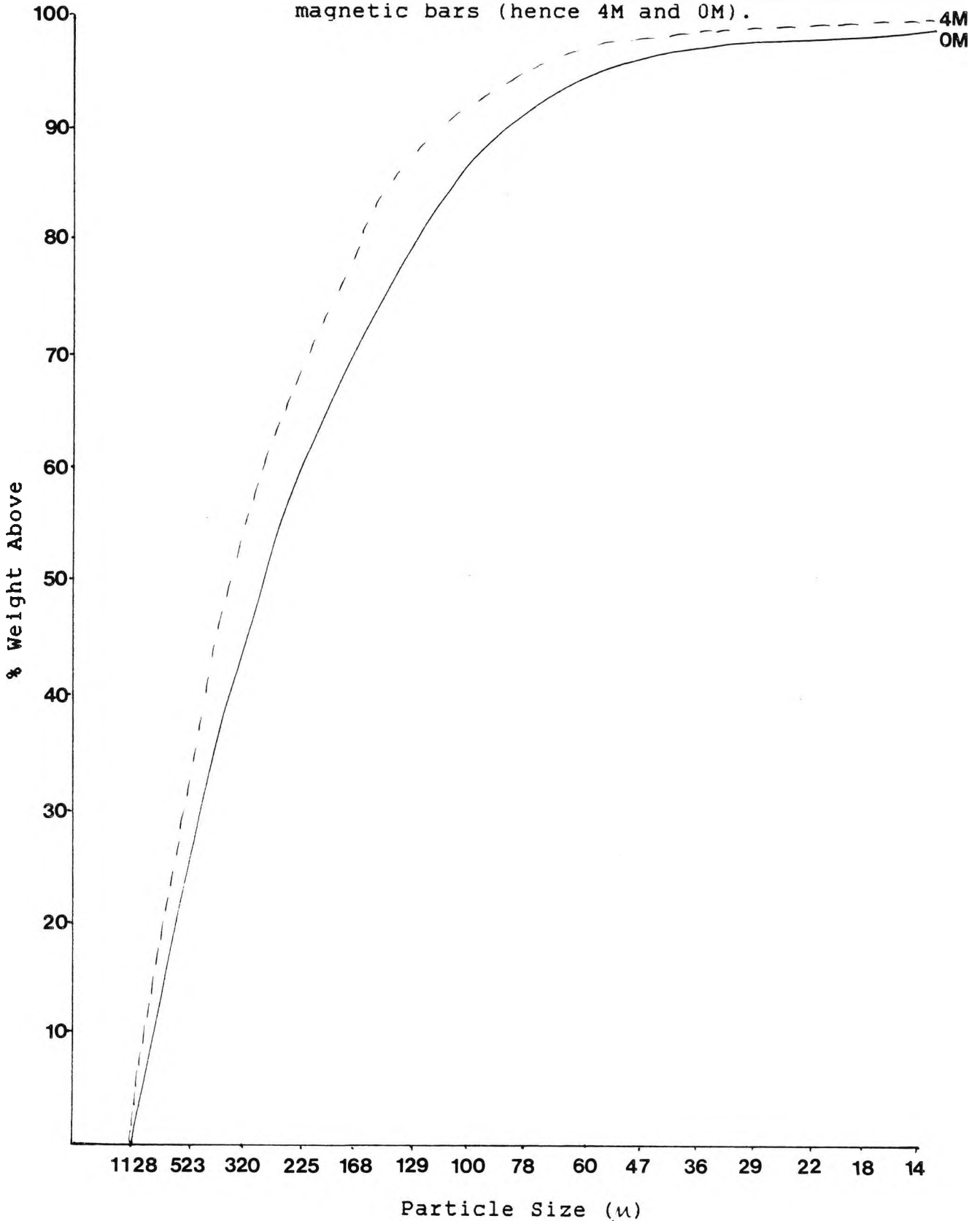


FIGURE 2.27 Percentage weight above against particle size of calcium phosphate crystals precipitated after four and a half hours following treatment with HDL units containing four and zero magnetic bars (hence 4M and 0M).

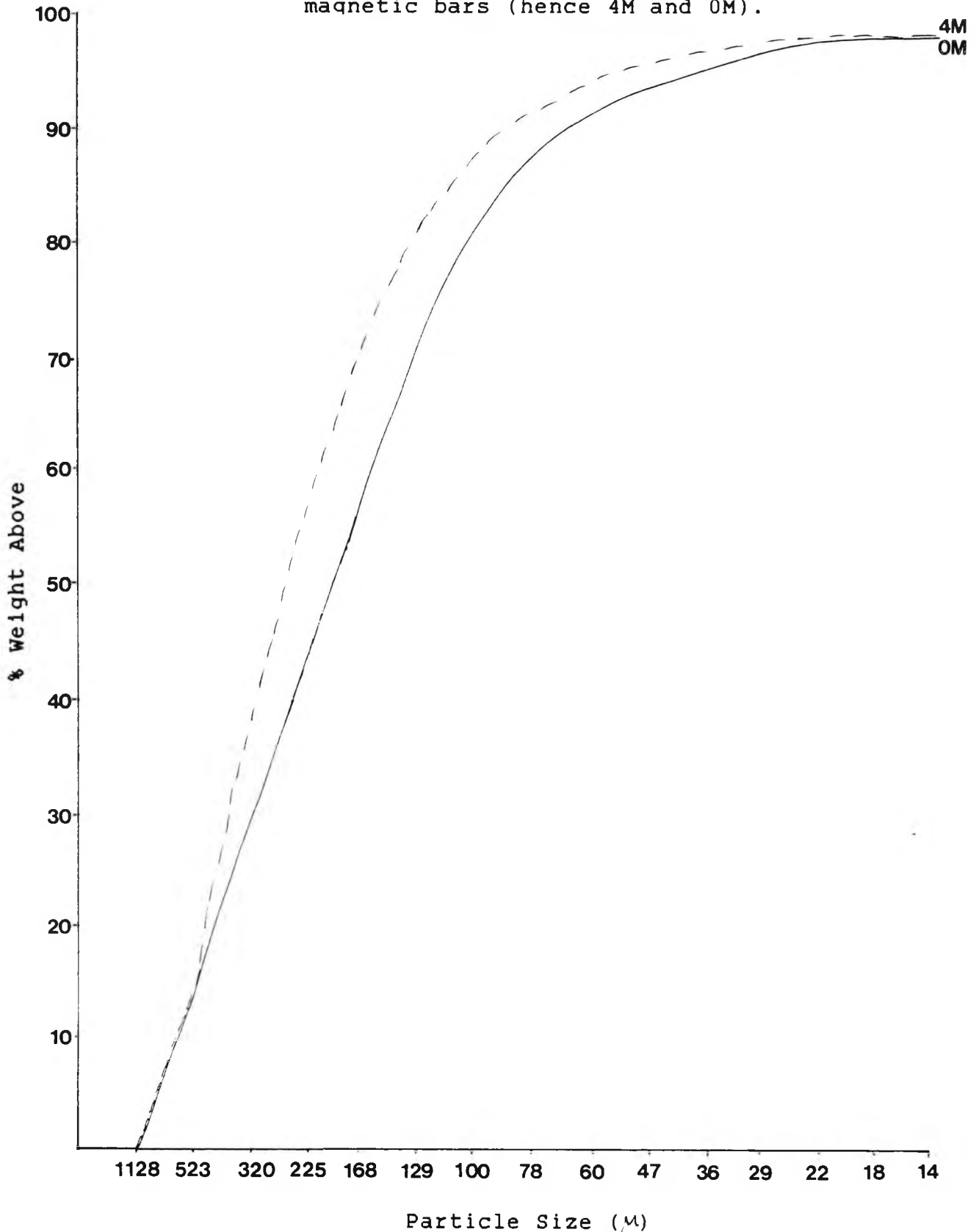


FIGURE 2.28      Compilation of data depicted in Figures 2.26 and 2.27 showing percentage weight above against particle size of calcium phosphate precipitated following treatment with HDL units containing four and zero magnetic bars (hence 4M and 0M).

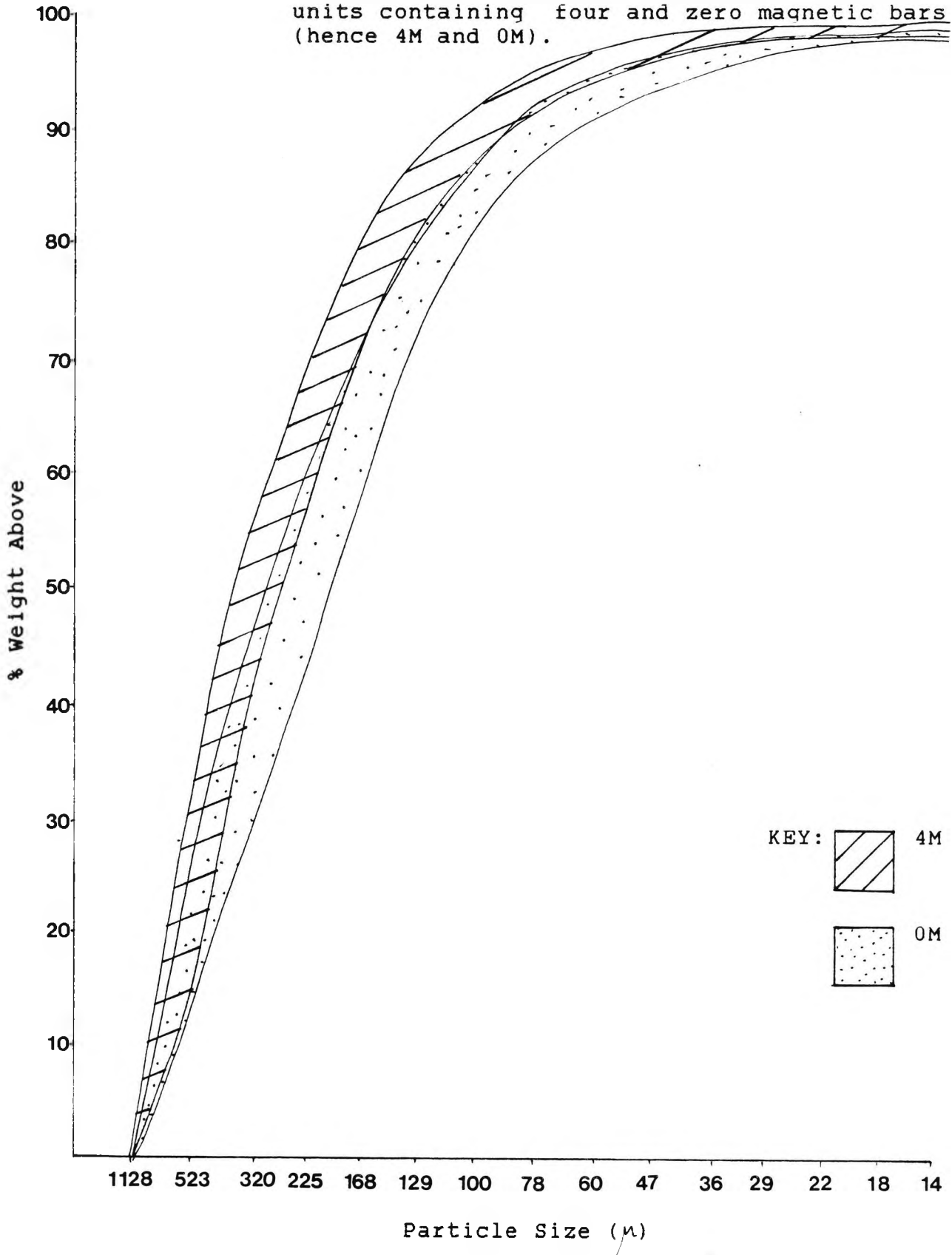


FIGURE 2.29 Percentage weight above against particle size of calcium phosphate crystals precipitated after two and a half hours following treatment with HDL units containing two and zero magnetic bars (hence 2M and 0M).

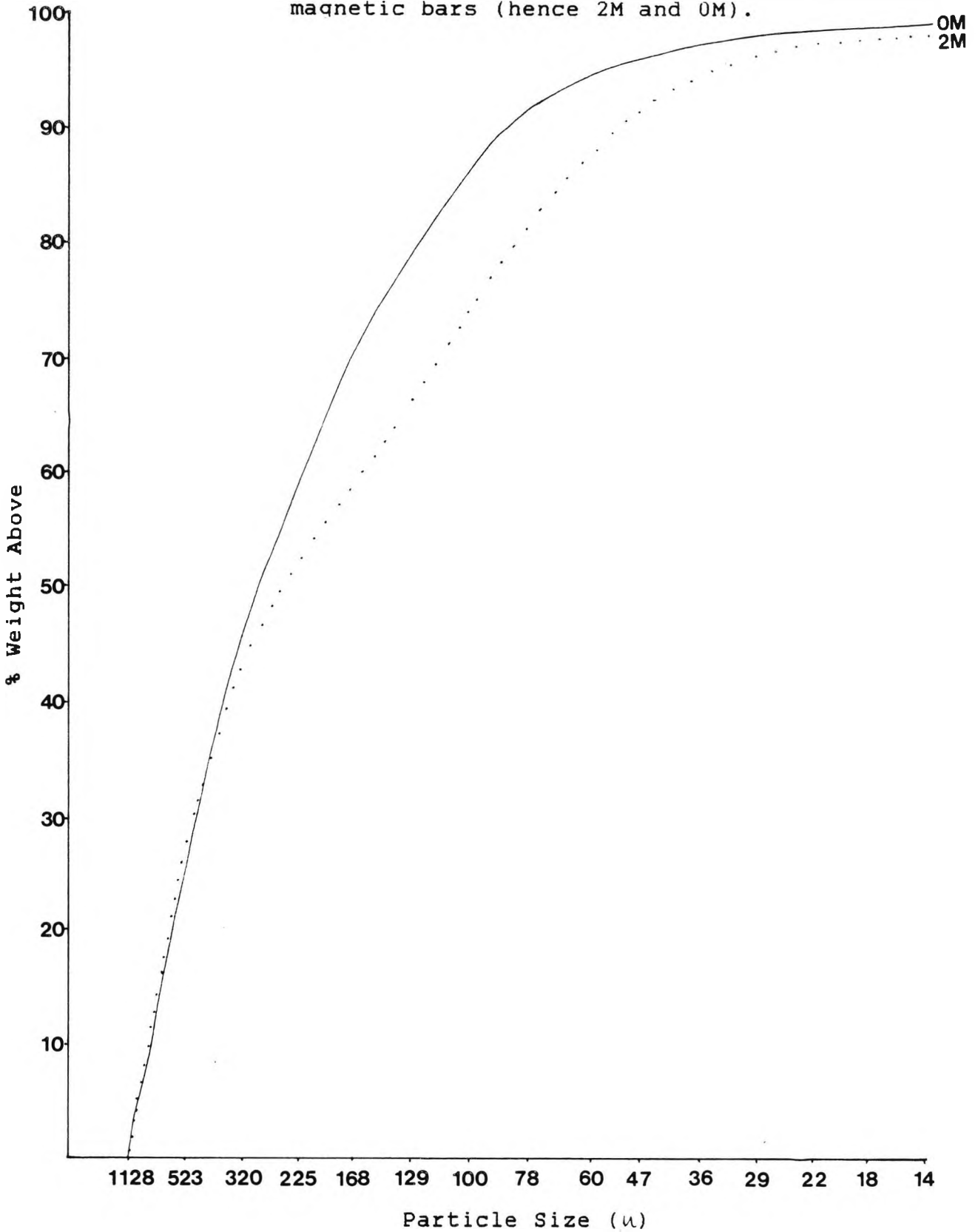


FIGURE 2.30 Percentage weight above against particle size of calcium phosphate crystals precipitated after four and a half hours following treatment with HDL units containing two and zero magnetic bars (hence 2M and 0M).

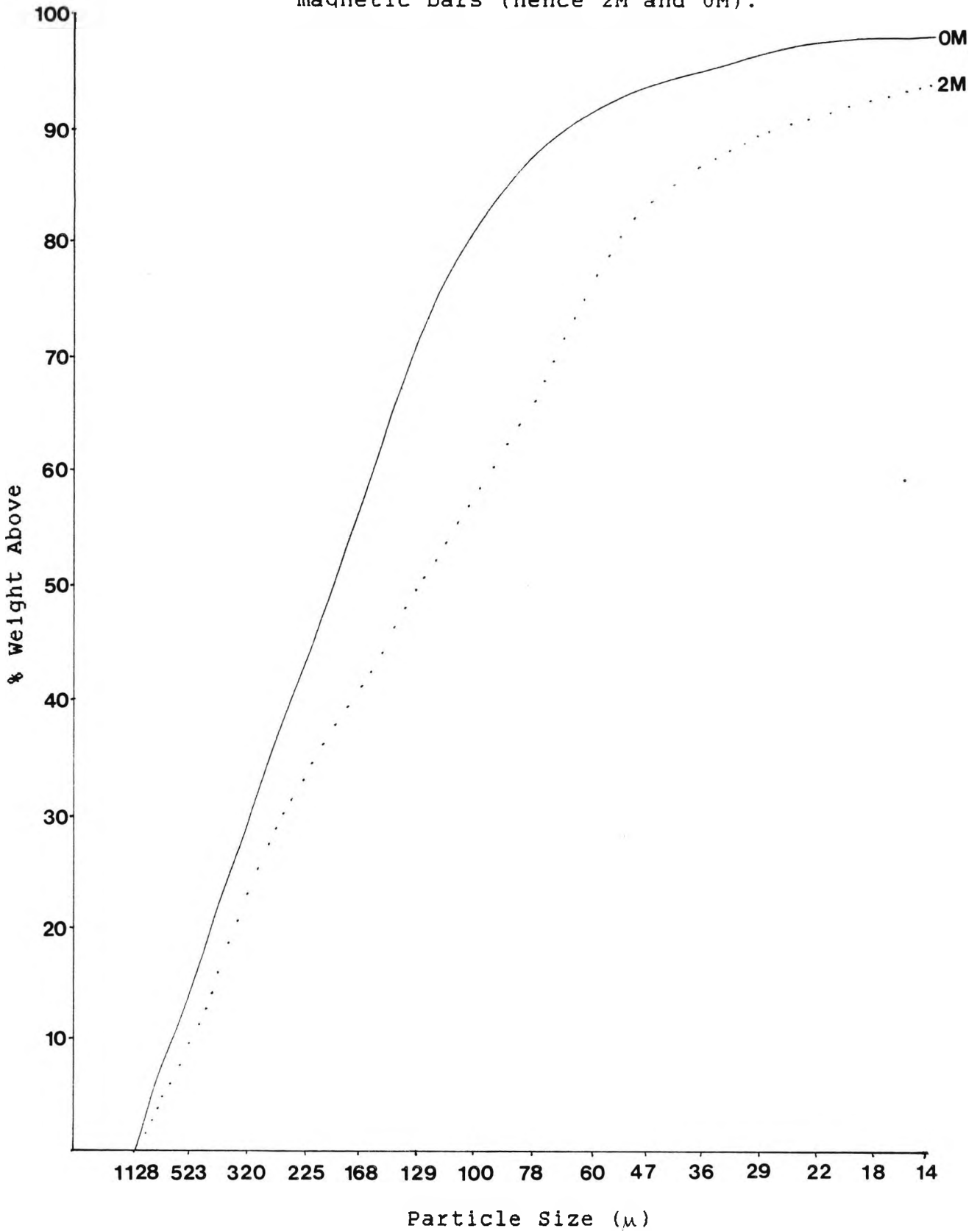


FIGURE 2.31 Compilation of data depicted in Figures 2.29 and 2.30 showing percentage weight above against particle size of calcium phosphate precipitated following treatment with HDL units containing two and zero magnetic bars (hence 2M and 0M).

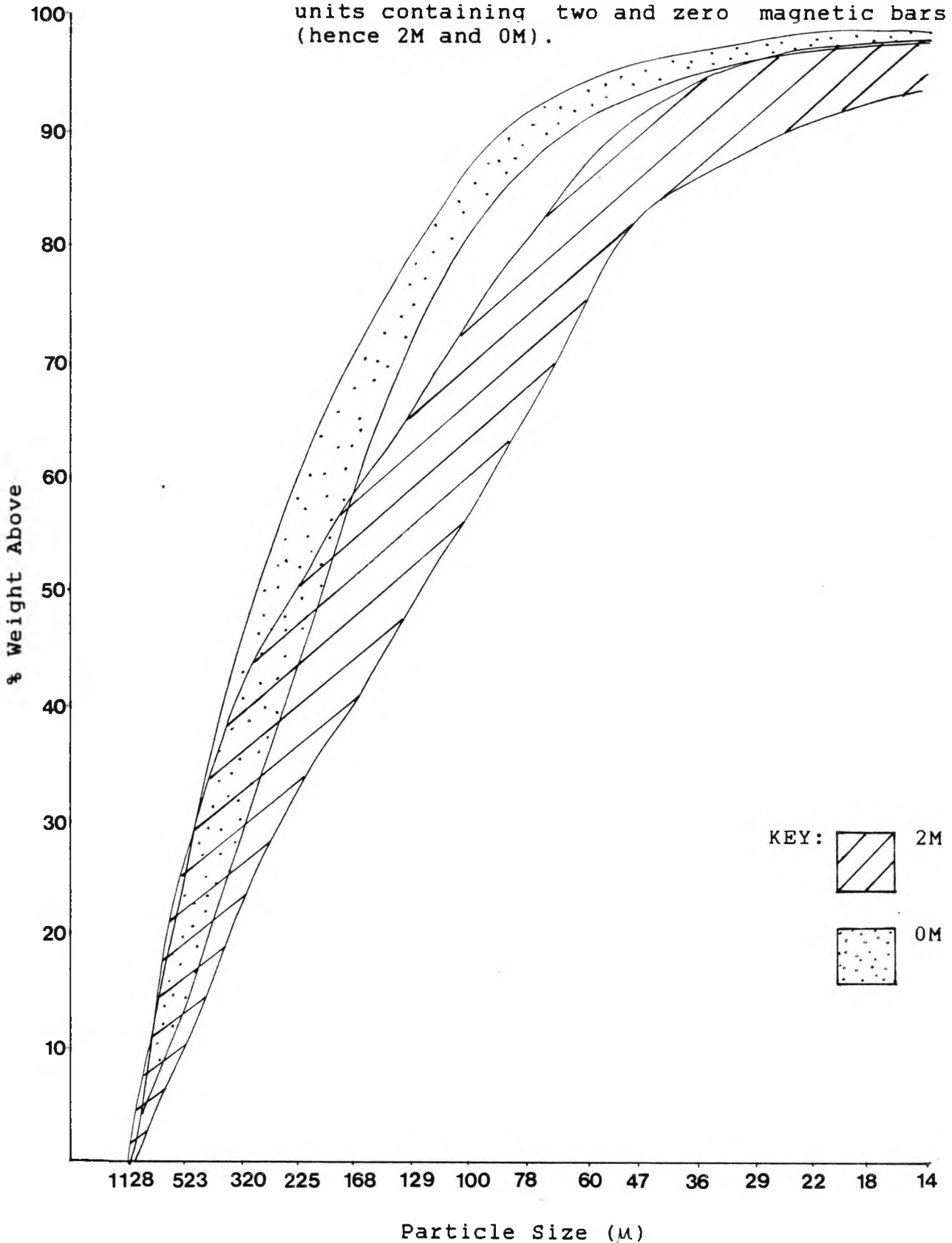


FIGURE 2.32 Percentage weight above against particle size of calcium phosphate crystals precipitated after two and a half hours following treatment with HDL units containing four and zero magnetic bars (hence 4M and 0M). (Repeat run).

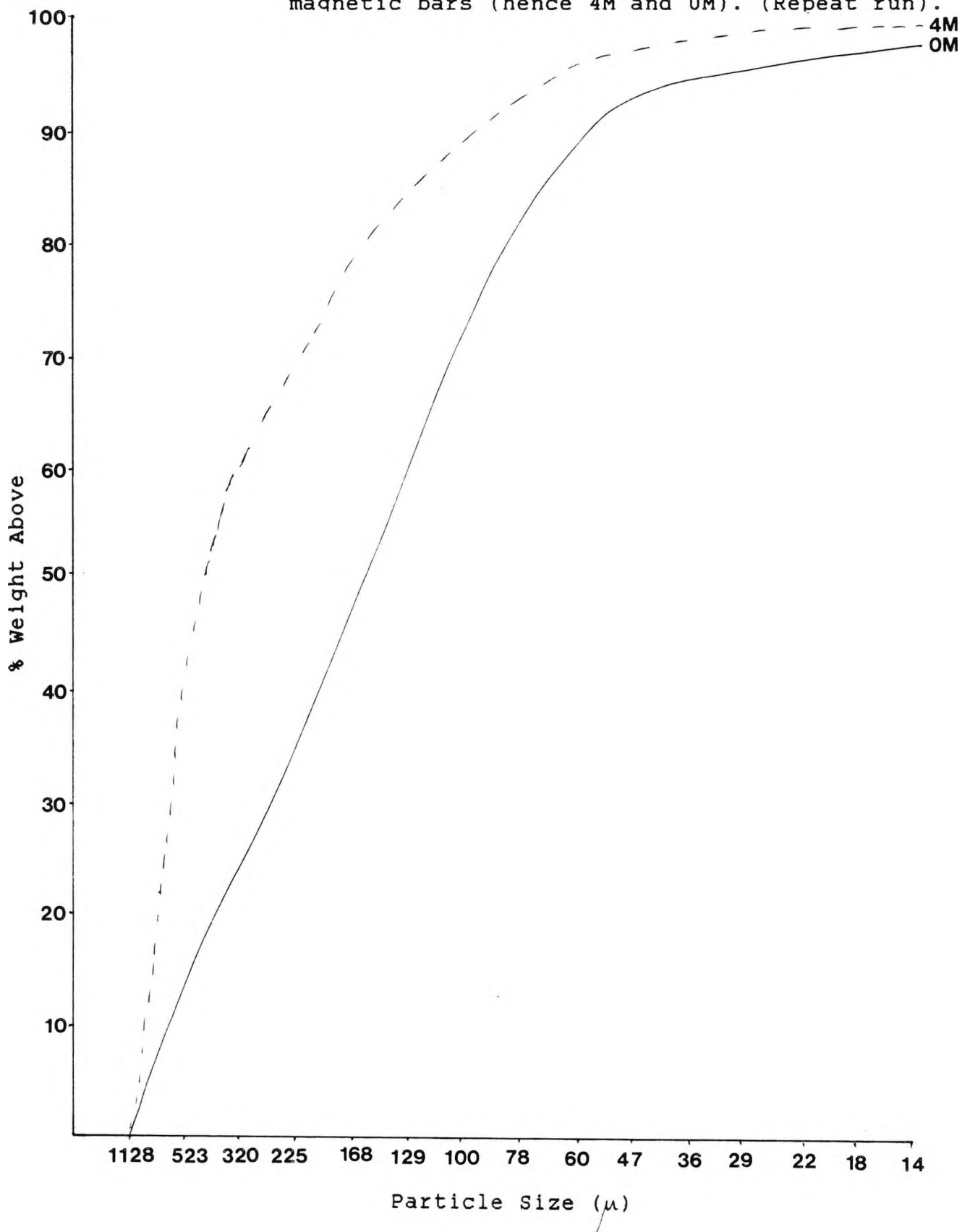


FIGURE 2.33 Percentage weight above against particle size of calcium phosphate crystals precipitated after four and a half hours following treatment with HDL units containing four and zero magnetic bars (hence 4M and 0M). (Repeat run.)

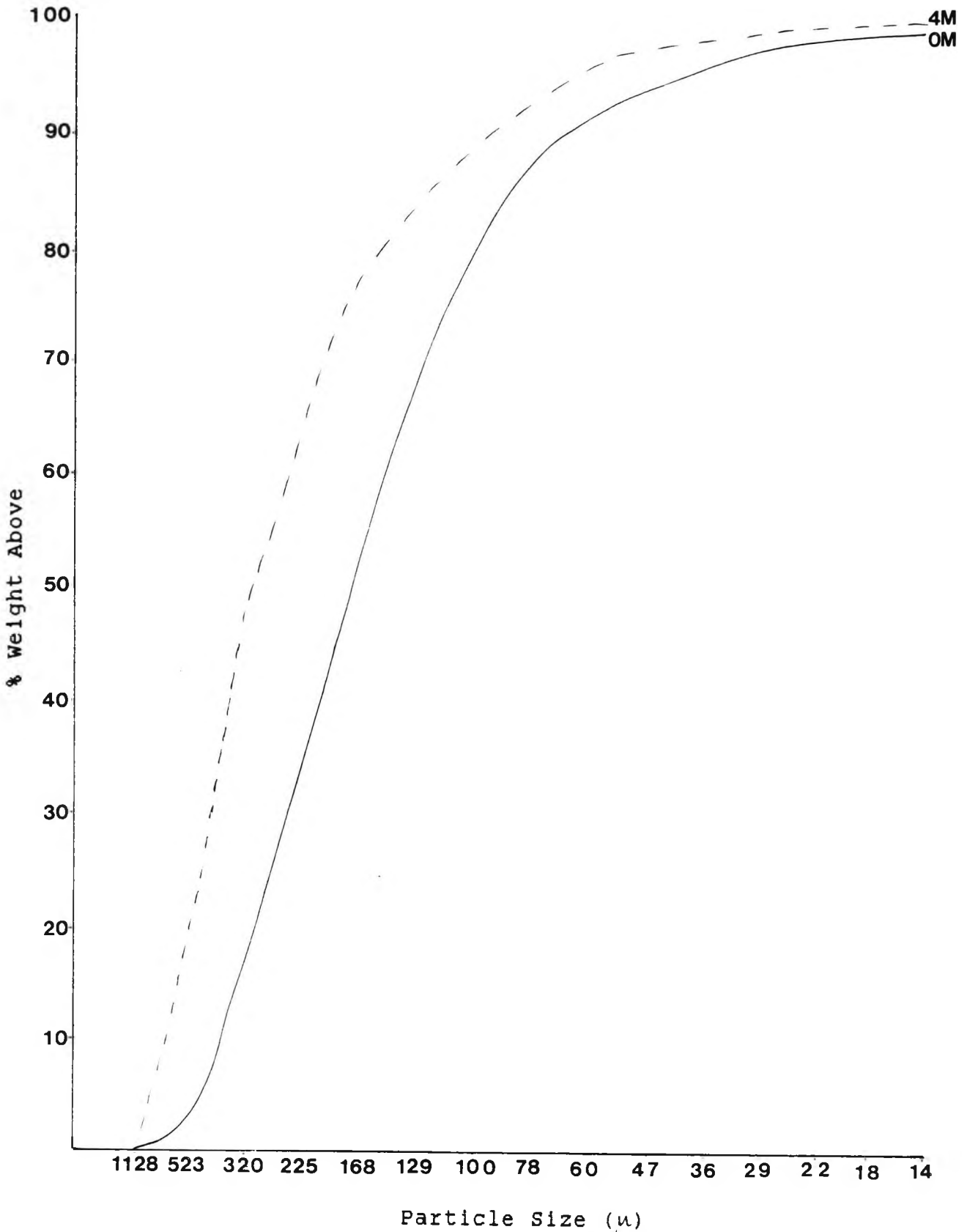


FIGURE 2.34 Compilation of data depicted in Figures 2.32 and 2.33 showing percentage weight above against particle size of calcium phosphate precipitated following treatment with HDL units containing four and zero magnetic bars (hence 4M and 0M). (Repeat run.)

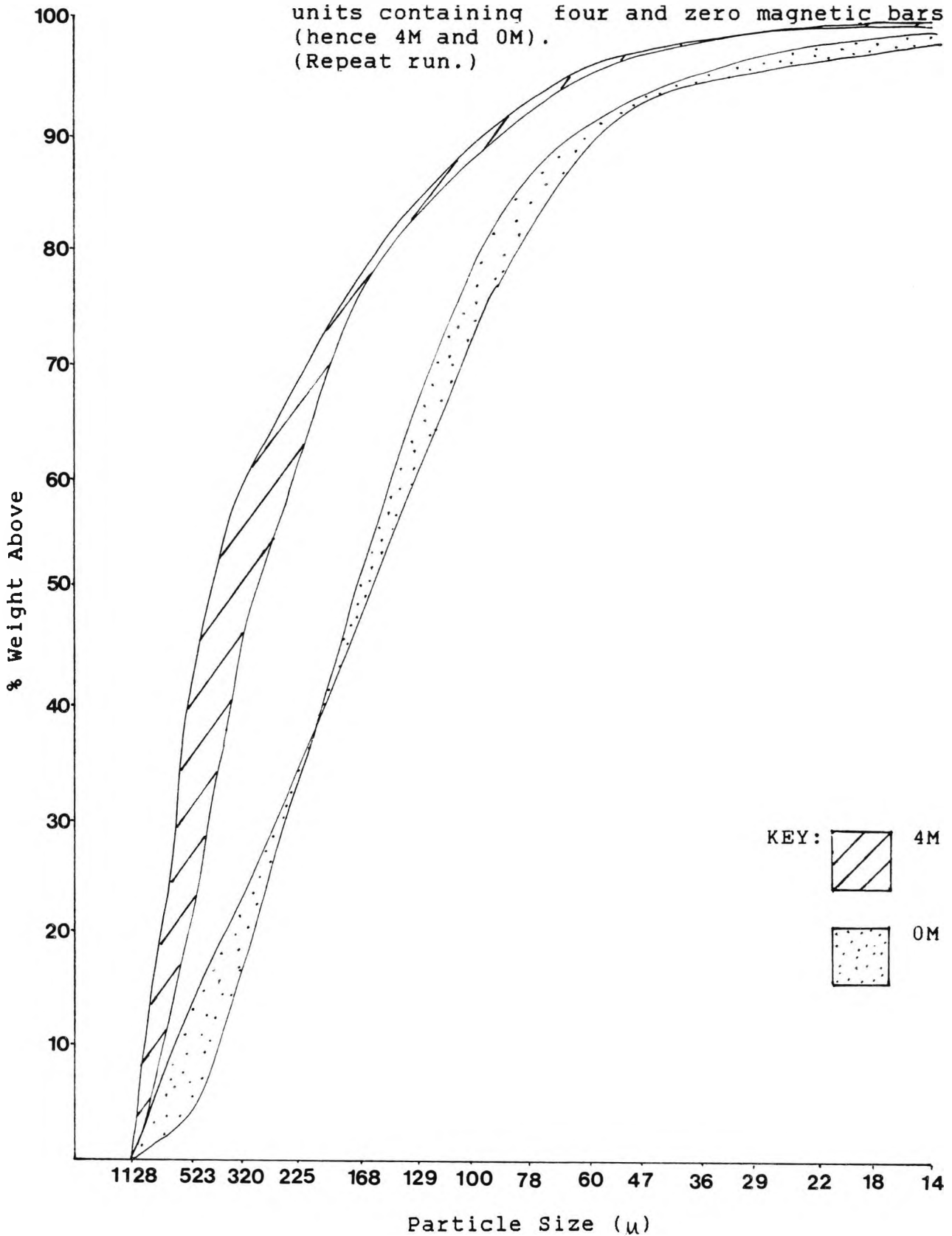


FIGURE 2.35 Percentage weight above against particle size of calcium phosphate crystals precipitated after two and a half hours following treatment with HDL units containing two and zero magnetic bars (hence 2M and 0M). (Repeat run.)

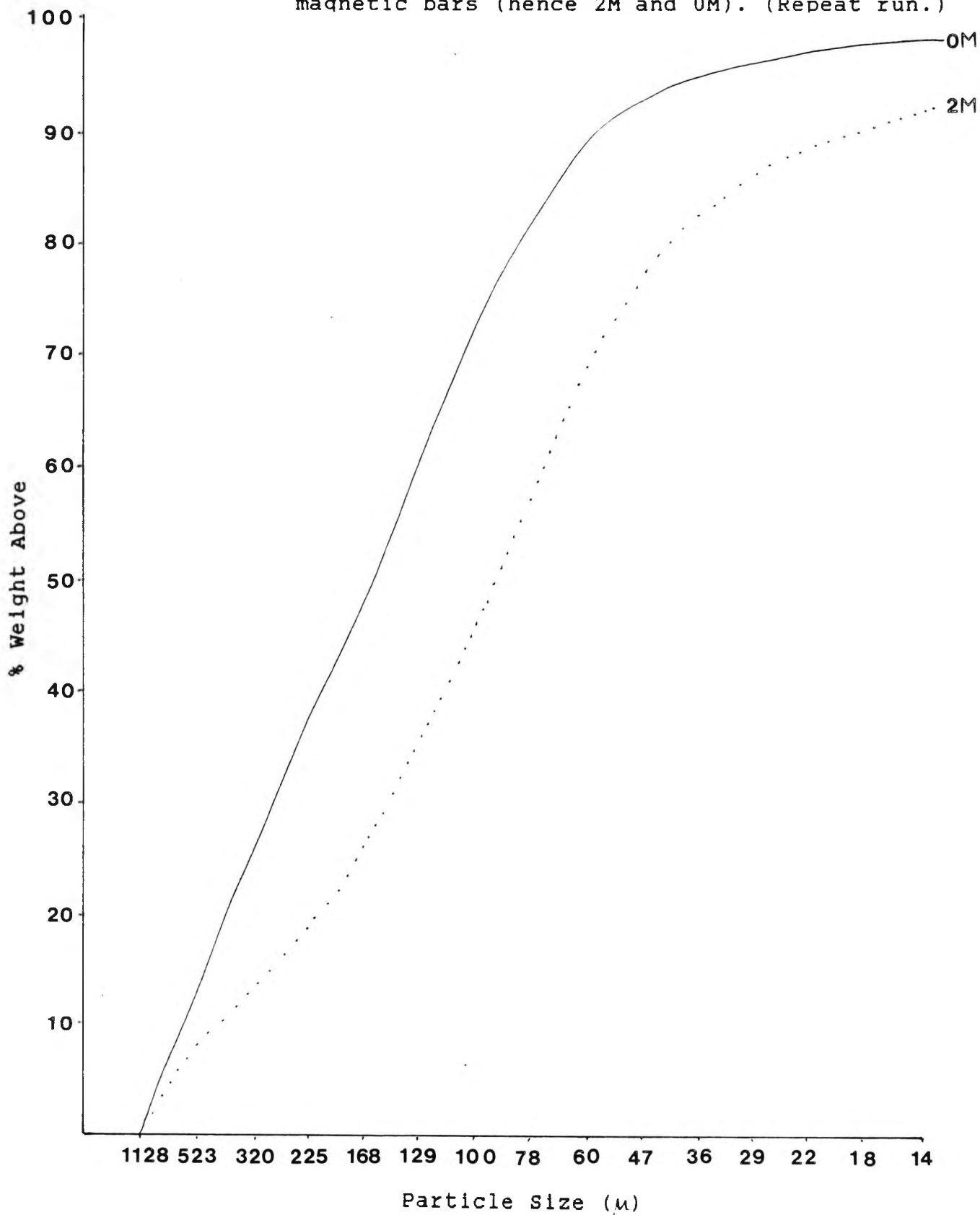


FIGURE 2.36 Percentage weight above against particle size of calcium phosphate crystals precipitated after four and a half hours following treatment with HDL units containing two and zero magnetic bars (hence 2M and 0M). (Repeat run.)

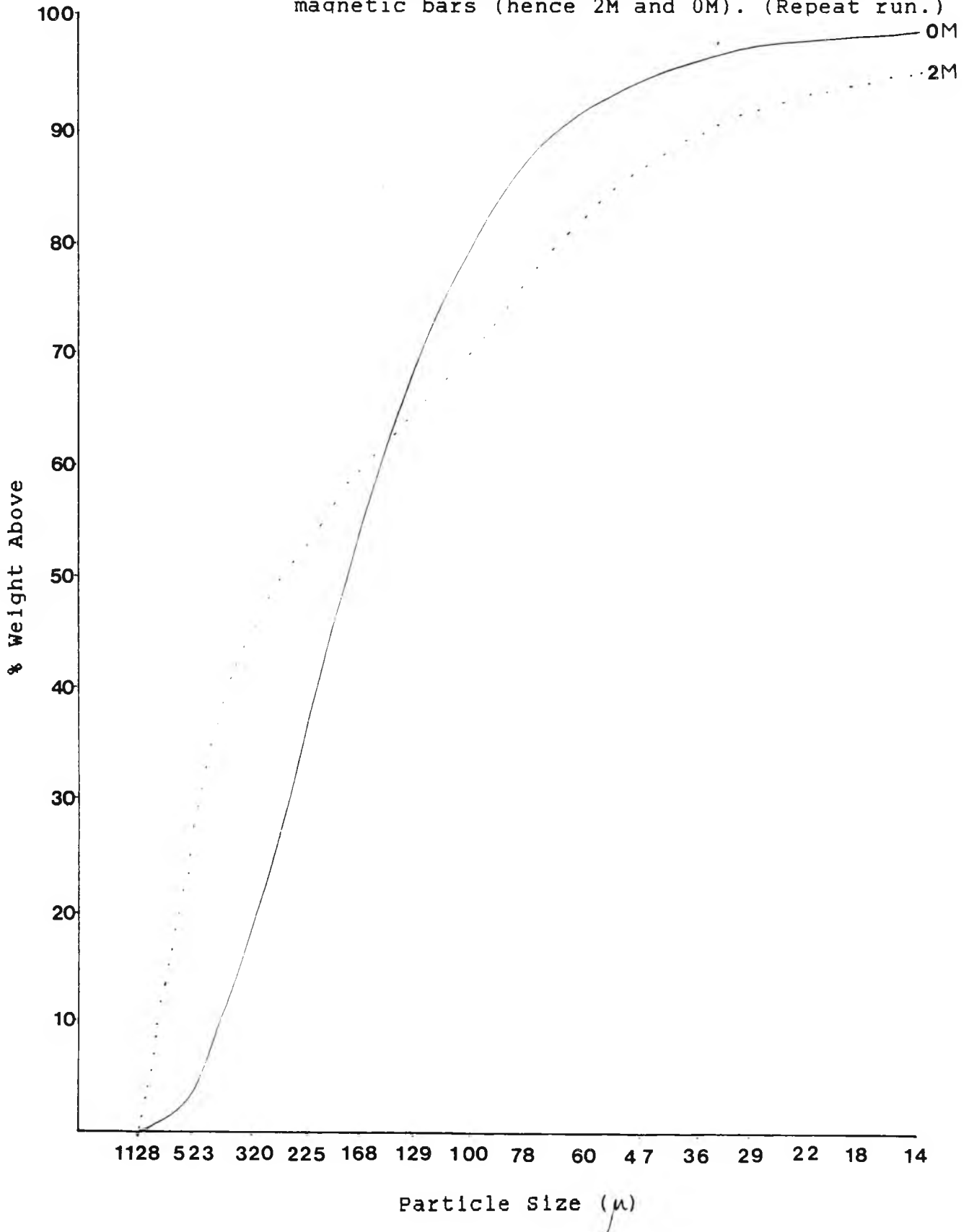
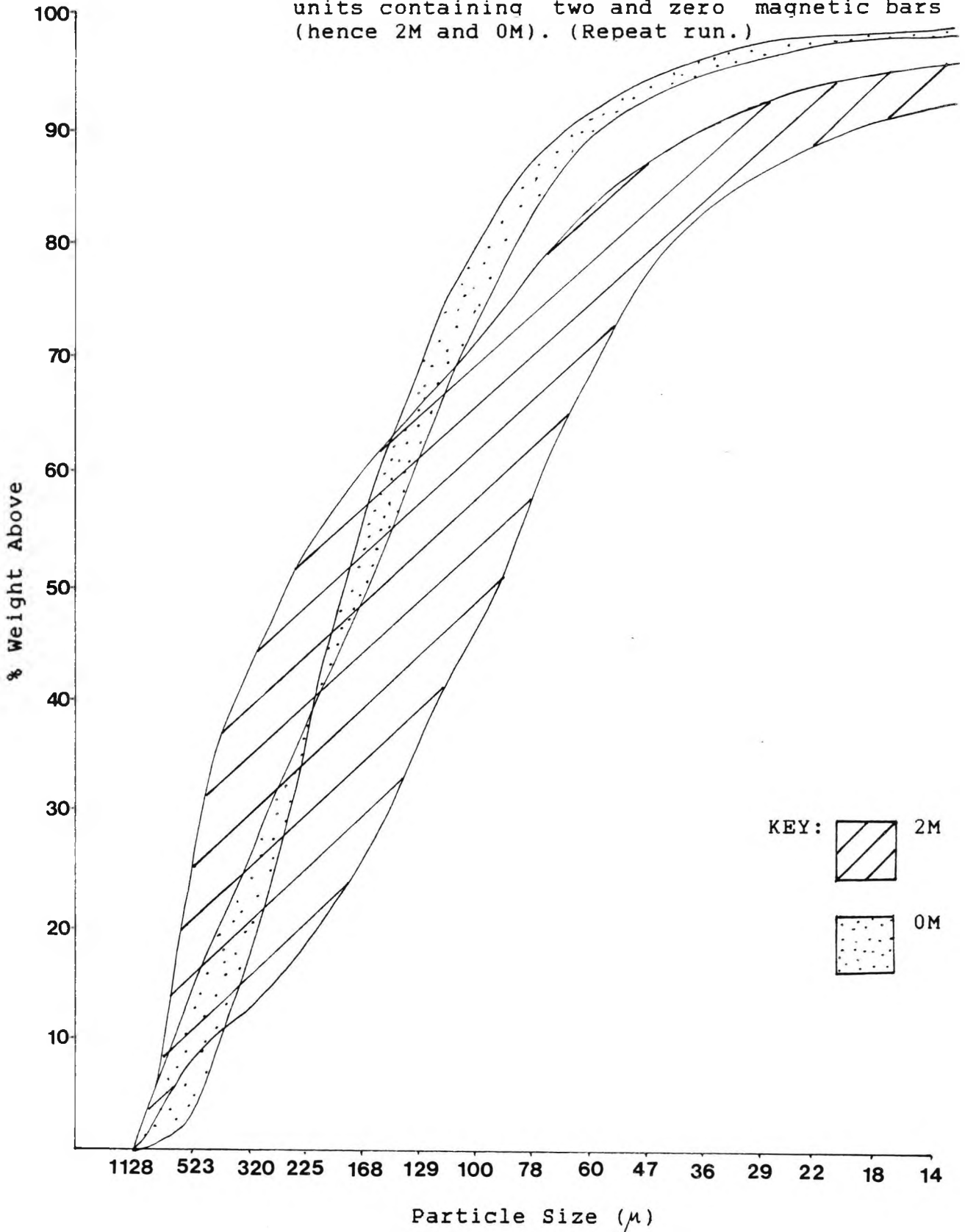


FIGURE 2.37      Compilation of data depicted in Figures 2.35 and 2.36 showing percentage weight above against particle size of calcium phosphate precipitated following treatment with HDL units containing two and zero magnetic bars (hence 2M and 0M). (Repeat run.)

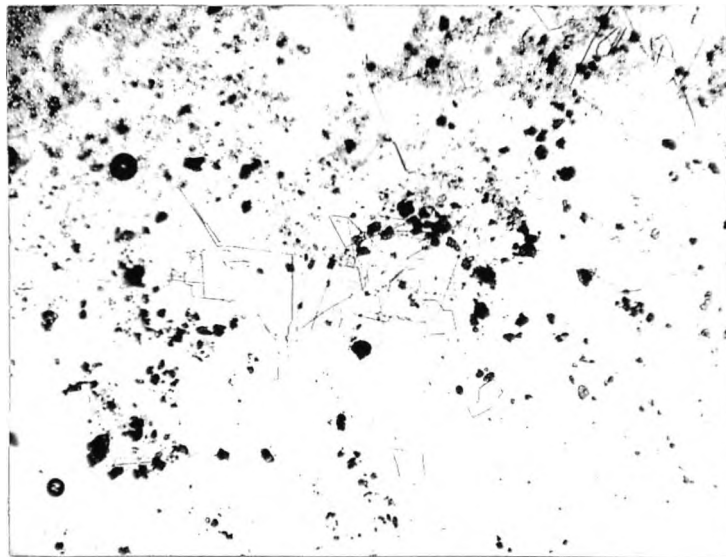




(a) 4M



(b) 3M



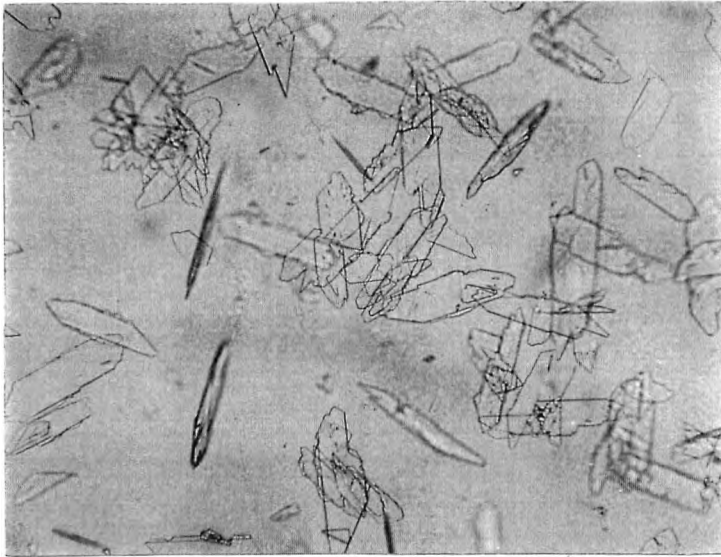
(c) 2M



(d) 0M

**FIGURE 2.38**

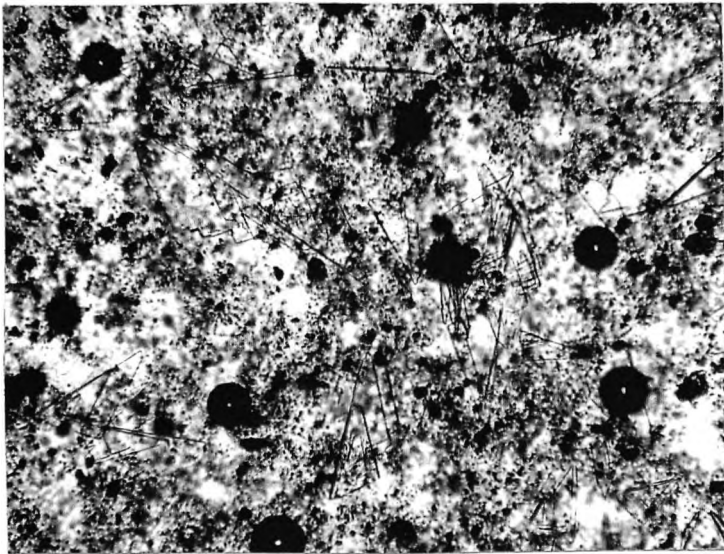
Optical micrographs showing calcium phosphate crystals precipitated, following treatment for one and a half hours with (a) four, (b) three, (c) two and (d) zero magnetic bars (hence 4M, 3M, 2M and 0M) [x73].



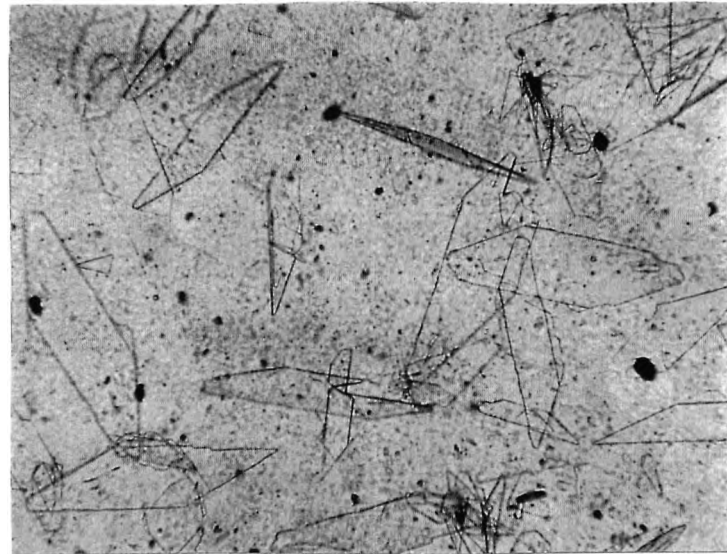
(a) 4M



(b) 3M



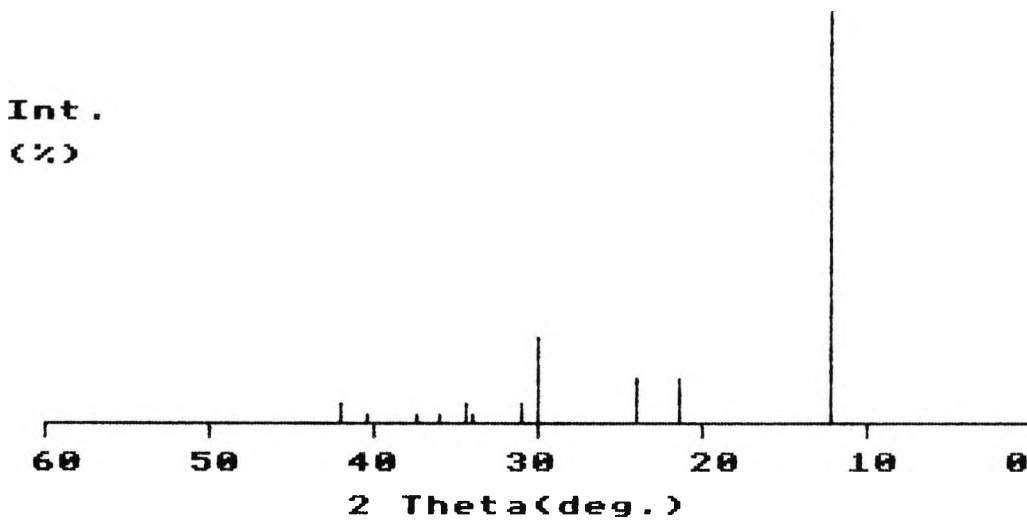
(c) 2M



(d) 0M

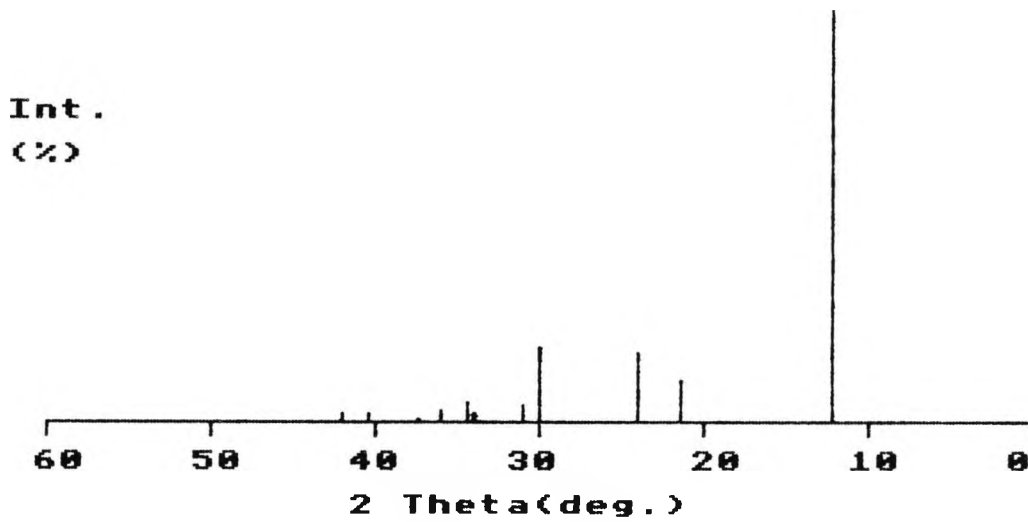
**FIGURE 2.39**

Optical micrographs showing calcium phosphate crystals precipitated, following treatment for two days with (a) four, (b) three, (c) two and (d) zero magnetic bars (hence 4M, 3M, 2M and 0M) [x73].



Rel. Int.	2theta	d
100	12.3	7.190
11	21.5	4.130
11	24.0	3.705
21	30.0	2.976
6	31.0	2.882
2	34.0	2.635
6	34.5	2.598
2	36.0	2.493
2	37.5	2.396
2	40.5	2.226
6	42.0	2.149

FIGURE 2.40(a) X-ray powder diffraction pattern for calcium phosphate crystals precipitated following treatment for two minutes with a control unit.



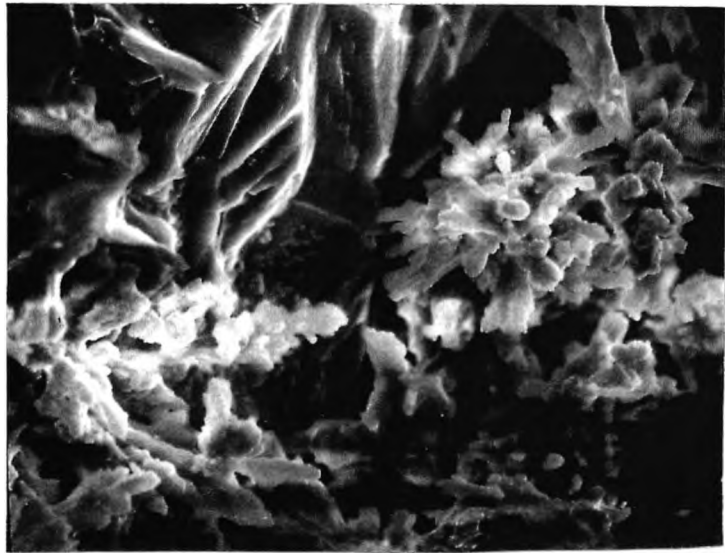
Rel. Int.	2theta	d
100	12.3	7.190
10	21.5	4.130
18	24.0	3.705
19	30.0	2.976
4	31.0	2.882
2	34.0	2.635
6	34.5	2.598
3	36.0	2.493
1	37.5	2.396
2	40.5	2.226
2	42.0	2.149

FIGURE 2.40(b) X-ray powder diffraction pattern for calcium phosphate crystals precipitated following treatment for two minutes with a unit containing two magnetic bars.

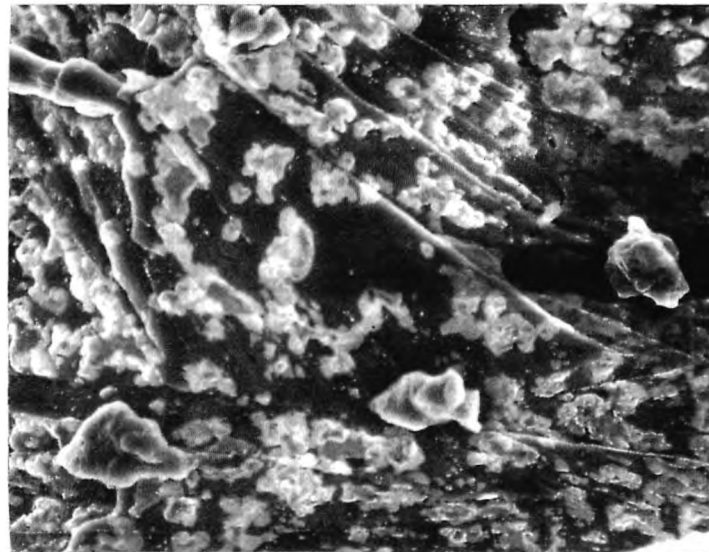


Rel. Int.	2theta	d
100	12.3	7.190
16	21.5	4.130
10	24.0	3.705
13	30.0	2.976
7	31.0	2.882
4	34.5	2.598
1	36.0	2.493
1	37.5	2.396
2	42.0	2.149

FIGURE 2.40(c) X-ray powder diffraction pattern for calcium phosphate crystals precipitated following treatment for two days with a unit containing four magnetic bars.



(a) 4M



(b) 0M

**FIGURE 2.41**

Electron micrographs showing barium sulphate crystals precipitated, following treatment for one hour with (a) four and (b) zero magnetic bars (hence 4M and 0M) [x300].

industrially monitored trials in steel pretreatment plants.

### Precipitation Experiments

The particle size data in Figs. 2.15 - 2.21 show that there is always a difference between the control and the full magnetic unit although there is not always consistent behaviour with units of intermediate strength. Since the field geometries of the units of intermediate strength are not symmetrical, this may account for the differences in behaviour. The data shown in Fig. 2.21 have been compiled from all the results in Figs. 2.15 - 2.20 and clearly show that there is a significant reduction in particle sizes of calcium sulphate precipitates obtained with magnetic units compared to those obtained from solutions treated with the control unit. These observations have been confirmed by optical microscopy and the micrographs of  $\text{CaSO}_4 \cdot 2\text{H}_2\text{O}$  obtained after treatment with the control and magnetic units for 1.5, and 4.5 hours are in Figs. 2.22 and 2.23, respectively.

The X-ray diffraction powder patterns of all the precipitates obtained for the  $\text{Ca}^{2+}\text{-SO}_4^{2-}\text{-H}_2\text{O}$  system were found to be those of  $\text{CaSO}_4 \cdot 2\text{H}_2\text{O}$ . There is some evidence for changes in morphology of the  $\text{CaSO}_4 \cdot 2\text{H}_2\text{O}$  crystals as is illustrated by differences in the relative intensity of the X-ray

diffraction powder lines in Fig. 2.24. This may be associated with an increase in clustering by spherulitic growth found in many samples after magnetic treatment and shown in Fig. 2.25 for crystals precipitated from treated samples by evaporation under an infrared lamp.

Particle size measurements on precipitates of calcium phosphate showed that there were differences between the effects of the magnetic fields produced by units containing four and two bars in the geometrical configurations depicted in Fig. 2.1. Figs. 2.26, 2.27 and 2.28 indicate that for the units containing four magnetic bars, the particle size increases on magnetic treatment, while Figs. 2.29, 2.30 and 2.31 reflect a decrease in particle size for units containing two magnetic bars. The data shown in Fig. 2.28 represent the combined results of Figs. 2.26 and 2.27, reinforcing the fact that the particle size of  $\text{Ca}_3(\text{PO}_4)_2$  precipitates obtained with units containing four magnetic bars increases after magnetic treatment compared to the control unit. Similarly, Fig. 2.31 consists of the data presented in Figs. 2.29 and 2.30 and indicates a reduction in the particle size of precipitates obtained with units comprising two magnetic bars compared to the control unit. The particle size data for a repeat experiment of  $\text{Ca}_3(\text{PO}_4)_2$  are shown in Figs. 2.32, 2.33, 2.34 and 2.35, 2.36, 2.37. Figs. 2.34 and 2.37 represent the combined

results of this repeat experiment and indicate a parallel with the previous experiment. X-ray diffraction powder patterns show that all the precipitates obtained are of the same phase (examples in Fig. 2.40).

As with calcium phosphate, barium sulphate was selected for study because it is sparingly soluble and thus, readily forms precipitates. The electron micrographs (Fig. 2.41) indicate that the particle size of crystals increases after magnetic treatment.

## 2.7 Discussion

The results emanating from the experimental work indicate that magnetic treatment has a profound influence on the behaviour of colloidal dispersions, or more precisely, on dispersed crystal nuclei.

There are essentially two major factors involved in crystallization by the deposition of solids from fluids, viz. solubility and nucleation. The rate of precipitation depends on the degree of supersaturation of the solution which should contain a greater concentration of solute than the equilibrium solubility at the temperature under consideration. Other than temperature, supersaturation is affected by pressure changes, pH and the concentration of

the solution. Nucleation eventually has to occur to enable the precipitated crystals to grow. Factors affecting nucleation are outlined in Chapter One where both heterogeneous and homogeneous nucleation are described.

Much of the work of The City University group has been concerned with aspects of crystallization that lead to scale formation. For scale formation to be controlled or prevented, the treatment must address itself to the issues of (1) solubility and (2) nucleation and crystal growth. Chemical means of reducing or preventing crystal (scale) growth include acid dosing and ion-exchange which are designed to control solubility by preventing the formation of supersaturated solutions, whilst other methods (such as the use of chemical inhibitors) control nucleation and/or growth. Seed crystals are sometimes mixed with the water for precipitation to take place on them, rather than on boiler walls or pipes, for instance, and affect both solubility and nucleation.

The results of the magnetic treatment of fluids that must be explained arise from observations in this work and other work carried out at The City University which show that the magnetic treatment of fluids can induce changes in particle size, crystallinity, crystal morphology, crystal phase, solubility and the rate of precipitation of crystals

precipitated from the fluid. Examples of each will now be presented.

#### CHANGES IN PARTICLE SIZE

Previous investigations at The City University have shown the particle size of calcium carbonate precipitates to increase following magnetic treatment (see Section 2.1).

In the present work, a decrease in the particle size of calcium sulphate dihydrate precipitates was evident where a full magnet was used compared to the control. Units of intermediate strength did not yield consistent results, a consequence of the asymmetric configuration of the magnetic bars. The particle size of calcium phosphate precipitates was seen to decrease where two magnetic bars were used and to increase in the case where four magnetic bars were used compared to the control unit. These opposing trends are due to the differing field geometries of the units. The particle size of barium sulphate precipitates was found to increase after magnetic treatment.

#### CHANGES IN CRYSTALLINITY

Associated with differences in crystal size are changes in crystallinity (the ability of precipitates to form crystals) observed after magnetic treatment.

An increase in aggregation was observed in the precipitation experiments for calcium sulphate dihydrate and calcium phosphate. Changes in crystallinity are further exemplified by previous experiments with basic tin(II) sulphate: an amorphous precipitate is obtained by the addition of an ammonia solution to tin(II) sulphate and a more crystalline product precipitated after magnetic treatment.

#### CHANGES IN MORPHOLOGY

There is also evidence of morphological changes. The application of a magnetic field alters the relative rates of growth of the external faces of a crystal.

Precipitates of calcium sulphate dihydrate indicate morphological changes following magnetic treatment as is evidenced by X-ray powder diffraction patterns. These results are comparable to those obtained by the precipitation of calcium oxalate [14] under similar conditions.

#### CHANGES IN CRYSTAL PHASE

Evidence also suggests that magnetic fields influence phase changes as is borne out in studies with zinc phosphate and calcium carbonate.

In this work, the X-ray powder diffractograms of calcium

sulphate dihydrate and calcium phosphate showed no change in crystal phase following magnetic treatment.

#### CHANGES IN SOLUBILITY

Higher solubility levels have been found in magnetically treated fluids compared to untreated fluids. For example, the solubility levels of calcium phosphate and barium sulphate were found to increase following magnetic treatment of solutions. Similar data have been obtained for aluminium hydroxide and zinc phosphate.

#### CHANGES IN THE RATE OF PRECIPITATION

Ellingsen and Kristiansen [12] found changes in the rate of precipitation of calcium carbonate after subjecting a solution to magnetic treatment.

The above can be monitored by measuring the settling rates and the accompanying loss of turbidity following magnetic treatment.

In this work, the results obtained lead to a requirement to explain the following:

- (a) the effects of the magnetic field on charged species in fluids;
- (b) the effects of the magnetic field on fluid-precipitate equilibria;

(c) the scientific basis for the overall observed effects.

(a) The effects of magnetic fields on charged species in fluids.

The effects of magnetic fields on charged species in fluids is covered by the theory of magnetohydrodynamics (MHD) [25]. MHD phenomena, sometimes referred to as magnetofluid dynamics (MFD) [26], essentially result from the mutual interaction between the magnetic field and the velocity of the conducting fluid flowing across it. The fluid conducts because it contains charged species that can move indefinitely. An electromagnetic force is produced in the fluid flowing through a transverse magnetic field. The resulting current and magnetic field combine to produce a force that resists and perturbs the fluid's motion. The current also generates an induced magnetic field which distorts the original magnetic field.

A charged particle is affected by three forces:

1. The ELECTROSTATIC FIELD,  $E$  (volt/m), arising from the attractive and repulsive forces on charged particles.
2. The MAGNETIC FORCE arising from the combined effects of the fluid velocity and the applied field,  $v \times B$  (Newtons per unit charge), and is orthogonal to  $v$  and  $B$ .

3. The INDUCED ELECTRIC FIELD,  $E_i$ , defined by the change in the magnetic field,  $B$ , with time.

The total force,  $E_T$  exerted on a particle per unit charge is denoted by:

$$E_T = E + vB$$

where  $E = E_{\perp} + E_i$ .

If a positively charged species of charge,  $q$ , passes through a magnetic field of strength,  $B$ , with a velocity,  $v$ , the interaction between the field, the charge and the velocity causes a force,  $F$ , to act on the charged species such that

$$F = qvB.$$

This constitutes the LORENTZ force, a modification of

$$E_T = E + vB,$$

which excludes the induced electric field component.

The force,  $F$ , acts at right angles to the plane established by the vectors of  $v$  and  $B$ .

A particle,  $M^{2+}$ , would carry a charge of  $3.2 \times 10^{-19}C$ .  
The strength of the magnetic fields used in HDL units is  
ca. 2500G.

Since

$$10^4G = 1Wb/m^2,$$

$$2500G = 0.25Wb/m^2.$$

The flow rate is known to be  $0.95m^3/hr$ .

Therefore,

$$\begin{aligned} \text{Flow rate through magnetic unit} \\ &= 0.95m^3/hr / r^2 \\ &= 0.95m^3/hr / 0.102m^2 \\ &= 0.003m/s \end{aligned}$$

$$F = qvB$$

$$\begin{aligned} F &= (3.2 \times 10^{-19})As (3 \times 10^{-3})m/s \\ &\quad (2.5 \times 10^{-1})kgm^2/s^2Am^2 \\ &= 2.4 \times 10^{-22} kgm/s^2 \end{aligned}$$

$$\begin{aligned} \text{Mass of 1mol } Ca^{2+} &= 1.66 \times 10^{-23} \times 40g \\ &= (6.64 \times 10^{-22})g \\ &= (6.64 \times 10^{-25})kg \end{aligned}$$

This shows that the Lorentz force,  $F$  (order

$10^{-22} \text{kgm/s}^{-2}$ ), acting on a calcium ion would be able to move the particle (order  $10^{-20} \text{kg}$ ).

Although the amount of energy generated by the Lorentz force is sufficient to influence particle interactions, the force generated, even summed over all ions present would be inadequate to carry out any substantial work such as descaling downstream, particularly as most of the energy would be dissipated as a result of normal collisions.

The physical bases of the interaction between a conducting medium and a magnetic field have been documented by Alfvén who won the Nobel Prize for physics in 1970 [27] [28]. A magnetic field alters the random course of motion of charged particles, whilst leaving neutral particles unaffected. A charged particle moving in a plane perpendicular to the magnetic field executes a circular motion, the radius of the circle being given by:

$$r = mc / |l| \cdot B \sqrt{8kT/\pi m}$$

where  $m$  is the mass,  $B$  is the intensity of the magnetic field,  $l$  is a linear dimension, and  $T$  is the temperature. The radius increases with the mass of the particle and with its thermal energy, but decreases as the intensity of the field increases. The direction of motion is opposite for

positive and negative particles. If a particle has a velocity component parallel to the field, then it produces a helical motion instead of a circle, as illustrated in Fig. 2.42-top. If the magnetic field is not of uniform intensity, then the radius of curvature of the helix in which a particle moves varies, as shown in Fig. 2.42-bottom.

(b) The effects of the magnetic field on fluid-precipitate equilibria.

The results of this work have been concerned with the effects of the magnetic field on solid-fluid equilibria at the point of crystallization. In the use of magnetic units for scale prevention, however, the effects are also seen in fluids that are not supersaturated as they pass through the magnetic field and therefore should not contain stable crystal nuclei.

The species present in solution that can be affected by the magnetic field should thus be accounted for. The crystal nucleation modification model considers the situation at the point of precipitation where the charged species in an inorganic fluid are water, ions and nuclei.

In undersaturated solutions, the effects would be the same for water and ions, but there must be other species present

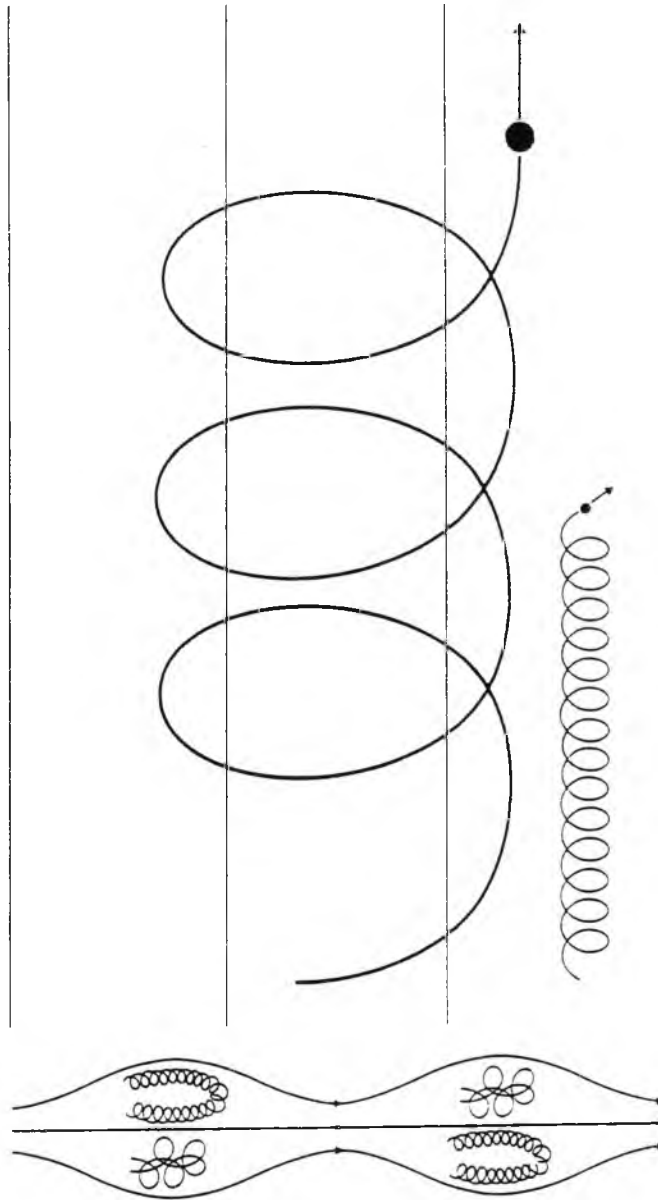
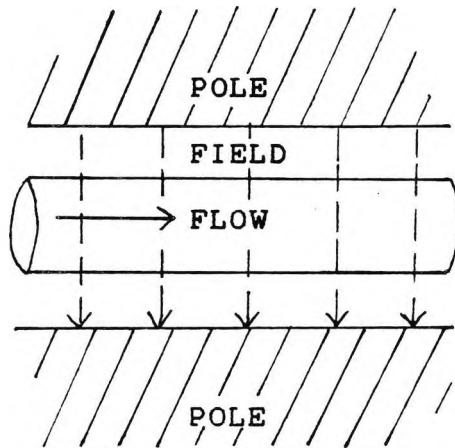
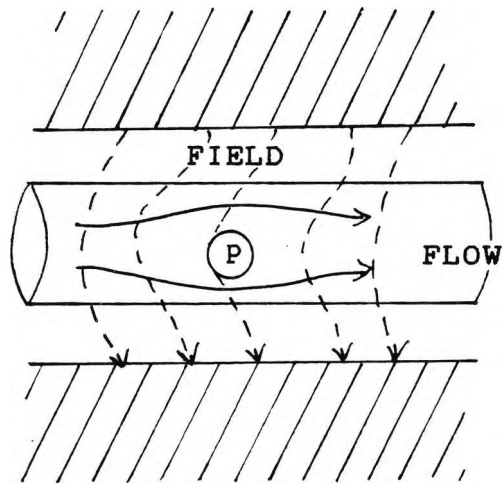


FIGURE 2.42 Motion of charged particles: (above) in a uniform magnetic field; (below) in a non-uniform magnetic field. The large sphere represents a positive ion, the small one an electron.



(a) Uniform jet of fluid passing through a uniform magnetic field between the poles of a magnet.



(b) Motion of particles in a fluid distorted owing to the non-uniform magnetic field. (Particle denoted by P.)

FIGURE 2.43

on which the magnetic field acts to achieve the observed downstream phenomena. It is suggested that these species must be clusters of hydrated anions and cations which are stable enough to have a finite lifetime in the fluid. Some clusters would not have the discrete crystal structure associated with nuclei, but would have structures that could be altered by field-charge interactions. The behaviour of the clusters would, moreover, be very similar to the behaviour of colloids in that they are dispersed very small particles with high surface charges.

As discussed in (a), charged particles describe a helical path in a uniform magnetic field, with positive and negative species moving in opposite directions. However, in a non-uniform field, the magnetic lines of flux are distorted and these in turn distort the particles' motion. This phenomenon is responsible for the changes in crystallization which can be achieved in various ways:

- (i) The nature of the charges at the surface of nuclei may be altered as a result of the interaction of the the magnetic field with the nuclei.

The nuclei on which crystals grow are usually very small particles which have a high surface to bulk charge ratio. Because of this, these particles should be affected by the

magnetic field. A given nucleus will consist of a minute crystal of the material precipitated with potentially growing faces each with its own surface charge characteristics. The interactions between the magnetic field and the nuclei could vary from aligning dipoles formed as a result of an imbalance in charge distribution, to movement of the nuclei according to the overall positive and overall negative charges to interactions between the magnetic fields and the charged surfaces of all potentially growing faces. Whatever the details of this interaction, however, changes must occur which would favour some growing faces rather than others and the favoured faces may well be different from those growing in the absence of magnetic fields.

(ii) The field could affect the transport of charged species to the crystal-solution interface.

For an inorganic crystal to grow, it must receive from the solution appropriate amounts of the constituent anions and cations. If these ions are affected by the magnetic field to set them in helical motion with anions and cations moving in opposite spirals, the regular supply of anions and cations to the crystal surface may be disrupted. Effects of this type, may also alter the rate of growth of the crystals and of specific faces of crystals.

(iii) Diffusion of ions through the diffusion barrier.

For a crystal to grow from a supersaturated solution, the constituent ions must cross a diffusion barrier at the crystal surface which changes the concentration gradient of ions from the supersaturated level in the fluid to zero at the crystal (see Fig. 2.44). Transport across the diffusion barrier could be affected by magnetic fields in two ways:

- (a) The influence of the magnetic field on the diffusion barriers at the surfaces of potentially growing faces may well affect the ease of transfer of anions and cations across the concentration barrier. This essentially means an increase or a decrease in the thickness of the diffusion barrier depending upon the exact nature of the field-surface charge interaction for a given face.
  
- (b) The transport of an ion through the energy barrier could be influenced by Lorentz effects. If the energy of a given ion is increased as a result of the Lorentz-type interactions, this extra energy will alter its diffusion through the concentration barrier at least until the excess energy is dissipated by collisions.

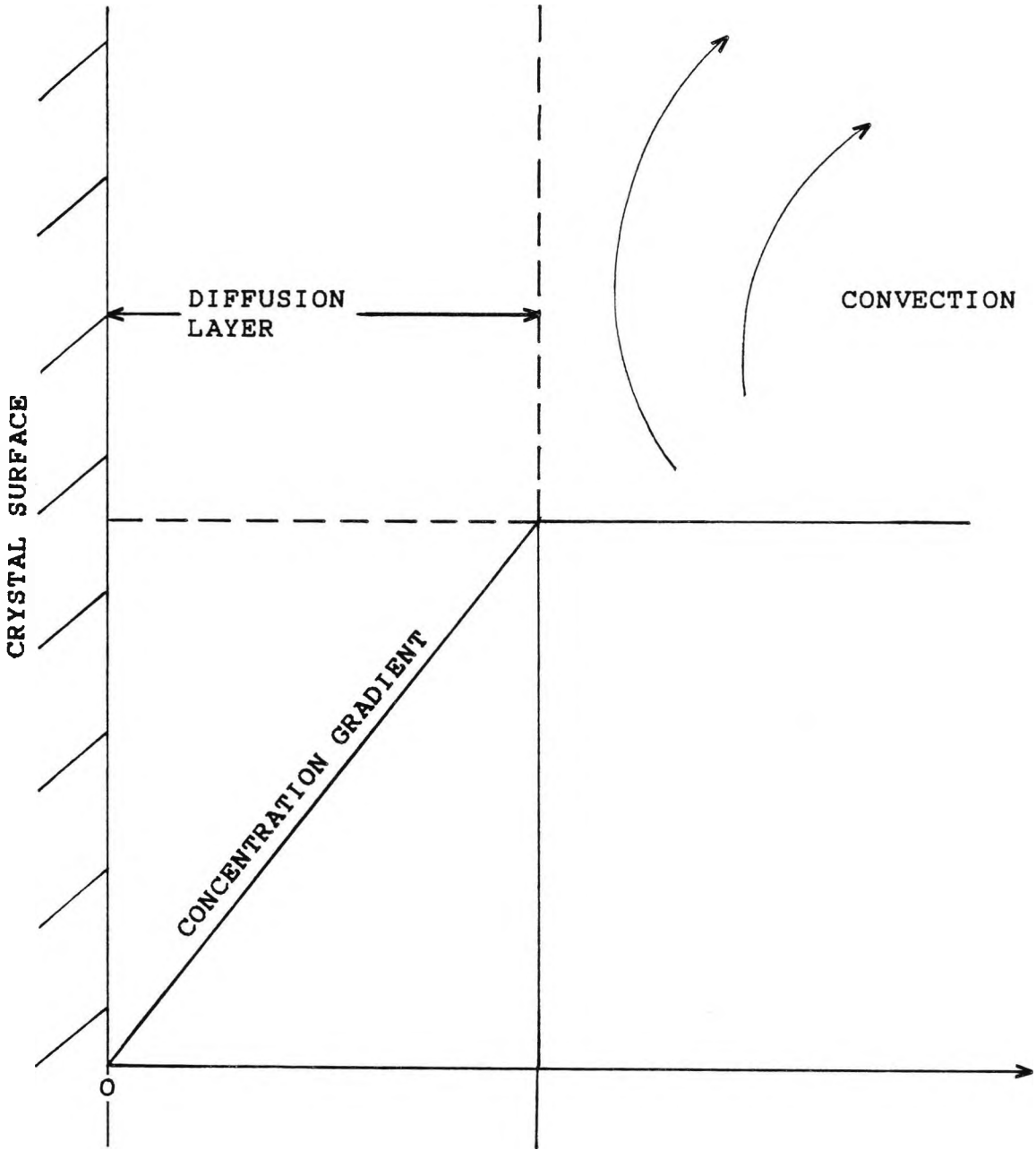


FIGURE 2.44 Diagram illustrating the diffusion layer set up between a growing face of a crystal and the solution.

(iv) Lorentz effects at the crystal surface.

If an ion in a supersaturated solution gains extra Lorentz energy which is dissipated on collision with the growing crystal surface, then that energy which is small in overall terms may be significant at the point of contact. It is possible that extra energy provided to the crystallizing system from ions carrying the Lorentz energy may contribute in determining the subsequent growth of the crystal.

It is likely that the effects of magnetic fields on fluid-precipitate equilibria involve a combination of the factors described above.

Zeta potential measurements, which lie beyond the scope of this work, could provide more answers as to how magnetic fields affect fluid-precipitate equilibria.

(c) The scientific basis for the overall observed effects.

In an attempt to ascribe a possible scientific basis to the effects observed, three explanations should be considered: (1) turbulence (2) the Lorentz effect and (3) crystal nucleation modification.

### Turbulence

Turbulence plays a role in preventing the aggregation of crystallites in the formation of scale and descaling processes, but its influence is secondary to that of the magnetic field on treated fluid. No evidence has been found that the effects on crystal growth, solubility and precipitation, described earlier, can be produced using control units of the same geometry as the magnetic units.

### The Lorentz Effect

In a saturated solution, ions which have gained extra Lorentz energy, should lose that energy rapidly by normal collisional processes. It is, therefore, unlikely that the Lorentz force contributes significantly to the observed phenomena, particularly in the light of recent experiments conducted by our research team [29] under static conditions, in which changes in crystallinity were noted. The one possible situation where the Lorentz energy could be important is where the excess energy is dissipated by collision with the growing crystal surface and so influence the crystal modification process.

### Crystal Nucleation Modification

Direct field-charge interactions on the nuclei provide the most satisfactory explanation of the effects of the magnetic field on crystallization. All the data observed can be accounted for by the combination of effects described in (b). The nuclei and growing crystallites have small, highly charged surfaces and when subjected to a magnetic field, the interaction is such as to modify the nature of the charges, both in general and on specific planes. In terms of the energy available, the interaction of the magnetic field with charged species, appears to be the major difference between fluids treated magnetically and those not. Thus, crystal nucleation modification constitutes the most feasible explanation for the observed data.

- (i) The impact of the magnetic field on the surface of particles affects the overall growth pattern leading to *changes in particle size*.
- (ii) Changes in the rates of growth of potentially growing faces are responsible for *changes in crystallinity and morphology*.
- (iii) *Changes in crystal phase* would arise because the relative energies available to growing crystals vary

in the presence and absence of a magnetic field.

(iv) *Differences in the solubility* of precipitates in fluids result from the disruption of fluid-precipitate equilibria as a direct consequence of crystal growth in systems.

(v) *Variations in the rate of precipitation* are induced by changes in the rate of growth of crystals subjected to a magnetic field compared with precipitation carried out under normal conditions.

Diffusion layers are set up in the interfacial regions between the faces of a growing crystal and the solution. The effect of the magnetic field on the diffusion layers and the surfaces of a crystal will be critical in determining the subsequent mode by which crystal growth proceeds.

REFERENCES

1. Joshi, K.M. and Kamat, P.V., *J. Indian Chem. Soc.*, 1966, 43, 9, 620-622.
2. Klassen, V.I., *Doklady Akademii Nauk. SSSR*, 1971, 197, 1104-5.
3. Drost-Hansen, W. and Kavjic, G., 'Conference on Electrolyte Precipitation in Aqueous Solution', University of Copenhagen, Proceeding abstr. book II (supplement), 1978.
4. Eliassen, R., Skrinde, R.T. and Davis, W.B, *J. Amer. Water Works Assoc.*, 1958, 50, 10, 1371-1385.
5. Raisen, E., *Corrosion* 84, 1984, 117.
6. Vonsovsky, S.V., *Uspekhi Fizicheskikh Nauk*, 1966, 90, 491.
7. Minenko, V.I. and Petrov, S.M., *Teploenergetica*, 1962, 9, 9, 63.
8. Ellingsen, F. and Fjeldsend, O., 'A Review of Scale Formation and Scale Prevention, with Emphasis on Magnetic Water Treatment', Citation Unknown.
9. Speranskiy, B.A., Vikhrev, V.V., Vinogradov, V.N. and Dolya, Y.I, *Prozh. Energ.*, 1973, 8, 43-44.
10. Duffy, E.A., Ph.D. Thesis, Clemson University, 1977.
11. American Petroleum Institute, 'Evaluation of the Principles of Magnetic Water Treatment', 1985, API Publication 960.
12. Ellingsen, F.T. and Kristiansen, H., *Vatten*, 1979, 35, 4, 309-315.

13. Donaldson, J.D. HDL Fluid Dynamics Symposium, London, 1988.
14. Grimes, S.M., HDL Fluid Dynamics Symposium, London, 1988.
15. Donaldson, J.D. and Grimes, S.M., *New Scientist*, Feb. 1988, 43-46.
16. Donaldson, J.D. and Grimes, S.M., *Cobalt News*, Dec. 1987, 2-4.
17. Malvern Instruments, '2600/3600 Particle Size Handbook', M.I., 1982.
18. West, A.R., 'Solid State Chemistry and its Applications', Wiley and Sons Ltd., U.K., 1984.
19. Nester, E.W., Roberts, C.E., Pearsall N.N. and McCarthy, B.J., 'Microbiology', Holt, Rinehart and Winston, U.S.A., 1978.
20. Wolfe, S.L., 'Biology of the Cell', Wadsworth Publishing Co., Calif., 1981.
21. DeRobertis, E.D.P. and DeRobertis, E.M.F., 'Cell and Molecular Biology', 7th Edn., Holt-Saunders, Japan, 1981.
22. Fifield, F.W. and Kealey, D., 'Analytical Chemistry', International Textbook Co., Ltd., London, 1983.
23. Weiss, J., 'Handbook of Ion Chromatography', Calif., 1986.
24. Wheeler, P., 'Investigating the Effects of Magnetic Fields on Fluids', The City University, London, 1987.
25. Shercliff, J.A., 'A Textbook of Magnetohydrodynamics', Pergamon Press, London, 1965.

26. Cramer, K.R. and Pai, S.I., 'Magnetofluid Dynamics for Engineers and Applied Physicists', Scripta Publishing Co. Ltd., U.S.A., 1973.
27. Alfvén, G., 'Worlds and Anti-Worlds', Moscow, 1968.
28. Alfvén, G., 'Magnetohydrodynamics', Symposium Proceedings, Moscow, 1958.
29. Prosser, J., Private Communication.

CHAPTER THREE

CEMENT

	Page	
3.1	Introduction	162
3.2	Portland Cements	163
3.3	Types of Portland Cement	166
3.4	Blended Portland Cements	169
3.5	Portland Cements with Additives	169
3.6	High Alumina Cement	170
3.7	Properties of Hardened Concrete	170
3.7.1	Strength	170
3.7.2	Deformation of Hardened Concrete	171
3.7.3	Resistance to Weather and Chemical Attack	173
3.8	Experimental Procedure	177
3.8.1	Tensile Strength Tests	179
3.8.2	Compressive Tests	188
3.9	Plaster of Paris	198
3.9.1	Fabrication of Specimens	198
3.10	Discussion	211
	References	213

CHAPTER THREE

CEMENT

3.1. Introduction

A cement can be defined as a finely ground substance forming, by the addition of an appropriate quantity of water, a binding paste capable of hardening both in air and under water and of binding together particulate material.

Various types of cement have been in use since ancient times. The Egyptians used calcined impure gypsum,  $\text{CaSO}_4 \cdot 2\text{H}_2\text{O}$ ; the Greeks and Romans used calcined limestone,  $\text{CaCO}_3$ , and later added aggregate - sand and crushed stone - to form concrete [1].

Hydraulic cements might be considered the most versatile binders yet known to man, enabling the development of massive constructions such as dams and foundations; slender, highly-stressed structures such as bridges and high-rise buildings; and paved areas such as roads and airfield runways, whilst they are equally suited to the manufacture of precast panels, building blocks, roofing tiles, pipes, and paving slabs as well as thin-walled items such as roofing sheet and rainwater fittings.

Hydraulic cements react exothermically with water to form hard, strong masses having an extremely low solubility. The reaction is irreversible. Setting is a gradual, stiffening process with the strength continuing to increase after hardening, sometimes taking several years to reach its ultimate value.

The cements currently made in the United Kingdom may be classified as follows:

- Portland cements;
- blended Portland cements;
- Portland cements with additives;
- high alumina cements.

The the first two major catagories have more diverse applications than the others which are generally required for special purposes.

### 3.2 Portland Cements

The method for producing modern Portland cement originates from that invented by Aspdin [2] in 1824, in Britain, when high temperatures were first used in the preparation of cements. The name derives from the similarity in colour and appearance to Portland stone, found in Dorset, England.

In compliance with BS12 [3], the cement is obtained by pulverizing clinker, consisting mainly of calcium silicates, obtained by heating to partial fusion a predetermined and homogeneous mixture of materials containing principally lime (CaO) and silica (SiO<sub>2</sub>) with a smaller proportion of alumina (Al<sub>2</sub>O<sub>3</sub>) and iron oxide (Fe<sub>2</sub>O<sub>4</sub>). Gypsum is usually added to prevent *flash set* from occurring, i.e. rapid setting on subsequent reaction with water. The resulting powder is the familiar Portland cement which, when mixed with water and the appropriate aggregate, hydrates to form set cement or concrete.

The term 'aggregate' embraces the gravels, sands and crushed stone such as granite, basalt, and harder types of limestone and sandstone. The aggregate reduces the cost of concrete production, controls the stiffening of the mix within a reasonable period of time and increases the fracture strength. In the absence of aggregates, set cement crumbles easily. Other additives, e.g. pozzolans fuel ash from power stations and blast furnace slag may be mixed with Portland cement to reduce costs. Some of these additives are beneficial in that they absorb Ca(OH)<sub>2</sub> liberated during the hydration of cement, thereby increasing the resistance of set cement to chemical attack.

RAW MATERIALS

(CaO, Al<sub>2</sub>O<sub>3</sub>, SiO<sub>2</sub>,  
Fe<sub>2</sub>O<sub>3</sub>, etc.)



Kiln, ~1500°C

CLINKER

(Ca<sub>3</sub>SiO<sub>5</sub>, Ca<sub>3</sub>Al<sub>2</sub>O<sub>6</sub>,  
β-Ca<sub>2</sub>SiO<sub>4</sub>, Ca<sub>2</sub>AlFeO<sub>5</sub>,  
etc.)



H<sub>2</sub>O, 25°C

SET CEMENT

(calcium silicate  
hydrates)

FIGURE 3.1 Stages in the manufacture and use of Portland cement.

### 3.3 Types of Portland Cement

The properties of cement can be modified by varying the composition of cement clinker or the amounts of additives.

TABLE 3.1

MAIN CONSTITUENTS OF PORTLAND CEMENTS.

NAME	EMPIRICAL FORMULA	ABBREVIATION	HEAT EVOLUTION AND HARDENING
Tricalcium silicate	$\text{Ca}_3\text{SiO}_5$	$\text{C}_3\text{S}$	Rapid
Dicalcium silicate	$\text{Ca}_2\text{SiO}_4$	$\text{C}_2\text{S}$	Slow
Tricalcium aluminate*	$\text{Ca}_3\text{Al}_2\text{O}_6$	$\text{C}_3\text{A}$	Rapid
Calcium aluminoferrate	$2\text{Ca}_2\text{AlFeO}_6$	$\text{C}_4\text{AF}$	Extremely slow

\* Sensitive to sulphate attack

*Ordinary Portland cement* (OPC) is the most common, general purpose cement, but is susceptible to sulphate attack and thus is not used in contact with seawater, for example. Two modes of sulphate attack manifest themselves. One is by the reaction of sulphate with the hydrated tricalcium aluminate present in hardened Portland cement, and the growth of the new crystalline mineral, ettringite, a less-dense calcium sulphoaluminate [4]. Consequent expansion may result in disruption of the cement paste if significant quantities

of soluble sulphates penetrate the interior of the concrete. However, concrete designed for full compaction at a restricted water/cement ratio is rendered less permeable and any action by sulphates will tend to be confined to its surface. The other form of sulphate attack is by the reaction of the aforesaid with  $\text{Ca(OH)}_2$  to form gypsum which also exerts a disruptive influence on hardened cement.

This problem is obviated by the application of *sulphate-resisting Portland cement* (SRPC) in which the tricalcium aluminate ( $\text{C}_3\text{A}$ ) content is reduced by augmenting the  $\text{Fe}_2\text{O}_3:\text{Al}_2\text{O}_3$  ratio in the raw materials and thereby increasing the amount of tetracalcium aluminoferrite ( $\text{C}_4\text{AF}$ ) [5], conferring upon the cement a characteristically darker hue.

The resistance of SRPC to acids is not substantially greater than that of ordinary Portland cement nor is it immune to the effects of some other dissolved salts, such as magnesium compounds, which may occur in natural waters and effluents.

*Rapid-hardening Portland cement* (RHPC) is similar in composition to the ordinary variety, although the  $\text{C}_3\text{S}$  content is greater than that of  $\text{C}_2\text{S}$  and the clinker is more finely ground. This does not render it 'quick-setting'; it merely gains strength more rapidly than OPC

after hardening. The finer grinding does, however, increase the rate of hydration in the initial stages engendering the increased rate of early hardening implied by its name. Because of the enhanced rate of heat evolution associated with this cement, it is unsuitable for use in massive structures as the stresses imposed would probably induce cracking. Conversely, it may be useful when concreting in low temperature environments where the heat developed on hydration may serve to prevent frost damage in the early, critical stages. Cement which hardens even more rapidly can be produced by intergrinding 1 to 2%  $\text{CaCl}_2$  with the rapid hardening clinker.

In *low heat Portland cement* (LHPC), the  $\text{C}_3\text{A}$  and  $\text{C}_3\text{S}$  contents are reduced, producing a concrete in which the development of strength and evolution of heat are relatively slow, although the ultimate strength and heat of hydration are virtually unaffected. It is intended primarily for use in large constructions, where the rate of heat evolution associated with OPC at the early stages may cause undesirable thermal stresses in the immature concrete. The BS 1370 [6] stipulates that the heat of hydration should not exceed 60 and 70kcal/kg at 7 and 28 days, respectively; typical figures for OPC are around 84 and 88kcal/kg at these ages. The heat evolved by most Portland cements is similar, but the rate at which it is evolved becomes an important

parameter when the heat of hydration poses a problem in construction.

### 3.4 Blended Portland Cements

*Portland blast furnace cement* has rather similar properties to OPC and is a blend of Portland cement clinker and granulated blast furnace slag in the proportions of 2 to 1 or thereabouts (BS 146 [7] permits the addition of up to 65% slag by weight of the combination). The slag is produced as a by-product in the extraction of iron, by reaction of limestone with silica, alumina and other components of the ore.

The mechanical properties of the cement are similar to those of OPC, but concrete made with it tends to gain strength more slowly and less heat is evolved in the process; it is often claimed to be more resistant to chemical attack [8].

### 3.5 Portland Cements with Additives

Special additives are incorporated with Portland cement to produce *masonry cement*, *hydrophobic cement*, *water-repellent cement* and *oil-well cement*. Until recently,

oil-well cement was chiefly manufactured for export, but the discovery of oil and gas in the North Sea has brought its use nearer home. Several grades are marketed, designed specifically for cementing in steel castings or for plugging shallow, medium and deep bore-holes in which high temperatures and pressures prevail. Apart from these specialized applications, oil-well cement is not used in the construction industry.

### 3.6 High Alumina Cement

*High alumina cement* has a relatively high alumina content, approximately 80 wt%  $Al_2O_3$  which is mainly present as  $CaAl_2O_4$  the amounts of iron oxide, silica and other impurities being kept to a minimum; this variety is useful as a *refractory concrete* up to 1800°C.

### 3.7 Properties of Hardened Concrete

#### 3.7.1 Strength

Concrete resists compression better than any other type of stress, and designs usually exploit this attribute. Compressive tests, if interpreted correctly, may be used to judge the quality of concrete.

Owing to the continuing hydration of cement, the strength of concrete increases with age. The source of cement (discussed earlier) and the curing conditions are influential factors in the actual gain of strength, particularly at the early stages. Where the thickness of the concrete is small, or in other conditions where the concrete may dry out rapidly, there may be little gain in strength with age. Alternatively, enhanced strength may be induced if the concrete is kept permanently wet, or where the volume of concrete is sufficiently great to prevent drying out within the mass.

### 3.7.2 Deformation of Hardened Concrete

The principal components of the deformation of hardened concrete are:

(i) elastic deformation, which occurs instantaneously and is dependent on the applied stress;

(ii) drying shrinkage, dependent on the extent of drying which occurs over a long period and is independent of the stress in the concrete. It is influenced by the humidity and temperature of the ambient air, the rate of air flow over the surface, and the ratio of surface area to volume of the concrete. For a given environment, the shrinkage of concrete

is affected by the amount of water present in the concrete at the time of mixing, and to a lesser extent by the cement content. Furthermore, aggregate and reinforcement shrinkage can contribute significantly to the drying shrinkage of the concrete;

(iii) creep, which also occurs over an extended period, but is dependent on the stress of the concrete. Creep strain is proportional to the logarithm of time upon load.

The magnitude of deformation depends primarily on the stress/strain ratio at the time of loading, but the mix proportions, the size of the specimen and even the climatic conditions must also be accounted for. On removal of the load, the concrete undergoes an immediate elastic recovery. Creep recovery is a slower process, and the concrete will not regain its original dimensions.

Concrete, like many other materials, is subject to expansion or contraction in response to temperature variations. The thermal expansion of concrete is largely governed by the type of aggregate used, the water content of the concrete and on the mix proportions. For most purposes, it is generally assumed that concrete has a thermal expansion of  $11 \times 10^{-6}$  per °C, although limestone aggregate concretes may have a coefficient of only 70% of this figure.

### 3.7.3 Resistance to Weather and Chemical Attack

#### (a) Resistance to Frost

The presence of numerous fine capillary channels in concrete may encourage water to penetrate to the interior of the mass without providing relief of the internal pressures generated if that water should freeze and consequently expand. The first indication of frost attack is often a pattern of cracks outlining the coarse aggregate particles, reflecting the fact that the bond between these and the mortar portion is inadequate to resist the pressure exerted by the freezing of absorbed water. Subsequent frosts may induce disintegration of the surface. The fine channels result predominantly from a high water/cement ratio.

The deliberate entrainment of a controlled quantity of air is sometimes necessary to improve durability and increase resistance to frost; the air is evenly distributed throughout the hardened mass. In contrast, the haphazard inclusion of relatively large air voids, such as may result from inadequate compaction, reduces the durability and strength of hardened concrete.

(b) Resistance to Sulphates

This property has been discussed in Section 3.3.

(c) Resistance to Seawater

Concrete is extensively used in docks, piers, jetties and marine structures of all types and thus, is particularly likely to be subject not only to ordinary stresses, but also to tidal wetting and drying; to erosion by waves, shingle and sand; and to exposure to severe frost. Structural design must therefore include precautions as a means of evading these perils. Steel, for example, readily rusts in seawater, and the concrete cover to steel reinforcement must be impermeable enough to prevent contact between the two. The value of a concrete having an adequate cement content, and capable of being fully compacted at a water/cement ratio not exceeding 0.45, cannot be too strongly emphasized. It is desirable for the aggregate to have not only a low permeability, but also a hardness able to resist potential abrasion by sand or shingle.

(d) Resistance to Industrial and Other Chemicals

All hardened Portland cements consist essentially of calcium compounds, and so, are vulnerable to attack by chemicals such as acids, sugars, fats and some oils. These aggressive agents may necessitate exclusion from contact with permanent structures, for example, by the interposition of a suitable, inert, impervious membrane.

However, in cases where spillage of aggressive materials is occasional, light or quickly diluted, attack may often be confined to the exposed surface of the concrete, provided an appropriately high cement content was originally selected and low permeability obtained through good compaction at a low water/cement ratio. Reaction of any aggressive agent with the cement then tends to be neutralized, preventing significant penetration into the body of the concrete.

High alumina cements are suitable for some aggressive environments owing to their refractory properties, but hydraulic cements are in general not 'chemical resistant' in the true sense; the supplier's advice should therefore be sought before using them in locations where the danger of attack is suspected.

(e) Resistance to Fire

The nature of concrete ensures that the temperatures produced by a fire cause no sudden, uniform and possibly disastrous changes in properties throughout the mass. The concrete initially expands as its temperature rises, but progressive loss of moisture from the cement paste results in shrinkage and thus helps to offset continued expansion of the aggregate at temperatures above 250°C. Heat energy is expended in driving off the moisture, and this inherently reduces the rate at which the temperature of the concrete surface rises. Moreover, the thermal conductivity of concrete is low (only about one-tenth of that of steel), so that a rise in surface temperature is not immediately communicated to the interior. Loss of concrete strength due to dehydration of the cement paste may thus be confined to the surface layers.

Concrete is incombustible, non-inflammable and highly resistant to fire. The degree of resistance varies slightly with the type of aggregate used, those having a low or regular thermal expansion eliciting the best results. Minerals such as gravel, flint and granite, which consist of or contain silica, are liable to undergo sudden increases in volume at certain temperatures because of the crystal changes (exhibits polymorphism: quartz, tridymite,

cristobalite) peculiar to this compound.

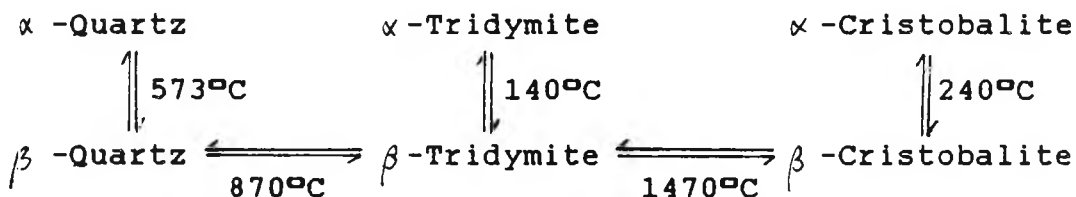


FIGURE 3.2 The three crystalline forms of silica and their high-temperature and low-temperature modifications.

In severe fires, the temperature may rise rapidly enough for the aforementioned mineral aggregates to generate internal stresses capable of forcing off the surface layers of the concrete. Prolonged exposure to such fires may cause progressive loss of concrete ('spalling').

Changes in volume are not brought about in response to heating lightweight aggregates, blast furnace slag and limestone which confer upon concretes excellent fire resistance.

### 3.8 Experimental Procedure

In view of the results of the studies of the magnetic treatment of fluids described in Chapter Two and because of

a comment in a Soviet publication [9] about the effects of magnetic treatment on the strength of cements, a study of the magnetic treatment of fluids relevant to the cement situation was carried out.

In this study, ordinary tap water and magnetically treated water (tap water passed through a magnetic field of 2.75 kilogauss for 1hr.) were each dispersed in the following types of cement:

- (i) ordinary Portland cement,
- (ii) sulphate-resisting Portland cement,
- (iii) oil-well cement.
- (iv) Plaster of Paris (Section 3.9)

A slurry, consisting of 10% sulphate-resisting Portland, was also subjected to a magnetic field under the conditions outlined above, before being dispersed in the same type of cement.

The ratio of water to ordinary Portland cement used was 1:3; that of water to sulphate-resisting Portland cement and water to oil-well cement, 1:2.

The water and cement were thoroughly mixed until homogeneity was achieved. Samples were then set in the form of dogbones (dumb-bell briquettes) and cubes. Tensile strength and compressive tests were performed on them, respectively,

after 7, 14, 21 and 28 days.

### 3.8.1 Tensile Strength Tests

Tensile strength can be defined as the maximum tensile stress which the test specimen is capable of supporting, the tensile stress being the tensile force carried by the test specimen per unit area of the original cross-sectional area of the central portion of the specimen.

Test specimens were fabricated in the form of dogbones (dumb-bell briquettes) in accordance with the dimensions specified in BS 6319 : Part 7 [10] (see Fig. 3.4) in order to fit into the jaws of the tensometer (see Fig. 3.3). The specimens were compacted by means of a table vibrator, allowed to dry and stored in water until tensile strength tests were performed. (Vibration in itself provides no compaction force. It merely agitates the particles; the compaction is then affected by gravity.)

The width and thickness of the central portion of the dogbones were measured after removing any loosely adhered particles. Tensile strength tests were conducted on a Hounsfield Tensometer. Specimens were positioned symmetrically in the jaws of the tensometer in axial

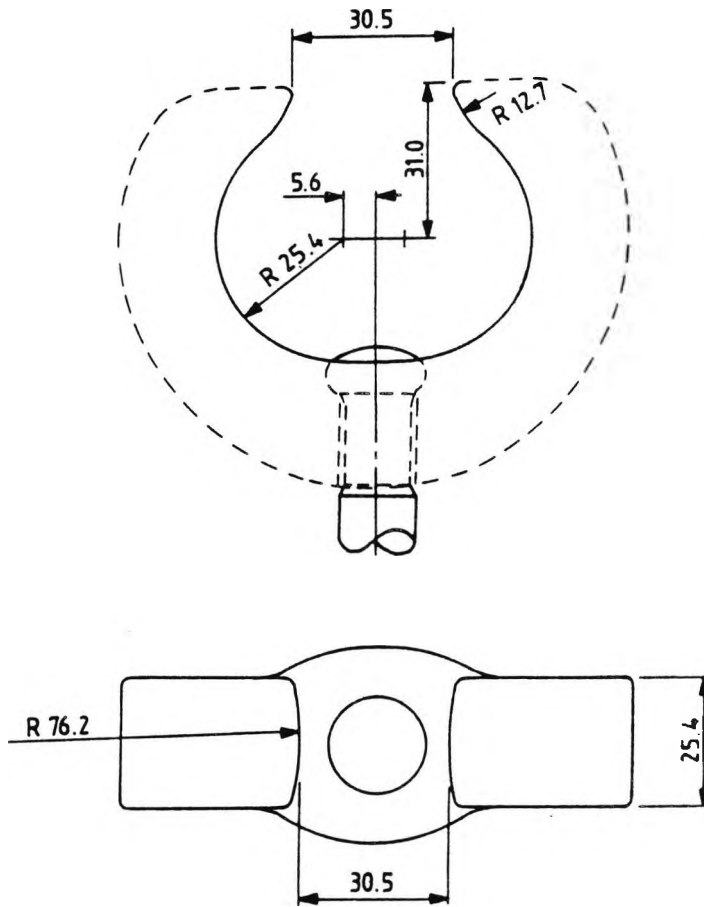


FIGURE 3.3 Jaws for briquette testing machine. (All dimensions are in millimetres.)

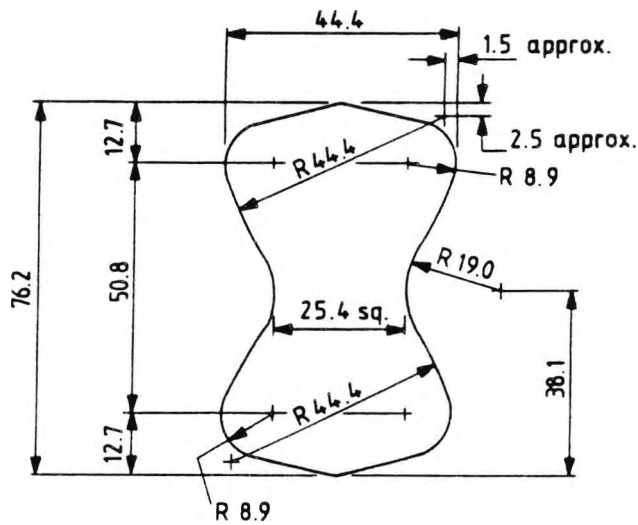


FIGURE 3.4 Dimensions of briquette test specimens. (All dimensions are in millimetres.)

TABLE 3.2

Dogbones: Dispersion of tap water in ordinary Portland cement.

TIME (Days)	SAMPLE NO.	WIDTH (mm)	THICKNESS (mm)	C.S.A. (mm <sup>2</sup> )	FORCE (kN)	T.S. (x10 <sup>-3</sup> N/mm <sup>2</sup> )
7	1	25.54	24.30	620.62	0.90	1.45
	2	25.51	24.39	622.19	0.78	1.25
	3	25.56	24.29	620.85	0.76	1.22
					MEAN	1.31
14	4	25.65	24.59	630.73	0.93	1.47
	5	25.55	24.46	624.95	0.73	1.17
	6	25.41	24.57	624.32	0.88	1.41
					MEAN	1.35
21	7	25.62	24.77	634.61	1.02	1.61
	8	25.45	24.79	630.91	1.07	1.70
	9	25.41	24.44	621.02	0.85	1.37
					MEAN	1.56
28	10	25.36	24.81	629.18	0.94	1.59
	11	25.58	24.58	628.76	0.99	1.57
	12	25.66	24.48	628.16	1.18	1.88
					MEAN	1.68

TABLE 3.3

Dogbones: Dispersion of magnetically treated water in ordinary Portland cement.

TIME (Days)	SAMPLE NO.	WIDTH (mm)	THICKNESS (mm)	C.S.A. (mm <sup>2</sup> )	FORCE (kN)	T.S. (x10 <sup>-3</sup> N/mm <sup>2</sup> )
7	1	25.62	24.42	625.64	0.79	1.26
	2	25.39	24.47	621.29	0.95	1.53
	3	25.63	24.73	633.83	0.73	1.15
					MEAN	1.31
14	4	25.54	24.50	625.73	1.02	1.63
	5	25.69	24.32	624.78	0.80	1.28
	6	25.60	24.49	626.94	1.00	1.60
					MEAN	1.50
21	7	25.70	24.63	632.99	1.00	1.58
	8	25.50	24.50	624.75	1.13	1.81
	9	25.87	24.56	635.37	1.04	1.64
					MEAN	1.68
28	10	25.60	24.28	621.57	0.97	1.56
	11	25.46	24.45	622.50	1.17	1.88
	12	25.55	24.60	628.53	1.20	1.91
					MEAN	1.78

TABLE 3.4

Dogbones: Dispersion of tap water in sulphate-resisting Portland cement.

TIME (Days)	SAMPLE NO.	WIDTH (mm)	THICKNESS (mm)	C.S.A. (mm <sup>2</sup> )	FORCE (kN)	T.S. (x10 <sup>-3</sup> N/mm <sup>2</sup> )
7	1	25.78	24.05	620.01	0.32	0.52
	2	25.83	24.07	621.73	0.36	0.58
	3	25.77	24.02	619.00	0.35	0.57
					MEAN	0.56
14	4	25.99	24.18	628.44	0.60	0.95
	5	25.50	24.12	615.06	0.47	0.76
	6	25.69	24.08	618.62	0.43	0.70
					MEAN	0.80
21	7	25.63	24.05	616.40	0.44	0.71
	8	25.67	24.11	618.90	0.70	1.13
	9	25.82	24.17	624.07	0.51	0.82
					MEAN	0.89
28	10	25.90	24.18	626.26	0.51	0.81
	11	25.86	24.12	623.74	0.80	1.28
	12	25.63	24.14	618.71	0.79	1.28
					MEAN	1.12

TABLE 3.5

Dogbones: Dispersion of magnetically treated water in sulphate-resisting Portland cement.

TIME (Days)	SAMPLE NO.	WIDTH (mm)	THICKNESS (mm)	C.S.A. (mm <sup>2</sup> )	FORCE (kN)	T.S. (x10 <sup>-3</sup> N/mm <sup>2</sup> )
7	1	25.96	24.20	628.23	0.55	0.88
	* 2	25.84	24.14	623.78	0.37	0.59
	3	25.68	24.06	617.86	0.56	0.91
					MEAN	0.90
14	4	25.73	24.21	622.92	0.50	0.80
	5	25.69	24.12	619.64	0.55	0.89
	6	25.68	24.19	621.20	0.62	1.00
					MEAN	0.90
21	7	25.61	24.05	615.92	0.81	1.32
	8	25.74	24.14	621.36	1.20	1.93
	9	26.08	24.13	629.31	0.60	0.95
					MEAN	1.40
28	10	25.80	24.21	624.61	0.96	1.54
	* 11	25.85	24.01	620.66	0.41	0.66
	12	25.53	24.05	614.00	0.77	1.25
					MEAN	1.40

\* On testing, these samples were found to have large air voids in their centres and thus, were considered invalid when calculating the mean.

TABLE 3.6

Dogbones: Dispersion of tap water in oilwell cement.

TIME (Days)	SAMPLE NO.	WIDTH (mm)	THICKNESS (mm)	C.S.A. (mm <sup>2</sup> )	FORCE (kN)	T.S. x10 <sup>-3</sup> N/mm <sup>2</sup>
7	1	25.84	24.15	624.04	0.37	0.59
	2	26.12	24.13	630.28	0.32	0.51
	3	25.82	24.18	624.33	0.30	0.48
					MEAN	0.53
14	4	25.81	24.24	625.63	0.44	0.70
	5	25.64	24.27	622.28	0.36	0.58
	6	25.62	24.26	621.54	0.40	0.64
					MEAN	0.64
21	7	25.80	24.18	623.84	0.64	1.03
	8	26.12	24.23	632.89	0.80	1.26
	9	25.73	24.19	622.41	0.67	1.08
					MEAN	1.12
28	10	25.75	24.17	622.38	0.61	0.98
	11	25.95	24.18	627.47	0.82	1.31
	12	25.80	24.19	624.10	0.73	1.17
					MEAN	1.15

TABLE 3.7

Dogbones: Dispersion of magnetically treated water in oilwell cement.

TIME (Days)	SAMPLE NO.	WIDTH (mm)	THICKNESS (mm)	C.S.A. (mm <sup>2</sup> )	FORCE (kN)	T.S. (x10 <sup>-3</sup> N/mm <sup>2</sup> )
7	* 1	25.72	24.24	623.45	1.45	2.33
	2	25.59	24.11	616.97	0.55	0.89
	* 3	25.82	24.18	624.33	0.86	1.38
						MEAN 0.89
14	4	25.64	24.17	619.72	0.41	0.66
	5	25.83	24.13	623.28	0.90	1.44
	6	26.13	24.09	629.47	0.51	0.81
						MEAN 0.97
21	7	26.14	24.19	632.33	0.80	1.27
	8	25.96	24.17	627.45	0.75	1.20
	9	25.79	24.21	624.38	0.63	1.00
						MEAN 1.16
28	10	25.58	24.21	619.29	0.80	1.29
	11	25.82	24.29	627.17	0.67	1.07
	* 12	25.73	24.23	623.44	0.54	0.87
						MEAN 1.18

\* These samples did not fail within the middle third and thus, in accordance with British Standards, were considered invalid when calculating the mean.

TABLE 3.8

Dogbones: Dispersion of 10% sulphate-resisting Portland cement and ordinary tap water, run through a magnet for one hour, in the same type of cement.

TIME (Days)	SAMPLE NO.	WIDTH (mm)	THICKNESS (mm)	C.S.A. (mm <sup>2</sup> )	FORCE (kN)	T.S. (x10 <sup>-3</sup> N/mm <sup>2</sup> )
7	1	25.74	24.11	620.59	0.43	0.69
	2	25.68	24.07	618.12	0.38	0.61
	3	25.65	24.24	621.76	0.40	0.64
					MEAN	0.65
14	4	25.79	24.18	623.60	0.57	0.91
	5	25.81	24.15	623.31	0.40	0.64
	6	25.56	24.08	615.48	0.59	1.62
					MEAN	1.06
21	7	26.22	24.17	633.74	0.93	1.47
	8	25.81	24.18	624.09	0.43	1.60
	9	25.71	24.03	617.81	0.42	0.68
					MEAN	1.25
28	10	25.05	24.03	625.98	0.76	1.21
	11	26.10	24.06	627.97	0.85	1.59
	12	25.79	24.24	625.15	0.67	1.60
					MEAN	1.47

alignment with the direction of pull. (Some inconsistency of results has been attributed to specimens being incorrectly positioned in the jaws.) A tensile force was applied to the test specimens such that the jaws separated at a rate of  $1 \pm 0.5$  mm/min until failure occurred. In compliance with BS 6319 : Part 7, if fracture occurred beyond the middle-third of the specimen, the test was considered invalid. Each test was performed in triplicate.

Tensile strength was calculated by dividing the load at failure by the cross-sectional area (C.S.A.). The mean tensile strength of the three specimens from the respective batch was then calculated.

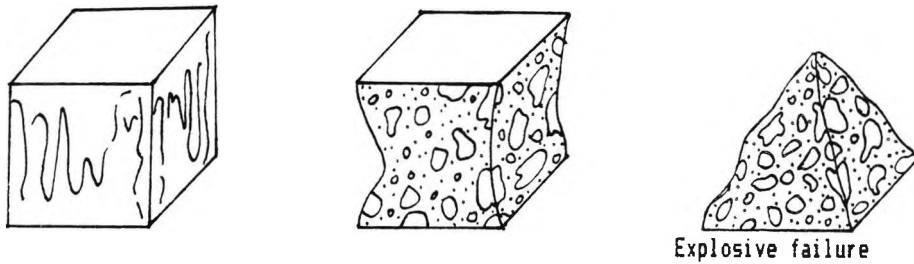
### 3.8.2 Compressive Tests

Compressive strength can be defined as the maximum stress carried by the test piece during a compressive test at the time of failure, the compressive stress being the compressive force carried by the test piece per unit area of original cross section.

The method used for the determination of the compressive strength of concrete cubes was that specified in BS 1881: Part 116 [11].

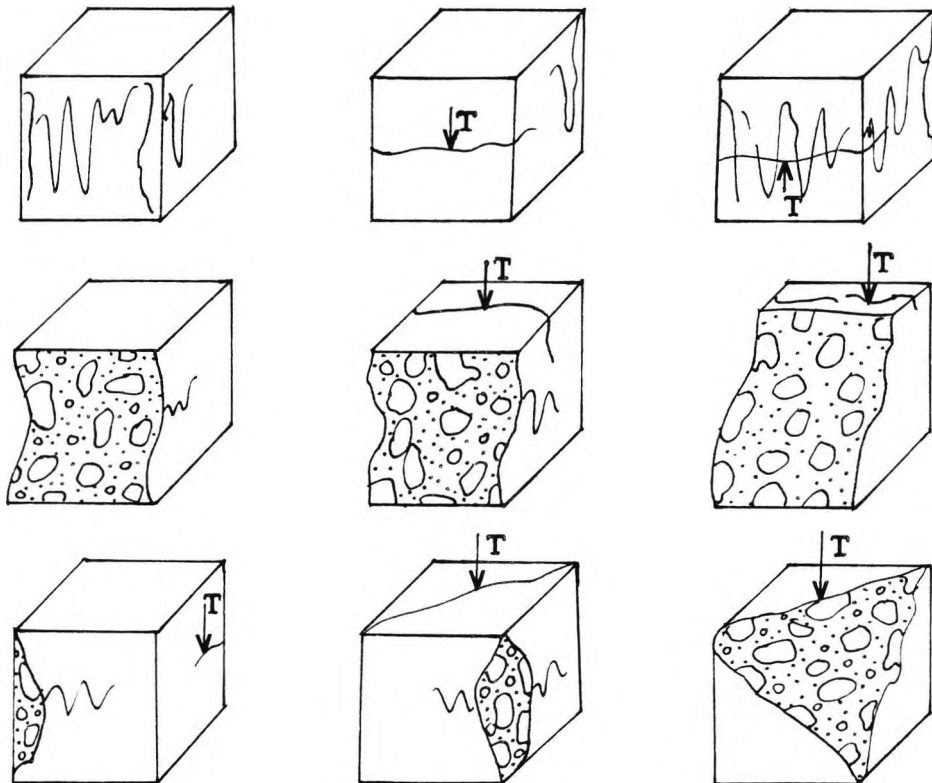
Cubes of the dimensions 50 x 50mm were prepared and compacted by means of a table vibrator, allowed to dry, then placed in water until tests were performed.

Prior to testing, samples were wiped clean of any extraneous material and the dimensions measured, i.e. the lateral depth and constant faces, in accordance with BS 1881 : Part 114 [12]. The mass was also determined. Specimens were then placed in an Avery Testing Machine after ensuring that the surfaces in contact with the cubes were cleaned, carefully aligning the axis of each specimen on the lower platen, with the centre of thrust of the instrument. The test cube was placed in the machine in such a manner that a load was applied to the opposite sides of the cube as cast (the lateral faces), i.e. not to the top and bottom. The load was applied, without shock, at a constant rate of approximately  $15\text{N/mm}^2$  per minute until no greater load could be sustained. The maximum load applied to the cube was then recorded. For examples of satisfactory and unsatisfactory failures, refer to Figs. 3.5 and 3.6, respectively. In satisfactory failures, all four exposed faces are cracked approximately equally, generally with little damage to the faces in contact with the platens. Irregular, unsatisfactory failures occur mainly due to misshapen specimens, but also due to poor alignment of the specimen in the testing machine,



NOTE. All four exposed faces are cracked approximately equally, generally with little damage to faces in contact with platens.

FIGURE 3.5 Satisfactory failures.



NOTE: T = tensile crack.

FIGURE 3.6 Some unsatisfactory failures.

TABLE 3.9

Cubes: Dispersion of tap water in ordinary Portland cement.

TIME (Days)	SAMPLE NO.	DIMENSIONS (mm)			MASS (kg)	MAX. LOAD (kN)	LOADED AREA (mm <sup>2</sup> )	COMP. STRENGTH (N/mm <sup>2</sup> )	MEAN
		Lateral Depth	Constant Faces						
7	1	50.80	50.93	51.42	0.266	29.7	2618.82	11.3	20.6
	2	50.73	50.92	51.61	0.267	59.1	2627.98	22.5	
	3	50.92	50.96	51.53	0.266	73.3	2625.97	27.9	
14	4	50.81	50.71	51.62	0.272	64.9	2617.65	24.8	25.1
	5	50.86	50.93	51.09	0.270	68.7	2602.01	26.4	
	6	50.90	50.89	51.61	0.272	63.1	2626.43	24.0	
21	7	50.95	50.97	51.43	0.274	95.4	2621.39	36.4	35.8
	8	50.88	50.70	51.41	0.273	90.7	2606.49	34.8	
	9	50.74	51.04	51.11	0.272	94.1	2608.65	36.1	
28	10	50.91	50.90	51.63	0.277	95.1	2627.97	36.2	37.4
	11	51.02	51.15	51.16	0.276	102.8	2616.32	39.3	
	12	51.04	50.92	51.44	0.274	96.5	2619.32	36.8	

TABLE 3.10

Cubes: Dispersion of magnetically treated water in ordinary Portland cement.

TIME (Days)	SAMPLE NO.	DIMENSIONS (mm)			MASS (kg)	MAX. LOAD (kN)	LOADED AREA (mm <sup>2</sup> )	COMP. STRENGTH (N/mm <sup>2</sup> )	MEAN
		Lateral Depth	Constant Faces						
7	1	50.91	50.92	51.40	0.274	77.2	2617.29	29.5	29.4
	2	50.91	50.90	51.40	0.273	78.2	2616.26	29.9	
	3	50.85	50.90	51.40	0.272	75.8	2616.26	29.0	
14	4	50.74	50.93	51.17	0.271	99.9	2606.09	38.3	35.0
	5	50.73	50.85	51.38	0.271	88.0	2612.67	33.7	
	6	50.74	50.91	51.04	0.270	85.6	2598.45	32.9	
21	7	51.06	51.40	50.99	0.279	96.5	2621.40	36.8	36.9
	8	50.78	51.00	51.08	0.275	93.6	2605.08	35.9	
	9	50.75	50.90	51.33	0.276	99.4	2612.70	38.0	
28	10	50.93	50.87	51.42	0.278	100.6	2615.74	38.5	39.3
	11	50.77	50.97	51.55	0.278	104.1	2627.50	39.6	
	12	50.91	50.97	51.04	0.276	103.7	2601.51	39.9	

TABLE 3.11

Cubes: Dispersion of tap water in sulphate-resisting Portland cement.

TIME (Days)	SAMPLE NO.	DIMENSIONS (mm)			MASS (kg)	MAX. LOAD (kN)	LOADED AREA (mm <sup>2</sup> )	COMP. STRENGTH (N/mm <sup>2</sup> )	MEAN
		Lateral Depth	Constant Faces						
7	1	50.46	50.92	50.97	0.277	237.0	2595.39	91.3	91.8
	2	50.58	50.81	50.88	0.277	236.2	2585.21	91.4	
	3	50.53	50.67	50.83	0.276	238.4	2575.56	92.6	
14	4	50.74	50.79	50.93	0.278	262.1	2586.73	101.3	103.7
	5	50.67	51.01	50.93	0.280	273.4	2597.94	105.2	
	6	50.81	51.23	50.90	0.283	273.0	2607.61	104.7	
21	7	50.64	50.85	51.25	0.281	292.1	2606.06	112.1	109.0
	8	50.55	50.91	51.13	0.279	274.5	2603.03	105.5	
	9	50.60	50.85	50.82	0.278	282.6	2584.20	109.4	
28	10	50.57	50.80	50.67	0.276	291.7	2574.04	113.3	112.7
	11	50.54	50.87	50.76	0.277	288.1	2582.16	111.6	
	12	50.48	50.89	50.89	0.278	293.1	2589.79	113.2	

TABLE 3.12

Cubes: Dispersion of magnetically treated water in sulphate-resisting Portland cement.

TIME (Days)	SAMPLE NO.	DIMENSIONS (mm)			MASS (kg)	MAX. LOAD (kN)	LOADED AREA (mm <sup>2</sup> )	COMP. STRENGTH (N/mm <sup>2</sup> )	MEAN
		Lateral Depth	Constant Faces						
7	1	50.69	50.81	51.30	0.281	233.7	2606.55	89.7	89.2
	2	50.57	50.95	51.13	0.280	226.5	2605.07	86.9	
	3	50.58	50.95	50.92	0.277	236.1	2594.37	91.0	
14	4	50.64	50.95	50.72	0.278	264.7	2605.07	101.6	103.8
	5	50.63	50.88	50.82	0.279	255.1	2585.72	98.7	
	6	50.60	50.91	50.89	0.280	287.7	2590.81	111.0	
21	7	50.63	51.22	50.87	0.284	296.6	2605.56	113.8	113.1
	8	50.79	51.21	50.94	0.282	304.4	2608.64	116.7	
	9	50.64	50.96	50.86	0.280	282.2	2591.83	108.9	
28	10	50.67	50.83	50.99	0.280	302.5	2591.82	116.7	117.6
	11	50.62	50.80	50.86	0.280	305.3	2583.69	118.2	
	12	50.53	50.99	50.89	0.281	306.0	2594.88	117.9	

TABLE 3.13

Cubes: Dispersion of tap water in oilwell cement.

TIME (Days)	SAMPLE NO.	DIMENSIONS (mm)			MASS (kg)	MAX. LOAD (kN)	LOADED AREA (mm <sup>2</sup> )	COMP. STRENGTH (N/mm <sup>2</sup> )	MEAN
		Lateral Depth	Constant Faces						
7	1	50.77	50.87	51.31	0.283	220.7	2610.14	84.6	86.0
	2	50.61	50.97	51.07	0.282	222.4	2603.04	85.4	
	3	50.58	51.02	51.02	0.281	229.4	2603.04	88.1	
14	4	50.60	50.88	51.93	0.283	222.5	2642.20	84.2	86.7
	5	50.67	50.87	51.32	0.284	220.4	2610.65	84.4	
	6	50.70	50.97	51.30	0.285	239.1	2614.76	91.4	
21	7	50.66	51.04	51.14	0.285	263.9	2610.19	101.1	101.1
	8	50.69	51.01	51.65	0.286	266.3	2634.67	101.1	
	9	50.69	50.97	51.51	0.285	265.6	2625.46	101.2	
28	10	50.54	50.99	51.48	0.287	283.1	2624.97	107.8	107.5
	11	50.60	51.09	50.97	0.284	277.6	2604.05	106.6	
	12	50.69	50.94	51.43	0.287	283.1	2619.84	108.1	

TABLE 3.14

Cubes: Dispersion of magnetically treated water in oilwell cement.

TIME (Days)	SAMPLE NO.	DIMENSIONS (mm)			MASS (kg)	MAX. LOAD (kN)	LOADED AREA (mm <sup>2</sup> )	COMP. STRENGTH (N/mm <sup>2</sup> )	MEAN
		Lateral Depth	Constant Faces						
7	1	50.93	51.36	50.93	0.286	221.6	2615.76	84.7	83.5
	2	50.84	50.95	51.40	0.287	222.1	2618.83	84.8	
	3	50.84	50.92	51.42	0.285	211.8	2617.29	80.9	
14	4	50.52	50.89	51.15	0.286	247.2	2603.02	95.0	96.1
	5	50.55	50.87	50.98	0.285	254.4	2593.35	98.1	
	6	50.42	50.97	50.99	0.285	247.6	2598.96	95.3	
21	7	50.55	50.99	51.02	0.285	272.1	2550.52	106.7	105.8
	8	50.65	50.95	51.25	0.286	284.6	2611.19	108.8	
	9	50.69	51.41	51.02	0.288	267.4	2622.94	101.9	
28	10	50.57	50.83	51.36	0.289	291.7	2610.63	111.7	113.8
	11	50.78	51.03	51.06	0.287	297.5	2605.59	114.2	
	12	50.60	50.96	51.42	0.289	302.4	2620.36	115.4	

TABLE 3.15

Cubes: Dispersion of 10% sulphate-resisting Portland cement and ordinary tap water, run through a magnet for one hour, in the same type of cement.

TIME (Days)	SAMPLE NO.	DIMENSIONS (mm)			MASS (kg)	MAX. LOAD (kN)	LOADED AREA (mm <sup>2</sup> )	COMP. STRENGTH (N/mm <sup>2</sup> )	MEAN
		Lateral Depth	Constant Faces						
7	1	50.64	50.81	50.67	0.271	196.8	2574.54	76.4	78.0
	2	50.55	50.91	50.90	0.272	220.3	2591.32	85.0	
	3	50.99	50.62	50.93	0.272	187.4	2578.08	72.7	
14	4	51.02	50.87	51.33	0.278	253.2	2611.16	97.0	92.4
	5	50.60	50.91	50.86	0.273	223.9	2589.28	86.5	
	6	50.88	50.99	51.21	0.279	244.7	2611.20	93.7	
21	7	50.70	50.83	50.94	0.276	234.6	2589.28	90.6	94.2
	8	51.07	50.83	51.13	0.278	252.6	2598.94	97.2	
	9	50.99	50.79	51.18	0.277	246.3	2599.43	94.8	
28	10	51.27	50.30	51.15	0.277	245.9	2572.85	95.6	96.2
	11	51.00	50.82	51.34	0.279	246.5	2609.10	94.5	
	12	50.69	50.88	51.21	0.277	256.8	2605.56	98.6	

or to a machine fault.

The cross-sectional area of the cubes was calculated and the compressive strength determined by dividing the maximum load by the cross-sectional area. The mean compressive strength of the three specimens from the respective batch was then calculated.

### 3.9 Plaster of Paris

#### 3.9.1 Fabrication of Specimens

Plaster of Paris,  $\text{CaSO}_4 \cdot 1/2\text{H}_2\text{O}$ , was sprinkled into (a) ordinary tap water and (b) magnetically treated water (obtained in the manner described in Section 3.8) and stirred continuously to produce a homogeneous mix, in each case. The ratio of water to Plaster of Paris used was 7:10. As with the cement, samples were moulded to form dogbones of the same dimensions. Moreover, industrially manufactured dogbones were supplied by Twyfords. Tensile strength tests were performed on all specimens. Prior to testing, specimens were placed in a kiln at  $38^\circ\text{C}$  for 24 hrs. unless stated otherwise (indicated on tables) to ensure adequate drying.

TABLE 3.16

Dogbones: Dispersion of tap water in Plaster of Paris.

TIME (Days)	SAMPLE NO.	WIDTH (mm)	THICKNESS (mm)	C.S.A. (mm <sup>2</sup> )	FORCE (N)	T.S. (x10 <sup>-3</sup> N/mm <sup>2</sup> )
7	1	25.58	24.25	620.32	780	1.26
	2	25.65	24.24	621.76	815	1.31
	3	25.48	24.10	614.07	885	1.44
	4	25.74	24.23	623.68	930	1.49
	5	25.71	24.07	618.84	500	0.81
	6	25.51	24.09	614.54	795	1.29
MEAN						1.27
8	* 7	26.70	24.47	653.35	900	1.38
	8	25.46	24.33	619.44	925	1.49
	9	25.60	24.10	616.96	600	0.97
	10	25.79	24.17	623.34	905	1.45
	11	25.71	24.09	619.35	815	1.32
	12	25.54	24.23	618.83	645	1.04
MEAN						1.26

\* Cast damaged during loan to industry and thus, specimen rendered invalid.

TABLE 3.17

Dogbones: Dispersion of magnetically treated water  
in Plaster of Paris.

TIME (Days)	SAMPLE NO.	WIDTH (mm)	THICKNESS (mm)	C.S.A. (mm <sup>2</sup> )	FORCE (N)	T.S. (x10 <sup>-3</sup> N/mm <sup>2</sup> )
7	1	25.90	24.22	627.30	810	1.29
	2	25.54	24.07	614.75	800	1.30
	3	25.56	24.08	615.48	760	1.23
	4	25.34	24.23	614.00	820	1.34
	5	25.65	24.11	618.42	765	1.24
	6	25.52	24.14	616.05	985	1.60
					MEAN	1.33
8	* 7	26.49	24.01	636.02	700	1.10
	8	25.40	24.28	616.71	735	1.19
	9	25.69	24.34	625.29	875	1.40
	10	25.47	24.36	620.45	860	1.39
	11	25.74	24.16	621.88	860	1.38
	12	25.51	24.25	618.62	825	1.33
					MEAN	1.34

\* Cast damaged during loan to industry and thus, specimen rendered invalid.

TABLE 3.18

Dogbones: Dispersion of tap water in Plaster of Paris.

TIME (Days)	SAMPLE NO.	WIDTH (mm)	THICKNESS (mm)	C.S.A. (mm <sup>2</sup> )	FORCE (N)	T.S. (x10 <sup>-3</sup> N/mm <sup>2</sup> )
7	1	25.81	24.16	623.57	330	0.53
	2	25.80	24.19	624.10	330	0.53
	3	25.73	24.23	623.44	395	0.63
MEAN						0.56
14	4	25.55	24.19	618.05	348	0.56
	5	26.06	24.29	633.00	305	0.48
	6	25.70	24.38	626.57	325	0.51
MEAN						0.52
21	7	25.66	24.17	620.20	290	0.47
	8	25.85	24.23	626.35	340	0.54
	9	25.72	24.37	626.80	330	0.53
MEAN						0.51
28	10	26.32	24.22	637.47	340	0.53
	11	25.56	24.20	618.55	335	0.54
	12	25.83	24.19	624.83	458	0.73
MEAN						0.60
OVERALL MEAN						0.55

N.B. Specimens not fired prior to testing.

TABLE 3.19

Dogbones: Dispersion of magnetically treated water  
in Plaster of Paris.

TIME (Days)	SAMPLE NO.	WIDTH (mm)	THICKNESS (mm)	C.S.A. (mm <sup>2</sup> )	FORCE (N)	T.S. ( $\times 10^{-3}$ N/mm <sup>2</sup> )
7	1	25.81	24.20	624.60	330	0.53
	2	25.79	24.65	635.72	370	0.58
	3	25.72	24.32	625.51	315	0.50
						MEAN 0.54
14	4	25.77	24.06	620.03	300	0.48
	5	25.62	24.21	620.26	390	0.63
	6	26.14	24.31	635.46	350	0.55
						MEAN 0.55
21	7	26.18	24.13	631.72	380	0.60
	8	25.80	24.30	626.94	398	0.63
	9	25.57	24.19	618.54	340	0.55
						MEAN 0.59
28	10	25.81	24.18	624.09	755	1.21
	11	25.71	24.16	621.15	885	1.42
	12	25.87	24.25	627.35	705	1.12
						MEAN 1.25
						OVERALL MEAN 0.73

N.B. Specimens not fired prior to testing.

TABLE 3.20  
 Industrially manufactured dogbones:  
 Dispersion of tap water in Plaster of Paris.

SAMPLE NO.	WIDTH (mm)	THICKNESS (mm)	C.S.A. (mm <sup>2</sup> )	FORCE (N)	T.S. ( $\times 10^{-3}$ N/mm <sup>2</sup> )
1	25.71	24.41	627.59	600	0.96
2	25.58	25.55	653.57	760	1.16
3	25.69	24.42	627.35	830	1.32
4	26.13	24.52	640.71	780	1.22
5	26.09	25.12	655.38	870	1.33
6	25.60	24.88	636.93	720	1.13
7	25.57	24.98	638.74	750	1.17
8	25.80	24.62	635.20	640	1.01
9	26.04	24.61	640.84	840	1.31
10	25.49	24.71	629.86	840	1.33
11	25.73	24.66	634.50	730	1.15
12	25.64	24.56	629.72	750	1.19
13	25.65	24.14	619.19	735	1.19
14	26.08	24.41	636.61	795	1.25
15	25.45	24.07	612.58	680	1.11
* 16	25.57	23.76	607.54	530	0.87
17	26.20	23.86	625.13	795	1.27
* 18	25.43	24.12	613.37	470	0.77
19	25.82	24.07	621.49	815	1.31
20	25.50	23.80	606.90	630	1.04
21	25.45	24.10	613.35	760	1.24
22	26.23	24.04	630.57	670	1.06
23	25.80	23.74	612.49	780	1.27
24	25.44	24.10	613.10	760	1.24

MEAN 1.19

\* These anomalously low values were rendered invalid.

TABLE 3.21

Industrially manufactured dogbones: Dispersion of magnetically treated water in Plaster of Paris.

SAMPLE NO.	WIDTH (mm)	THICKNESS (mm)	C.S.A. (mm <sup>2</sup> )	FORCE (N)	T.S. (x10 <sup>-3</sup> N/mm <sup>2</sup> )
1	25.51	25.21	643.12	750	1.17
2	26.46	24.53	649.06	820	1.26
3	26.03	24.95	649.45	875	1.34
4	25.96	25.10	651.60	770	1.18
5	26.04	24.29	632.51	810	1.28
6	25.95	24.82	644.08	640	0.99
7	25.74	24.66	634.75	720	1.13
8	26.26	24.87	653.09	800	1.22
9	27.06	24.24	655.93	585	0.90
10	26.00	24.24	656.24	890	1.36
11	26.01	24.03	625.02	900	1.44
12	26.04	24.09	627.30	810	1.29
13	27.59	24.55	677.34	720	1.06
14	26.12	24.58	642.03	665	1.04
15	26.78	24.01	642.99	740	1.15
16	25.92	24.53	635.82	830	1.31
17	25.72	24.73	636.06	860	1.35
18	26.00	24.32	632.32	790	1.25
19	26.24	24.86	652.33	885	1.36
20	25.78	24.59	633.93	865	1.36
21	26.22	24.44	640.82	810	1.26
22	26.63	25.44	677.47	870	1.29
23	26.25	24.19	634.99	830	1.31
24	25.71	24.75	636.32	770	1.21

MEAN 1.23

TABLE 3.22

Dogbones: Mean tensile strength measurements ( $\times 10^{-3}$  N/mm<sup>2</sup>) of specimens containing OPC and tap water (TW) and, OPC and magnetically treated water (MTW), indicating percentage increase in specimens containing MTW.

TIME (Days)	TW SPECIMENS	MTW SPECIMENS	% INCREASE
7	1.31	1.31	0
14	1.35	1.50	11.1
21	1.56	1.68	7.7
28	1.68	1.78	6.0

TABLE 3.23

Dogbones: Mean tensile strength measurements ( $\times 10^{-3}$  N/mm<sup>2</sup>) of specimens containing SRPC and TW and, SRPC and MTW, indicating percentage increase in specimens containing MTW.

TIME (Days)	TW SPECIMENS	MTW SPECIMENS	% INCREASE
7	0.56	0.90	60.7
14	0.80	0.90	12.5
21	0.89	1.40	57.3
28	1.12	1.40	25.0

TABLE 3.24

Dogbones: Mean tensile strength measurements ( $\times 10^{-3}$  N/mm<sup>2</sup>) of specimens containing oilwell cement and TW and, oilwell cement and MTW, indicating percentage increase in specimens containing MTW.

TIME (Days)	TW SPECIMENS	MTW SPECIMENS	% INCREASE
7	0.53	0.89	67.9
14	0.64	0.97	51.6
21	1.12	1.16	3.6
28	1.15	1.18	2.6

TABLE 3.25

Dogbones: Mean tensile strength measurements ( $\times 10^{-3}$  N/mm<sup>2</sup>) of specimens containing SRPC and TW and, magnetically treated slurry of 10% SRPC and tap water dispersed in SRPC, indicating percentage increase in specimens containing slurry.

TIME (Days)	TW SPECIMENS	SLURRY SPECIMENS	% INCREASE
7	0.56	0.65	16.1
14	0.80	1.06	32.5
21	0.89	1.25	40.5
28	1.12	1.47	31.3

TABLE 3.26

Cubes: Mean compressive strength measurements (N/mm<sup>2</sup>) of specimens containing OPC and tap water (TW) and, OPC and magnetically treated water (MTW), indicating percentage increase in specimens containing MTW.

TIME (Days)	TW SPECIMENS	MTW SPECIMENS	% INCREASE
7	20.6	29.4	42.7
14	25.1	35.0	39.4
21	35.8	36.9	3.1
28	37.4	39.3	5.1

TABLE 3.27

Cubes: Mean compressive strength measurements (N/mm<sup>2</sup>) of specimens containing SRPC and TW and, SRPC and MTW, indicating percentage change in specimens containing MTW.

TIME (Days)	TW SPECIMENS	MTW SPECIMENS	% CHANGE
7	91.8	89.2	- 2.8
14	103.7	103.8	0.1
21	109.0	113.1	3.8
28	112.7	117.6	4.4

TABLE 3.28

Cubes: Mean compressive strength measurements (N/mm<sup>2</sup>) of specimens containing oilwell cement and TW and, oilwell cement and MTW, indicating percentage change in specimens containing MTW.

TIME (Days)	TW SPECIMENS	MTW SPECIMENS	% CHANGE
7	86.0	83.5	- 2.9
14	86.7	96.1	10.8
21	101.1	105.8	4.6
28	107.5	113.8	5.9

TABLE 3.29

Cubes: Mean compressive strength measurements (N/mm<sup>2</sup>) of specimens containing SRPC and TW and, magnetically treated slurry of 10% SRPC and tap water dispersed in SRPC, indicating percentage change in specimens containing slurry.

TIME (Days)	TW SPECIMENS	SLURRY SPECIMENS	% CHANGE
7	91.8	78.0	- 15.0
14	103.7	92.4	- 10.9
21	109.0	94.2	- 13.6
28	112.7	96.2	- 14.6

TABLE 3.30

Dogbones: Mean tensile strength measurements ( $\times 10^{-3} \text{N/mm}^2$ ) of specimens containing Plaster of Paris and TW and, Plaster of Paris and MTW indicating percentage increase in specimens containing MTW.

TIME (Days)	TW SPECIMENS	MTW SPECIMENS	% INCREASE
7	1.27	1.33	4.7
8	1.26	1.34	6.3

TABLE 3.31

Dogbones: Mean tensile strength measurements ( $\times 10^{-3} \text{N/mm}^2$ ) of specimens containing Plaster of Paris and TW and, Plaster of Paris and MTW indicating percentage change in specimens containing MTW.

TIME (Days)	TW SPECIMENS	MTW SPECIMENS	% CHANGE
7	0.56	0.54	- 3.6
14	0.52	0.55	5.8
21	0.51	0.59	15.7
28	0.60	1.25	108.3

TABLE 3.32

Dogbones: Mean tensile strength measurements ( $\times 10^{-3} \text{N/mm}^2$ ) of industrially manufactured specimens containing Plaster of Paris and TW and, Plaster of Paris and MTW indicating percentage increase in specimens containing MTW.

TW SPECIMENS	MTW SPECIMENS	% INCREASE
0.56	0.65	3.4

TABLE 3.33

Summary of data showing overall percentage change in strength of cement samples containing MTW as measured against similarly prepared samples containing ordinary TW.

Composition of specimens	% Change in strength of specimens containing MTW compared with those containing TW after 28 days	
	Dogbones	Cubes
MTW/OPC	+ 6	+ 5
MTW/SRPC	+25	+ 4
MW/Oilwell cement	+ 3	+ 6
Magnetically treated slurry of SRPC/SRPC	+32	-15

TABLE 3.34

Summary of data showing overall percentage change in strength of Plaster of Paris samples containing MTW as measured against similarly prepared samples containing ordinary TW.

Composition of Specimens	Dogbones
MTW/Plaster of Paris	+ 5 (after 6 days) + 6 (after 12 days)
MTW/ Plaster of Paris (Industrially prepd. samples)	+ 3
MTW/Plaster of Paris	+33 (after 28 days) (not fired)

### 3.10 Discussion

The results obtained from the work described in this chapter indicate that the use of hard water, passed through a magnetic field for cement hydration, leads to an increase in both tensile and compressive strengths for ordinary Portland cement, sulphate-resisting Portland cement and oilwell cement. No compressive strength tests were carried out for Plaster of Paris, but the tensile strength was found to increase with the use of water that had passed through a magnetic field.

Following the discussion at the end of Chapter Two, it is suggested that the interaction between the magnetic field and pre-nuclear clusters in hard water alters the nature of these clusters and their subsequent chemical reaction. In this particular case, the subsequent reaction of the clusters with cement particles appears to result in more efficient aggregation of the hydrated cement particles to produce set cements with increased tensile and compressive strengths.

To test the direct effect of magnetic fields on hydrated cement particles, slurries of cement were passed through a magnetic field and these slurries were used to produce a cement-water mix for setting tests. In comparison with

duplicate experiments with the slurry not treated magnetically, an increase in tensile, but not compressive strength, was observed. The difference in the compressive strength behaviour between water and slurry treatment suggests that the effect of the magnetic field on the slurry is two-fold and that the results of the interaction between the field and slurry particles are found in addition to the reaction with clusters in the hard water.

REFERENCES

1. West, A.R., 'Solid State Chemistry and its Applications', Wiley and Sons Ltd., U.K., 1984.
2. Blezard, R.G., *Chemistry and Industry*, Sept. 1981, 18, 630-636.
3. British Standards Institution, 'Specification for ordinary and rapid-hardening Portland cement', BS 12, BSI, 1978.
4. Shirley, D.E., 'Introduction to Concrete', Cement and Concrete Association, U.K., 1980.
5. British Standards Institution, 'Sulphate-resisting Portland cement', BS 4027 : Part 2, BSI, 1972.
6. British Standards Institution, 'Specification for low heat Portland cement', BS 1370, BSI, 1979.
7. British Standards Institution, 'Portland blast furnace cement', BS 146 : Part 2, BSI, 1973.
8. Barnbrook, G., 'Concrete Practice', Cement and Concrete Association, U.K., 1976.
9. Belova, V., *Soviet Science Review*, May 1972, 150-156.
10. British Standards Institution, 'Testing of resin compositions for use in construction', BS 6319 : Part 7, BSI, 1985.
11. British Standards Institution, 'Specification for compression testing machines for concrete, BS 1881 : Part 116, BSI, 1986.

12. British Standards Institution, 'Specification for compression testing machines for concrete, BS 1881 : Part 114, BSI, 1986.

CHAPTER FOUR  
DISPERSION STUDIES

	Page	
4.1	Introduction	217
4.2	Tin(II) Carboxylates as Curing Catalysts for Silicone Resins	218
4.2.1	Introduction to Silicones	218
4.2.2	Analytical Techniques	226
4.2.3	Experimental	241
4.2.3(a)	Scope of this Work	241
4.2.3(b)	Preparation of Carboxylates	242
4.2.3(c)	Preparation of Dispersants	244
4.2.4	Curing Results	247
4.2.5	Mössbauer Results	247
4.2.6	Discussion	247
4.3	Dispersion of Calcium Hydroxide in Processing Aids	257
4.3.1	Thermal Analysis	260
4.3.2	Tablet Formation	265
4.3.3	Scattering Ability	266
4.3.4	Results of DTA	266
4.3.5	Results of Tablet Formation	266
4.3.6	Results of Scattering Ability	266
4.3.7	Discussion	273
4.4	The Determination of a Suitable Form of Administering Cobalt to Ruminants	274

	Page	
4.4.1	Introduction	274
4.4.2	Scope of this Work	277
4.4.3	Experimental Procedure and Results	278
4.4.4	Discussion	283
	References	285

CHAPTER FOUR  
DISPERSION STUDIES

4.1 Introduction

The manufacture and use of composite materials has become particularly important over the last decade. The aim, in the production of composites, is to maximize properties such as strength, electrical conductivity, heat transfer and chemical reactivity by mixing different phases until these requirements are fulfilled. Previous work at The City University has been concerned, for example, with dispersion of natural fibres in structural composites [1], conducting metal oxides in polymers for use as antistatic plastics [2] and viscous catalyst media in resins for low temperature use [3].

In this work, the aspect of composite materials considered is the problem of dispersion of fine powders in suitable media to maximize the chemical reactivity of the powder while minimizing the disadvantages associated with handling and susceptibility to atmospheric attack.

Three dispersion systems have been studied:

1. Catalysts containing a tin(II) carboxylate.

2. Calcium hydroxide-processing aid composites for fluoroelastomers.
3. Cobalt oxide in ruminant feedstock.

## 4.2 Tin(II) Carboxylates as Curing Catalysts for Silicone Resins

### 4.2.1 Introduction to Silicones

Silicones may be defined as polymeric materials based on the inorganic siloxane backbone,  $(-\text{Si}-\text{O}-)_n$ , the other valencies on the silicone atom usually being occupied by organic groups or hydrogen. The thermally stable silicon-oxygen bonds confer a high degree of chemical inertness on these materials; the physical properties of silicones are retained over a wide temperature range, typically from  $-50$  to  $250^\circ\text{C}$ , which renders them valuable for many demanding applications.

Silicone polymers may be divided into three major categories: fluids, elastomers and resins.

The fluids and elastomers are based on a linear structural arrangement. The former are colourless in appearance and of a relatively low molecular weight. They exhibit little change in viscosity with temperature and thus, are ideal for

use as lubricants and hydraulic fluids. However, these fluids play a more important role as a constituent of water repellents for treating paper and fabrics. Certain liquid silicones are also used as surfactants to control or eliminate foam formation in various processes, whilst others constitute the basis of damping fluids and release agents.

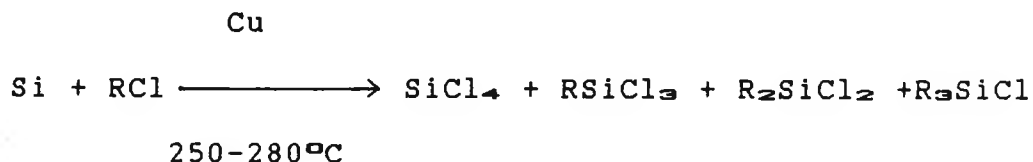
Silicone elastomers, owing to their remarkable thermal and oxidative stability, chemical resistance and excellent dielectric properties, are used as potting compounds for encapsulating electric parts, wire coatings, gasket materials and adhesives. Their physiological inertness enables them to be used as construction material for artificial organs for surgical implantation. Further, the release properties of silicone elastomers have led to their extensive use in producing moulds - ideal for the casting of plastics, plaster, or low melting point alloys.

Silicone resins are highly cross-linked, comprising a rigid, three-dimensional structure. They can vary in consistency from very flexible substances to hard, brittle, glassy materials and are employed as water-repellent coatings, mould release agents, nonstick surfaces for cooking utensils (although not as successfully as polytetrafluoroethylene), and as with fluids, in treating paper and fabrics. Some of

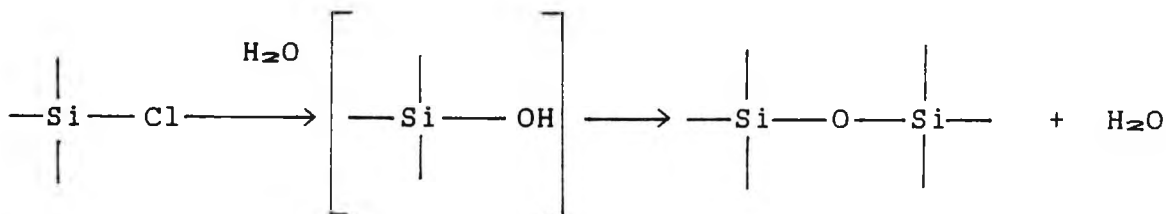
the more unusual properties of polysiloxanes are demonstrated by the behaviour of Super Balls and Silly Putty.

### Preparation of Silicones

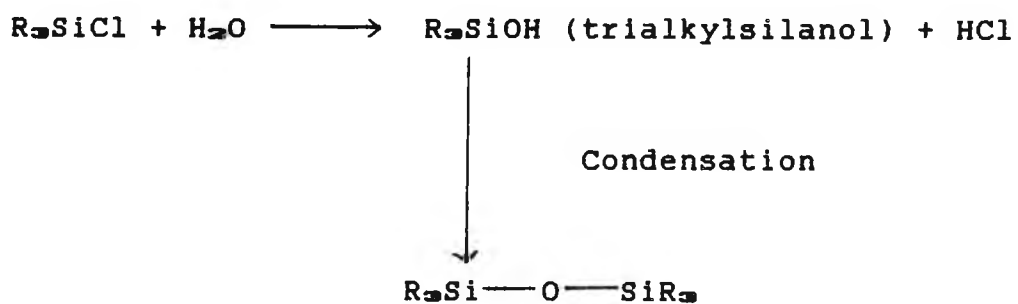
Silicones, or polysiloxanes, as they are sometimes referred to, are prepared by hydrolysis of alkylsilicon or arylsilicon halides. The halogen derivatives themselves are made from silicon and alkyl or aryl halides by heating at 250 to 280°C in the presence of a copper catalyst. This is the preferred procedure for preparing methyl- and phenylchlorosilanes.



Hydrolysis of the halides yields the corresponding unstable silanols which undergo condensation to form the siloxane linkage:

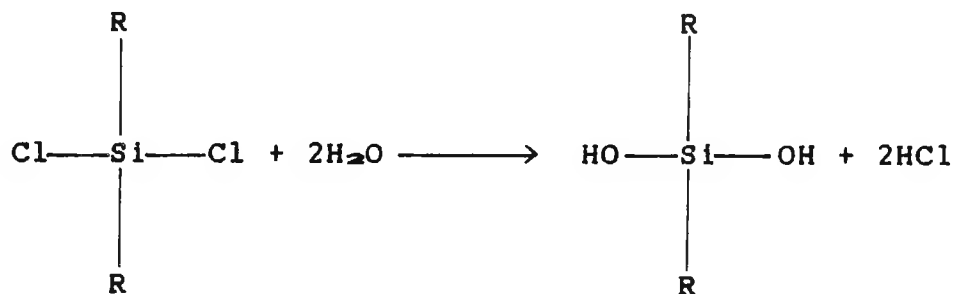


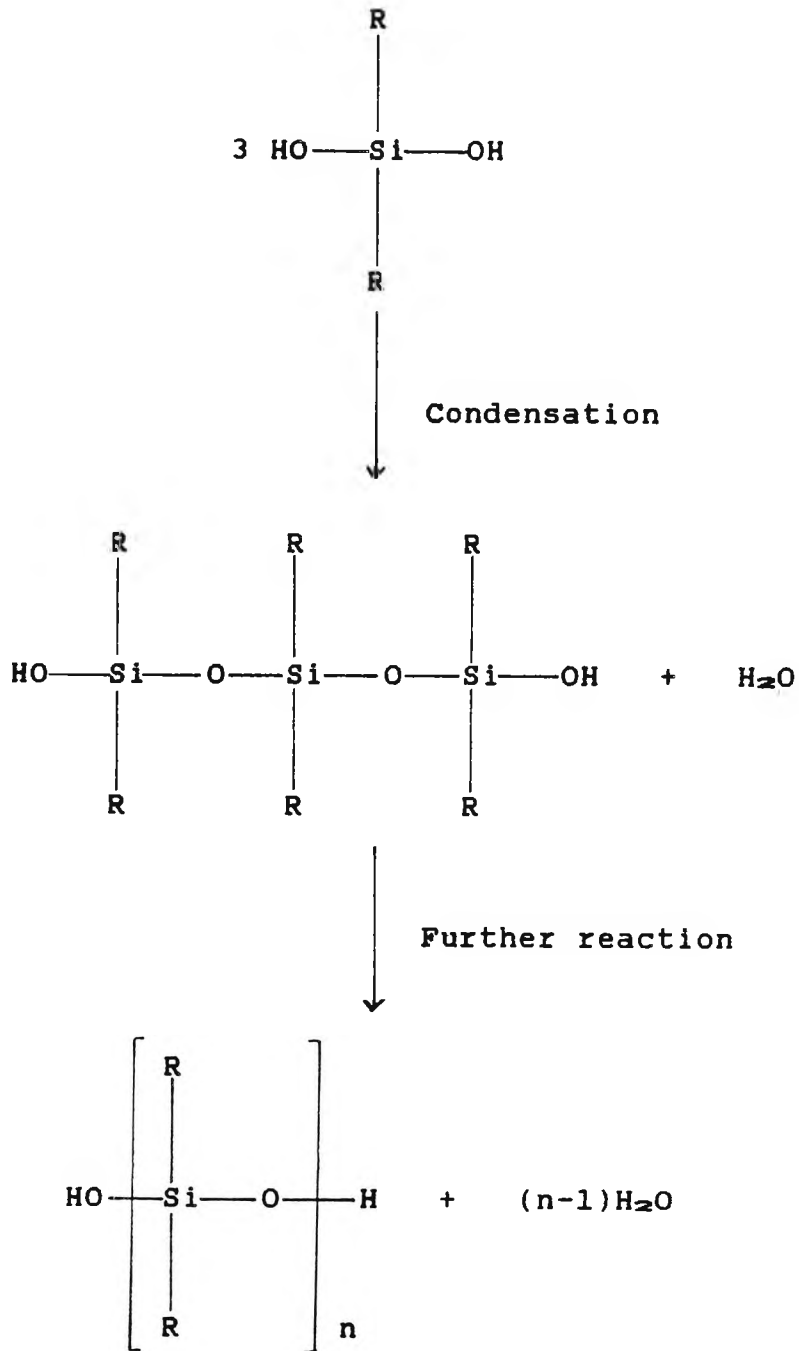
Hydrolysis of the trialkylchlorosilane leads to a dimer (a disiloxane), since this compound is only monofunctional.



Thus,  $R_3SiCl$  is frequently used as a terminator, to regulate the chain length of silicone polymers.

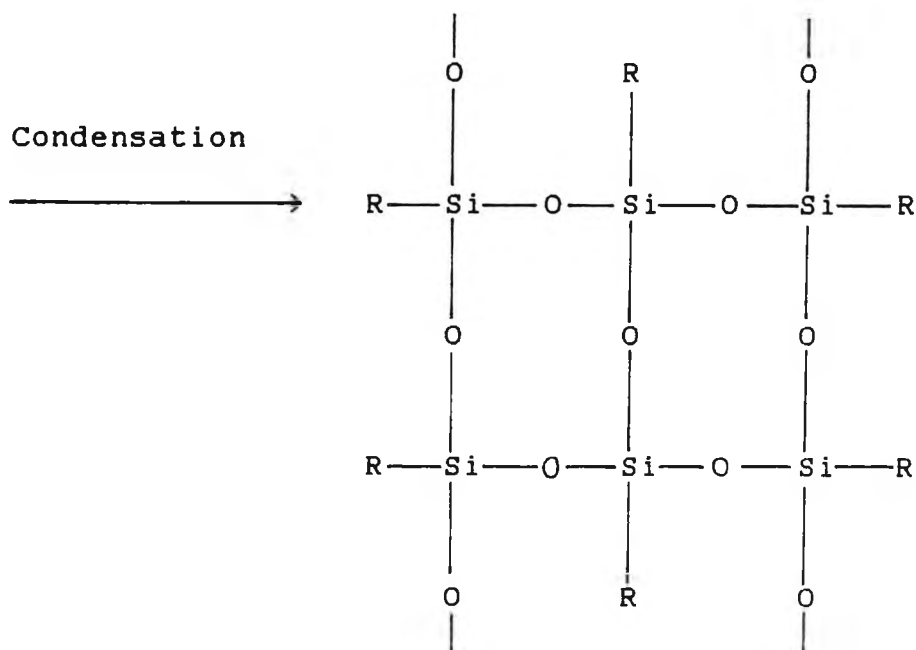
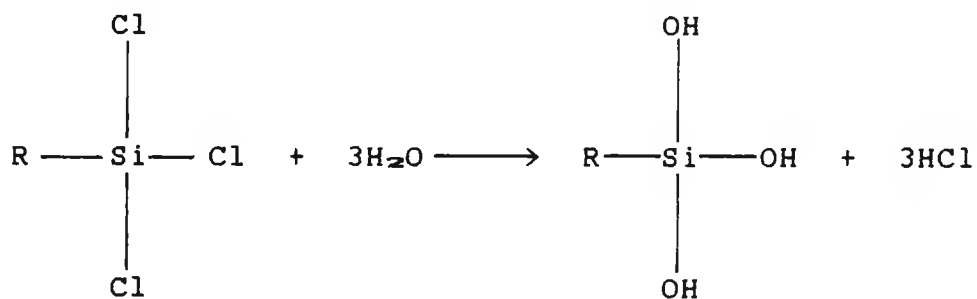
Hydrolysis of the dialkyldichlorosilane yields a linear polymer:





Two dimensional silicone

Crosslinked polysiloxanes are prepared via the hydrolysis of trichlorosilanes:

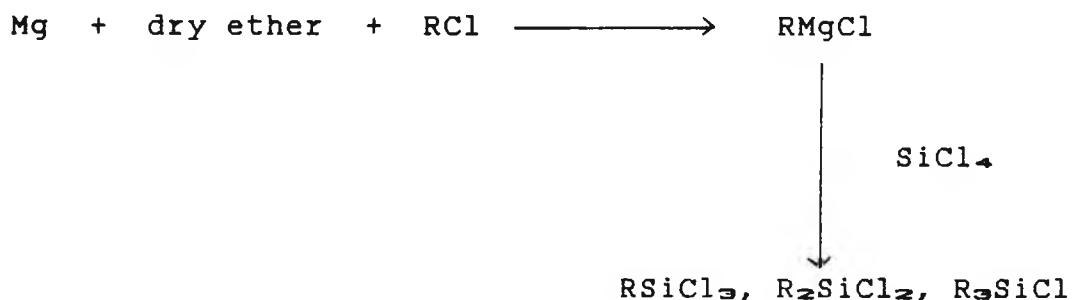


Three dimensional silicone

They may also be prepared by hydrolysis of mixtures of di-

and trichlorosilanes, the degree of crosslinking being determined by the molar ratio of these compounds (the greater the proportion of the trichloro-derivative, the greater the extent of crosslinking). The nature of the polymers are, in addition, dependent on the alkyl or aryl substituent. Generally, these polymers range from oily liquids to rubbery solids.

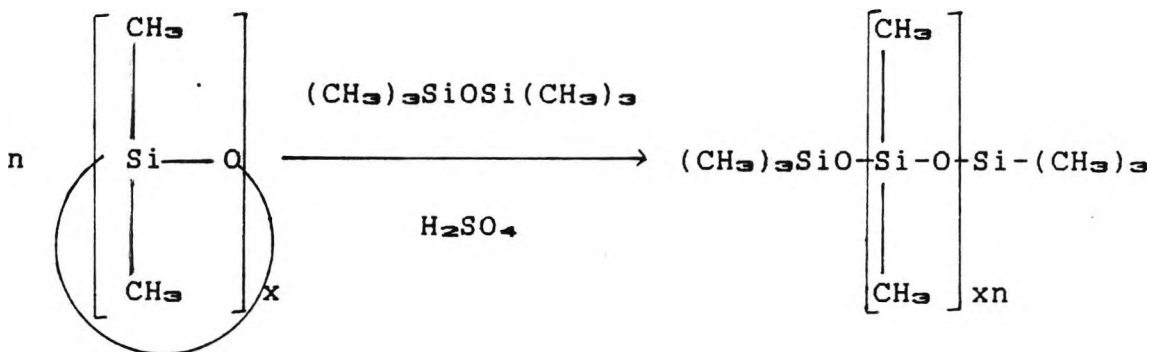
Though the method employing a copper catalyst is preferred in the production of methyl and phenyl substituted compounds, a Grignard-type synthesis is commonly used for other alkyl and aryl substituted substances:



As a general method of preparing polysiloxanes, hydrolysis of the halides is not satisfactory because of the tendency to form cyclic siloxanes (mainly trimers or tetramers) under the conditions of hydrolysis, although some silicone resins are synthesized in this way. To obtain high molecular weight polymers, the cyclic products are purified by distillation and polymerized by acid- or base-catalyzed, ring-opening

reactions.

In the presence of sulphuric acid, ring-opening and further condensation occur to give linear siloxane polymers. Silicone fluids are prepared by adding some hexamethyldisiloxane, during the polymerization reaction, eliciting the production of polysiloxanes with unreactive trimethylsiloxyl terminal groups. The molecular weight, and hence viscosity, of the oils can be controlled by the amount of hexamethyldisiloxane added.



The use of tin carboxylate catalysts to cure silicone resins is described in Section 4.2.3.

Preliminary investigations on silicone resin tin catalysts were carried out at The City University by Nicholides [4] who varied the following parameters: (a) the catalyst used, (b) the catalyst concentration, (c) the solvent used, and (d) the temperature. She used tin(II), alkali metal tin(II)

and transition metal tin carboxylate catalysts and found (1) that stannous octoate was the most efficient catalyst under ambient conditions, (2) that increasing the catalyst concentration caused an exponential decrease in cure time, (3) that the rate of cure is independent of the solvent used and (4) that a drop in temperature from room temperature to 2°C caused a 30 fold decrease in the catalytic activity of tin(II) octoate.

One problem with the use of tin(II) carboxylates is that their solutions in carboxylic acids are of very different viscosity from the silicones and mixing is difficult. The aim of this work was to study the use of solid tin(II) carboxylates dispersed in a medium of ethylene glycol and octoic acid to produce fluids of viscosity similar to that of the silicones.

#### 4.2.2 Analytical Techniques

Section 4.2.3(b) concerns the preparation of tin(II) carboxylates, the corresponding transition metal carboxylates, and their transition metal tin derivatives. The analytical techniques adopted and the principles involved are briefly outlined.

### Elemental Analyses

The tin(II) content of the carboxylates was determined by Donaldson and Moser's method [5] which is suitable for both tin(II) and total tin analyses. The transition metal concentrations were determined by atomic absorption spectrometry on a Perkin Elmer 370 Spectrometer. Carbon and hydrogen analyses were conducted by the 'Microanalysis Service' operated by the Department of Chemistry at The City University. Water was determined in hydrated products by thermogravimetry.

Mössbauer spectroscopy was used in this part of the work to characterize products and follow reactions. A brief description of this technique now follows.

### MÖSSBAUER SPECTROSCOPY

#### General Principles

The Mössbauer effect, first observed by R.L. Mössbauer in 1957 [6], is the recoilless emission and resonant reabsorption of  $\gamma$ -radiation between the ground and usually

the first excited state of the nucleus and gives an energy distribution dictated by the Heisenberg Uncertainty Principle. A radioactive nucleus will emit  $\alpha$ ,  $\beta$ , and  $\gamma$  radiation. The emission of  $\gamma$ -radiation emanates from the decay of an excited spin state of a nucleus to the ground state. Classically, the energy of the  $\gamma$ -ray would be degraded by recoil of the nucleus and could not then be resonantly reabsorbed by another identical nucleus. The Mössbauer effect is, however, a solid state effect; crystalline lattices are used as emitters, in which the emitting nucleus is rigidly bound to the surrounding nuclei and hence, has a large apparent mass within which the recoil energy can be dissipated. A monochromatic  $\gamma$ -ray is thus emitted and can be resonantly reabsorbed. Experiments are conducted at liquid nitrogen or liquid helium temperatures to minimize thermal motions of the lattice atoms.

In this study, only  $^{119}\text{Sn}$  Mössbauer spectra were recorded. To obtain a Mössbauer spectrum, the source, emitting radiation of energy,  $E$ , is subjected to a Doppler velocity,  $v$ , relative to the absorber. The modulation of  $\gamma$ -radiation incident on the absorber,  $E_\gamma$ , produces an energy shift,  $\Delta E$ , denoted by the expression:

$$\Delta E = v \frac{E_\gamma}{c}$$

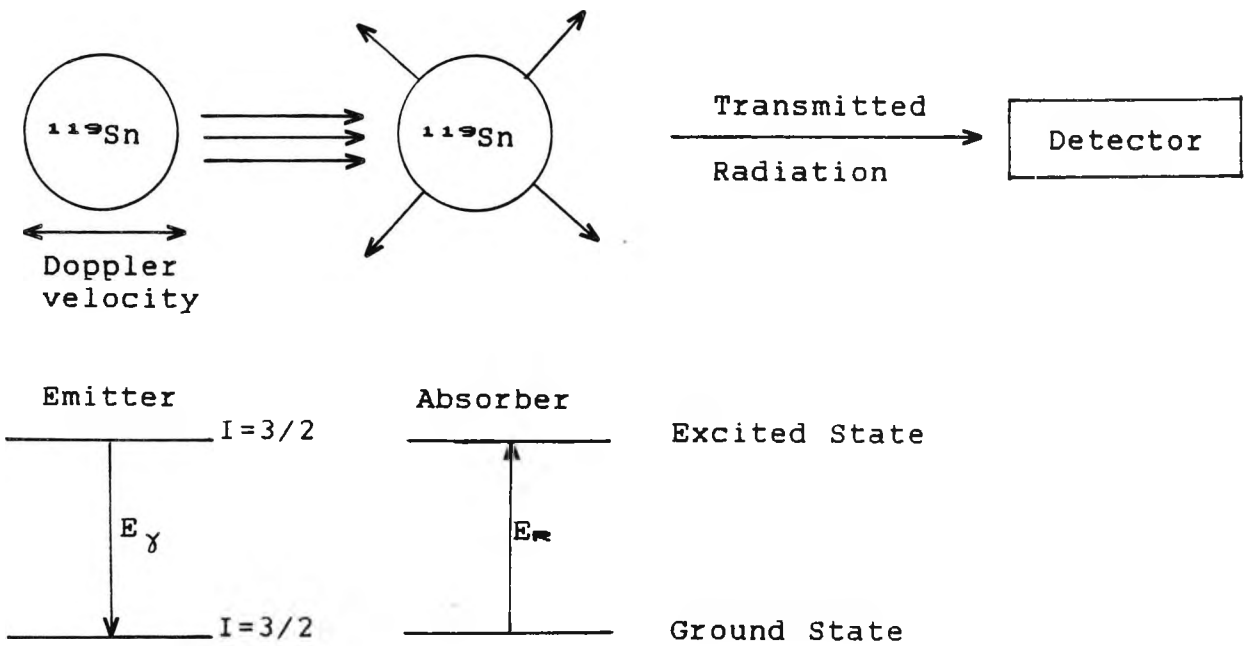


FIGURE 4.1 Fundamental features of the Mössbauer effect.

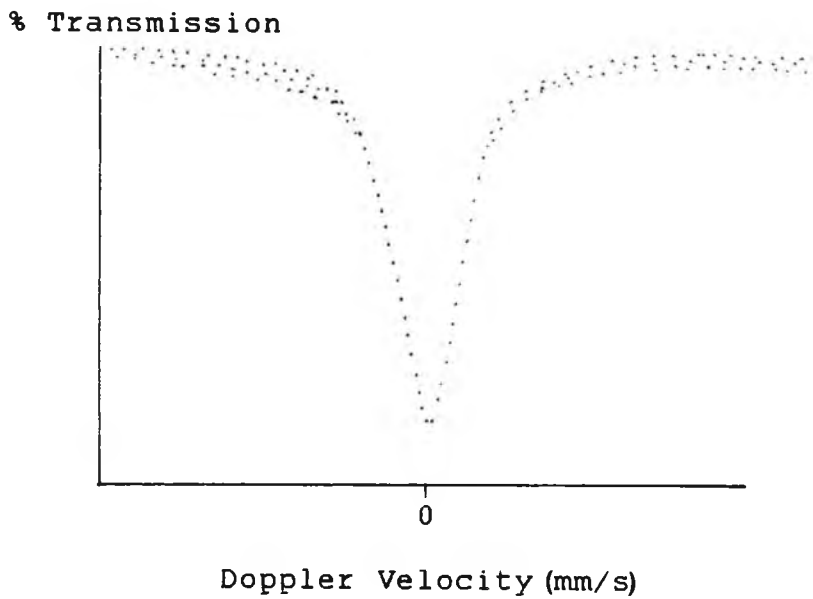


FIGURE 4.2 Mössbauer spectrum obtained when source and absorber are in identical environments.

where  $c$  is the velocity of light.

If the source and absorber are identical, maximum resonance will occur at zero velocity.

The Mössbauer spectrum is usually plotted as the percentage transmission (number of counts registered by the detector) against the Doppler velocity (Fig 4.2).

Maximum resonance will occur when  $E_\gamma = E_R$ , where  $E_R$  is the energy separation of the ground and excited states of absorbing nuclei.

### Chemical Shift

The chemical isomer shift is a direct function of the s-electron density at the Mössbauer nucleus, but shows induced secondary effects due to changes in shielding of the s-electrons by p-, d-, or f-electrons. As already mentioned, a nucleus in chemical surroundings, different from those of the source does not absorb at the same frequency, i.e. the energy gap between the ground and excited states of the source and absorber are unequal. Under these circumstances, the energy of the  $\gamma$ -radiation applied to the source is modulated by the Doppler motion, resulting in maximum

absorption resonance at a point other than when the Doppler velocity is zero and leading to a shift in the Mössbauer line referred to as the chemical isomer shift. Thus, if the Mössbauer spectrum of an  $\alpha$ -Sn absorber is recorded relative to a  $\text{BaSnO}_3$  source, a spectrum, as shown in Fig. 4.4, is obtained. This is due to the fact that the excited and ground state nuclei differ in radius to a small but significant extent and so the electrostatic interaction with the surrounding electrons changes on excitation. The effect is only important for s-electrons; the energy of the nucleus alters by an amount proportional to the change in nuclear radius,  $\delta R$ , and the s-electron density at the nucleus. Although  $\delta R$  is the same in both source and absorber the electron density is dependent upon the chemical environment.

The chemical shift provides information on the s-electron density at the nucleus which, in turn, gives an estimate of the bond character of atoms or ions chemically attached to the Mössbauer nucleus.

The chemical shift is expressed as follows:

$$\delta = k \cdot \frac{\Delta R}{R} \{ |\psi_0|_A^2 - |\psi_0|_S^2 \}$$

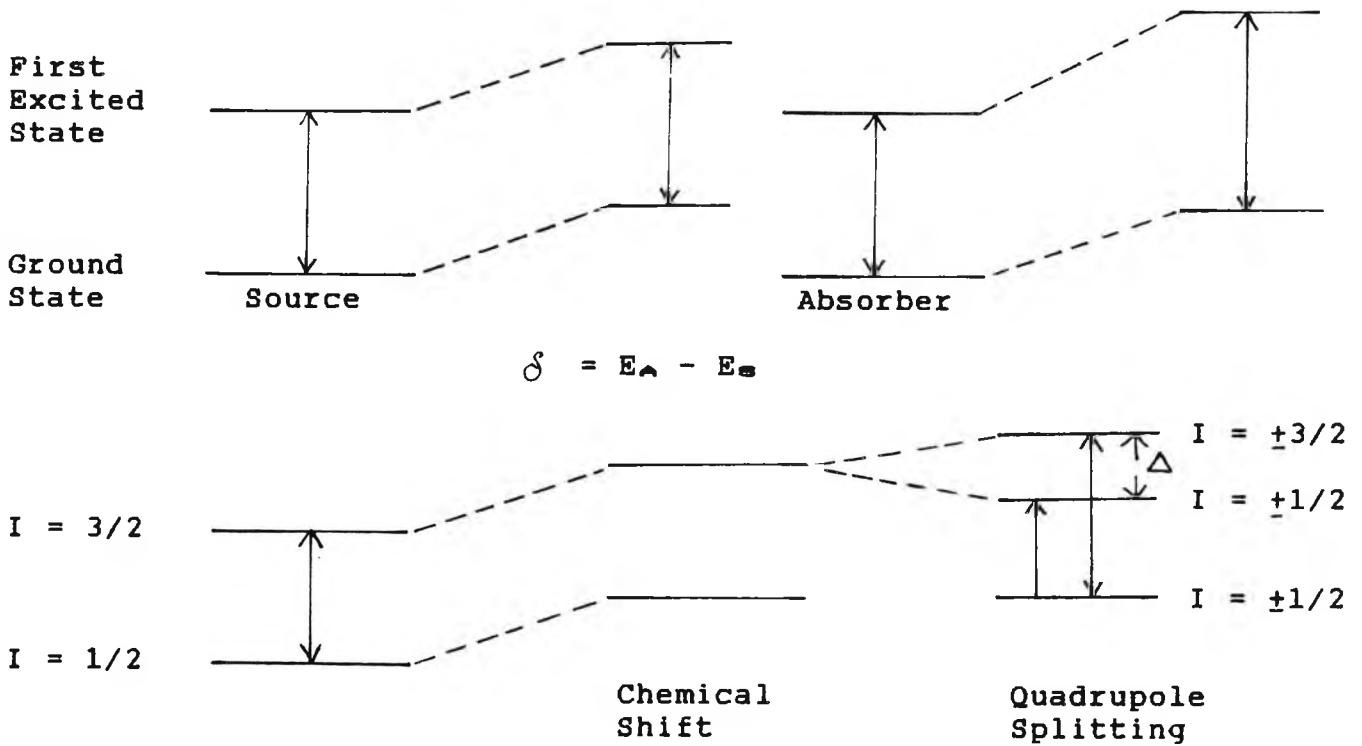


FIGURE 4.3 Origin of chemical shift and quadrupole splitting.

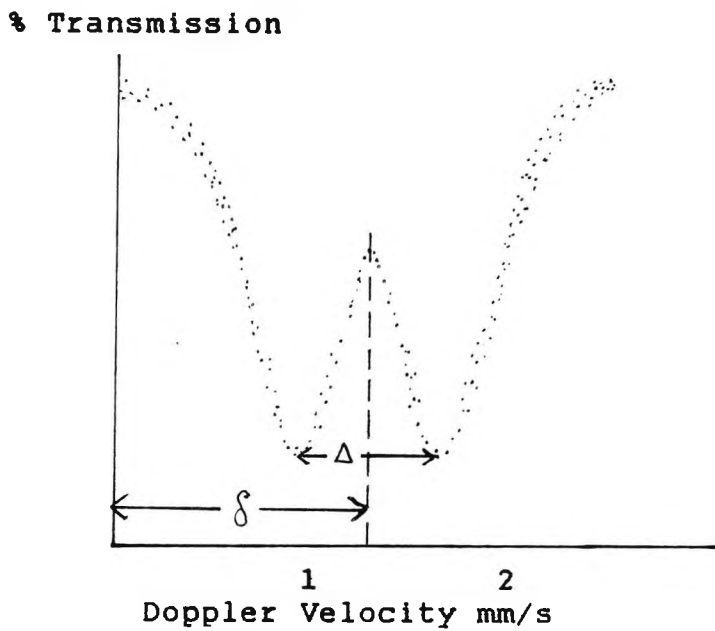


FIGURE 4.4 Mössbauer spectrum of an  $\alpha$ -Sn absorber, using a  $BaSnO_3$  source, showing chemical shift and quadrupole splitting.

where  $k = \text{constant}$

$R = \text{radius of nucleus in ground state}$

$\Delta R = \text{difference between nuclear radii in ground and excited states}$

$|\psi_0|^2 = \text{s-electron density at nucleus}$

The value of  $\Delta R/R$  is characteristic of each transition and may be of either sign. A positive value for  $\Delta R/R$  [7] implies that the s-electron density at the nucleus of the absorber is greater than that of the source and corresponds to an increase in the chemical isomer shift. The sign, in this case, further indicates that the nucleus contracts on de-excitation. Conversely, when  $\Delta R/R$  is negative, the reduction of s-electron density at the nucleus results in a decrease in the isomer shift.  $|\psi_0|^2$  includes contributions from all the occupied s-electron orbitals, but is naturally more sensitive to changes which take place in the outer valence shells. Although d- and f- orbitals have zero density at their nuclei, they have a significant indirect interaction with the Mössbauer nucleus by shielding the s-electrons from the latter.

#### Quadrupole Splitting

The derivation of the expression for the chemical isomer

shift assumes that the nucleus is spherical with a uniform charge distribution. However, a nucleus with a spin greater than  $I_{1/2}$ , has a nuclear quadrupole moment,  $eQ$ , so that even if the charge density within the nucleus is constant, the distorted shape causes the charge distribution to be non-spherical. Nuclei with spins of  $I=0$  or  $I=1/2$  are spherically symmetrical and do not possess quadrupole moments. The nuclear quadrupole moment is the departure of the nuclear charge from sphericity and can be positive or negative depending on whether the nucleus is prolate (elongated) or oblate (flattened), respectively, along the spin-axis.

The quadrupole splitting is brought about by the interaction of the nuclear quadrupole moment with the electric-field gradient, produced as a result of an imbalance in the p, d, or f electron density about the nucleus. An electric-field gradient may arise either in the valence shell, when the ligands are dissimilar or when the coordination geometry is less than cubic.

The quadrupole splitting occurs due to a splitting in the nuclear energy levels. In the case of  $^{119}\text{Sn}$ , transitions take place between the spin states  $I_{\text{g}}=1/2$  and  $I_{\text{e}}=3/2$ ; the ground state is unsplit and the excited state has two energy levels;  $I_{\text{e}}=\pm 1/2$  and  $\pm 3/2$  separated by

$$\Delta = (e^2qQ/2)(1+n^2/3)^{1/2}$$

where  $n$  is the electric field gradient,  $q$  is a point charge and  $Q$  is the nuclear quadrupole moment.

It follows that the Mössbauer spectrum consists of a doublet with a separation of  $\Delta$ , the quadrupole splitting, the centroid of the doublet corresponding to the isomer shift.

The quadrupole splitting is therefore a measure of the s-electron density; it increases with an increase in the electric field gradient at the nucleus. High symmetry (cubic, tetrahedral, octahedral) gives a zero quadrupole splitting and a single line spectrum.

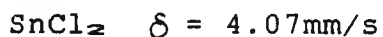
#### Magnetic Hyperfine Interactions

The Mössbauer line can also be split owing to a magnetic hyperfine interaction, set up as a result of an external, applied magnetic field or an internal magnetic field. If an atom has one or more unpaired d- or f-electrons, an imbalance in s-electron density at the nucleus is induced, thereby generating a local magnetic flux density. The resultant spectrum contains a number of resonant lines, symmetrical about the centroid.

Applications in the Chemistry of Tin

Mössbauer spectroscopy has drawn attention to many fundamental issues in the understanding of the chemistry of tin.

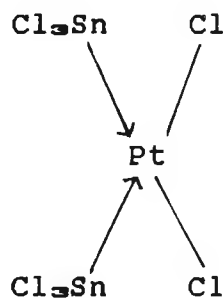
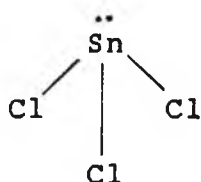
Sn(IV) and Sn(II) having outer configurations of  $4d^{10}5s^0$  and  $4d^{10}5s^2$ , respectively, can readily be distinguished between by reference to their chemical isomer shifts, the more positive values, as in the case of Sn(II) compounds, being associated with greater s-electron density,



The isomer shift also provides information on the bonding to the tin atom, i.e. ionic or covalent.  $\alpha$ -Sn is adopted as the reference point and arbitrarily assigned zero. Thus, an increase in isomer shift with respect to  $\alpha$ -Sn corresponds to an increase in s-electron density about the nucleus and hence a decrease in ionic character. Conversely, for Sn(IV) compounds, a decrease in isomer shift corresponds to a decrease in s-electron density, with more negative values accentuating the degree of ionicity. The actual value of the isomer shift, in each case, reflects the extent of ionicity or covalency of the bond to the tin atom.



The donation of the lone pair of electrons of the tin atom to another metal atom, during complex formation, is an additional factor resulting in a reduction of the s-electron density around the tin nucleus and hence, a decrease in isomer shift. As the lone pair now forms a dative bond, the complex is effectively a Sn(IV) species.



### Instrumentation

In this work, a Cryophysics MS-102 Microprocessor Mössbauer Spectrometer was used, the basic arrangement of which is diagrammatically represented in Fig. 4.6.

The spectrometer consists of two major components: the Doppler velocity drive which modulates the gamma energy emitted by the source, and the multichannel analyzer which stores an accumulated total of  $\delta$ -counts, (using binary memory storage like a computer), in one of several hundred individual registers known as channels. Each channel is held open in turn for a short time interval (of fixed length)

by a stable constant frequency clock. Any  $\gamma$ -counts registered by the detection system during this time period are added to those already accumulated and stored in the channel. The sequential accessing of the channels is completed in about  $1/20$  of a second and is repeated *ad infinitum*.

The time pulses from the clock may also be used to synchronize a voltage waveform, which is used as a command signal to the servo-amplifier controlling an electro-mechanical vibrator. The voltage increases linearly with time causing the source to move with constant acceleration and spend equal time intervals at each velocity increment. The multichannel analyzer and the Doppler drive are synchronized so that the velocity changes linearly from  $-v$  to  $+v$  with increasing channel number. In this way, the source is always moving at the same velocity when a given channel is open.

$\gamma$ -rays passing through the absorber are detected by a gas-filled proportional counter. The pulse is amplified before passing through a discriminator which rejects most of the non-resonant background radiation and is finally fed into the multichannel analyzer. In this study, a computerized output was obtained.

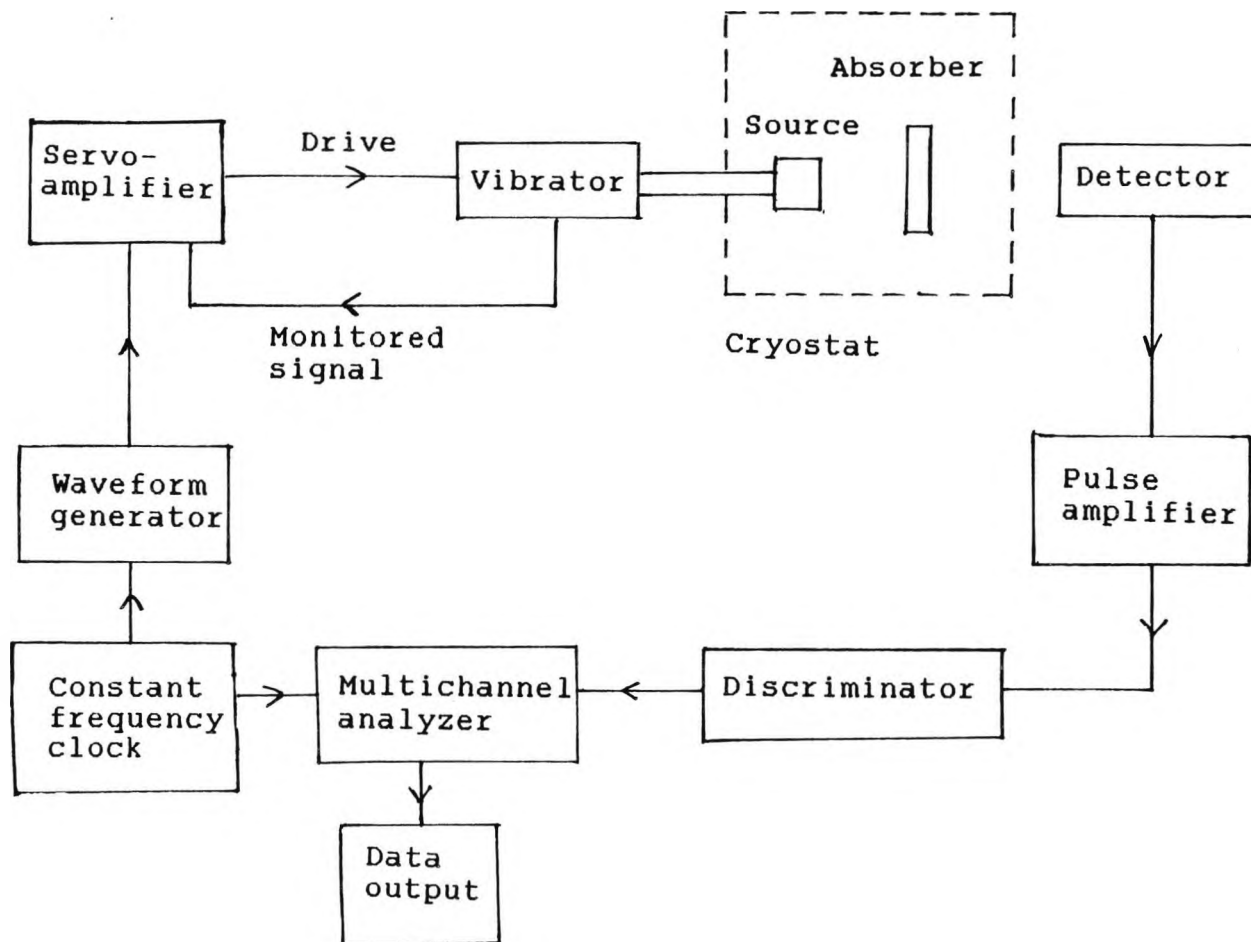


FIGURE 4.6 A schematic representation of a Mössbauer spectrometer.

It is often necessary to cool the absorber, and sometimes the source to 80K using liquid N<sub>2</sub> or to 4.2K using liquid He, to increase the recoilless fractions. In this instance, the absorber was encased in a cryostat and cooled accordingly. Mössbauer resonances may be recorded at room temperature, although it may take a considerably long time. The main exceptions to this are <sup>57</sup>Fe and <sup>119</sup>Sn.

A Ca<sup>119</sup>SnO<sub>3</sub> source, having a natural line width of  $\Gamma_{1/2} = 0.38\text{mm/s}$  was used in this work. The isomer shifts were recorded relative to a BaSnO<sub>3</sub> standard source.

#### 4.2.3 Experimental

##### 4.2.3(a) Scope of this Work

In this study, the effect of tin(II) carboxylates, as potential curing catalysts for silicone resins, have been determined. Following on from preliminary investigations in which materials such as stannous formate and stannous acetate have been shown to be effective curing agents, the present work examines the performance of these carboxylates, their transition metal counterparts, and transition metal-tin derivatives. Furthermore, a comparison is drawn between the rate of cure in non-magnetic and magnetic

silicone resins.

#### 4.2.3(b) Preparation of Carboxylates

##### TIN(II) CARBOXYLATES

Tin(II) formate [8] and tin(II) acetate [9] were prepared by the literature methods as follows:

##### Tin(II) Formate

Tin(II) formate was allowed to crystallize out from a solution obtained by refluxing blue-black tin(II) oxide with a 60% aqueous solution of formic acid. The white anhydrous crystals were filtered and dried *in vacuo* over KOH pellets. Tin(II) formate is moderately stable in air, although it eventually deteriorates with a loss of crystallinity and the oxidation of tin(II) to tin(IV).

##### Tin(II) Acetate

Tin(II) acetate was prepared by dissolving blue-black tin(II) oxide (0.2 mole) in a 50% aqueous solution of acetic acid (300ml) and refluxing for approximately one and a half hours. The resulting solution was filtered hot and concentrated by rotary evaporation. On cooling, a white powder was obtained and dried *in vacuo* over KOH. The compound is fairly stable in air, but eventually

deteriorates to give tin(IV) impurities. Tin(II) acetate melts between 182.5-183°C and boils between 239-241°C with some decomposition.

#### TRANSITION METAL CARBOXYLATES: COBALT AND NICKEL

##### Transition Metal Formates

0.1 mole of the appropriate carbonate was added to a 50% v/v aqueous solution of formic acid and refluxed for approximately one hour. The solution was then hot-filtered, allowed to cool, re-filtered under vacuum and finally dried *in vacuo* over KOH pellets. The products were crystalline in appearance.

##### Transition Metal Acetates

The general procedure as described for the preparation of transition metal formates was closely adhered to. The transition metal acetates were powdered.

#### COMPLEX DERIVATIVES OF TIN(II) CARBOXYLATES:

##### COBALT AND NICKEL

##### Complex Tin(II) Formates

Tin(II) oxide (0.05 mole) [10] was dissolved in a 50% v/v aqueous solution of formic acid (200ml) by refluxing for one hour. The solution was filtered hot and the appropriate

metal carbonate (0.05 mole) added before continuing to reflux. Again, the solution was hot-filtered and the filtrate subjected to rotary evaporation to remove any excess solvent before being dried *in vacuo* over KOH pellets. The cobalt and nickel compounds were of a pale pink and pale green pulverulent appearance, respectively.

#### Complex Tin(II) Acetates

Tin(II) oxide (0.01 mole) was dissolved in 50% v/v acetic acid (50ml) and the transition metal carbonate (0.005 mole) added to the clear filtrate [10] obtained after hot-filtering. The mixture was refluxed to complete dissolution and re-filtered, any excess solvent being reduced by rotary evaporation. The crystals obtained on cooling, were filtered and washed with diethyl ether, and stored *in vacuo* over KOH. It should be noted that any excess of tin(II) oxide or the metal carbonate only gives rise to coprecipitation of stannous acetate or the metal acetate, respectively.

#### 4.2.3(c) Preparation of Dispersants

The selected catalyst in each case was accurately weighed and dispersed in a known quantity of solvent consisting of ethylene glycol, which has a similar viscosity to that of

TABLE 4.1 Elemental analyses for tin(II) carboxylates.

	%Sn	%C	%H
Tin(II) Formate $\text{Sn}(\text{HCOO})_2$	55.9 (56.86)	10.61 (11.51)	0.93 (0.96)
Tin(II) Acetate $\text{Sn}(\text{CH}_3\text{COO})_2$	50.2 (50.13)	20.12 (20.29)	2.42 (2.55)

TABLE 4.2 Elemental analyses for transition metal carboxylates.

	%T.M.	%C	%H
Cobalt(II) Formate $\text{Co}(\text{HCOO})_2 \cdot 2\text{H}_2\text{O}$	31.5 (31.86)	12.03 (12.93)	3.42 (3.27)
Cobalt(II) Acetate $\text{Co}(\text{CH}_3\text{COO})_2 \cdot 4\text{H}_2\text{O}$	23.1 (23.66)	20.05 (19.29)	4.66 (5.66)
Nickel(II) Formate $\text{Ni}(\text{HCOO})_2 \cdot 2\text{H}_2\text{O}$	31.6 (31.72)	12.23 (12.98)	3.23 (3.27)
Nickel(II) Acetate $\text{Ni}(\text{CH}_3\text{COO})_2 \cdot 4\text{H}_2\text{O}$	23.4 (23.59)	19.90 (19.31)	5.37 (5.67)

TABLE 4.3 Elemental analyses for transition metal tin carboxylates.

	%T.M.	%Sn	%C	%H
Cobalt tin formate $\text{Co}_3\text{Sn}_4(\text{HCOO})_{14} \cdot 8\text{H}_2\text{O}$	11.2 (12.40)	32.7 (33.29)	12.41 (11.79)	1.77 (2.12)
Cobalt tin acetate $\text{CoSn}_2(\text{CH}_3\text{COO})_6 \cdot 5\text{H}_2\text{O}$	8.1 (7.96)	31.0 (30.20)	18.81 (19.46)	3.07 (3.81)
Nickel tin formate $\text{Ni}_3\text{Sn}_4(\text{HCOO})_{14} \cdot 8\text{H}_2\text{O}$	11.7 (12.35)	29.6 (33.31)	13.20 (11.80)	3.25 (2.12)
Nickel tin acetate $\text{NiSn}_2(\text{CH}_3\text{COO})_6 \cdot 5\text{H}_2\text{O}$	7.8 (8.0)	31.50 (32.10)	19.30 (19.50)	2.67 (3.80)

(Theoretical data indicated in parentheses.)

the resin, and octoic acid. The catalyst and ethylene glycol concentration were varied; that of octoic acid was kept constant. (Earlier investigations have proved 0.05ml to be the optimum volume of octoic acid for 5.0g of resin.)

A pre-dispersion of the catalyst in the appropriate medium was achieved by grinding the former to a fine powder and mixing with the latter. The resulting mixture was stirred into 5.0g of silicone resin, a free-flowing, viscous gum, for approximately 2-3 minutes, and the time required to obtain a hard cure noted. Curing was considered to have reached completion at the point at which the resin could be cleanly removed from the reaction vessel. At this stage, the polymer could not be deformed or indented with applied pressure. Each cure was accomplished in duplicate and a mean time subsequently obtained. Mössbauer data were also collected for the cured resins. The materials were water repellent, resistant to attack by acid and organic solvents, and thermally stable up to 600°C.

The same catalyst was employed in the curing of both, a non-magnetic and magnetic silicone resin having similar chemical and physical properties, with the exception that iron filings were dispersed in the latter. The non-magnetic and magnetic silicone resins were of a cream and grey hue, respectively.

#### 4.2.4 Curing Results

The cure times for the silicone resins using the prepared carboxylates are set out in Tables 4.4 and 4.5.

#### 4.2.5 Mössbauer Results

The Mössbauer data for the carboxylate catalysts and cured resins are given in Table 4.6.

#### 4.2.6 Discussion

The efficiency of tin(II) catalysts has long been known. Berridge [11] first reported the use of stannous octoate (tin(II) 2-ethylhexanoate), naphthenate and oleate as curing agents for the low molecular weight ethoxy resin:

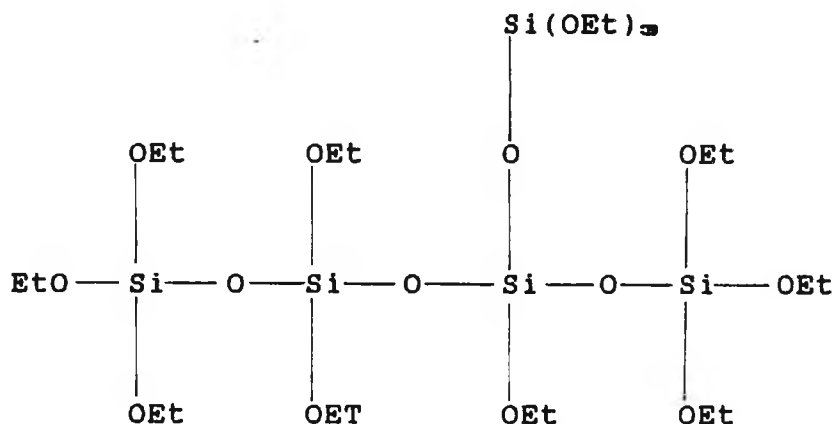


TABLE 4.4 Mean cure time for 5.0g of non-magnetic and magnetic silicone resins, following the addition of the appropriate formate dispersed in ethylene glycol and octoic acid.

Compound	Mass(g)	E.G.(ml)	O.A.(ml)	Non-Mag. Resin		Mag. Resin	
				Mean Cure Time (mins.)	Temp.(°C)	Mean Cure Time (mins.)	Temp.(°C)
Tin(II) Formate	0.30	0.25	0.05	18.4	14.0	21.0	12.0
	0.30	0.50	0.05	16.8	14.0	19.3	12.0
	0.25	0.25	0.05	14.8	14.0	20.5	12.0
	0.25	0.50	0.05	14.5	14.0	21.3	12.0
Cobalt Tin Formate	0.30	0.25	0.05	12.9	14.9	11.0	17.0
	0.30	0.50	0.05	11.4	14.9	11.0	17.0
	0.25	0.25	0.05	10.9	14.9	12.2	16.6
	0.25	0.50	0.05	9.6	14.9	12.2	16.6
Cobalt(II) Formate	0.30	0.25	0.05	No cure	16.0	No cure	16.0
	0.25	0.25	0.05	after 24hrs.	16.0	after 24hrs.	16.0
Nickel Tin Formate	0.30	0.25	0.05	13.9	14.8	11.8	16.0
	0.30	0.50	0.05	12.8	13.5	11.2	17.0
	0.25	0.25	0.05	12.0	15.0	11.6	16.0
	0.25	0.50	0.05	14.8	15.5	12.0	16.0
Nickel(II) Formate	0.30	0.25	0.05	No cure	16.0	No cure	16.0
	0.25	0.25	0.05	after 24hrs.	16.0	after 24hrs.	16.0

TABLE 4.5 Mean cure time for 5.0g of non-magnetic and magnetic silicone resins, following the addition of the appropriate acetate dispersed in ethylene glycol and octoic acid.

Compound	Mass(g)	E.G.(ml)	O.A.(ml)	Non-Mag. Resin		Mag. Resin	
				Mean Cure Time (mins.)	Temp.(°C)	Mean Cure Time (mins.)	Temp.(°C)
Tin(II) Acetate	0.30	0.25	0.05	3.9	21.5	7.4	18.5
	0.30	0.50	0.05	2.8	21.5	5.5	19.5
	0.25	0.25	0.05	4.2	21.5	9.6	18.5
	0.25	0.50	0.05	3.9	20.5	9.2	18.5
Cobalt Tin Acetate	0.30	0.25	0.05	13.8	17.0	16.4	18.0
	0.30	0.50	0.05	16.4	17.0	6.4	18.0
	0.25	0.25	0.05	10.4	17.0	17.1	16.5
	0.25	0.50	0.05	18.5	15.0	14.8	18.5
Cobalt(II) Acetate	0.30	0.25	0.05	No cure	16.0	No cure	19.0
	0.25	0.25	0.05	after 24hrs.	16.0	after 24hrs.	19.0
Nickel Tin Acetate	0.30	0.25	0.05	5.5	20.0	10.8	19.5
	0.30	0.50	0.05	6.3	20.0	7.9	19.5
	0.25	0.25	0.05	6.2	20.5	4.5	19.5
	0.25	0.50	0.05	6.1	20.5	9.8	19.5
Nickel(II) Acetate	0.30	0.25	0.05	No cure	16.0	No cure	16.0
	0.25	0.25	0.05	after 24hrs.	16.0	after 24hrs.	16.0

TABLE 4.6 Mössbauer data for carboxylates and cured silicone resins.

SAMPLE	$\delta$ (mm/s)	$\Delta$ (mm/s)	$\delta$ (mm/s)
Tin(II) Formate	3.27	1.73	-
Tin(II) Octoate*	3.22	2.02	-
Tin(II) Formate/ Tin(II) Octoate	3.25	1.73	-
Tin(II) Acetate	3.33	1.75	0.02
Tin(II) Formate/E.G.	3.28	1.76	-
Tin(II) Formate/E.G./ O.A./Non-Mag.Resin	0.06	-	-
Tin(II) Formate/E.G./ O.A./Mag.Resin	0.08	-	-
Tin(II) Acetate/E.G./ O.A./Non-Mag.Resin	-0.15	-	-
Tin(II) Acetate/E.G./ O.A./Mag.Resin	0.03	-	-
Tin(II) Octoate/ Non-Mag. Resin*	0.11	-	-
Cobalt Tin Formate	3.31	1.67	-
Cobalt Tin Acetate	3.08	1.83	1.02

\* Values obtained by Nicholides [4].

In each case, the resin was found to cure in 15 minutes, although increasing the concentration of the catalyst did not engender an increase in the rate of cure. A comparison of the activity of stannous octoate with other metal catalysts, viz. Pb, Sb, Fe and Ti, proved the superiority of the former.

Moreover, stannous octoate was used to cure dimethylpolysiloxane fluids [12]: the catalyst incorporated at the level of 2% by weight, cured the fluid in 30 minutes, producing an elastomer which when stretched or deformed, reverted to its original cured shape. Dimethylpolysiloxane fluids have also been cured by higher tin(II) carboxylates [13]: stannous neodecanoate gave a 30 minute cure, too, but in this instance 10 wt.% catalyst was required, whilst the use of stannous ricinoleate was accompanied by a discolouration of the cured resin.

Karpel [14] describes the application of stannous octoate, at the level of 0.1-1.0%, in the vulcanization of silicone elastomers, the rate of cure being controllable to some extent by the concentration of catalyst used.

In the present work, the use of solids dispersed in suitable liquid media as catalysts was investigated. The tin and transition metal tin derivatives of carboxylic acids were

tested as potential curing agents. The results were encouraging in that cure times were achieved in about 20 minutes or less for the formates and acetates used.

The results indicate that for the formates, the rate of cure increases when the tin carboxylate is complexed with a transition metal. In the case of the acetates, this situation is reversed; the tin acetate was found to affect a cure more rapidly than the transition metal tin derivatives. Transition metal carboxylates were found not to produce a cure at all.

These findings point to an increase in the catalytic activity of the complex tin formates and a reduction in the catalytic activity of the complex tin acetates when compared with the corresponding tin carboxylates. Thus, the transition metal modifies the behaviour of the tin species whilst an increase in alkyl chain length may retard catalytic activity. Further, the fact that the transition metal carboxylates did not affect a cure suggests that tin may be reacting with octoic acid to form tin(II) octoate.

Most catalysts function effectively at room temperature, but their efficiency drops in response to a decrease in temperature, as is manifested by some of the results of this work. This compares favourably with the data obtained by

Nicholides.

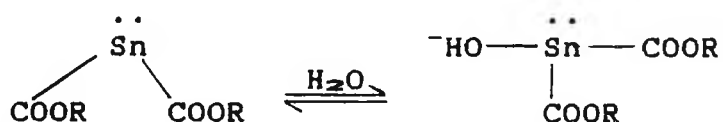
The inclusion of iron filings in silicone resins, hence the term 'magnetic' silicone resins, seems to retard the curing reaction. A possible explanation for this may be that the small, highly charged species repel one another, enhancing the stability of the dispersion and, in so doing, reduce or completely inhibit the rate of cure.

The Mössbauer data indicate that, on curing, the tin(II) species is transformed to tin(IV). The data serves as a comparison between the tin in the pure compounds and that in the catalyzed resins. The spectra show that the isomer shift falls in the region of 3.22 - 3.33mm/s for the pure compounds and decreases dramatically for the cured resins. This implies a reduction in s-electron density around the tin nucleus for catalyzed resins, and that the Sn-O bonding is largely covalent. Moreover, the quadrupole splitting, evident in the spectra of the pure carboxylates and consistent with a highly distorted environment around the tin nucleus, is absent in spectra of the cured resins. The Sn(IV) peak at -0.15 - 0.08mm/s is characteristic of tin octahedrally bound by six oxygens. This type of environment is explained in the mechanism set out in the following section. Similarly, for halide systems [4], viz. SnBr<sub>2</sub>.ethylene glycol, SnCl<sub>2</sub>.propylene glycol and

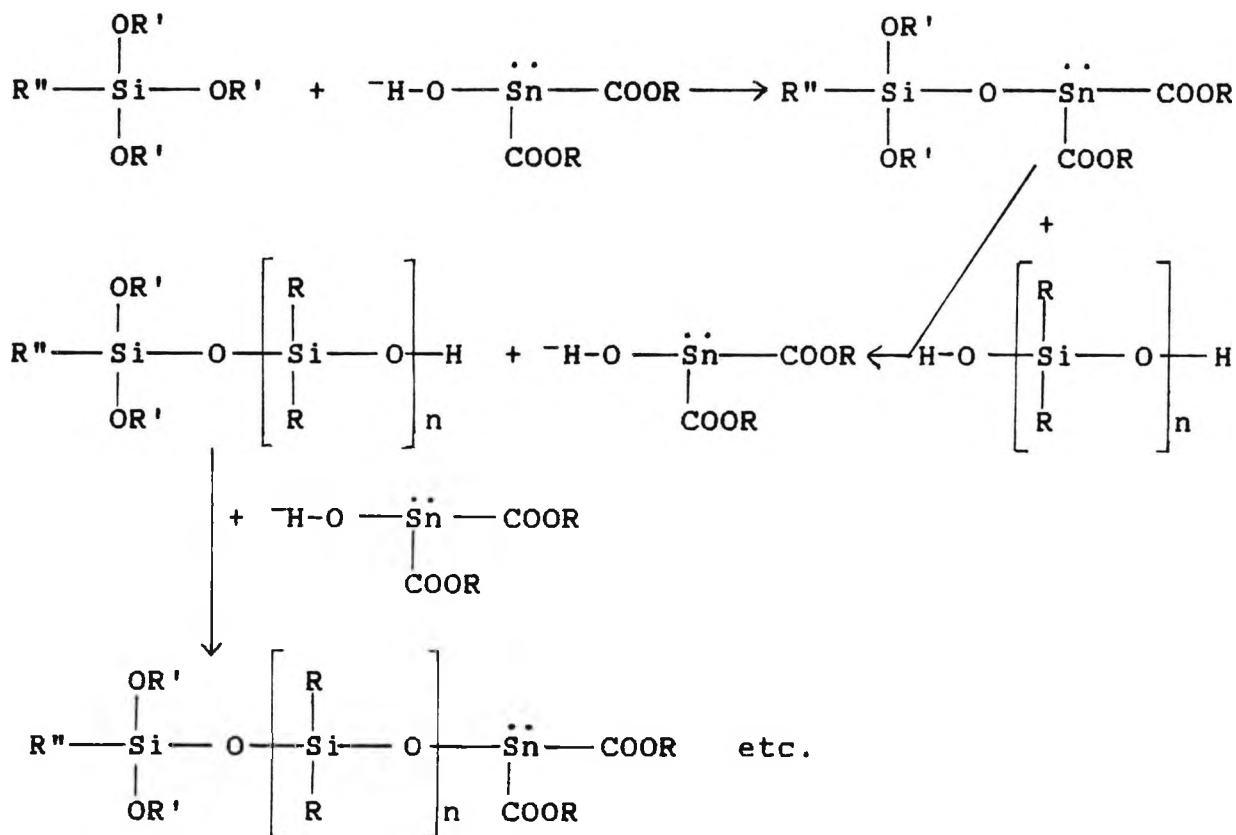
Two mechanisms can be postulated for the tin catalysed curing of silicone resins:

MECHANISM A

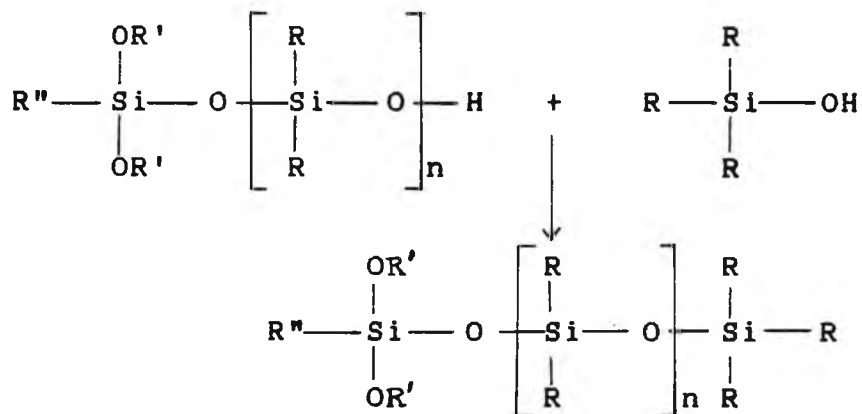
Initiation:



Propagation:



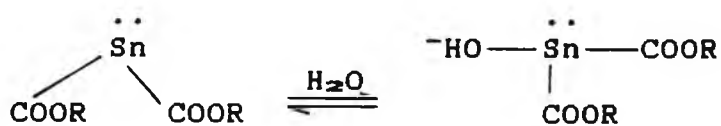
Termination:



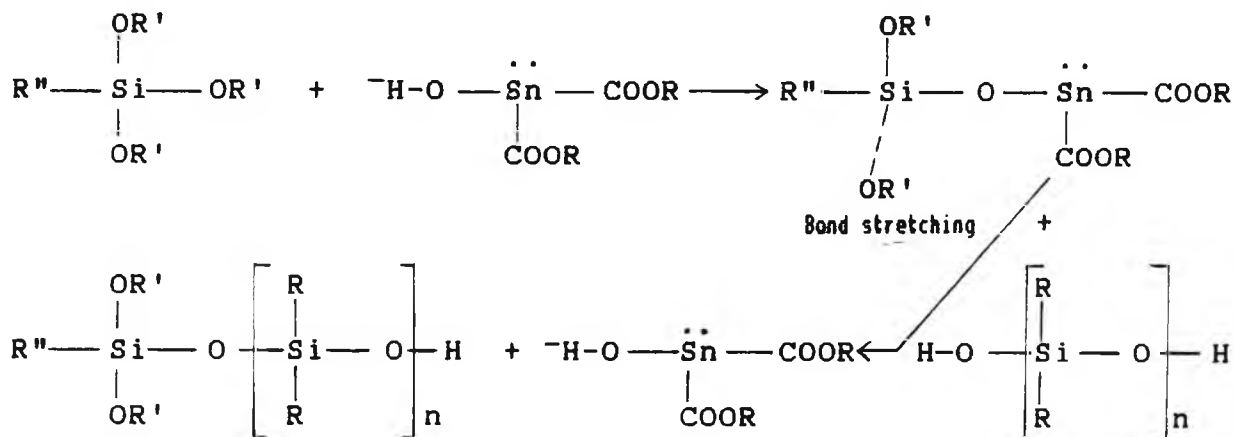
where R and R' = alkyl  
and R'' = alkyl, alkoxy or polyalkoxysiloxy

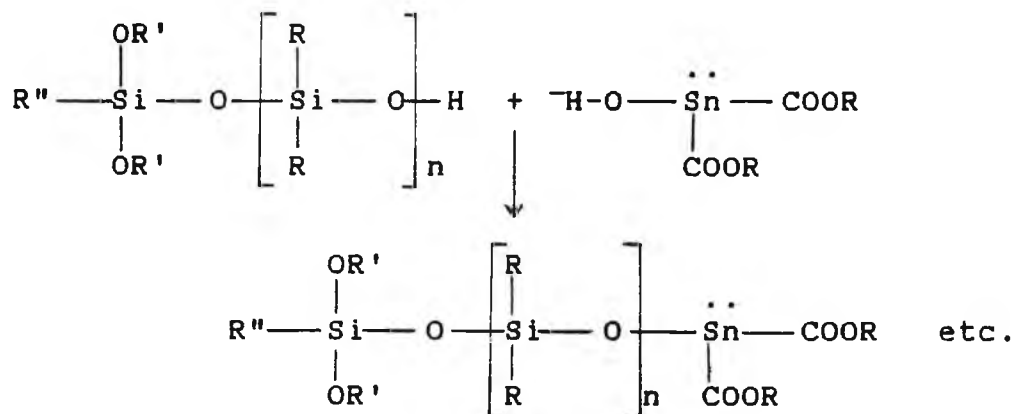
MECHANISM B

Initiation:

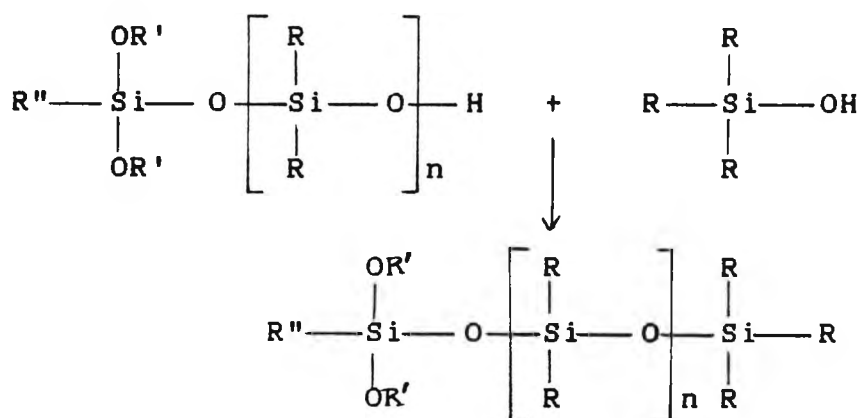


Propagation:

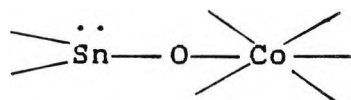




Termination:



Alternatively, where tin is complexed with a transition metal, a transition metal tin complex intermediary will be formed.



The complex ion can modify the behaviour of the tin species.

$\text{SnCl}_2$ .glycerol, the chemical shift, in each case, decreases for the cured resin when compared with the pure compound. However, for these same systems, the quadrupole splitting increases and has been attributed to a greater degree of disorder about the tin nucleus.

#### 4.3 Dispersion of Calcium Hydroxide in Processing Aids

The formulation of fluorocarbon elastomeric compounds is relatively simple. Unlike compounds of other elastomers, which typically contain ten or more compounding ingredients, fluoroelastomeric compounds, such as those of Viton or Fluorel, normally comprise not more than four or five ingredients as shown below [15]:

<u>Ingredient</u>	<u>Parts by Weight</u>
Fluorocarbon elastomer	100
Metal oxide/hydroxide	3 - 15
Filler	10 - 30
Curing agents	0.5 - 3.0
Processing aid	0.5 - 2.0

Most fluoroelastomers conform to this type of formulation in which the only variables are usually the metal oxide or

hydroxide and its amount, the filler, and the curing agent. A processing aid might be used depending on the processing requirements.

Metal oxides and hydroxides are used as acid acceptors in the curing reaction, whilst the addition of processing aids enhances transfer mouldability. Fluorocarbon elastomers are difficult to release from mould cavities accompanied and/or aggravated by dirty mould surfaces. The problem is associated with diamine curing agents. However, compounds of the polymers Viton E-60C and Fluorel 2170, are reported to be relatively free from mould dirtying and sticking. Nevertheless, the use of a good mould lubricant and proper preconditioning of mould surfaces are essential to good release. Preconditioning by baking on an emulsion-applied low molecular weight polyethylene and subsequent use of a lubricant prepared from a mixture of isopropyl myristate polyethylene emulsion has been beneficial. It is often possible, however, to avoid using a processing aid by substituting it with a low viscosity polymer such as Viton A-35 [16].

In this study, detailed in Sections 4.3.1, 4.3.2 and 4.3.3., an attempt was made to determine the optimum proportions of  $\text{Ca(OH)}_2$  to processing aid (supplied by J.R. McShane) required to reduce the health hazards involved in the

manufacture of fluoroelastomers, whilst complying with the specified regulations of parts by weight of the aforementioned components.

### Procedure

Sets of  $\text{Ca(OH)}_2$ -processing aid composites were prepared in the following manner:

5.0g of  $\text{Ca(OH)}_2$  were dispersed in various quantities of three processing aids:

(a) VPA 2: 0.1g, 0.3g, 0.5g, 0.7g, 0.9g

(b) PPA 791: 0.1g, 0.3g, 0.5g, 0.7g, 0.9g

(c) PPA 790: 0.1g, 0.3g, 0.5g, 0.7g, 0.9g

In all cases, the wax was melted and  $\text{Ca(OH)}_2$  dispersed in it, stirring thoroughly. The mixtures were then subjected to the action of an agate ball-mill for 30 minutes.

The following tests were performed on each composite to determine its physical properties:

1. Thermal Analysis
2. Tablet Formation
3. Scattering Ability

#### 4.3.1 Thermal Analysis

Thermal analysis is the generic term encompassing a group of related techniques whereby some physical parameter of a system under investigation is determined as a dynamic function of temperature. The main parameter important in methods of thermal analysis is the change in heat content.

#### Differential Thermal Analysis

Differential thermal analysis (DTA) is a technique in which the temperature difference between a test sample and an inert reference sample is recorded as a function of temperature, or time, as the two specimens are subjected to identical temperature regimes in an environment heated or cooled at a controlled rate [17]. Any physical or chemical change, evident in the test sample, involving the evolution of heat, will cause the sample's temperature to rise temporarily above that of the reference material, thus engendering an exothermic peak on the DTA plot. Conversely, any process accompanied by the absorption of heat will cause the temperature of the test sample to lag behind that of the reference sample, resulting in an endothermic peak. A hypothetical DTA trace is shown in Fig. 4.7.

However, even where no physical or chemical process occurs,

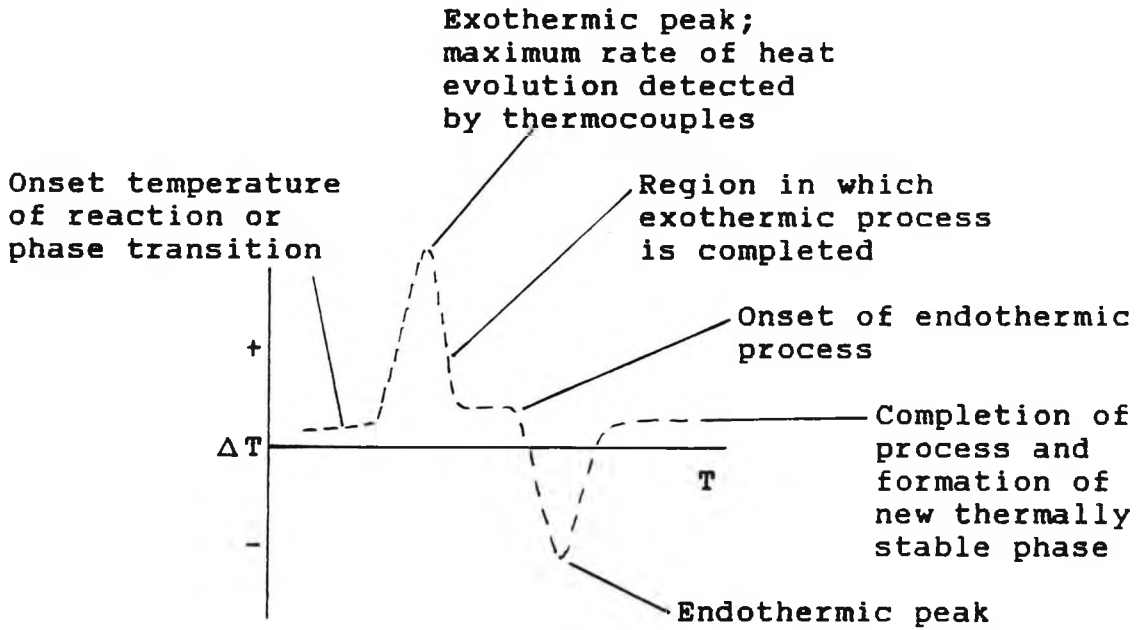


FIGURE 4.7 Hypothetical DTA trace indicating an exothermic and endothermic peak.

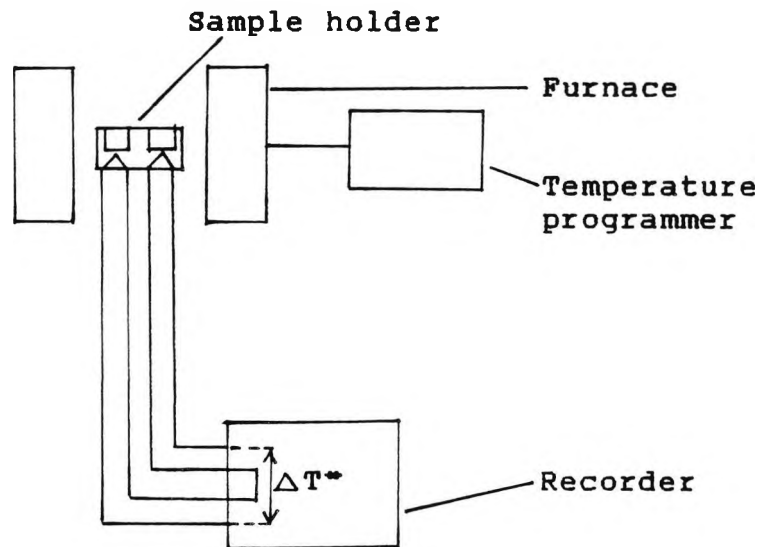


FIGURE 4.8 Block diagram of DTA apparatus.

\* Temperature difference between sample and inert reference material.

a small and steady differential temperature normally develops between test and reference materials. This is primarily due to differences in the heat capacity and thermal conductivity of the two materials, but is also influenced by other factors, such as sample mass and packing density. Consequently, DTA can be used to study transitions in which no heat is evolved or absorbed by the sample, as may be the case in certain solid-solid phase changes. The difference in the heat capacity [18] of the sample before and after the transition has occurred will then be reflected in a new steady differential temperature being established between the test and reference samples. The baseline of the differential curve will accordingly show a sudden discontinuity at the transition temperature, while the gradients of the curve in the regions above and below this temperature will usually differ significantly.

Clearly, the peaks due to chemical changes may ensue not only from reactions of the sample itself, but also from secondary reactions of evolved decomposition products. Such reactions can often occur catalytically on the surface of the residual solid.

To rely entirely on the evidence obtained by DTA in the elucidation of a problem is undesirable. Thus, thermogravimetry (TG) is commonly employed in conjunction with

DTA.

### Thermogravimetry

In dynamic thermogravimetry, as used in this work, changes in the weight of a sample, subjected to a uniform rate of increase in temperature are recorded. (Static thermogravimetry measures the change in weight of a sample with time at a constant temperature.) This enables any DTA peak due to a chemical reaction involving a weight change to be identified. If a DTA peak arises at a temperature where the sample weight remains constant, it may be assumed that either a solid state reaction, or a phase transition, has occurred. Therefore, the TG curve provides information on the thermal stability and composition of the initial sample, on any intermediate compound that may be formed, and on the composition of any residue.

### Differential Thermogravimetry

Differential thermogravimetry is a technique expressing the results of TG by yielding the first derivative of the TG curve with respect to either temperature (T) or time (t):

$$dm / dt = f (T \text{ or } t)$$

The area under the curve is proportional to the total change in mass of the sample.

Several advantages may be attributed to DTG, as have been outlined by Erdey *et al* [19]: DTG curves are more reproducible than DTA curves (the results of the latter indicate even those changes in state that are not accompanied by a loss in mass); DTG measurements reveal the precise temperatures of the onset, the maximum rate and the termination of the change, whereas DTA curves extend over a wider temperature interval owing to subsequent warming of the material after reaction; the effect of rapid changes is to encourage overlapping of TG curves, complete with the difficulties implicit in interpretation, the DTG curves of the same transitions are usually more distinct with prominent peaks.

#### Instrumentation

In this work, a Stanton Redcroft STA 780 Simultaneous Thermal Analyzer was used and samples heated to 600°C unless stated otherwise. The instrument is designed to give temperature, TG, DTA and DTG curves simultaneously, facilitating the correlation of data for the same substance.

The DTA apparatus consists of four major components, as is

illustrated in Fig. 4.8:

1. Sample holder - measuring system. This comprises the thermocouples and sample containers.
2. Furnace - heat source having a large uniform temperature zone.
3. Temperature programmer - supplies energy to the furnace in such a manner as to ensure a reproducible (and preferably linear) rate of change of temperature.
4. Recording system - method of indicating and/or recording the e.m.f. (suitably amplified) from the differential- and temperature-measuring thermocouples.

#### 4.3.2 Tablet Formation

Tablets of the dimensions 13x1mm were produced from samples containing 5g  $\text{Ca(OH)}_2$  and 1g processing aid with the aid of a Specac die. The die was placed in Bechmann Hydraulic Press and samples were compressed using a 10 ton load for 30 seconds.

#### 4.3.3 Scattering Ability

1.0g of the various  $\text{Ca(OH)}_2$ -processing aid composites were dropped from a height of 15cm onto a piece of glass and the mean diameter was estimated. Measurements were taken in the vertical, horizontal and diagonal directions. Each sample was tested in triplicate.

#### 4.3.4 Results of DTA

The thermal data for the  $\text{Ca(OH)}_2$ -processing aid composites are set out in Tables 4.7, 4.8, 4.9 and 4.10.

#### 4.3.5 Results of Tablet Formation

The strength of tablets containing  $\text{Ca(OH)}_2$ -processing aid composites are indicated in Table 4.11.

#### 4.3.6 Results of Scattering Ability

Table 4.12 shows the extent of scattering of the  $\text{Ca(OH)}_2$ -processing aid composites.

TABLE 4.7

Thermal data for calcium hydroxide and processing aids.

SAMPLE	TEMP. (°C)	%WT. LOSS	INFERENCE
Ca(OH) <sub>2</sub>	355	22.0	Endothermic reaction; decomp. : Ca(OH) <sub>2</sub> → CaO+H <sub>2</sub> O
	553	0	Endothermic reaction; m.p.
VPA 2	51	-	Endothermic reaction; sharp peak, m.p.
	258	95.0	Endothermic reaction; decomp. and volatilization.
PPA 790	66	-	Endothermic reaction; m.p.
	143	73.0	Endothermic reaction; decomp. and volatilization.
PPA 791	66	-	Endothermic reaction; m.p.
	136	99.0	Endothermic reaction; decomp. and volatilization.

TABLE 4.8

Thermal data for calcium hydroxide-processing aid composites.

SAMPLE	TEMP. (°C)	%WT. LOSS	INFERENCE
5.0g Ca(OH) <sub>2</sub> - 0.1g VPA 2	51	0	Endothermic reaction; m.p. of wax.
	346	22.5	Endothermic reaction; decomp. of Ca(OH) <sub>2</sub> .
5.0g Ca(OH) <sub>2</sub> - 0.3g VPA 2	51	0	Endothermic reaction; m.p. of wax.
	350	23.0	Endothermic reaction; decomp. of Ca(OH) <sub>2</sub> .
5.0g Ca(OH) <sub>2</sub> - 0.5g VPA 2	54	0	Endothermic reaction; m.p. of wax.
	365	17.0	Endothermic reaction; decomp. of Ca(OH) <sub>2</sub> .
5.0g Ca(OH) <sub>2</sub> - 0.7g VPA 2	58	0	Endothermic reaction; m.p. of wax.
	365	18.5	Endothermic reaction; decomp. of Ca(OH) <sub>2</sub> .
5.0g Ca(OH) <sub>2</sub> - 0.9g VPA 2	58	0	Endothermic reaction; m.p. of wax.
	365	18.5	Endothermic reaction; decomp. of Ca(OH) <sub>2</sub> .
5.0g Ca(OH) <sub>2</sub> - 1.0g VPA 2	125	0	Endothermic reaction; m.p. of wax.
	326	2.3	Endothermic reaction; m.p. of Ca(OH) <sub>2</sub> .
	371	28.0	Endothermic reaction; decomp. of Ca(OH) <sub>2</sub> .

TABLE 4.9

Thermal data for calcium hydroxide-processing aid composites.

SAMPLE	TEMP. (°C)	%WT. LOSS	INFERENCE
5.0g Ca(OH) <sub>2</sub> - 0.1g PPA 790	66	2.5	Endothermic reaction; m.p. of wax.
	320	22.5	Endothermic reaction; decomp. of Ca(OH) <sub>2</sub> .
5.0g Ca(OH) <sub>2</sub> - 0.3g PPA 790	66	4.0	Endothermic reaction; m.p. of wax.
	349	19.5	Endothermic reaction; decomp. of Ca(OH) <sub>2</sub> .
5.0g Ca(OH) <sub>2</sub> - 0.5g PPA 790	73	4.0	Endothermic reaction; m.p. of wax.
	350	19.5	Endothermic reaction; decomp. of Ca(OH) <sub>2</sub> .
5.0g Ca(OH) <sub>2</sub> - 0.7g PPA 790	94	4.0	Endothermic reaction; m.p. of wax.
	360	17.5	Endothermic reaction; decomp. of Ca(OH) <sub>2</sub> .
5.0g Ca(OH) <sub>2</sub> - 0.9g PPA 790	106	0	Endothermic reaction; m.p. of wax.
	365	18.0	Endothermic reaction; decomp. of Ca(OH) <sub>2</sub> .
5.0g Ca(OH) <sub>2</sub> - 1.0g PPA 790	129	0	Endothermic reaction; m.p. of wax.
	326	6.5	Endothermic reaction; m.p. of Ca(OH) <sub>2</sub> .
	370	19.0	Endothermic reaction; decomp. of Ca(OH) <sub>2</sub> .

TABLE 4.10

Thermal data for calcium hydroxide-processing aid composites.

SAMPLE	TEMP. (°C)	%WT. LOSS	INFERENCE
5.0g Ca(OH) <sub>2</sub> - 0.1g PPA 791	57	0	Exothermic reaction; phase change.
	243	2.0	Exothermic reaction; phase change.
	365	22.5	Endothermic reaction; decomp. of Ca(OH) <sub>2</sub> .
5.0g Ca(OH) <sub>2</sub> - 0.3g PPA 791	73	0	Exothermic reaction; phase change.
	300	4.0	Exothermic reaction; phase change.
	365	20.0	Endothermic reaction; decomp. of Ca(OH) <sub>2</sub> .
5.0g Ca(OH) <sub>2</sub> - 0.5g PPA 791	80	6.0	Exothermic reaction; phase change.
	304	2.0	Exothermic reaction; phase change.
	365	19.5	Endothermic reaction; decomp. of Ca(OH) <sub>2</sub> .
5.0g Ca(OH) <sub>2</sub> - 0.7g PPA 791	80	8.0	Exothermic reaction; phase change.
	302	2.5	Exothermic reaction; phase change.
	365	17.5	Endothermic reaction; decomp. of Ca(OH) <sub>2</sub> .

TABLE 4.10 contd.

Thermal data for calcium hydroxide-processing aid composites.

SAMPLE	TEMP. (°C)	%WT. LOSS	INFERENCE
5.0g Ca(OH) <sub>2</sub> - 0.9g PPA 791	94	7.0	Exothermic reaction; phase change.
	300	2.0	Exothermic reaction; phase change.
	365	19.0	Endothermic reaction; decomp. of Ca(OH) <sub>2</sub> .
5.0g Ca(OH) <sub>2</sub> - 1.0g PPA 791	130	7.0	Exothermic reaction; sharp peak, phase change.
	326	0	Exothermic reaction; sharp peak, phase change.
	375	8.0	Endothermic reaction; decomp. of Ca(OH) <sub>2</sub> .

TABLE 4.11

Strength of tablets containing 5g calcium hydroxide-  
1g processing aid.

PROCESSING AID	DESCRIPTION OF TABLET
VPA 2	Fairly strong
PPA 790	Not very strong
PPA 791	Brittle

TABLE 4.12

Dropping of calcium hydroxide-processing aid composites  
from a fixed height and estimation of extent of scattering.

MASS OF P.A. IN Ca(OH) <sub>2</sub> -P.A. COMPOSITE (G)	MEAN DIAMETER (CM)		
	Ca(OH) <sub>2</sub> - VPA 2	Ca(OH) <sub>2</sub> - PPA 790	Ca(OH) <sub>2</sub> - PPA 791
0.1	23.00	25.25	30.00
0.3	23.67	44.17	42.67
0.5	30.08	51.08	38.17
0.7	33.17	45.42	36.42
0.9	31.17	43.33	35.67

#### 4.3.7 Discussion

The thermograms suggest that by dispersing calcium hydroxide in a processing aid, the dehydration of the former is suppressed, that is, the decomposition temperature is generally greater than for calcium hydroxide alone. Furthermore, the thermograms of each processing aid indicate a definite melting point. This peak, although present on the thermograms of the composites, is more difficult to discern. The melting points of the waxes are, on average, higher in composite form compared with the waxes alone which implies that the melting points are suppressed when the waxes are compounded with calcium hydroxide. Phase changes are evident on the thermograms of the  $\text{Ca(OH)}_2$ -PPA 791 composites, but are absent on the thermograms of both calcium hydroxide and PPA 791.

A comparison of the results obtained for tablet formation showed that the  $\text{Ca(OH)}_2$ -VPA 2 composite was strongest and possibly most suitable for use as a dispersant.

With reference to the degree of scattering, it was evident that this property generally increased in the case of the  $\text{Ca(OH)}_2$ -VPA 2 composites with the percentage of processing aid. This trend was not so clear where the  $\text{Ca(OH)}_2$ -PPA 790 and  $\text{Ca(OH)}_2$ -PPA 791 composites were

concerned. Another observation was that the scattering of the PPA composites was more extensive than that of the VPA mixtures. This may tentatively be attributed to the fact that the PPA processing aids were found to be lighter and so less dense than VPA 2, and thus tended to be carried further when dropped.

In view of the results emanating from these experiments and with due consideration to the application of the compounding ingredients, exploited in the manufacture of fluoro-elastomers, it would probably be advantageous to use VPA 2 in preference to PPA 790 and PPA 791, since the dust-suppressant properties of the former substantially surpass those of the latter and thus minimize the health hazards involved.

#### 4.4 The Determination of a Suitable Form of Administering Cobalt to Ruminants

##### 4.4.1 Introduction

The term *cobalt* is thought to have been derived from the German *Kobold*, literally translated as 'goblin' or 'mischievous spirit', originating from the 16th century, first being applied by miners of the Harz mountains in Germany to an ore which did not yield the expected copper

when smelted by the normal procedure, but on roasting, emitted toxic fumes of arsenic [20]. A similar word, encountered in Saxony, *kobelt*, appears to have been generally applicable to ores which were not readily reduced. When G. Brandt [21] isolated the element in 1735, he referred to it as 'cobalt rex' and was the first to describe its properties. Moreover, it was he who discovered the magnetic behaviour of the metal, thus initiating its scientific study, although its true elemental nature was not established until 1780, following a thorough investigation by Bergman.

Cobalt forms an important constituent of vitamin B<sub>12</sub>, or cyanocobalamin, essential for the normal maturation and development of erythrocytes. Vitamin B<sub>12</sub> was first detected in 1926 by G. R. Minot and W. P. Murphy [22] who found that the inclusion of liver in the diet cures patients suffering from pernicious anaemia. Despite several attempts over the years to isolate the liver-factor, little progress was made, as the disease could not be evoked *in vivo* and afflicted patients were required to assay the potency of liver-factor concentrates. However, in 1948, the liver-factor, called vitamin B<sub>12</sub> was finally isolated in a red crystalline form by E. L. Smith *et al.* [23], in England E. L. Rickes *et al.* [24], in the United States.

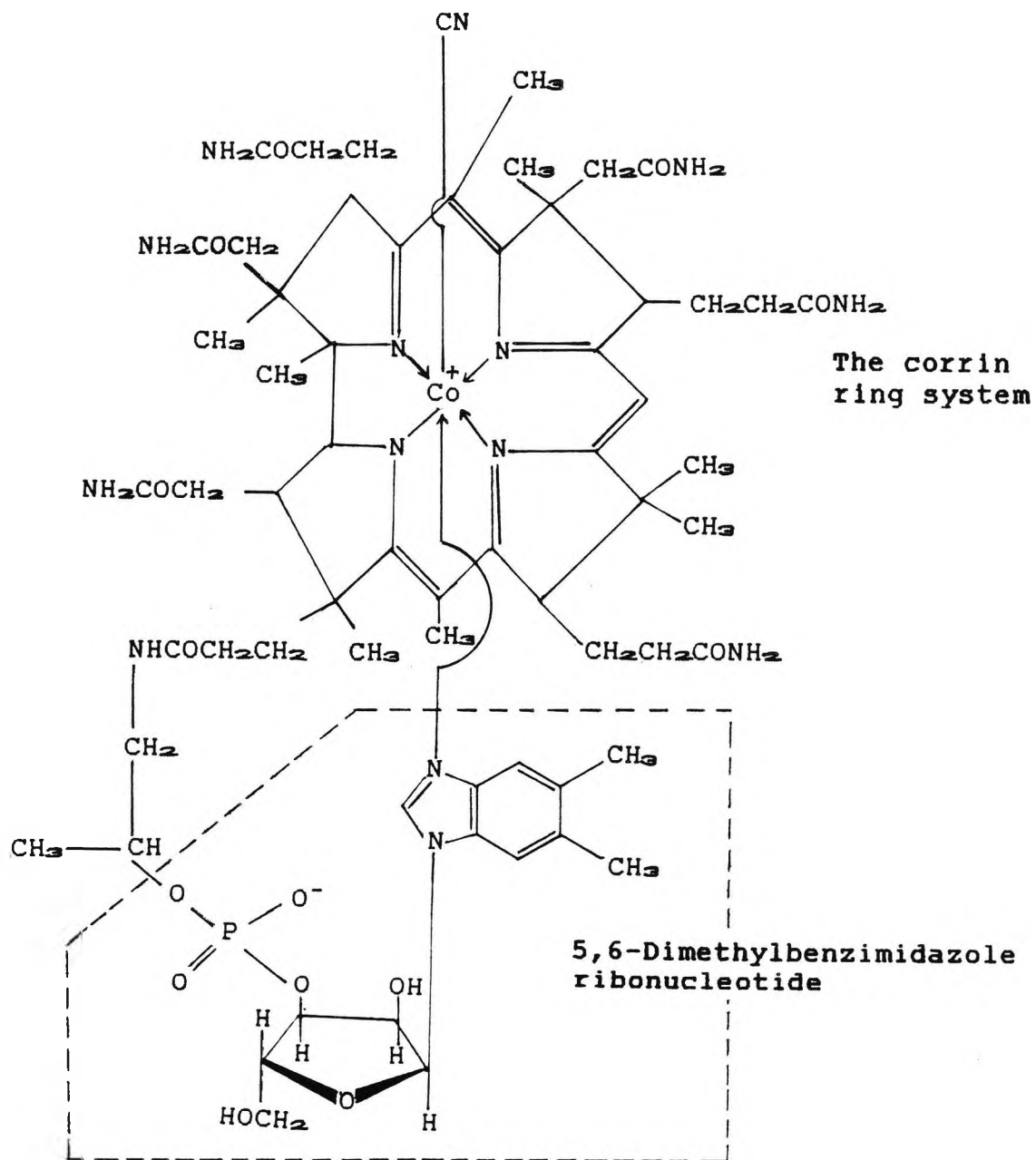


FIGURE 4.9 Structure of vitamin B<sub>12</sub> (cyanocobalamin).

The elucidation of the structure of vitamin B<sub>12</sub> posed a problem, ultimately solved in 1957 [25], by a combination of chemical and X-ray diffraction methods. Vitamin B<sub>12</sub> was found to consist of two characteristic components: the larger being the corrin ring system, resembling the porphyrin ring system present in haemoglobin, containing four pyrrole-type rings but in which a pair of these five membered rings is joined directly rather than through a methane bridge. Coordinated to the four inner nitrogen atoms of the corrin ring system is an atom of cobalt, long known to be essential for growth. The second major component of the vitamin was found to be a ribonucleotide, exceptional in containing 5,6-dimethylbenzimidazole as a base, in the unusual  $\alpha$ -N-glycosyl linkage with D-ribose, rather than the  $\beta$ -linkage present in most other nucleotides. This ribonucleotide is attached to the corrin by a coordination bond between the other nitrogen atom of the nucleotide and the cobalt atom and, by an ester linkage between the 3'-phosphate group of the ribonucleotide and a side chain of the corrin ring. Cyanide occupies one of the coordination positions of the cobalt atom; hence the name cyanocobalamin.

#### 4.4.2 Scope of this Work

The objective of this study was to compound cobalt oxide

with a compatible medium, adding the minimum amount of the latter, to enable its use as feedstock. Moreover, a commercially presentable form for administering the oxide was sought.

The cobalt oxide used in this investigation had a black, powdered appearance and consisted of 95%  $\text{Co}_2\text{O}_3$  and 5%  $\text{CoO}$ . It was manufactured by Hoboken, in Belgium.

Attempts were made to disperse the cobalt oxide in four media: PEG 400, PEG 600 and carnuba wax, PEG 4000 and a polyunsaturate.

#### 4.4.3 Experimental Procedure and Results

##### (a) The Dispersion of Cobalt Oxide in PEG 400

Initially, the cobalt oxide was dispersed in PEG 400, a clear, viscous liquid at 25°C and moderately hygroscopic, the mixture being 'kneaded' with a pallet until a 'plastercine-like' consistency was achieved. A thermogravimetric analysis was performed on the final product to evaluate the percentage of cobalt oxide in the sample. The T.G. revealed that the composite comprised 84.5% cobalt oxide and ca. 0.5%  $\text{H}_2\text{O}$ , the remainder being PEG 400. Several samples were subsequently prepared, their

percentage compositions in close proximity to the above. It was not possible to use less than 0.5g PEG 400, owing to its high viscosity (i.e. greater than 85mPa).

TABLE 4.13

Percentage composition of cobalt oxide/PEG 400 samples

% Cobalt Oxide	% PEG 400
94.5	5.5
94.0	6.0
93.5	6.5
93.0	7.0
92.5	7.5
92.0	8.0
91.5	8.5
91.0	9.0
90.5	9.5
90.0	10.0
88.0	12.0
87.75	12.25
87.5	12.5

In this section, the dispersions produced were by 'agglomeration', a process in which small particles are gathered into larger sized units. Several methods of forming agglomerated materials exist, including: agitation,

extrusion, compression and fusion.

Agglomerates prepared by agitation are termed 'prills'. These are formed by collision and adherence of the bulk particles in the presence of a liquid binder or wetting agent to produce a 'snowball' effect [26]. The strength and hardness of the prills are determined by the binders and wetting agents used.

Agglomerated products formed by extrusion are termed 'pellets' and are formed when a material is forced out of an orifice which is usually cylindrical.

When aggregation is achieved by compaction, the agglomerates produced are known as 'tablets'. In this operation, a powder is compressed between two opposing surfaces or compacted in a die or cavity. Some tableting machines use the action of two opposing plungers which function within a cavity.

Agglomerates formed by fusion are termed 'melts'. The sintering process utilizes fusion as a means of size enlargement. This process is applied mainly for ores, minerals and powdered metals. Generally, heated air is passed through a loose bed of finely ground material and the particles fuse together without the aid of a binder. Sintering is frequently accompanied by the volatilization of

impurities and removal of undesired moisture.

In this work, the agglomerates formed were by agitation, extrusion and compression.

(i) The Formation of Prills:-

The samples, listed in Table 4.13, were each spun in an agate ball-mill (ca. 8cm in diameter) together with three agate balls (1cm in diameter) for 20 minutes. In each case, aggregation of the particles occurred; a greater degree was evident in samples containing higher percentages of PEG 400. However, a variation in the size of particles was observed.

After a week had elapsed, samples of the following percentages of cobalt oxide were again subjected to the action of the ball-mill: 90.5, 92.5 and 94.5. As before, aggregation occurred, although the results were not as satisfactory as those previously obtained, i.e. the extent of aggregation was not as pronounced. In addition, uniformity in spheroid size was still not achieved.

With samples of higher percentages of cobalt oxide, an attempt was made at hand rolling the spheroids, produced by ball-milling, between two hard surfaces, using a circular motion, the smooth surfaces being sandwiched between one's hand and the bench top, the sample secured between the

surfaces. The aim was to increase the number of spheroids as well as the degree of uniformity. However, the spheroids produced earlier only disintegrated.

Spheroids of uniform size were later produced by forming an agglomeration consisting of cobalt oxide, PEG 600 and carnauba wax in the ratio of 18:2:1 respectively, i.e. 85.7% cobalt oxide. The mixture was warmed in a beaker in order to melt the wax. Spheroids appeared during this process which, on cooling, were found to harden.

(ii) The Formation of Pellets:-

After the samples were ball-milled, an attempt was made to produce pellets of approximately 5mm in length and 1mm in diameter. The optimum mass to be placed in the extruder was found to be 30g. The pellets were formed by extruding the sample through an orifice and severing at the requisite length. Samples containing 87.5% cobalt oxide were moist in appearance, whilst samples of higher percentages proved too difficult to extrude, despite the application of substantial pressure.

(b) The Dispersion of Cobalt Oxide in PEG 4000

An endeavour was made to establish whether or not PEG 4000 (white, waxy flakes; viscosity greater than 90mPa) would prove to be a compatible dispersing medium for cobalt oxide.

The former had to be melted prior to use, but was found to cool down and resolidify too rapidly, preventing the production of a good dispersion.

(c) The Dispersion of Cobalt Oxide in a Polyunsaturate and the Formation of Tablets

17.5g of cobalt oxide were dispersed in 2.5g of a polyunsaturate (i.e. 86.6% oxide) and spun in a ball-mill for 20 minutes. Tablets of the dimensions 13x6mm were then produced by feeding the sample into a Specac die. The die was evacuated and placed in a Beckmann hydraulic press and the sample compressed using a one ton load for 30 seconds. The resulting tablets were not particularly hard and had a tendency to flake.

4.4.4 Discussion

The aim of this study was to produce a dispersion containing the maximum amount of cobalt oxide possible in a compatible medium for use as feedstock for ruminants. Two interesting materials were prepared for this purpose.

The dispersion containing the highest percentage of cobalt oxide was achieved by mixing 86.6% of the latter with a polyunsaturate and prepared in the form of tablets.

A second method in which the final product took the form of spheroids, or prills, involved dispersing 85.7% of cobalt oxide in carnauba wax and PEG 600.

Both these products were sent to Belgium for assessment to establish whether they would be commercially acceptable and were shown to be satisfactory.

Neither animals nor plants are able to synthesize vitamin B<sub>12</sub>; it is only manufactured by certain micro-organisms. The vitamin is required in mere traces by animals, normal human blood containing 0.0002  $\mu$ g of vitamin B<sub>12</sub> per millilitre. In man, the amount of cobalt present in a normal diet safeguards the human system from any vitamin B<sub>12</sub> deficiency. However, in ruminants reared on cobalt-deficient pasture, the absence of this element results in loss of appetite, retarded growth and anaemia accompanied by long, rough hair coat, emaciation, pale mucous membranes, decreased milk flow, and scaliness of the skin; in severe cases, death may ensue. The same animals, when administered a vitamin B<sub>12</sub> supplement, have been shown to make a spectacular recovery.

REFERENCES

1. Ahmed, A.S., Ph.D. Thesis, The City University, London, 1987.
2. Lawrence, S.A., Ph.D. Thesis, The City University, London, 1984.
3. Grimes, S.M., Private Communication.
4. Nicholides, A., Ph.D. Thesis, The City University, London, 1984.
5. Donaldson, J.D., and Moser, W., *Analyst*, 1959, 84, 10.
6. Mössbauer, R.L., *Z. Physik*, 1958, 151, 124.
7. Gibb, T.C., 'Principles of Mössbauer Spectroscopy', Chapman and Hall, London, 1980.
8. Donaldson, J.D., and Knifton, J.F., *J. Chem. Soc.*, 1964, 4801.
9. Donaldson, J.D., Moser, W., and Simpson, W.B., *J. Chem. Soc.*, 1961, 839.
10. Arifin, Z.B, Ph.D. Thesis, The City University, London, 1981.
11. Berridge, C.A., U.S.P. 2,843,555, 1958.
12. Smith, F.A., U.S.P. 3,109,826, 1963.
13. Smith, R.A., U.S.P. 3,931,047, 1976.
14. Karpel, S., *Tin and its Uses*, 1984, 142, 6-9.
15. Arnold, R.G., Barney, A.L., and Thompson, D.C., *Rubber Chemistry and Technology*, 1973, 46, 3, 619-652.

16. Sweet, G.C., 'Developments in Rubber Technology - I', Applied Science Publishers Ltd., U.K., 1978.
17. Pope, M.I., and Judd, M.D., 'Differential Thermal Analysis, Heyden and Son Ltd., U.K., 1977.
18. Blazek, A., 'Thermal Analysis', Nostrand Reinhold Company Ltd., London, 1973.
19. Erdey, L., Paulik, F., and Paulik, J., *Nature*, 1954, 174, 885.
20. Betteridge, W., 'Cobalt and its Alloys', Ellis Horwood Ltd., U.K. 1982.
21. Battelle Memorial Institute, 'Cobalt Monograph', Centre D'Information Du Cobalt, Brussels, 1960.
22. Minot, G.R., and Murphy, W.P., *J. Amer. Med. Assos.*, Aug. 1926, 87, 470-476.
23. Smith, E.L., *Nature*, 1948, 162, 144-145.
24. Rickes, E.L., Brink, N.G., Koniuszy, F.R., Wood, T.R., and Folkers, K., *Science*, 1948, 108, 134.
25. Lehninger, A.L., 'Biochemistry', Worth Publishers Inc., New York, 1979.
26. Donbavand, J., Ph.D. Thesis, 1982, The City University, London.